Studies on the Precision Control of Polymer Structure Based on Heteroatom-Mediated Living Radical Polymerization Reaction

Eiichi Kayahara

2011

Studies on the Precision Control of Polymer Structure Based on Heteroatom-Mediated Living Radical Polymerization Reaction

Eiichi Kayahara

2011

Acknowledgement

The studies presented in this thesis have been carried out under the direction of Professor Shigeru Yamago at the Department of Polymer Chemistry of Kyoto University during 2008-2011 and at the Division of Molecular Materials Science of Osaka City University during 2005-2008. This thesis is concerned with studies on the precision control of polymer structure using organoheteroatom-mediated living radical polymerization.

The author would like to express his sincerest gratitude to Professor Shigeru Yamago for his kind guidance, valuable suggestions, and constant encouragement throughout this work.

The author would like to express my gratitude to Professor Takeshi Fukuda, Professor Atsushi Goto, and Dr. Yungwan Kwak at Kyoto University for the kinetic studies. And I would like to thank Professor Keiji Morokuma and Dr. Lung Wa Chung at Kyoto University for the theoretical calculations.

The author also wishes to thank to Ms. Tomoko Terada and Ms. Toshiko Hirano of Institute for Chemical Research, Kyoto University for the measurement of Mass and NMR analyses. The author also wishes to thank to Ms. Matsumi Doe and Ms. Rika Miyake of Osaka City University for the measurement of Mass and NMR analyses.

The author must make special mention of Dr. Masashi Kotani, Dr. Ray Biswajit, Mr. Hiroto Yamada, and Mr. Noriaki Kondo for their great assistance and collaborations.

The author has learned a great deal from Dr. Yasuyuki Nakamura, Dr. Takeshi Yamada, Ms. Yuu Kobayashi, Mr. Kazunobu Takemura, Mr. Atsushi Matsumoto, and Mr. Manabu Togai. The author also would like to thank them for their advice and collaborations. The author heartily thanks to Dr. Na Pan, Dr. Atanu Kotal, Dr. Shenyong Ren, Ms. Eri Mishima, Mr, Tsubasa Hamano, Mr. Yu Ukai, Mr. Kazuya Ueki, Mr. Yoshiki Watanabe, Mr. Shota Konishi, Ms. Tokiko Ueda, Mr. Takehiro Fujita, Mr. Yusuke Okumura, Mr. Takahiro Iwamoto, Ms. Yukie Kitada, Mr. Keita Horie, Mr. Yoshitaka Umeda, Mr. Kotaro Saiki, Mr. Koji Nakanishi, Mr. Lin Liu, Mr. Sinji Suzuki, Mr. Tomoki Tamura, Mr. Sora Tomita, and all of members of Professor Yamago's group for their active collaborations and kindness.

The author also would like to express his gratitude to Professor Christopher C. Cummins and the members of Professor Cummins's group; Dr. Alexander R. Fox, Dr. Nicholas A. Piro, Dr. Brandi M. Cossairt, Mr. Jared S. Silvia, Mr. Paresh Agarwal at Massachusetts Institute of

Technology and Mr. Ayumi Takaoka of Professor Peters's group at California Institute of Technology.

The author acknowledges financial support from Japan Society for the Promotion of Science (JSPS Research Fellowships for Young Scientists) and Kyoto University Global COE Program "International Center for Integrated Research and Advanced Education in Materials Science".

Finally, the author would like to express his deep appreciation to his family, especially his parents Mr. Fumio Kayahara and Ms. Kazuyo Kayahara for their constant assistance and encouragement.

Eiichi Kayahara

Department of Polymer Chemistry
Graduate School of Engineering
Kyoto University
2011

Contents

General Introduction

Heteroatom-containing organic compounds play key roles in modern science and technologies. These compounds are widely utilized in the biological and material sciences as, for examples, pharmaceuticals, biological probes, photonic and electronic devices, catalysts and ligands for catalysts. They are also used for precursors of a variety of reactive carbon species in organic synthesis, such as carbanions, carbocations, and carbon-centered radicals. Thus, organic chemists have focused much efforts to create novel heteroatom compounds with a hope that such molecules would possess new or improved properties.

Among synthetic transformations using organoheteroatom compounds, halogen atom transfer (AT) and organochalcogen group transfer (GT) radical addition (RA) reactions of organoheteroatom compounds with alkenes and alkynes have attracted attentions as new tools for forming carbon-carbon or carbon-heteroatom bond (Scheme 1a).[1-3] Nowadays, these reactions allow to access novel heteroatom compounds including biologically active molecules and tailor-made polymers.[1-3] The widespread interests in ATRA and GTRA are primarily associated with the synthetic advantages of radical reactions; since radicals are neutral and highly reactive species, the reaction usually proceeds under mild conditions with high functional group compatibility which cannot tolerate under ionic reactions.

ATRA and GTRA proceed thorough the radical chain reaction (Scheme 1b). Carbon-centered radical (R•) generaged from organoheteroatom compound R-XL_n adds to alkene or alkyne to generate adduct radical **1**, which undergoes bimolecular homolytic substitution (S_H2) reaction with R-XL_n to give the desired product with the regeneration of a R radical through transition state **2**.[4-6] A sufficiently fast S_H2 reaction is crucial for the success of ATRA and GTRA, because **1** also undergoes unwanted termination reactions such as homo-coupling and disproportionation reaction which usually occur at a diffusion-controlled rate.

The ATRA was discovered by Khrasch for the first time in 1945. He reported the addition of halomethanes to alkenes in the presence of radical initiators,[7,8] and this reaction is now known as the Kharasch reaction (Scheme 2). Despite of the novelty, synthetic potentials of the Kharasch reaction was rather low because the combination of haloalkanes and alkene substrates was quite limited. However, synthetic potential of the Kharasch reaction has been considerably increased after the finding of the iodine-transfer radical addition reaction by Curran in 1986.[9-14] Curran showed that

Scheme 1. (a) Atom transfer (AT) and group transfer (GT) addition reactions and (b) their mechanism

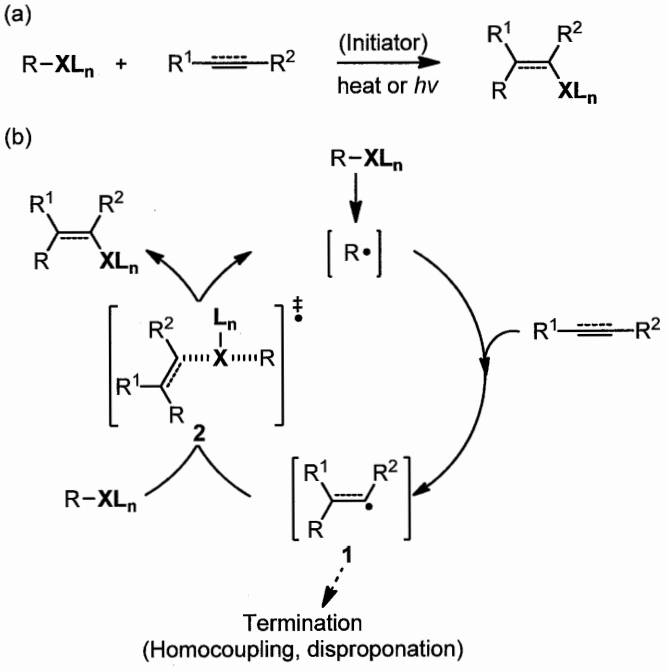

Scheme 2. Khrasch reaction.

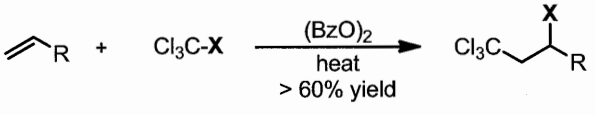

acyclic organoiodide **3** was transformed to cyclic vinyliodide **4** under radical conditions (Scheme 3). The reaction involves the generation of carbon-centered radical **5** from **3** under photoirradiation in the presence of $(Bu_3Sn)_2$. The 5-*exo-dig* intramolecular radical cyclization to alkyne followed by the iodine-transfer from **3** to give **4**.[13] Curran also demonstrated that this type of reaction could be extended to intermolecular addition reaction. The ATRA and GTRA are synthetically more valuable than the similar transformation under reductive conditions, such as tinhydride-mediated addition reaction of organohalogen and chalcogens to alkenes and alkynes, because heteroatom functionality is retained in the products which can be used to further synthetic transformations. Phenylselenyl-group[15-17] and phenyltellanyl-group transfer[18-25] radical addition reactions of organoselenides, organotellurides, respectively, have been subsequently reported.

Scheme 3. Iodine atom transfer radical addition reaction.

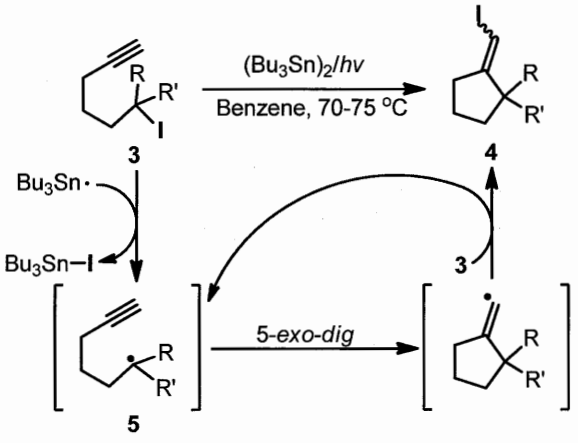

The S_H2 reaction is usually reversible. However, the equilibrium shifted to the product side forming **4** in the reaction shown in Scheme 3 because of the formation of thermodynamically more stable product possessing sp^2-carbon iodine bond from **3** having less stable sp^3-carbon iodine bond. In contrast, if an alkene was used as an acceptor instead of an alkyne, the carbon-heteroatom bond in the product should be similar stability to that in the substrate. Consequently, the product would regenerate a carbon-centered radical under the reaction condition, which then reacts with an alkene in ATRA or GTRA manner to give the doubly inserted product. If the iteration of this sequence successfully occurs, a polymerization having heteroatom substituent at the polymer end with controlled molecular weight distribution will form. Such polymerization, so called controlled/living radical polymerization (LRP), is of ever-increasing importance in polymer chemistry both in the academic and the industrial areas due to the potentials to create novel functional polymeric materials with new or improved properties.[26-29]

Our group has already found in 2002 that several organotellurium compounds having methyltellanyl group serve as efficient chain transfer agents for LRP, and demonstrated that this organo*te*llurium-mediated living *r*adical *p*olymerization (TERP) is a powerful method for the synthesis of structurally well-defined homopolymers and block copolymers .[30,31] For example, when styrene is heated in the presence of organotellurium compound **6a**, polystyrene with predetermined number average molecular weight (M_n) from styrene/**6a** ratio with narrow molecular weight distribution (MWD) formed (Scheme 4). Furthermore, our group has also developed in 2004 that organostibines **6b** bearing dimethylstibanyl group also serve as chain transfer agents for highly controlled LRP.[32] This organo*sti*b*i*ne-mediated living *r*adical *p*olymerization (SBRP) showed higher control of MWD than TERP. The characteristic features of these methods are high versatility in

polymerizing varieties of monomers under mild condition without catalyst.[33-35]

Scheme 4. Organoheteroatom-mediated living radical polymerization.

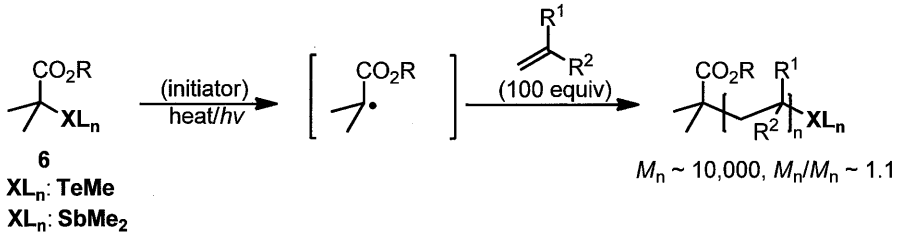

6
a: **XL_n**: **TeMe**
b: **XL_n**: **$SbMe_2$**

On the other hand, organoiodine compounds have been also used for the LRP (IRP), but the level of control in molecular weight and MWD is usually modest.[36-38] A binary system consisting from organobromides or chlorides and transition metal catalysts, such as ruthenium and copper complexes also promote LRP of varieties of conjugated monomers. This method so called transition metal catalyzed LRP or atom transfer radical polymerization (ATRP) involves redox reaction between the organohalogen compounds and metal species, and the polymerization proceeds different mechanism from the one shown in Scheme 1b.[39-44]

The rate of S_H2 reaction of group 16 and 17 heteroatom compounds with an alkyl radical has been systematically determined thorough kinetic experiments by Newcomb and Curran (Table 1).[45-49] The rate constant increases 10 and 100 times in going from the compounds having third row elements (XL_n = Cl, SPh, entries 1 and 5) to those having the fourth row elements (XL_n = Br, SePh, entries 2, 3, and 6-8) and further to those having fifth row elements (XL_n = I, TePh, entries 4, 9, and 10) in the periodic table of the elements when the leaving substituent R is same. On the other hand, the results also reveal that the reactivity of the heteroatom compounds with the same row are virtually same. Although Kambe and Sonoda reported that phenyltellanyl group transfer reaction with vinyl radical takes place about 10 times faster than iodine atom transfer reaction does by competition experiments, this fact had not received appropriate attentions.[18,50,51] Consequently, organohalogen compounds, particularly organobromine and iodine compounds, had been widely used as radical precursors.

Table 1. Rate constants of the S_H2 reaction of organohalogen and organochalcogen compounds towards alkyl radical.

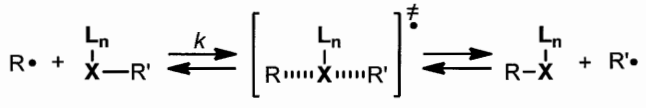

Entry	L_nX-R	R•	Temperature (°C)	k (M^{-1} S^{-1})
1	**PhS**-$C(CH_3)(CN)_2$	*n*-Octyl	50	5.0×10^{5} [c]
2	**PhSe**-CH_2CO_2Et	*n*-Octyl	50	1.0×10^{5} [c]
3	**PhSe**-$C(CH_3)(CO_2Et)_2$	*n*-Octyl	50	8.0×10^{5} [c]
4	**PhTe**-CH_2CO_2Et	*n*-Octyl	50	2.3×10^{7} [c]
5	**Cl**-$C(CH_3)_3$	*n*-Octyl	50	6.0×10^{2} [d]
6	**Br**-$C(CH_3)(CO_2Et)_2$	*n*-Octyl	50	1.0×10^{6} [c]
7	**Br**-$C(CH_3)_3$	*n*-Octyl	50	5.0×10^{3} [d]
8	**Br**-$CH_2CO_2Et_2$	*n*-Octyl	50	0.7×10^{5} [c]
9	**I**-$C(CH_3)_3$	*n*-Octyl	50	3.0×10^{6} [d]
10	**I**-$CH_2CO_2Et_2$	*n*-Octyl	50	2.6×10^{7} [c]
11	**Me_2Sb**-PSt[a]	PSt[b]	60	1.1×10^{4} [e]
12	**MeTe**-PSt[a]	PSt[b]	60	5.7×10^{3} [f]
13	**I**-PSt[a]	PSt[b]	60	1.2×10^{3} [g]

[a]Polystyrene macro chain transfer agent bearing heteroatom group at the polymer end was used. [b]Polystyryl radical. [c]The values were taken from ref. 49. [d]The values were taken from ref. 45. [e]The values were taken from ref. 32 and 52. [f]The values were taken from ref. 53. [g]The values were taken from ref. 54.

Recently, our group has shown that the S_H2 reaction of methyltellanyl-substituted polystyrene (PSt-TeMe)[52] with polystyryl (PSt) radical takes place ca. 5 times faster than that of iodine-substituted polystyrene (PSt-I)[53] with PSt radical (entries 12 *vs* 13). Our group further clarified that the S_H2 reaction of dimethylstibanyl-substituted polystyrene (PSt-$SbMe_2$) with PSt radical takes place ca. 10 times faster than that PSt-I (entries 11 *vs* 13).[32,52] These result strongly indicates the reactivity differences among the heteroatom compounds in the same row.

The organoheteroatom-mediated LRP predominately proceed through the S_H2 reaction, namely the degenerative transfer mechanism (Scheme 5), and higher MWD control is expected when the S_H2 reaction proceeds faster.[55] Therefore, the kinetic data are consistent with the observation in MWD control in using these heteroatom compounds; SBRP usually shows higher control than TERP, and TERP also exhibits higher control than organo*i*odine-mediated *r*adical

*p*olymerization (IRP). These results suggest that if one can attain higher reactivity of the S_H2 reaction, higher control of LRP would be possible.

Scheme 5. Degenerative chain transfer mechanism of organoheteroatom-mediated LRP.

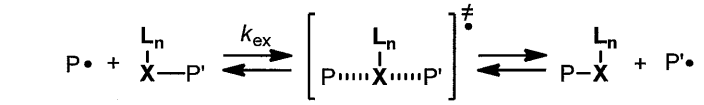

Diheteroatom compounds (X-X) possessing heteroatom-heteroatom σ bond take place S_H2 reaction with carbon-centered radicals giving corresponding organoheteroatom compounds. Indeed, diphosphines,[56-58] disulfides,[59,60] diselenides,[61-65] ditellurides,[66-68] and iodine[38,69] have been already demonstrated to be excellent precursors for organophosphines, sulfides, seleneides, tellurides, and iodides. Our group has recently found a new synthetic route to organostibine chain transfer **7** agents by trapping of a radical generated from azo-initiators with tetramehyldistibine (Scheme 6). Since the coupling reactions take place under neutral conditions, **7** bearing various polar functional groups were successfully synthesized.[70] Furthermore, **7** allowed to access α-functional living polymers with highly controlled and defined structure. The reaction of dimethylditelluride and diphenylditelluride with AIBN was also examined by our group. While the reaction gave the desired organotellurium chain transfer agents, the yields were low (ca. 15%).[71] The reaction of molecular iodine with azo-compound has been recently used for the in situ synthesis of organoiodine chain transfer agent.[72]

Scheme 6. Reaction of tetramethyldistibine with azo-compounds.

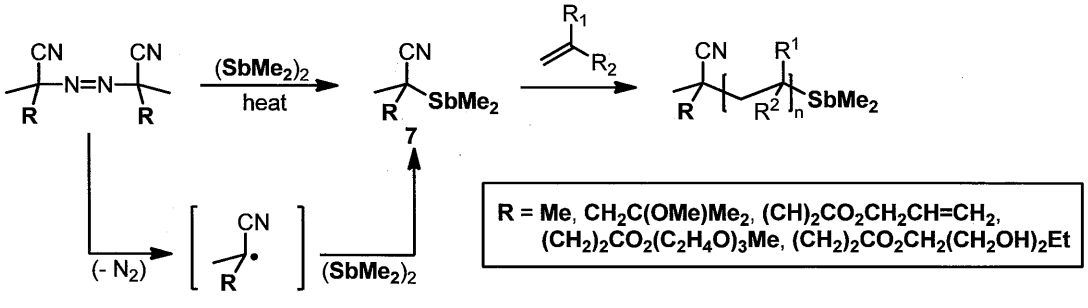

Furthermore, diheteroatom compounds possessing σ bond between different heteroatom have recently been utilized for the synthesis of organoheteroatom compounds under radical conditions. Barton and coworkers reported that an alkyl radical generated from a Barton ester reacted with

tris(triphenylthio)stibine to give organostibine adduct **8**, which was oxidized to give an alcohol (Scheme 7a).[73] Due to the mild reaction conditions, this method was applied to the key step in the synthesis of (+)-cyclophellitol (Scheme 7b).[74]

Scheme 7. Reaction of tris(triphenylthio)stibine with Barton ester.

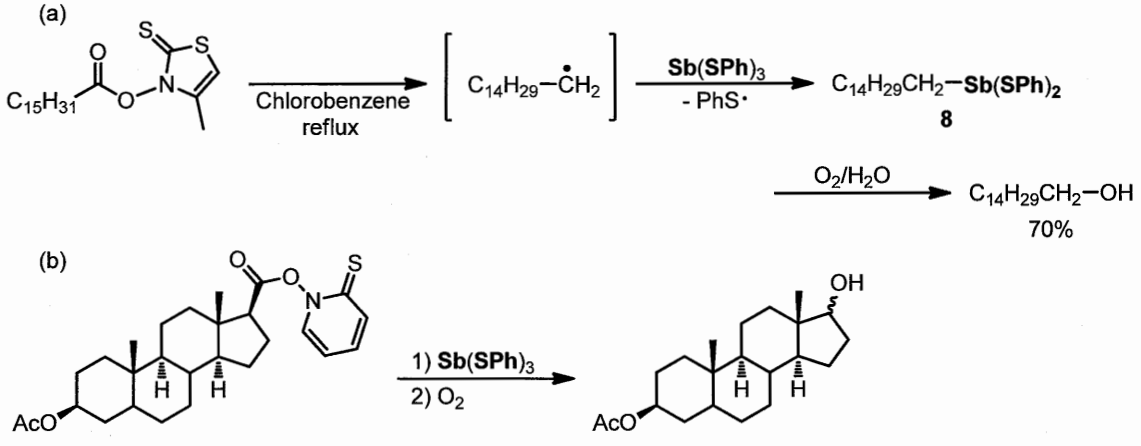

Armido et al. recently reported a highly efficient radical phosphonation of alkyl and aryl radicals with Me_3SnPPh_2 or Me_3SiPPh_2.[75] The reaction proceeds through the radical chain reaction, in which the generated carbon-centered radical undergoes the S_H2 reaction at phosphorus atom of Me_3SnPPh_2 or Me_3SiPPh_2 to give the phosphines **9** and regenerate Me_3Sn or Me_3Si radicals (Scheme 8).

Scheme 8. Radical phosphonation using Sn-P and Si-P compounds

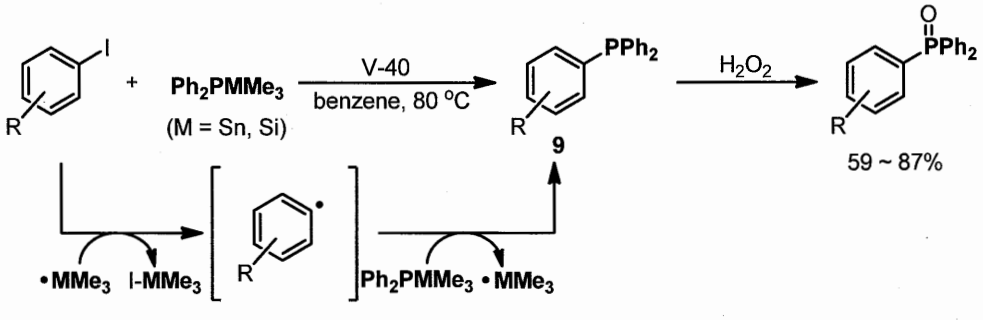

Diheteroatom compounds have also been utilized to increase the efficiency of ATRA and GTRA reactions and the control of LRP. Yang et al. recently reported a remarkable increase in the the efficiency of phenylselenyl-GT radical cyclization reaction was observed by the addition of diphenyldiselenide.[76] The initially generated carbon-centered radical **10** undergoes the 5-*exo-trig*

intramolecular radical cyclization to alkene to lead to the cyclized alkyl radical **11**, which further undergoes the S_H2 reaction with diphenyldiselenide to give organoselenide **12**. Oxidation of **12** by H_2O_2 gave alkene product (Scheme 9).

Scheme 9. Addition Effect of diheteroatom compounds in GTRA.

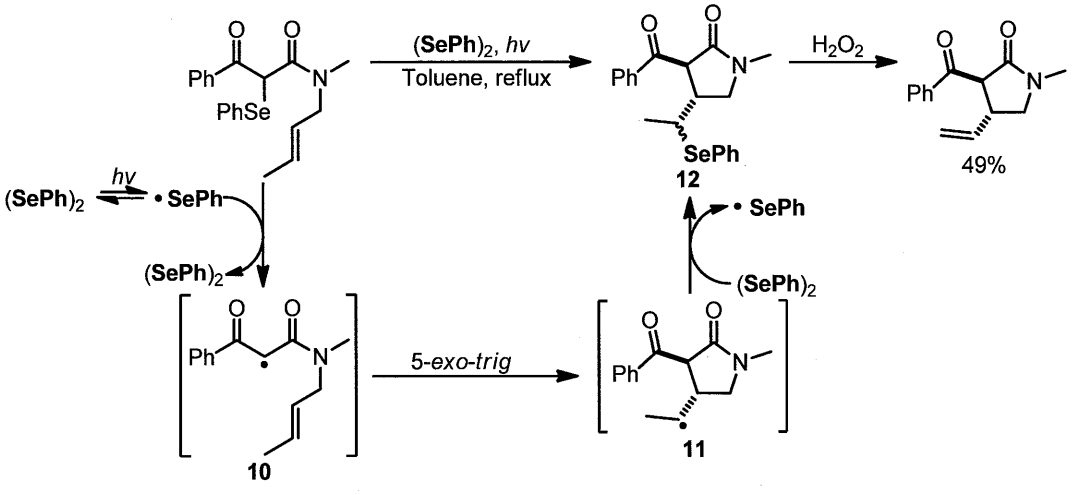

Furthermore, our group reported that the addition of ditelluride in TERP of styrene and methyl methacrylate (MMA) considerably increased the MWD control (Table 2, entries 1 *vs.* 2).[31] The same effect on the increase of MWD control was also observed in SBRP of styrene and MMA by the addition of distibine (entries 3 and 4)[70] and transition metal catalyzed polymerization of methyl acrylate using iron catalyst by the addition of iodine (entries 5 and 6).[77]

Table 2. Addition Effect of diheteroatom compounds in organoheteroatom-mediated LRP.

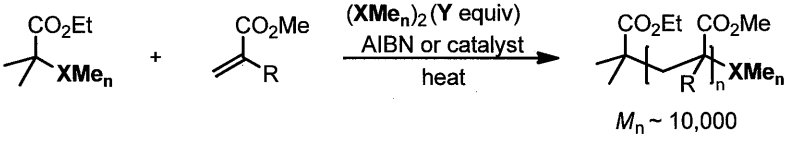

Entry	XMe_n	R	Y (equiv)	M_w/M_n
1	**TeMe**	Me	0	1.38
2	**TeMe**	Me	1	1.15
3	**$SbMe_2$**	Me	0	1.24
4	**$SbMe_2$**	Me	0.1	1.05
5	**I**	H	0	1.90
6	**I**	H	0.5	1.28

The reactivity of group 16 diheteroatom compounds toward 5-hexenyl radical has been already examined thorough kinetic experiments by Russel and coworkers (Table 3).[49,78,79] The reactivity becomes higher when the elements become heavier, and the rate constants of the S_H2 reaction with diphenyl diselenide and diphenyl ditelluride are about 150 and 650 times higher than that of dimethyl disulfide (entries 4-5 *vs.* 3).[78] Considering such high reactivity of ditellurides, we were rather surprised for the low yields observed in the synthesis of organotellurium chain transfer agents from azo initiators and ditellurides.

Our group has recently shown that the S_H2 reaction of PSt and PMMA radicals with dimethyl ditelluride takes place about 100 and 60 times higher than that of PSt and PMMA radicals with PSt-TeMe and PMMA-TeMe, respectively (entries 6 and 7).[80] This increased capping reaction of the polymer-end radical is responsible for the observed increased MWD control by the addition of ditelluride. The results also suggest that the higher control of LRP would be possible by employing appropriate diheteroatom compounds.

Table 3. Rate constants of the S_H2 reaction of organohalogen and organochalcogen compounds towards alkyl radical.

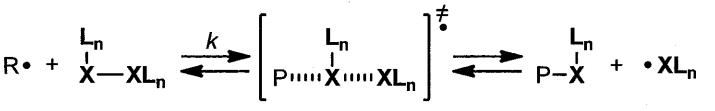

Entry	L_nX-XL_n	R•	Temperature (°C)	k (M^{-1} S^{-1})
1	**MeS-SMe**	*n*-Undecyl	25	6.0×10^{4} [c]
2	**PhS-SPh**	*n*-Undecyl	25	2.0×10^{5} [c]
3	**PhS-SPh**	5-Hexenyl	~45	1.7×10^{5} [d]
4	**PhSe-SePh**	5-Hexenyl	~45	2.6×10^{7} [d]
5	**PhTe-TePh**	5-Hexenyl	~45	1.1×10^{8} [d]
6	**MeTe-TeMe**	PSt[a]	60	5.1×10^{5} [e]
7	**MeTe-TeMe**	PMMA[b]	60	1.8×10^{5} [e]

[a]Polystyryl radical. [b]PolyMMA radical. [c]The values were taken from ref. 78,79. [e]The values were taken from ref. 80.

Outline of This Thesis

While significant progress in the AT and GT radical reaction has been achieved recently for the precise control of polymer structure by LRP using organoheteroatom compound, the development of a more powerful method than the currently available methods is still needed to

create new polymeric materials with increased or new properties. Furthermore, in addition to the control of molecular weigh and MWD, new methods to control polymer-end structure are also needed. Moreover, understanding of the reactivity of heteroatom and diheteroatom compounds under radical or non-radical condition is needed in order to further enhance the ability of macromolecular engineering.

This thesis entitled in "**Studies on the Precision Control of Polymer Structure Based on Heteroatom-Mediated Living Radical Polymerization Reaction**" consists of seven chapters and devotes to the development of new methods to control macromolecular structrure based on heteroatom-mediated LRP.

Chapter 1 describes the optimization of untransferable substituent *L* on tellurium atom to achieve higher control in TERP (Scheme 10). Several new organotellurium compounds possessing alkyl, aryl or heteroaryl groups as *L* were synthesized, and the effect of the substituents in S_H2 reactions was clarified through polymerization reaction and kinetic study. Aryltellanyl-substituted organotellurium compounds showed higher reactivity to the S_H2 reaction and proved to be better chain transfer agents for TERP than alkyl-substituted derivatieves.

Scheme 10. Substituent effects in radical-mediated organotellanyl group transfer reactions

Rate of *k*: ***L* = Aryl > Alkyl**
Controllability of MWD: ***L* = Aryl > Alkyl**

Chapter 2 focuses on the substituent effect on the antimony atom in SBRP (Scheme 11a). 2-Methyl-2-diphenylstibanylpropionitrile **13a** was synthesized and the ability to control SBRP and S_H2 reaction was compared with the dimethylstibanyl analogue **13b** which has been used for SBRP so far. While **13a** successfully polymerized acrylates in a highly controlled manner, the controllability was slightly decreased for styrene polymerization. Furthermore, polymerization of methacrylates could not be controlled at all. The results were in sharp contrast that **13b** is efficient chain transfer agents for acrylates, methacrylates, and styrenes. The effect of the substituents were clarified thorough kinetic studies and chain extension experiments (Scheme 11b).

Scheme 11. Substituent effects in radical-mediated organotellanyl group transfer reactions

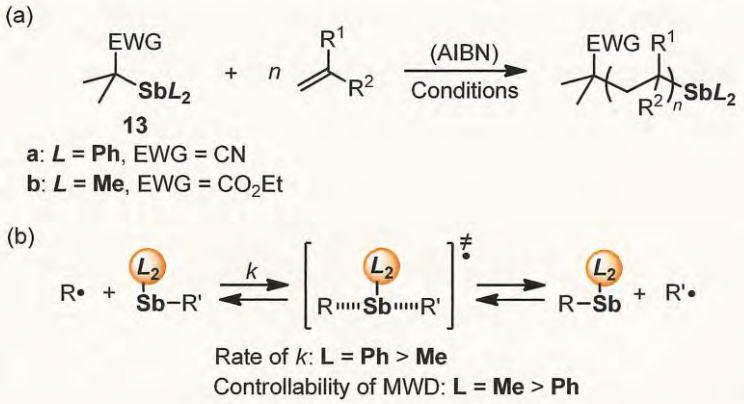

Chapter 3 describes the development of bismuth-based new chain transfer agents for LRP. While synthetic radical chemistry of organobismuth compounds were not known, newly synthesized organobismuthines severed as excellent precursors for carbon-centered radicals and promoted highly controlled LRP (Scheme 12a). The organo*bis*muthine-mediated living *r*adical *p*olymerization (BIRP) showed excellent control for the polymerization of both conjugated and unconjugated vinyl monomers. BIRP was also effective for the synthesis of block copolymers. The mechanism as well as the origin of high controllability in BIRP was clarified by kinetic studies (Scheme 12b).

Scheme 12. Organo*bis*muthine-mediated living *r*adical *p*olymerization (BIRP).

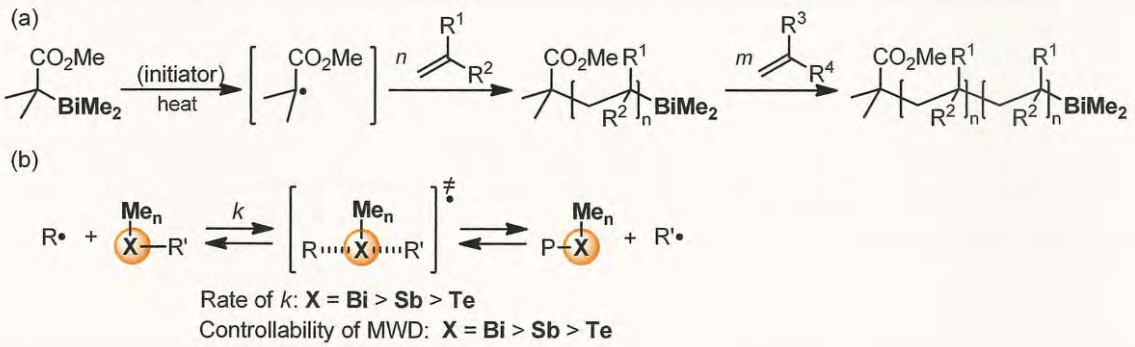

Chapter 4 describes the development of an arylthiobismuthine cocatalyst for BIRP (Scheme 13). Organobismuthine bearing the sterically bulky aryl group on the sulfur atom was designed and synthesized for the first time. BIRP in the presence of the thiobismuthine cocatalyst showed higher control of MWD than that in the absence of the cocatalyst. The binary system could be applied for the synthesis of high molecular weight polystyrenes ($M_n \sim 2 \times 10^5$) and ultra-high molecular weight

poly(butyl acrylate)s ($M_n \sim 3 \times 10^6$) with controlled macromolecular structure ($M_w/M_n \sim 1.06$-1.43). The mechanism of action of the cocatalyst during the polymerization reaction was clarified by several control experiments.

Scheme 13. Development of cocatalyst in BIRP.

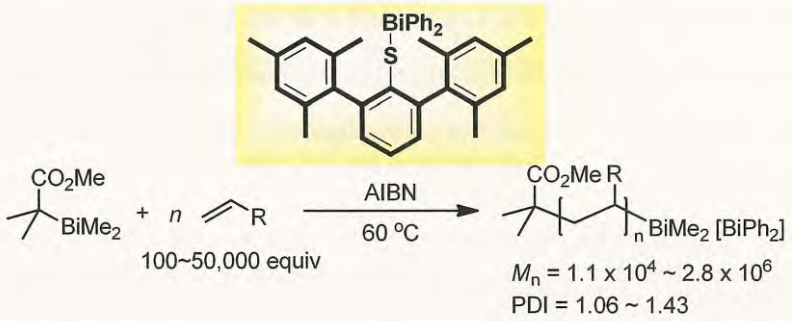

Chapter 5 describes the synthesis of ω-vinylidene functionalized polymethacrylate by selective transformation of the heteroatom polymer-end group. Treatment of polymethacrylates bearing organotellanyl, organostibanyl, and organobismuthanyl ω-polymer end groups with 2,2,6,6-tetramethylpiperidine 1-oxyl (TEMPO) under thermal or photochemical conditions quantitatively gave ω-vinylidene polymethacrylates (Scheme 14). The effect of the end group structure on the thermal stability of poly(methyl methacrylate) was also examined.

Scheme 14. Synthesis of ω- vinylidene functionalized polymethacrylates

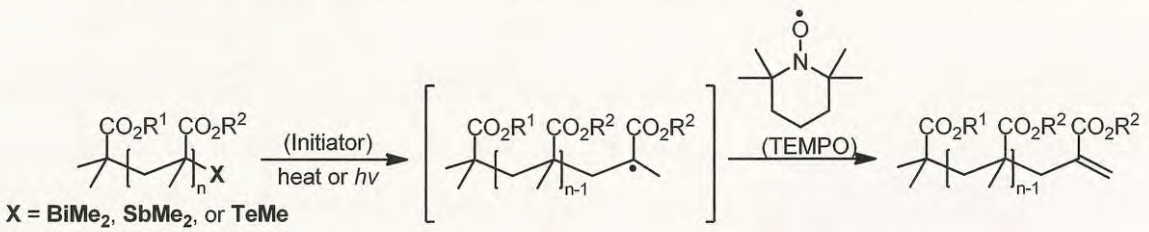

Chapter 6 describes generation of carboanions from organostibines and bismuthines via stibine-metal and bismuth-metal exchange reaction. The heteroatom species were selectively and quantitatively transformed by treatment of several organometallic reagents, such as alkyl lithiums, tetraalkylzinc dilithiums, and alkylmagnesium halides. The exchange reaction was compatible with various polar functional groups and applicable for the polymer-end organostibine and bismuthine species. The subsequent reaction with various electrophiles gave structurally well-defined ω-end functionalized polymer (Scheme 15). Reactivities of heteroatom groups were examined by

competition experiments.

Scheme 15. Synthesis of ω-end functionalized polymer via stibine-metal and bismuthine-methal exchange reaction

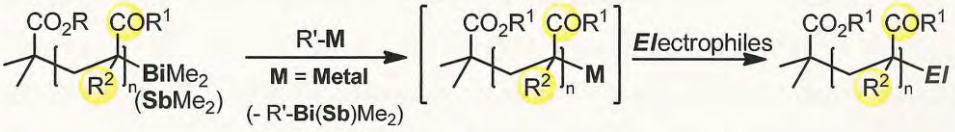

Chapter 7 describes the theoretical study on the S_H2 reaction of dichalcogenides with carbon-centered radical (Scheme 16). The density functional theory (DFT) calculation suggests that the kinetic reactivity becomes higher when the heteroatom compounds become heavier, and the results are good agreement with the experimental data. On the other hand, the thermodynamic stability of the products is higher in the reaction of lighter heteroatom compounds. Thus, both kinetic reactivity and thermodynamic stability must be considered to design efficient cocatalyst for LRP. The energy decomposition and molecular orbital analyses were carried out to clarify the origin of the reactivity difference of each chalcogen atoms.

Scheme 16. Homolytic substitution reaction of dichalcogenides with carbon-centered radical.

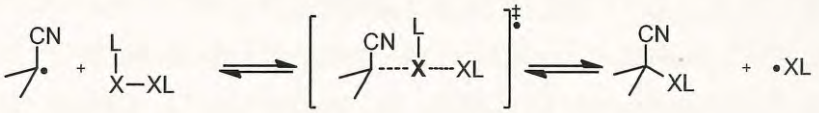

References

(1) Curran, D. P. In *Comprehensive Organic Synthesis*; Trost, B. M., Fleming, I., Eds.; Pergamon: Oxford, 1991; Vol. 4, p 745-831.

(2) *Radicals in Organic Synthesis*; Renaud, P.; Sibi, M., Eds.; Wiley-VCH: Weinheim, Germany, 2001.

(3) Zard, S. Z. *Radical Reaction in Organic Synthesis*; Oxford University Press: New York, 2003.

(4) Schiesser, C. H.; Smart, B. A.; Tran, T.-A. *Tetrahedron* **1995**, *51*, 3327-3338.

(5) Schiesser, C. H.; Smart, B. A. *Tetrahedron* **1995**, *51*, 6051-6060.

(6) Schiesser, C. H.; Wild, L. M. *Tetrahedron* **1996**, *52*, 13265-13314.

(7) Kharash, M. S.; Jensen, E. V.; Urry, W. H. *Science* **1945**, *102*, 128-130.

(8) Kharasch, M. S.; Urry, W. H.; Jensen, E. V. *J. Am. Chem. Soc.* **1945**, *67*, 1626-1626.

(9) *Radical Addition Reaction*; Curran, D. P., Ed.; Pergamo Press: Oxford, U.K., 1991; Vol. 4.

(10) Curran, D. P.; Chen, M. H.; Kim, D. *J. Am. Chem. Soc.* **1986**, *108*, 2489-2490.

(11) Curran, D. P.; Chen, M. H. *J. Am. Chem. Soc.* **1987**, *109*, 6558-6560.

(12) Curran, D. P.; Chen, M. H.; Kim, D. *J. Am. Chem. Soc.* **1989**, *111*, 6265-6276.

(13) Curran, D. P.; Chen, M. H.; Spletzer, E.; Seong, C. M.; Chang, C. T. *J. Am. Chem. Soc.* **1989**, *111*, 8872-8878.

(14) Curran, D. P. *Aldrichimica Acta* **2000**, *33*, 104-110.

(15) Byers, J. H.; Harper, B. C. *Tetrahedron. Lett.* **1992**, *33*, 6953-6954.

(16) Curran, D. P.; Thoma, G. *J. Am. Chem. Soc.* **1992**, *114*, 4436-4437.

(17) Curran, D. P.; Eichenberger, E.; Collis, M.; Roepel, M. G.; Thoma, G. *J. Am. Chem. Soc.* **1994**, *116*, 4279-4288.

(18) Han, L. B.; Ishihara, K.; Kambe, N.; Ogawa, A.; Ryu, I.; Sonoda, N. *J. Am. Chem. Soc.* **1992**, *114*, 7591-7592.

(19) Han, L.-B.; Ishihara, K.-I.; Kambe, N.; Ogawa, A.; Sonoda, N. *Phosphorus, Sulfur Silicon Relat. Elem.* **1992**, *67*, 243 - 246.

(20) Chen, C.; Crich, D.; Papadatos, A. *J. Am. Chem. Soc.* **1992**, *114*, 8313-8314.

(21) Crich, D.; Chen, C.; Hwang, J.-T.; Yuan, H.; Papadatos, A.; Walter, R. I. *J. Am. Chem. Soc.* **1994**, *116*, 8937-8951.

(22) Engman, L.; Gupta, V. *J. Chem. Soc. Chem. Commun.* **1995**, 2515-2516.

(23) Engman, L.; Gupta, V. *J. Org. Chem.* **1997**, *62*, 157-173.

(24) Lucas, M. A.; Schiesser, C. H. *J. Org. Chem.* **1996**, *61*, 5754-5761.

(25) Lucas, M. A.; Schiesser, C. H. *J. Org. Chem.* **1998**, *63*, 3032-3036.

(26) *Handbook of Radical Polymerization*; Matyjaszewski, K.; Davis, T. P., Eds.; Wiley-Interscience: New York, 2002.

(27) Moad, G.; Solomon, D. H. *The Chemistry of Radical Polymerization*; Elsevier: Amsterdam, 2006.

(28) Braunecker, W. A.; Matyjaszewski, K. *Prog. Polym. Sci.* **2007**, *32*, 93-146.

(29) Destarac, M. *Macromol. React. Eng.* **2010**, *4*, 165-179.

(30) Yamago, S.; Iida, K.; Yoshida, J. *J. Am. Chem. Soc.* **2002**, *124*, 2874-2875.

(31) Yamago, S.; Iida, K.; Yoshida, J. *J. Am. Chem. Soc.* **2002**, *124*, 13666-13667.

(32) Yamago, S.; Ray, B.; Iida, K.; Yoshida, J.; Tada, T.; Yoshizawa, K.; Kwak, Y.; Goto, A.; Fukuda, T. *J. Am. Chem. Soc.* **2004**, *126*, 13908-13909.

(33) Yamago, S. *Proc. Jpn. Acad., Ser. B* **2005**, *81*, 117-128.

(34) Yamago, S. *J. Polym. Sci. Part A: Polym. Chem.* **2006**, *44*, 1-12.

(35) Yamago, S. *Chem. Rev.* **2009**, *109*, 5051-5068.

(36) Oka, M.; Tatemoto, M. *Contemporary Topics in Polymer Science*; Plenum: New York, 1984.

(37) Matyjaszewski, K.; Gaynor, S.; Wang, J.-S. *Macromolecules* **1995**, *28*, 2093-2095.

(38) David, G.; Boyer, C.; Tonnar, J.; Ameduri, B.; Lacroix-Desmazes, P.; Boutevin, B. *Chem. Rev.* **2006**, *106*, 3936-3962.

(39) Matyjaszewski, K.; Xia, J. *Chem. Rev.* **2001**, *101*, 2921-2990.

(40) Kamigaito, M.; Ando, T.; Sawamoto, M. *Chem. Rev.* **2001**, *101*, 3689-3746.

(41) Ouchi, M.; Terashima, T.; Sawamoto, M. *Acc. Chem. Res.* **2008**, *41*, 1120-1132.

(42) Matyjaszewski, K.; Tsarevsky, N. V. *Nature Chem.* **2009**, *1*, 276-288.

(43) Ouchi, M.; Terashima, T.; Sawamoto, M. *Chem. Rev.* **2009**, *109*, 4963-5050.

(44) Rosen, B. M.; Percec, V. *Chem. Rev.* **2009**, *109*, 5069-5119.

(45) Newcomb, M.; Sanchez, R. M.; Kaplan, J. *J. Am. Chem. Soc.* **1987**, *109*, 1195-1199.

(46) Newcomb, M.; Kaplan, J. *Tetrahedron. Lett.* **1988**, *29*, 3449-3450.

(47) Curran, D. P.; Bosch, E.; Kaplan, J.; Newcomb, M. *J. Org. Chem.* **1989**, *54*, 1826-1831.

(48) Newcomb, M. *Acta Chem. Scand.* **1990**, *44*, 299-310.

(49) Curran, D. P.; Martin-Esker, A. A.; Ko, S. B.; Newcomb, M. *J. Org. Chem.* **1993**, *58*, 4691-4695.

(50) Kim, S.; Song, H. J.; Choi, T. L.; Yoon, J. Y. *Angew. Chem. Int. Ed.* **2001**, *40*, 2524-2526.

(51) Kim, S.; Song, H.-J. *Synlett* **2002**, 2110,2112.

(52) Kwak, Y.; Goto, A.; Fukuda, T.; Yamago, S.; Ray, B. *Z. Phys. Chem.* **2005**, *219*, 283-293.

(53) Goto, A.; Kwak, Y.; Fukuda, T.; Yamago, S.; Iida, K.; Nakajima, M.; Yoshida, J. *J. Am. Chem. Soc.* **2003**, *125*, 8720-8721.

(54) Goto, A.; Ohno, K.; Fukuda, T. *Macromolecules* **1998**, *31*, 2809-2814.

(55) Goto, A.; Fukuda, T. *Prog. Polym. Sci.* **2004**, *29*, 329-385.

(56) Okazaki, R.; Hirabayashi, Y.; Tamura, K.; Inamoto, N. *J. Chem. Soc., Perkin Trans. 1* **1976**, 1034-1036.

(57) Akinori, S.; Hideki, Y.; Koichiro, O. *Angew. Chem. Int. Ed.* **2005**, *44*, 1694-1696.

(58) Cossairt, B. M.; Cummins, C. C. *New J. Chem.* **2010**, *34*, 1692-1699.

(59) Heiba, E.-A. I.; Dessau, R. M. *J. Org. Chem.* **1967**, *32*, 3837-3840.

(60) Benati, L.; Montevecchi, P. C.; Spagnolo, P. *J. Chem. Soc., Perkin Trans. 1* **1991**, 2103-2109.

(61) Perkins, M. J.; Turner, E. S. *J. Chem. Soc., Chem. Commun.* **1981**, 139-140.

(62) Back, T. G.; Krishna, M. V. *J. Org. Chem.* **1988**, *53*, 2533-2536.

(63) Ogawa, A.; Yokoyama, H.; Yokoyama, K.; Masawaki, T.; Kambe, N.; Sonoda, N. *J. Org. Chem.* **1991**, *56*, 5721-5723.

(64) Renaud, P. *Top. Curr. Chem.* **2000**, *208*, 81-112.

(65) Tsuchii, K.; Doi, M.; Hirao, T.; Ogawa, A. *Angew. Chem. Int. Ed.* **2003**, *42*, 3490-3493.

(66) Ogawa, A.; Yokoyama, K.; Yokoyama, H.; Obayashi, R.; Kambe, N.; Sonoda, N. *J. Chem. Soc., Chem. Commun.* **1991**, 1748-1750.

(67) Ogawa, A.; Yokoyama, K.; Obayashi, R.; Han, L.-B.; Kambe, N.; Sonoda, N. *Tetrahedron* **1993**, *49*, 1177-1188.

(68) Takagi, K.; Soyano, A.; Kwon, T. S.; Kunisada, H.; Yuki, Y. *Polymer Bulletin* **1999**, *43*, 143-150.

(69) Balczewski, P.; Mikolajczyk, M. *New. J. Chem.* **2001**, *25*, 659-663.

(70) Yamago, S.; Yamada, T.; Togai, M.; Ukai, Y.; Kayahara, E.; Pan, N. *Chem. Eur. J.* **2009**, *15*, 1018-1029.

(71) Yamago, S.; Iida, K.; Nakajima, M.; Yoshida, J. *Macromolecules* **2003**, *36*, 3793-3796.

(72) Goto, A.; Hirai, N.; Nagasawa, K.; Tsujii, Y.; Fukuda, T.; Kaji, H. *Macromolecules* **2010**, *43*, 7971-7978.

(73) Barton, D. H. R.; Bridon, D.; Zard, S. Z. *J. Chem. Soc. Chem. Commun.* **1985**, 1066-1068.

(74) Ziegler, F. E.; Wang, Y. *J. Org. Chem.* **1998**, *63*, 7920-7930.

(75) Santiago, E. V.; Christian, M. k.-L.; Stefan, G.; Armido, S. *Angew. Chem. Int. Ed.* **2007**, *46*, 6533-6536.

(76) Yang, D.; Lian, G.-Y.; Yang, H.-F.; Yu, J.-D.; Zhang, D.-W.; Gao, X. *J. Org. Chem.* **2009**, *74*, 8610-8615.

(77) Kamigaito, M.; Onishi, I.; Kimura, S.; Kotani, Y.; Sawamoto, M. *Chem. Comm.* **2002**, 2694-2695.

(78) Russell, G. A.; Tashtoush, H. *J. Am. Chem. Soc.* **1983**, *105*, 1398-1399.

(79) Newcomb, M. *Tetrahedron* **1993**, *49*, 1151-1176.

(80) Kwak, Y.; Tezuka, M.; Goto, A.; Fukuda, T.; Yamago, S. *Macromolecules* **2007**, *40*, 1881-1885.

Chapter 1

Optimization of Organotellurium Transfer Agents for Highly Controlled Living Radical Polymerization

Abstract

Several new organotellurium transfer agents for living radical polymerization have been developed. Transfer agents possessing aryltellanyl groups, such as phenyltellanyl, *p*-methoxyphenyltellanyl, and *p*-trifluoromethylphenyltellanyl groups, showed higher control in styrene polymerization than that bearing conventional methyltellanyl group and gave structurally well-defined polystyrenes with predetermined number-average molecular weights and narrow molecular weight distribution. Kinetic studies were carried out to clarify the substituent effects, and aryltellanyl groups underwent ca. 2~4 times faster tellanyl group transfer reaction than methyltellanyl group towards a polystyrene-end radical. As the faster group transfer reaction leads to the higher control of molecular weight distribution, this high reactivity of aryltellanyl groups is the origin of the observed high control.

Introduction

Controlled/living radical polymerization (LRP) has been recognized as one of the most efficient methods for the controlled synthesis of macromolecules possessing a variety of polar functional groups with defined monomer sequences and architechtures.[1,2] Stable free radical polymerization,[3,4] atom transfer radical polymerization,[5,6] and degenerative transfer polymerization including reversible addition-fragmentation chain transfer radical polymerization[7,8] and catalytic chain transfer polymerization[9] are the three representative processes for conducting LRP. Organo*i*odine-mediated *r*adical *p*olymerization (IRP)[10-12] is operationally simple and effective in polymerization of several vinyl monomer, though the level of control in molecular weight and its distribution is usually modest. We recently found that several organotellurium compounds shown in Chart 1 bearing methyltellanyl group serve as excellent chain transfer agents for living radical polymerization.[13-20] This organo*te*llurium-mediated living *r*adical *p*olymerization (TERP) shows high versatility in polymerizing a variety of monomers and gives living polymers with number-average molecular weights (M_ns) predicated from the monomer/transfer agent ratio and with narrow molecular weight distributions (MWDs). In addition, ease of the end group transformation giving ω-end functionalized polymers and block copolymers makes TERP as a powerful method for the synthesis of novel polymeric materials for various applications.

Chart 1. Representative structure of organotellurium chain transfer agents.

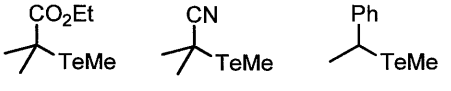

Mechanistic studies revealed that both IRP and TERP proceed mainly via a degenerative transfer mechanism, in which the polymer end radical P undergoes an iodine atom transfer (XL = I) or tellanyl group transfer (X = Te) reaction, respectively, with the corresponding dormant species P'XL to generate new radical P' and dormant species PXL (Scheme 1).[13,21] The difference between organoiodine and tellurium is, however, the rate of the iodine atom transfer (AT) and methyltellanyl group transfer (GT) reactions; the rate constant, k_{ex}, of the methyltellanyl GT reaction is ca. 5 times faster than that of the iodine AT reaction. The results are consistent with theoretical predictions that the faster exchange reaction leads to a narrow MWD for the resulting polymer.[22] The results are also consistent with the previous reports showing the reactivity of phenyltellanyl GT reaction higher than the iodine AT reaction towards vinyl radicals,[23-25] though an inverse reactivity was reported

towards alkyl radicals.[26]

Scheme 1. Degenerative transfer [atom transfer (AT) or group transfer (GT)] mechanism of organo*i*odine-mediated *r*adical *p*olymerization (IRP) and organo*te*llurium-mediated living *r*adical *p*olymerization (TERP)

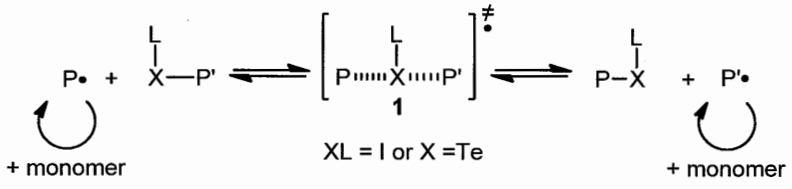

Since the organotellanyl GT reaction proceeds through transition state **1** (Scheme 1, X = Te), the untransferable substituent L would affect the rate of the GT reaction and, thus, the MWD control. Despite this, there is no report on the effect of the L group on the GT reactions. We have used exclusively a chain transfer agent (CTA) possessing methyltellanyl group (L = Me) due to their ease of preparation and purification. In this chapter, we report the first study on the effect of substituent L in organotellanyl GT reactions, which should lead to the generation of new, highly efficient transfer agents for TERP.

Result and discussions

Synthesis of organotellurium CTAs. Phenyltellanyl- (**2a**), *p*-methoxyphenyltellanyl- (**2b**), *p*-trifluoromethylphenyltellanyl- (**2c**), 2-furyltellanyl- (**2d**), and *n*-butyltellanyl- (**2e**) substituted organotellurium CTAs were prepared by a method similar to that used for the synthesis of methyltellanyl derivative **2f**[14] (Scheme 2). For example, reaction of phenyl lithium and tellurium powder generated phenyltellanyl lithium, which was treated with ethyl 2-bromoisobutyrate gave **2a** in 51% yield. Aryl lithium generated from corresponding aryl bromide and 2 equiv of *t*-butyl

Scheme 2. Synthesis of organotellurium CTAs **2**.

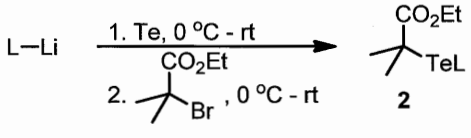

a: L = Ph (51%), **b**: L = C_6H_5OMe-*p* (78%),
c: L = $C_6H_5CF_3$-*p* (56%), **d**: L = 2-furyl (17%),
e: L = Bu-*n* (49%)

lithium was employed for the synthesis of **2b** and **2c**. 2-Furyl lithium was prepared by the deprotonation of furan and *n*-butyl lithium for the synthesis of **2d**. Commercial *n*-butyl lithium was used for the synthesis of **2e**.

Polymerization of styrene. The efficiencies of CTAs **2a~f** were examined in the bulk polymerization of styrene (100 equiv). High monomer conversion was observed in all cases after heating at 100 °C for 24 h. Polystyrenes with M_ns predetermined from the styrene/**2** ratio ($M_n \approx$ 10,000) and narrow MWD ($M_w/M_n < 1.25$) were obtained in all cases (Table 1, entries 1–6). CTAs **2a~c** showed higher MWD controls ($M_w/M_n < 1.10$) than conventional CTA **2f** (entries 1–3 vs 6), but **2d** and **2e** showed slightly lower control than **2f** (entries 4 and 5). The GPC traces of polystyrene samples by using CTAs **2c** or **2f** were shown in Figure 1. While organostibine **2g**[27] exhibit better MWD control than **2f** (entry 7), it is worth noting that **2a~c** shows higher MWD controls than **2g**.

We also examined the bulk polymerization of styrene in the presence of 2,2′-azobis(isobutyronitrile) (AIBN) (1.0 equiv) at 60 °C (entries 8–13). The polymerization reached to a high monomer conversion after heating at 60 °C, and polystyrenes with narrow MWDs were obtained in all cases (M_w/M_n = 1.17–1.33). Although the level of MWD control was slightly lower than that without AIBN, it is still acceptable. The lower control in the presence of AIBN can be attributed to an increase in the formation of dead polymers originated from the radical species derived from the azo-initiator upon its consumption.[22] Not only for the styrene polymerization, but also *n*-buthyl acrylate (100 equiv) was successfully polymerized under the controlled manner by **2a** in the presence of AIBN at 60 °C (87% conv., M_n = 13,000, M_w/M_n = 1.18).

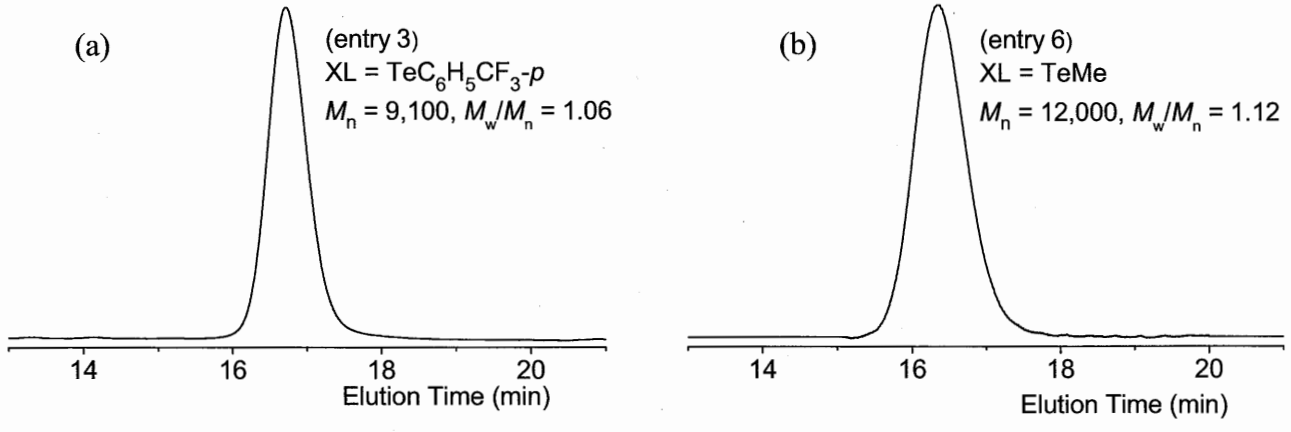

Figure 1. GPC traces of polystyrene samples obtained by using (a) CTA **2c** (entry 3) and (b) CTA **2f** (entry 6).

Table 1. Effects of heteroatom and substituent of CTA **2** in polymerization of styrene with and without 2,2′-azobis(isobutyronitrile) (AIBN).

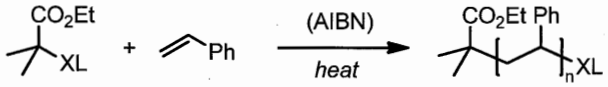

2 (100 equiv) **3**

a: XL = TePh, **b**: XL = TeC_6H_5OMe-*p*, **c**: XL = $TeC_6H_5CF_3$-*p*,
d: XL = Te-2-furyl, **e**: XL = TeBu-*n*, **f**: XL = TeMe,
g: XL = $SbMe_2$, **h**: XL = $BiMe_2$

entry	Transfer agent (XL)	AIBN (equiv)	Conv. (%)[b]	M_n (theo)[c]	M_n (exp)[d]	M_w/M_n[d]
1	**2a** (TePh)	0	99	10,300	12,200	1.08
2	**2b** (TeC_6H_5OMe-*p*)	0	90	9,400	11,400	1.09
3	**2c** ($TeC_6H_5CF_3$-*p*)	0	81	8,400	9,100	1.06
4	**2d** (Te-2-furyl)	0	88	9,200	7,800	1.23
5	**2e** (TeBu-*n*)	0	99	10,300	11,100	1.25
6	**2f** (TeMe)	0	98	10,200	12,000	1.12
7[e]	**2g** ($SbMe_2$)	0	82	8,500	7,700	1.14
8	**2a** (TePh)	1.0	100	10,400	9,500	1.24
9	**2b** (TeC_6H_5OMe-*p*)	1.0	100	10,400	12,100	1.17
10	**2c** ($TeC_6H_5CF_3$-*p*)	1.0	99	10,300	10,600	1.16
11	**2d** (Te-2-furyl)	1.0	99	10,300	10,800	1.24
12	**2e** (TeBu-*n*)	1.0	100	10,400	10,300	1.33
13	**2f** (TeMe)	1.0	100	10,400	9,700	1.22
14[e]	**2g** ($SbMe_2$)	0.5	99	10,300	8,700	1.17

[a]Bulk polymerization was carried out at 100 °C (for 24 h for entries 1–6, and for 48 h for entry 7) and 60 °C (for 11 h for entries 9–14, and for 19 h for entry 15). [b]Monomer conversion was determined by ^{1}H NMR. [c]The theoretical number-average molecular weight (M_n) was obtained as the product of monomer/**2** ratio and monomer conversion. [d]The experimental M_n and MWD (M_w/M_n) were obtained by size exclusion chromatography calibrated by polystyrene standards. [e]The values taken from ref. 27.

Kinetic study. The effects of the substituent *L* on the GT reaction were quantitatively analyzed through kinetic experiments. Polystyrene macro-CTAs **3a**~**e** (P-XL, M_n = 3,000–3,800, M_w/M_n = 1.06–1.24) were prepared from **2a**~**e** and styrene and were subjected to polymerization with a large excess of styrene (2.1–3.3 mM) and with different concentrations of AIBN at 60 °C. The time dependent consumption of the macro-CTA and the formation of the chain-elongated

polymer were analyzed by a gel permeation chromatography (GPC) method developed by Fukuda and coworkers.[28-31]

The second-order rate constant k_{ex} for the GT reaction and the first-order rate constant k_d for thermal C-TeL bond dissociation were successfully obtained for each CTA, except for the 2-furyltellanyl derivative, in which sufficient base line separation by GPC could not be obtained (Table 2). The exchange constant C_{ex} (k_{ex}/k_p), in which k_p is the propagation constant of styrene polymerization (340 M^{-1} s^{-1} at 60 °C),[32] was also calculated. The rate constant k_{ex} for the phenyltellanyl-, *p*-methoxyphenyltellanyl-, and *p*-trifluoromethylphenyltellanyl GT reactions were determined to be 9.6–15 x 10^3 M^{-1} s^{-1}, the values of which are 1.6–2.6 times faster than that of the methyltellanyl group transfer reaction (entries 1–3 vs 5). As the faster GT reaction leads to higher MWD control, the kinetic data are consistent with the observed higher MWD control using **2a~c** possessing aryl substituents than that using methyltellanyl derivative **2f**.[33] Butyltellanyl group undergoes slightly slower transfer reaction than methyltellanyl group (entry 4 vs 5), and the results are also consistent with the polymerization results. The faster aryltellanyl GT reactions can be explained by considering the stabilizing effect of the aryl group on the transition state by delocalizing the spin density on the tellurium atom. Both electron withdrawing and donating groups at the *para* position on the phenyl group slightly enhance the group transfer reactions (entries 2 and 3 vs 1), suggesting that the transition state possesses weak ambiphilic character. Despite of significant effect of L on the MWD control, its effect on the transition state and its structure would be rather small because the difference of k_{ex} value is within three times. Therefore, the organotellanyl GT reaction should take place nearly a concerted manner without formation of any meaningful intermediate in all cases.[15,34]

We have already reported that dimethylstibanyl GT reaction takes place much faster than methyltellanyl GT reaction (entry 6).[27,35] However, the current results reveal that the aryltellanyl group transfer reactions takes place similar rate to or even faster than dimethylstibanyl one. The results clearly indicate that both heteroatom and untransferable substituents affect the group transfer reactions and thus, the control over the molecular weight distribution in living radical polymerization. The rate of phenyltellanyl group transfer reaction is 8 times faster than that of the iodine atom transfer reaction (entry 1 vs 8), and the results are virtually identical to the previous report involving a vinyl radical.[12] Therefore, the current work also confirms the higher reactivity of the organotellanyl group than that of the iodine atom towards carbon-centered radicals.

Table 2. Kinetic parameters for the activation of polystyrene heteroatom transfer agents **3** (P-XL) in styrene polymerization at 60 °C[a]

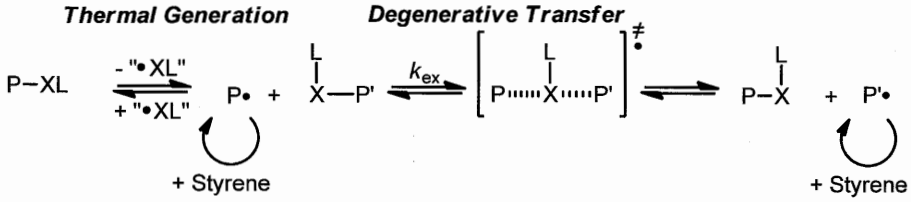

Entry	XL	k_{ex} (x 10^3 M^{-1} s^{-1})	C_{ex}	k_d (x 10^{-5} s^{-1})
1	TePh	9.6	28	1.0
2	TeC_6H_5OMe-*p*	12	35	4.4
3	$TeC_6H_5CF_3$-*p*	15	44	0.5
4	TeBu-*n*	3.5	10	1.2
5[b]	TeMe	5.8	17	1.2 [15][c]
6[d]	$SbMe_2$	11	32	~0
7[e]	I	1.2	3.5	~0

[a]The XL denotes heteroatom and its untransferable substituent. The k_d, k_{ex} and k_p are the rate constants of thermal dissociation of C-X bond, degenerative transfer reaction, and propagation reaction respectively, and the C_{ex} is the exchange constant (= k_{ex}/k_p), where the k_p value of styrene polymerization (340 M^{-1} s^{-1} at 60 °C) was taken from ref 32. [b]The values taken from ref. 13. [c]Data obtained at 100 °C. [d]The values taken from ref. 27. [e]The values taken from ref. 21.

The rate constants k_d for the thermal dissociation in the polystyrene dormant species were very small in all cases (k_d < 5 x 10^{-5} s^{-1} at 60 °C), but the results clearly revealed that organotellurium compounds also serve as radical initiators by C-Te bond homolysis.[36] The results are in sharp contrast to organostibine and iodine transfer agents, which do not show apparent bond homolysis (entries 6 and 8). Since the addition of an azo-initiator causes the formation of dead polymers upon its consumption and decrease the MWD control,[22] efficient thermal generation contributes considerably to the precise control of polymerization reactions.

Conclusions

In summary, we have shown that the untransferable substituent *L* on the tellurium atom considerably influences the group transfer reaction and leads to an increase in the control over the

molecular weight distribution in TERP. A significant high-level of control was observed using organotellurium transfer agents possessing aryl group as the untransferable substituent *L*. This finding would lead to the design of new heteroatom compounds for controlling radical reactions and the living radical polymerization.

Experimental Section

General. All reaction conditions dealing with oxygen- and moisture sensitive compounds were carried out in a dry reaction vessel under nitrogen or argon atmosphere. ^{1}H NMR (400 MHz) and ^{13}C NMR (100 MHz) spectra were measured for a $CDCl_3$ solution of a sample. ^{1}H NMR spectra are reported in parts per million (δ) from internal tetramethylsilane or residual solvent peak, and ^{13}C NMR from solvent peak. IR spectra (absorption) are reported in cm^{-1}. High resolution mass spectra (HRMS) were obtained under electron impact ionization conditions. Analytical gel permeation chromatography (GPC) was performed with two linearly connected polystyrene mixed gel columns, which were calibrated with polystyrene and poly(methyl methacrylate) standards. Chloroform was used as an eluant. Preparative/recycling GPC was carried out under nitrogen atmosphere with two linearly connected polystyrene mixed gel columns in a glove box as previously described.[37]

Materials. Unless otherwise noted, materials were obtained from commercial suppliers and were used as received. Styrene and methylmethacrylate were washed with 5% aqueous sodium hydroxide solution and were distilled over calcium hydride under reduced pressure and stored under nitrogen atmosphere. 2,2′-Azobis(isobutyronitrile) (AIBN) was recrystalized from methanol and stored in a refrigerator. Ethyl 2-methyltellanyl-2-methylpropionate (**2f**) was prepared as reported.[14]

Ethyl 2-phenyltellanyl-2-methylpropionate (2a). To a suspension of tellurium powder (5.72 g, 45 mmol) in 50 mL of THF was slowly added phenyllithium (51 mL, 0.98 M solution in cyclohexane and diethyl ether, 50 mmol) over 0.5 h at 0 °C. The resulting mixture was stirred for 0.5 h at room temperature. Ethyl 2-bromoisobutyrate (7.44 mL, 50 mmol) was added to this solution at 0 °C, and the resulting solution was stirred at room temperature for 1.5 h. Water, which was deoxygenated by bubbling nitrogen gas for 0.5 h before use, was added to this solution, and the aqueous layer was separated under nitrogen atmosphere. The remaining organic phase was washed successively with deoxygenated saturated aqueous NH_4Cl solution and saturated aqueous NaCl solution, dried over $MgSO_4$, and filtered under nitrogen atmosphere. Solvent was removed under reduced pressure followed by distillation under reduced pressure (bp. 91 °C/0.2 mmHg) to give a

98:2 mixture of **2a** and diphenyl ditelluride (7.34 g: yield of **2a** was 51%). This mixture was further purified by preparative GPC under nitrogen atmosphere followed by vacuum distillation to give pure sample (>99% pure) as yellow oil. IR (neat) 2979, 1714, 1265, 1146, 1106, 1018, 735, 692; HRMS (EI) *m/z*: Calcd for $C_{12}H_{16}O_2Te$ $(M)^+$, 322.0213; Found 322.0225; ^1H NMR (400MHz, $CDCl_3$) 1.18 (t, J = 7.2 Hz, 3H, CH_3), 1.73 (s, 6H, $C(CH_3)_2$), 4.07 (q, J = 7.2 Hz, 2H, OCH_2), 7.26-7.30 (m, 2H, ArH), 7.39-7.43 (m, 1H, ArH), 7.88-7.90 (m, 2H, ArH); ^{13}C NMR (100 MHz, $CDCl_3$) -14.13, 28.74, 30.18, 61.12, 113.79, 129.26, 129.34, 142.23, 176.89.

Ethyl 2-(*p*-methoxyphenyl)tellanyl-2-methylpropionate (2b). *t*-Butyllithium (64.50 mL, 1.55 M solution in *n*-pentane, 100 mmol) was added dropwisely to a stirred solution of 4-bromoanisole (6.26 mL, 50 mmol) in THF (200 mL) at -78 °C under nitrogen. After being stirred for 1 h at this temperature, the reaction mixture was allowed to warm to room temperature by removing the cooling bath over 0.5 h. Tellurium powder (5.72 g, 45 mmol) was added to this solution in one portion, and the resulting mixture was stirred for 0.5 h at room temperature. Ethyl 2-bromoisobutyrate (7.44 mL, 50 mmol) was added to this solution at 0 °C, and the resulting solution was stirred at room temperature for 2 h. Water, which was deoxygenated by bubbling nitrogen gas for 0.5 h before use, was added to this solution, and the aqueous layer was separated under nitrogen atmosphere. The remaining organic phase was washed successively with deoxygenated saturated aqueous NH_4Cl solution and saturated aqueous NaCl solution, dried over $MgSO_4$, and filtered under nitrogen atmosphere. Solvent was removed under reduced to give a 70:30 mixture of **2b** and di-*p*-methoxyphenyl ditelluride. (13.60 g: yield of **2b** was 78%). This mixture was further purified by preparative GPC under nitrogen atmosphere followed by vacuum distillation to give pure sample (>99% pure) as yellow oil. IR (neat) 2956, 1711, 1585, 1487, 1246, 1146, 1028, 823; HRMS (EI) *m/z*: Calcd for $C_{13}H_{18}O_3Te$ $(M)^+$, 352.0318; Found 350.0325; ^1H NMR (400MHz, $CDCl_3$) 1.20 (t, J = 7.2 Hz, 3H, CH_3), 1.69 (s, 6H, $C(CH_3)_2$), 3.82 (s, 3H, OCH_3), 4.08 (q, J = 7.2 Hz, 2H, OCH_2), 6.80 (d, J = 8.8 Hz, 2H, ArH), 7.78 (d, J = 8.8 Hz, 2H, ArH) ; ^{13}C NMR (100 MHz, $CDCl_3$) -13.88, 28.25, 29.67, 55.07, 60.79, 103.72, 114.91, 143.72, 160.54, 176.74.

Ethyl 2-(*p*-trifluoromethyl)tellanyl-2-methylpropionate (2c). *t*-Butyllithium (64.50 mL, 1.55 M solution in *n*-pentane, 100 mmol) was added dropwisely to a stirred solution of 4-bromobenzotrifluoride (7.60 mL, 50 mmol) in THF(200 mL) at -78 °C under nitrogen. After being stirred for 1 h at this temperature, the reaction mixture was allowed to warm to room temperature by removing the cooling bath over 0.5 h. Tellurium powder (5.72 g, 45 mmol) was

added to this solution in one portion, and the resulting mixture was stirred for 0.5 h at room temperature. Ethyl 2-bromoisobutyrate (7.44 mL, 50 mmol) was added to this solution at 0 °C, and the resulting solution was stirred at room temperature for 2 h. Water, which was deoxygenated by bubbling nitrogen gas for 0.5 h before use, was added to this solution, and the aqueous layer was separated under nitrogen atmosphere. The remaining organic phase was washed successively with deoxygenated saturated aqueous NH_4Cl solution and saturated aqueous NaCl solution, dried over $MgSO_4$, and filtered under nitrogen atmosphere. Solvent was removed under reduced pressure followed by distillation under reduced pressure (bp. 78-82 °C/0.5-0.7 mmHg) to give a 90:10 mixture of **2c** and diphenyl ditelluride (9.71 g: yield of **2c** was 56%). This mixture was further purified by preparative GPC under nitrogen atmosphere followed by vacuum distillation to give pure sample (>99% pure) as yellow oil. IR (neat) 2982, 1714, 1392, 1325, 1268, 1129, 829, 681; HRMS (EI) *m/z*: Calcd for $C_{13}H_{18}O_3Te$ $(M)^+$, 390.0086; Found 390.0060; ^1H NMR (400MHz, $CDCl_3$) 1.18 (t, J = 7.2 Hz, 3H, CH_3), 1.75 (s, 6H, $C(CH_3)_2$), 4.09 (q, J = 7.2 Hz, 2H, OCH_2) , 7.15 (d, J = 7.6 Hz, 2H, ArH), 8.01 (d, J = 8.4 Hz, 2H, ArH) ; ^{13}C NMR (100 MHz, $CDCl_3$) -13.77, 28.40, 30.99, 61.02, 117.72, 122.62, 125.46 (q, J_{C-F} = 3.8 Hz), 131.06 (q, J_{C-F} = 32 Hz), 141.93, 176.26.

Ethyl 2-(2-furyl) tellanyl-2-methylpropionate (2d). *n*-Butyllithium (36.8 mL, 1.51 M solution in hexanes, 55.6 mmol) was added dropwisely to a stirred solution of furan (4.4 mL, 60.9 mmol) in THF(100 mL) at -15 °C under nitrogen. After being stirred for 30 min at this temperature, the reaction mixture was allowed to warm to room temperature by removing the cooling bath over 0.5 h. Tellurium powder (6.04 g, 47.61 mmol) was added to this solution in one portion, and the resulting mixture was stirred for 1 h at room temperature. Ethyl 2-bromoisobutyrate (8.04 mL, 52.9 mmol) was added to this solution at 0 °C, and the resulting solution was stirred at room temperature for 2 h. Water, which was deoxygenated by bubbling nitrogen gas for 0.5 h before use, was added to this solution, and the aqueous layer was separated under nitrogen atmosphere. The remaining organic phase was washed successively with deoxygenated saturated aqueous NH_4Cl solution and saturated aqueous NaCl solution, dried over $MgSO_4$, and filtered under nitrogen atmosphere. Solvent was removed under reduced pressure followed by distillation under reduced pressure (bp. 102-103 °C/1.0-1.1 mmHg) to give a 97:3 mixture of **2d** and difuran ditelluride (2.62 g: yield of **2d** was 17%). This mixture was further purified by preparative GPC under nitrogen atmosphere followed by vacuum distillation to give pure sample (>99% pure) as yellow oil. IR (neat) 2980, 1715, 1462, 1267, 1148, 1107, 999, 746; HRMS (EI) *m/z*: Calcd for $C_{10}H_{14}O_3Te$ $(M)^+$, 312.0005;

Found 312.0016; ^{1}H NMR (400MHz, $CDCl_3$) 1.22 (t, J = 7.0 Hz, 3H, CH_3), 1.74 (s, 6H, $C(CH_3)_2$), 4.12 (q, J = 7.2 Hz, 2H, OCH_2), 6.40 (t, J = 1.6 Hz, 1H, ArH), 6.89 (d, J = 1.6 Hz, 1H, ArH), 7.62 (d, J = 1.6 Hz, 1H, ArH); ^{13}C NMR (100 MHz, $CDCl_3$) -13.81, 28.46, 33.64, 61.06, 112.03 123.50, 128.72, 149.31, 176.09.

Ethyl 2-(*n*-butyl) tellanyl-2-methylpropionate (2e). To a suspension of tellurium powder (5.72 g, 45 mmol) in 50 mL of THF was slowly added *n*-butyllithium (31 mL, 1.6 M solution in hexane, 50 mmol) over 0.5 h at 0 °C. The resulting mixture was stirred for 0.5 h at room temperature. Ethyl 2-bromoisobutyrate (7.59 mL, 50 mmol) was added to this solution at 0 °C, and the resulting solution was stirred at room temperature for 2 h. Water, which was deoxygenated by bubbling nitrogen gas for 0.5 h before use, was added to this solution, and the aqueous layer was separated under nitrogen atmosphere. The remaining organic phase was washed successively with deoxygenated saturated aqueous NH_4Cl solution and saturated aqueous NaCl solution, dried over $MgSO_4$, and filtered under nitrogen atmosphere. Solvent was removed under reduced pressure followed by distillation under reduced pressure (bp. 67-70 °C/1.0-1.2 mmHg) to give pure sample (>99% pure) as yellow oil (6.61 g: yield of **2e** was 49 %). IR (neat) 2958, 1722, 1463, 1382, 1267, 1145, 1109, 1028; HRMS (EI) *m/z*: Calcd for $C_{10}H_{14}O_3Te$ $(M)^+$, 302.0526; Found 302.0532; ^{1}H NMR (400MHz, $CDCl_3$) 0.92 (t, J = 7.2 Hz, 3H., CH_3), 1.26 (t, J = 7.2 Hz, 3H, $TeCH_2$), 1.38 (sext, J = 7.2 Hz, 2H, CH_2), 1.74 (s, 6H, $C(CH_3)_2$), 1.78 (quint, J = 7.6 Hz, 2H, CH_2), 2.92 (m, J = 7.6 Hz, 2H, CH_2), 4.15 (q, J = 7.2 Hz, 2H, OCH_2); ^{13}C NMR (100 MHz, $CDCl_3$) -7.38, 13.39, 13.86, 25.27, 28.47, 33.78, 60.79, 177.02.

General procedure for synthesis of macro-CTA. Phenyltellanyl-substituted Polystyrene macro-CTAs (3a). Styrene (1.72 mL, 15 mmol) and **2a** (111 μL, 0.5 mmol) were heated at 100 °C for 24 h. The resulting polystyrene was dissolved with 3 mL of $CHCl_3$, which was deoxygenated by bubling nitrogen gas for 0.5 h before use, and was poured into vigorously stirred 200 mL of methanol, which was deoxygenated by bubbling nitrogen gas for 0.5 h before use, under nitrogen atmosphere in a glove box. The precipitated polymer was collected by filtration and was dried under reduced pressure to give 1.51 g of **3a** (97 % yield). GPC analysis indicated the polymer formed with M_n = 3,100 and M_w/M_n = 1.11.

General procedure for the kinetic study. Peak resolution Method for detemining k_{act}.[28] This method is based on the GPC observation of an early stage of the polymerization containing a macro-CTA **3a** as a probe polymer P_0–X. When P_0–X is activated, the released P_0 radical will propagate until it is deactivated to give a new adduct P_1-X. (The subscripts 0 and 1 denoted the

number of activation.)Since P_0–X and P_1–X are generally different in chain length and its distribution, they may be distinguishable by GPC. By following the change in [P_0–X.], k_{act} can be determined from the first-order plot

$$\ln(S_0/S) = k_{act}t \qquad (1)$$

where S_0 and S are the concentrations (or the GPC peak areas) of P_0–X at times zero and t, respectively. A lower initial concentration of P_0–X leads to a larger number of monomer units added to P_0 radical during an activation-deactivation cycle. In fact, with a sufficiently low [P_0–X.]$_0$ (2.4 mM in this case), the GPC curves were composed of two defined peaks as shown in Figure S1, thus allowing accurate resolution. The lower-molecular weight component corresponds to the unreacted P_0–X, and the higher-molecular weight one corresponds to P_1–X (plus other minor components such as those originated from AIBN). Figure 2 shows the plot of $\ln(S_0/S)$ vs t for various concentrations of AIBN. The plot is linear in all cases, giving a well-defined value of k_{act}. Note that this experimental condition is so designed as to determine k_{act} with the highest possible accuracy, and accordingly is different from that in the usual work which aims at the preparation of low-polydispersity, well-defined polymers.

General procedure for determination of k_{act} at 60 °C for 3a in styrene polymerization. A schlenk flask was charged with the styrene solution (2.5 mL) of **3a** (M_n = 3,100, M_w/M_n = 1.11, 2.4–2.8 mM) and AIBN (0–41.1 mM) under nitrogen atmosphere in a glove box. The flask was equipped with stopcock, and was immersed in an oil bath at 60 °C with magnetic stirring (t = 0 min). After a prescribed time t, an aliquot (0.1 mL) of the solution was taken out with a syringe, quenched in the air at room temperature, and then diluted with $CHCl_3$ to a known concentration to be analyzed by GPC. Figure 2 shows examples of time-dependent GPC chromatograms under [**3a**]$_0$ = 2.4 mM and [AIBN]$_0$ = 41.1 mM in styrene. Figures 3 and 4 show the first-order plot of **3a** and monomer (M) concentrations ([**3a**]$_0$/[**3a**] and [M]$_0$/[M]), respectively under various AIBN concentrations. In all examined cases, the plot is approximately linear, and the slopes of each line of Figures 3 and 4 give k_{act} and k_p[P•], respectively. Figure 5 shows plot of k_{act} vs k_p[P•]. The k_d was determined from the intercept and the k_{cx} from the slope.

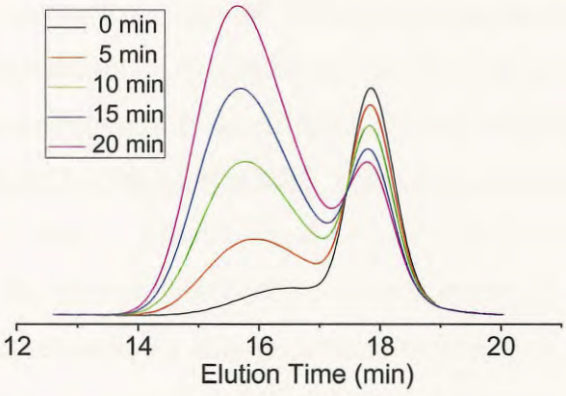

Figure 2. GPC traces for the polymerization of styrene in the presence of **3a** and AIBN at 60 °C: $[\mathbf{3a}]_0$ = 2.4 mM/$[AIBN]_0$ = 41.1 mM.

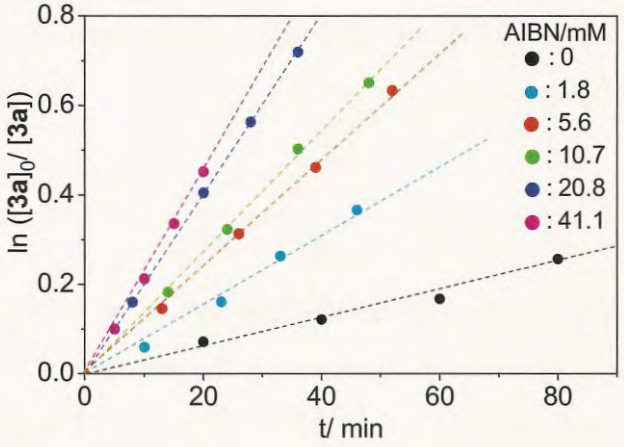

Figure 3. Plot of $\ln([\mathbf{3a}]_0/[\mathbf{3a}])$ vs t for the polymerization of styrene in the presence of **3a** and AIBN at 60 °C: $[\mathbf{3a}]_0$ = 2.4–2.8 mM/$[AIBN]_0$ = 0–41.1 mM (as indicated in the figure).

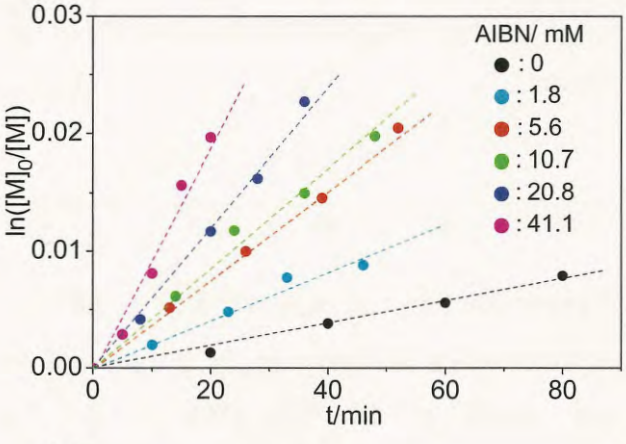

Figure 4. Plot of $\ln([M]_0/[M])$ vs t for the polymerization of styrene in the presence of 3a and AIBN at 60 °C: $[3a]_0$ = 2.4–2.8 mM/$[AIBN]_0$ = 0–41.1 mM (as indicated in the figure).

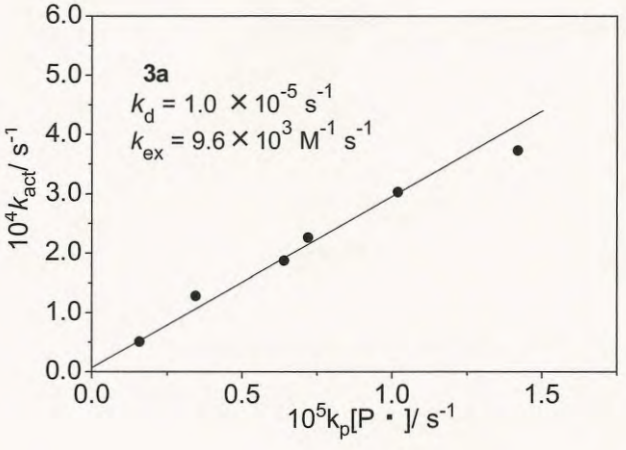

Figure 5. Plot of k_{act} vs $k_p[P\bullet]$ for the polymerization of styrene in the presence of **3a** and AIBN at 60 °C: $[\mathbf{3a}]_0$ = 0–41.1 mM/$[AIBN]_0$ = 0–41.1 mM.

Determination of k_{act} at 60 °C for 3b in styrene polymerization. **3b** (M_n = 3,800, M_w/M_n = 1.06) was obtained according to general experiment procedures. k_{act} at 60 °C for **3b** in styrene polymerization was determined as well as general procedure. Figures 6 and 7 show the plot of $\ln([\mathbf{3b}]_0/[\mathbf{3b}])$ and $\ln([M]_0/[M])$ for various concentrations of AIBN. Figure 8 shows plot of k_{act} vs $k_p[P\bullet]$. The k_{act} was determined.

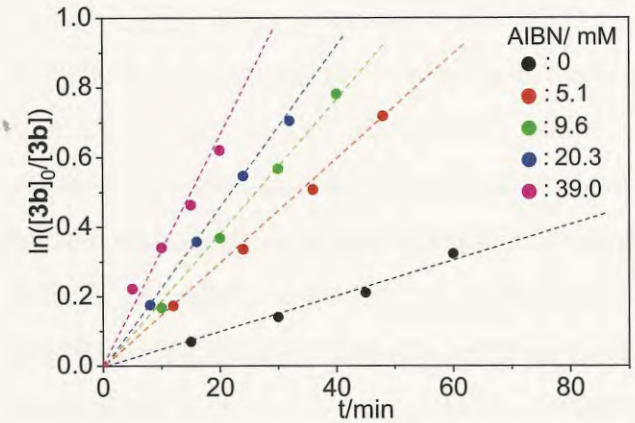

Figure 6. Plot of $\ln([\mathbf{3b}]_0/[\mathbf{3b}])$ vs t for the polymerization of styrene in the presence of **3a** and AIBN at 60 °C: $[\mathbf{3b}]_0$ = 2.3-2.6 mM/$[AIBN]_0$ = 0–39.0 mM (as indicated in the figure).

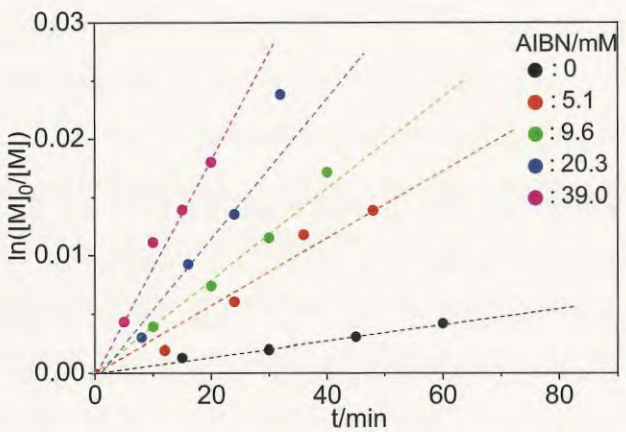

Figure 7. Plot of $\ln([M]_0/[M])$ vs t for the polymerization of styrene in the presence of 3b and AIBN at 60 °C: $[3b]_0$ = 2.3–2.6 mM/$[AIBN]_0$ = 0–39.0 mM (as indicated in the figure).

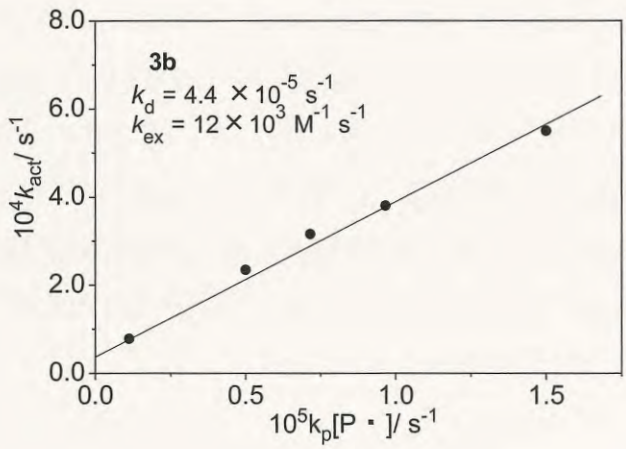

Figure 8. Plot of k_{act} vs $k_p[P\bullet]$ for the polymerization of styrene in the presence of **3a** and AIBN at 60 °C: $[\mathbf{3b}]_0$ = 2.3–2.6 mM/$[AIBN]_0$ = 0–39.0 mM.

Determination of k_{act} at 60 °C for 3c in styrene polymerization. 3c (M_n= 3,000, M_w/M_n = 1.07) was obtained according to typical experiment procedures. k_{act} at 60 °C for **3c** in styrene polymerization was determined as well as general procedure. Figure 9 and 10 show the plot of $\ln([\mathbf{3c}]_0/[\mathbf{3c}])$ and $\ln([M]_0/[M])$ for various concentrations of AIBN. Figure 11 shows plot of k_{act} vs $k_p[P\bullet]$. The k_{act} was determined by the peak resolution method.

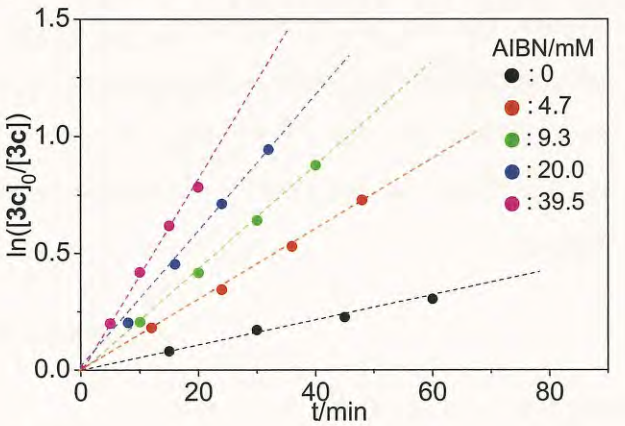

Figure 9. Plot of $\ln([\mathbf{3c}]_0/[\mathbf{3c}])$ vs t for the polymerization of styrene in the presence of **3a** and AIBN at 60 °C: $[\mathbf{3c}]_0$ = 3.0–3.3 mM/$[AIBN]_0$ = 0–39.5 mM (as indicated in the figure).

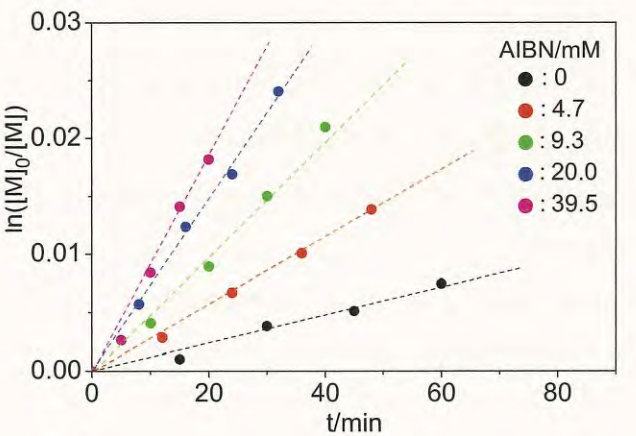

Figure 10. Plot of $\ln([M]_0/[M])$ vs t for the polymerization of styrene in the presence of 3b and AIBN at 60 °C: $[\mathbf{3c}]_0$ = 3.0–3.3 mM/$[AIBN]_0$ = 0–39.5 mM (as indicated in the figure).

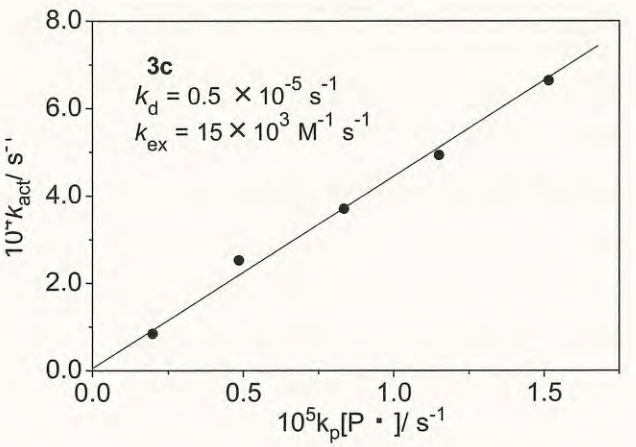

Figure 11. Plot of k_{act} vs $k_p[P\bullet]$ for the polymerization of styrene in the presence of **3c** and AIBN at 60 °C: $[\mathbf{3c}]_0$ = 3.0–3.3 mM/$[AIBN]_0$ = 0–39.5 mM.

Determination of k_{act} at 60 °C for 3d in styrene polymerization. **3d** (M_n = 3800, M_w/M_n = 1.08) was obtained according to typical experiment procedures. k_{act} at 60 °C for **3d** in styrene polymerization was determined as well as general procedure. Figure 12 and 13 show the plot of $\ln([\mathbf{3d}]_0/[\mathbf{3d}])$, $\ln([M]_0/[M])$, for various concentrations of AIBN. Figure 14 shows plot of k_{act} vs $k_p[P\bullet]$. The k_{act} was determined by the peak resolution method.

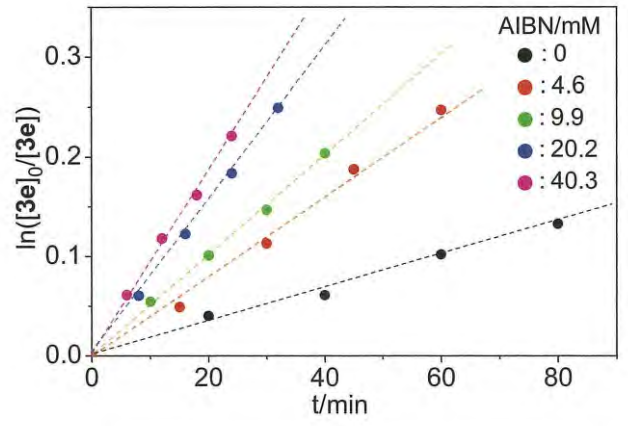

Figure 12. Plot of $\ln([\mathbf{3d}]_0/[\mathbf{3d}])$ vs t for the polymerization of styrene in the presence of **3d** and AIBN at 60 °C: $[\mathbf{3d}]_0$ = 2.1–2.7 mM/$[AIBN]_0$ = 0–40.3 mM (as indicated in the figure).

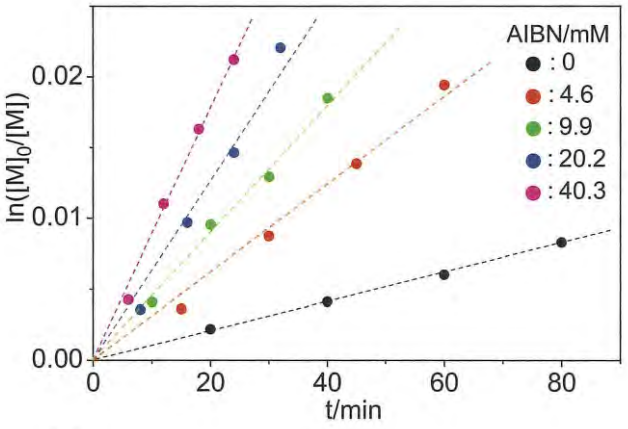

Figure 13. Plot of $\ln([M]_0/[M])$ vs t for the polymerization of styrene in the presence of **3d** and AIBN at 60 °C: $[\mathbf{3d}]_0$ = 2.1–2.7 mM/$[AIBN]_0$ = 0–40.3 mM (as indicated in the figure).

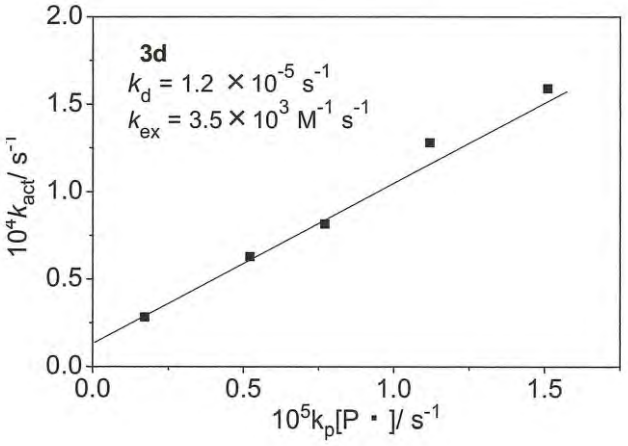

Figure 14. Plot of k_{act} vs $k_p[P\bullet]$ for the polymerization of styrene in the presence of **3c** and AIBN at 60 °C: $[\mathbf{3c}]_0$ = 2.1–2.7 mM/$[AIBN]_0$ = 0–40.3 mM.

Table 3. Experiment conditions for kinetics experiment.

XL	M_n	M_w/M_n	**3** (mM)	AIBN (mM)	k_d (s^{-1})	k_{ex} (M^{-1} s^{-1})
3a (TePh)	3,100	1.11	2.4–2.8	0–41.1	1.0×10^{-5}	9.6×10^{3}
3b (TeC_6H_4MeO-*p*)	3,800	1.06	2.3–2.6	0–39.0	3.9×10^{-5}	1.2×10^{4}
3c ($TeC_6H_4CF_3$-*p*)	3,000	1.07	3.0–3.3	0–39.5	2.4×10^{-6}	1.5×10^{4}
3d (TeBu-*n*)	3,700	1.24	2.1–2.7	0–40.3	1.3×10^{-5}	3.5×10^{3}
3e (Te-2-furyl)	3,800	1.08	2.2–3.0	0–40.9	nd	nd

nd: Not determined.

References

(1) *Handbook of Radical Polymerization*; Matyjaszewski, K.; Davis, T. P., Eds.; Wiley-Interscience: New York, 2002.

(2) Moad, G.; Solomon, D. H. *The Chemistry of Radical Polymerization*; Elsevier: Amsterdam, 2006.

(3) Hawker, C. J.; Bosman, A. W.; Harth, E. *Chem. Rev.* **2001**, *101*, 3661-3688.

(4) Wayland, B. B.; Poszmik, G.; Mukerjee, S. L.; Fryd, M. *J. Am. Chem. Soc.* **1994**, *116*, 7943-7944.

(5) Matyjaszewski, K.; Xia, J. *Chem. Rev.* **2001**, *101*, 2921-2990.

(6) Kamigaito, M.; Ando, T.; Sawamoto, M. *Chem. Rev.* **2001**, *101*, 3689-3746.

(7) Moad, G.; Rizzardo, E.; Thang, S. H. *Polymer* **2008**, *49*, 1079-1131.

(8) Moad, G.; Rizzardo, E.; Thang, S. H. *Aust. J. Chem.* **2009**, *62*, 1402-1472.

(9) Gridnev, A. A.; Ittel, S. D. *Chem. Rev.* **2001**, *101*, 3611-3660.

(10) Oka, M.; Tatemoto, M. *Contemporary Topics in Polymer Science*; Plenum: New York, 1984.

(11) Matyjaszewski, K.; Gaynor, S.; Wang, J.-S. *Macromolecules* **1995**, *28*, 2093-2095.

(12) David, G.; Boyer, C.; Tonnar, J.; Ameduri, B.; Lacroix-Desmazes, P.; Boutevin, B. *Chem. Rev.* **2006**, *106*, 3936-3962.

(13) Goto, A.; Kwak, Y.; Fukuda, T.; Yamago, S.; Iida, K.; Nakajima, M.; Yoshida, J. *J. Am. Chem. Soc.* **2003**, *125*, 8720-8721.

(14) Yamago, S.; Iida, K.; Yoshida, J. *J. Am. Chem. Soc.* **2002**, *124*, 2874-2875.

(15) Kwak, Y.; Goto, A.; Fukuda, T.; Kobayashi, Y.; Yamago, S. *Macromolecules* **2006**, *39*, 4671-4679.

(16) Yamago, S.; Iida, K.; Yoshida, J. *J. Am. Chem. Soc.* **2002**, *124*, 13666-13667.

(17) Yamago, S.; Iida, K.; Nakajima, M.; Yoshida, J. *Macromolecules* **2003**, *36*, 3793-3796.
(18) Yusa, S.; Yamago, S.; Sugahara, M.; Morikawa, S.; Yamamoto, T.; Morishima, Y. *Macromolecules* **2007**, *40*, 5907-5915.
(19) Yamago, S. *Proc. Jpn. Acad., Ser. B* **2005**, *81*, 117-128.
(20) Yamago, S. *J. Polym. Sci. Part A: Polym. Chem.* **2006**, *44*, 1-12.
(21) Goto, A.; Ohno, K.; Fukuda, T. *Macromolecules* **1998**, *31*, 2809-2814.
(22) Goto, A.; Fukuda, T. *Macromolecules* **1997**, *30*, 4272-4277.
(23) Han, L. B.; Ishihara, K.; Kambe, N.; Ogawa, A.; Ryu, I.; Sonoda, N. *J. Am. Chem. Soc.* **1992**, *114*, 7591-7592.
(24) Kim, S.; Song, H. J.; Choi, T. L.; Yoon, J. Y. *Angew. Chem. Int. Ed.* **2001**, *40*, 2524-2526.
(25) Kim, S.; Song, H.-J. *Synlett* **2002**, 2110,2112.
(26) Curran, D. P.; Martin-Esker, A. A.; Ko, S.-B.; Newcomb, M. *J. Org. Chem.* **1993**, *58*, 4691-4695
(27) Yamago, S.; Ray, B.; Iida, K.; Yoshida, J.; Tada, T.; Yoshizawa, K.; Kwak, Y.; Goto, A.; Fukuda, T. *J. Am. Chem. Soc.* **2004**, *126*, 13908-13909.
(28) Goto, A.; Terauchi, T.; Fukuda, T.; Miyamoto, T. *Macromol. Rapid. Commun.* **1997**, *18*, 673-681.
(29) Fukuda, T.; Goto, A.; Ohno, K. *Macromol. Rapid Commun.* **2000**, *21*, 151-165.
(30) Goto, A.; Fukuda, T. *Prog. Polym. Sci.* **2004**, *29*, 329-385.
(31) Fukuda, T. *J. Polym. Sci. Part A* **2004**, *42*, 4743-4755.
(32) Gilbert, R. G. *Pure Appl. Chem.* **1996**, *68*, 1491-1494.
(33) We previously reported that 1-phenyltellanyl-1-phenylethane (A) was less efficient for PDI control than corresponding 1-methyltellanyl derivative in styrene polymerization (ref 14). However, the current results suggest that the previous results were affected by unexpected factors presumably a small amount of impurities present in the transfer agent because of the difficulty to obtain pure A.
(34) Yamago, S.; Miyazoe, H.; Goto, R.; Hashidume, M.; Sawazaki, T.; Yoshida, J. *J. Am. Chem. Soc.* **2001**, *123*, 3697-3705.
(35) Kwak, Y.; Goto, A.; Fukuda, T.; Yamago, S.; Ray, B. *Z. Phys. Chem.* **2005**, *219*, 283-293.
(36) The k_d value is less accurate than the kex value because the former is more sensitive to the experimental error. Furthermore, as the kd values obtained this study were very small, we do not think that detailed comparison of the substituent effects on the k_d is significant.
(37) Yamago, S. *Jpn. Kokai Tokkyo Koho* **2005**, JP2005300277.

Chapter 2

Substituent Effect on the Antimony Atom in Organostibine-Mediated Living Radical Polymerization

Abstract

The substituent effect on the antimony atom in organostibine-mediated living radical polymerization (SBRP) has been studied. 2-Diphenylstibanyl-2-methylpropionitrile (**1a**) was synthesized as an organostibine chain transfer agent (CTA), and its effect was compared to the previously reported dimethylstibanyl analogue **1b**. Both CTAs successfully polymerized butyl acrylate (BA) in a highly controlled manner giving poly(butyl acrylate)s possessing number average molecular weights close to the theoretical values determined by BA/**1** ratios and narrow molecular weight distribution. The controllability of styrene polymerization by **1a** was slightly decreased but still acceptable level. However, **1a** did not control the polymerization of methyl methacrylate (MMA). The results are in sharp contrast that **1b** can highly control the polymerization of styrene and MMA. Kinetic studies using diphenylstibanyl-substituted polystyrene macro CTA **2** in styrene polymerization revealed that the degenerative chain transfer reaction of diphenylstibanyl group takes place faster than that of dimethylstibanyl group, suggesting that the reactivity of diphenylstibanyl group is not the origin of the low control. Chain extension experiments revealed the formation of considerable amount of dead polymers when **1a** was used as a CTA, and the frequent occurrence of termination reaction is most probable origin of the low control. The addition of tetraphenyldistibine significantly increased the control of styrene and MMA polymerization, and structurally well defined polystyrene and poly(methyl methacrylate) were obtained by applying a binary system consisting from **1a** and tetraphenyldistibine.

Introduction

Controlled/living radical polymerization (LRP) has become an indispensable method for the synthesis of well-defined, advanced polymeric materials, because it allows the polymerization of a variety of functional vinyl monomers to give products with well-controlled molecular weights and molecular weight distributions.[1-6] Since radical species at the polymer end in radical polymerization undergoes undesired termination and disproportionation reactions forming dead polymers nearly diffusion controlled rate, LRP so far reported relies on the reversible generation of polymer-end radicals from dormant species (Figure 1a).[7] Therefore, once polymer end radical is generated from dormant species, it reacts with monomer before deactivating to the dormant species. This reversible radical generation decreases the concentration of radical species in solution and minimizes undesirable side reactions. Furthermore, the rapid deactivation makes it possible to elongate all of the polymer chains with similar chain lengths. The faster deactivation leads to the higher control of polymerization under the ideal condition without any side reactions, and polymers possessing predicted number average molecular weight (M_n) and narrower molecular weight distribution (MWD) are formed.

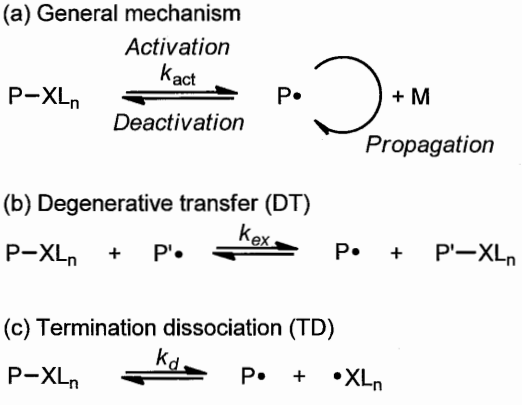

Figure 1. (a) General mechanism of LRP, and (b) degenerative transfer mechanism and (c) termination dissociation mechanism for the activation/deactivation reaction of dormant species P-XL$_n$ and polymer-end radical P•. P and M denote polymer and monomer, respectively.

Organotellurium-,[8-17] and organostibine-,[18-20] mediated LRP (TERP and SBRP, respectively) are new class of LRP methods we have developed recently.[21-24] These methods are synthetically highly valuable in polymerizing a variety of monomers, e.g., conjugated and non-conjugated monomers, bearing variety of polar functional groups in a controlled manner. These

methods are also advantageous for making end-functionalized polymers and block copolymers through the selective polymer-end group transformations. The mechanistic studies revealed that these methods predominantly proceeds by the degenerative chain transfer (DT) mechanism for the activation/deactivation reaction (Figure 1b), while the thermal dissociation (TD) mechanism also contributes to a small extent (Figure 1c). The rate constant k_{ex} of DT, which corresponds to the deactivation and activation rates for P radical and P'XL_n dormant species, respectively, is a function of the heteroatom species X and also the untransferable substituent *L* on the heteroatom. When *L* = Me in styrene polymerization, the k_{ex} for dimethylstibanyl group (XL_n = $SbMe_2$)[18,25] is larger than that for methyltellanyl group (XL_n = TeMe).[10,26] It is worth noting that the k_{ex} value of methyltellanyl group is still ca. 2 times faster than that of iodine atom (XL_n = I).[27] The results are consistent with the MWD control of LRP: SBRP usually gives polymers with narrowest MWD followed by SBRP, TERP, and then organoiodine-mediated LRP.

In chapter 1, we have shown that the untransferable substituent *L* on the tellurium atom influences the DT reaction as well as the MWD control in TERP.[14] For example, the k_{ex} of phenyltellanyl group is ca. 2 times larger than that of methyltellanyl group. As a result, a chain transfer agent (CTA) possessing phenyltellanyl group showed higher control in MWD than that having methyltellanyl group. These results prompted us to investigate the reactivity of CTA **1a** possessing diphenylstibanyl group, as we have used dimethylstibanyl substituted CTA **1b** in SBRP so far due to the ease of its preparation and purification. In this chapter, we report the effect of untransferable substituent on antimony thorough polymerization reactions and kinetic studies (Scheme 1). We have recently reported the addition of tetrametyldistibine is effective to increase the control of MWD.[20] Therefore, we also examined the effect of tetraphenyldistibine on the control.

Results and Discussion

Preparation of CTA 1a. Diphenylstibanyl substituted organostibine CTA **1a** was synthesized by the analogous method for the synthesis of **1b** (Scheme 1). Thus, isobutyronitrile was treated with lithium diisopropylamide in THF at -78 °C, and the resulting anion was quenched by diphenylstibanyl bromide.[28] After aqueous work up under nitrogen atmosphere, **1a** was isolated in 38% yield as a white solid by distillation followed by recrystallization from hexane. This compound was easily oxidized in air but was stored for long period (> 6 months) under nitrogen atmosphere. Our previous studies using organotellurium CTAs suggested that 2-methyl-2-methyltellanyl-

propionate and 2-methyl-2-methyltellanylpropionitrile showed similar control in the polymerization of various monomers.[10] Therefore, **1a** is an appropriate CTA for comparing the substituent effects on the antimony atom.

Scheme 1. Synthesis of diphenylstibanyl substituted organostibine CTA **1a**.

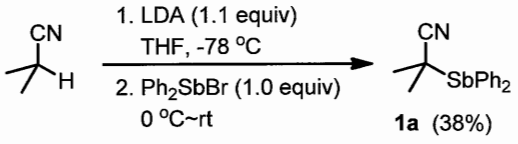

Substituent effects of CTAs. The efficiencies of organostibine CTA **1a** were first examined in the bulk polymerization of butyl acrylate (BA). When a mixture of **1a**, 2,2'-azobis-isobutyronitrile (AIBN) (0.1 equiv), and BA (100 equiv) was heated at 60 °C for 4.5 h, monomer conversion reached to 89% as judged by ^{1}H NMR analysis. Gel permeation chromatography (GPC) analysis indicated the formation of poly(butyl acrylate) (PBA) with the number average molecular weight (M_n) close to the theoretical value from monomer/**1a** ratio [M_n (theo) = 11500, M_n (exp) = 11000] and a narrow MWD (M_w/M_n = 1.17) (Table 1, entry 1). The level of control using **1a** is virtually identical to that of **1b** (entry 11). Polymerization of BA proceeded slowly without AIBN at 100 °C suggesting that **1a** also serves as a radical initiator (entry 2). While the MWD is slightly broad (M_w/M_n = 1.32), the level of control is still acceptable. Since this is a living polymerization, PBAs with high molecular weights were also prepared in a controlled manner by increasing the BA/**1a** ratio (entries 3 and 4).

Polymerization of styrene and methyl methacrylate (MMA) was next examined. CTA **1a** controlled the polymerization of styrene when the targeted molecular weight is low (M_n ~ 2,500) to give the controlled polystyrenes with narrow MWDs (M_w/M_n = 1.31–1.38) with and without AIBN (entries 5 and 6). The control became slightly decreased when the targeted molecular weight increased (M_n ~ 10,000), but the resulting polystyrenes possessed acceptable level of MWDs (M_w/M_n = 1.42–1.55) (entries 7 and 8). Polymerization of MMA in the presence of **1a**, however, was not controlled with and without AIBN at 60 and 100 °C, respectively, and poly(methyl methacrylate)s (PMMAs) with considerably high M_ns from the theoretical values and broad MWDs were formed in both cases (entries 9 and 10). The results are in sharp contrast to the polymerization using **1b**, that exhibits excellent control of the polymerization of not only BA but also styrene and MMA (entries 12 and 13).

Table 1. Effect of substituent of CTA **1a** and **1b** in polymerization of styrene, butyl acrylate, and methyl methacrylate with and without 2,2'-Azobis-isobutyronitrile (AIBN).

a: L = Ph, EWG = CN
b: L = Me, EWG = CO_2Et

Entry	CTA	Monomer (equiv)[a]	Conditions (°C/h)	Conv. (%)[b]	M_n (theo)[c]	M_n (exp)[d]	M_w/M_n[d]
1	**1a**	BA (100)	60/2[f]	87	11,500	11,000	1.17
2	**1a**	BA (100)	100/70	68	9,100	8,000	1.32
3	**1a**	BA (200)	60/3[f]	94	24,400	21,900	1.22
4	**1a**	BA (300)	60/4.5[f]	82	31,500	31,100	1.31
5	**1a**	styrene (30)	60/36[f]	81	2,500	2,400	1.38
6	**1a**	styrene (30)	100/40	89	3,100	2,500	1.31
7	**1a**	styrene (100)	60/48[f]	85	8,900	9,900	1.55
8	**1a**	styrene (100)	100/51	84	9,100	8,300	1.42
9	**1a**	MMA (100)	60/8[f]	89	9,300	32,100	2.35
10	**1a**	MMA (100)	100/24	95	9,900	26,900	2.12
11[e]	**1b**	BA (100)	60/1[f]	84	11,000	10,900	1.13
12[e]	**1b**	St (100)	60/19[g]	99	10,300	8,700	1.17
13[e]	**1b**	MMA (100)	60/4[h]	100	10,000	11,000	1.24

[a]Monomer abbreviation: BA = *n*-butyl acrylate, MMA = methyl methacrylate. [b]Monomer conversion determined by ^{1}H NMR analysis. [c]The theoretical number-average molecular weight [M_n(theo)] was calculated from [(MW of monomer) × (monomer/**1** ratio) × conversion/100] + (MW of **1**), where MW is the molecular weight. [d]Number-average molecular weight (M_n) and molecular weight distribution (MWD = M_w/M_n) were obtained by size exclusion chromatography calibrated against polystyrene standards for entries 5–8 and PMMA standards for the others. [e]Data taken from ref 18. [f]AIBN (0.1 equiv) was added. [g]AIBN (0.5 equiv) was added. [h]AIBN (0.3 equiv) was added.

Chain extension experiment. To confirm the livingness of the current polymerization, chain extension experiment was carried out (Scheme 2). Polystyrene macro-CTA **2** (M_n = 2,400, M_w/M_n = 1.38, Table 1, entry 5) was treated with 200 equiv of styrene at 60 °C for 72 h in the presence of AIBN (0.1 equiv), and the chain extended polystyrene with M_n of 18,400 and M_w/M_n of 1.51 was obtained. According to the GPC traces of polystyrene before and after the chain extension (Figure

2a), 86% of macro-CTA **2** was living as the dormant species and chain extended. However, 14% of **2** was inactive and already became dead polymer as determined by GPC using the method reported by Fukuda.[29] A chain extension experiment using dimethylstibanyl substituted polystyrene macro-CTA **3**, on the other hand, contained only 6% of dead polymer (Figure 2b). Termination reaction of polymer end radicals cannot be completely suppressed in LRP, and the formation of ca. 5% of dead polymer was reported in the nitroxide-mediated LRP and atom transfer radical polymerization.[29,30] However, since lower termination reaction should lead to the higher control of LRP, the less formation of dead polymer using **1b** over **1a** plays a significant role in the level of control.

Scheme 2. Chain extension experiment using (a) diphenyl- or (b) dimethylstibanyl substituted macro-CTAs in the styrene polymerization.

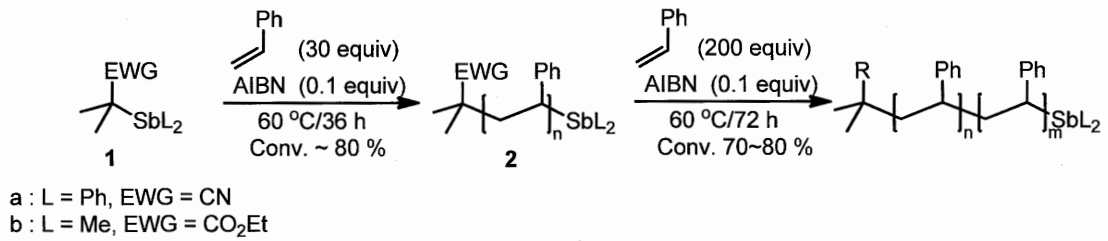

(a) (b)

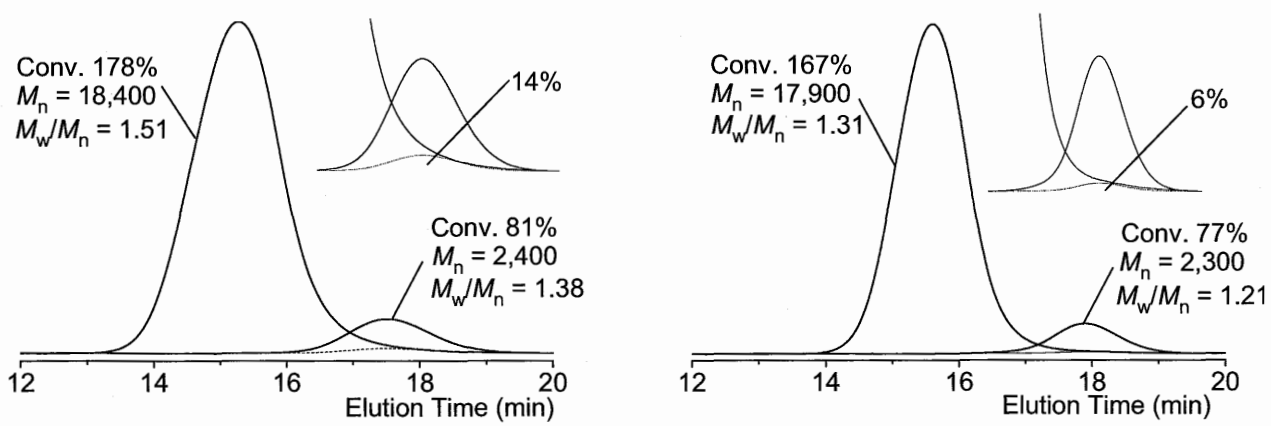

Figure 2. GPC traces of polystyrene samples before and after the chain extension using (a) macro -CTA **2a** and (b) macro-CTA **2b**.

Effect of tetraphenyldistibine. We have recently reported that the addition of tetramethyldistibine is effective to increase the MWD control in the SBRP of styrene and MMA using **1b**[20]. Therefore, we examined the effect of tetraphenyldistibine in the polymerization of

styrene and MMA in the presence of **1a** (Table 2). When tetraphenyldistibine (0.02 equiv) was added to the polymerization of styrene (30 equiv) in the presence of **1a** (1.0 equiv) and AIBN (0.1 equiv), polystyrene with controlled M_n (= 2,500) and MWD (M_w/M_n = 1.11) was obtained after 33 h heating at 60 °C (entry 1). When the targeted molecular weight increased (M_n ~ 10,000), structurally controlled polystyrene was also obtained with narrow MWD (M_w/M_n = 1.18) (entry 2). Addition of 0.05 equiv of tetraphenyldistibine further increased the control (M_w/M_n = 1.10 at 52% monomer conversion), but considerable rate retardation was observed (entry 3). The rate retardation was also observed by the addition of tetramethyldistibine.[31] Therefore, amount of the distibine must be controlled to maximize the effect of the distibine.

Table 2. Effect of tetraphenyldistibine on styrene and methyl methacrylate polymerization in the presence of CTA **1a**.[a]

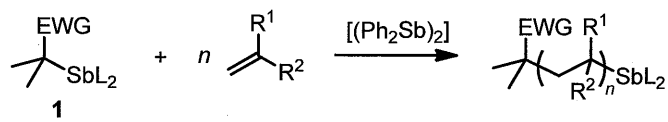

a: L = Ph, EWG = CN
b: L = Me, EWG = CO_2Et

Entry	Monomer (equiv)[b]	$(SbPh_2)_2$ (equiv)	Conditions (°C/h)	Conv. (%)[c]	M_n (theo)[d]	M_n (exp)[e]	M_w/M_n[e]
1	styrene (30)	0.02	60/33	87	3,100	2,500	1.11
2	styrene (100)	0.02	60/48	84	9,100	8,700	1.18
3	styrene (100)	0.05	60/57	52	5,800	4,800	1.10
4	MMA (100)	0.2	60/8	89	9,300	12,000	1.32
5	MMA (100)	0.5	60/8	89	9,300	10,100	1.27
6	MMA (100)	1.0	60/12	92	9,600	9,900	1.25

[a]Polymerization was carried out in bulk in the presence of AIBN (0.1 equiv). [b]Monomer abbreviation: MMA = methyl methacrylate. [c]Monomer conversion determined by ^{1}H NMR analysis. [d]The theoretical number-average molecular weight [M_n (theo)] was calculated from [(MW of monomer)×(monomer/**1a** ratio)×conversion/100] + (MW of **1a**), where MW is the molecular weight. [e]Number-average molecular weight (M_n) and molecular weight distribution (MWD = M_w/M_n) were obtained by size exclusion chromatography calibrated against polystyrene standards for entries 1–3 and PMMA standards for entries 4–6.

Significant increase of the control was also observed in the polymerization of MMA by the addition of tetraphenyldistibine. The rate retardation was not observed by the addition of the distibine, and the control increased as the increase of the amount of the distibine added from 0.2

equiv to 0.5 equiv, and further to 1.0 equiv. Structurally well controlled PMMAs (M_w/M_n = 1.25–1.32) were obtained in all cases (entries 4–6).

From an analogy of the reactivity of ditellurides and tetramethyldistibine towards radicals[31-33], tetraphenyldistibine acts as a capping agent for the polymer end radicals and enhances the deactivation of polymer-end radicals to the dormant species (Scheme 3). The enhanced deactivation reaction led to the formation of controlled polymers. The addition of distibine shifts the equilibrium from the polymer-end radical to dormant species in styrene polymerization presumably due to the low reactivity of polystyrene dormant species with diphenylstibanyl radical. In such cases, diphenylstibanyl radical may dimerize to tetraphenyldistibine.

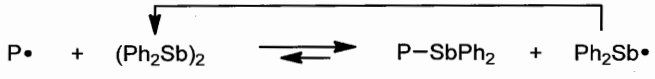

Scheme 3. Plausible deactivation mechanism of polymer-end radical P by distibine

Kinetic Experiment. The effects of the diphenylstibanyl group on the activation/deactivation mechanism (Figure 1) were evaluated by kinetic experiments in the polymerization of styrene using a protocol developed by Fukuda.[7,34,35] Thus, polystyrene macro-CTA **2a** (M_n = 2,500, M_w/M_n = 1.11, Table 2, run 1), which was prepared from **1a** and styrene in the presence of tetraphenyldistibine, was heated with a large excess of styrene (30 mM of **2a**) by changing the amount of AIBN (0~20 mM) at 60 °C. The time dependent consumption of **2a** and the formation of the chain-elongated polymer were analyzed by GPC peak resolution method. The activation rate constant k_{act} of the dormant species can be expressed by $k_{act} = k_d + k_{ex}[P•]$, where k_d and k_{ex} are the first- and second-order rate constants for the TD and DT processes, respectively (Figure 1). Thus, the measurement of k_{act} as a function of [P•] unambiguously determines the TD and DT processes.

The results revealed that the current polymerization also proceeds mainly through DT mechanism (Figure 1b). The rate constant k_{ex} was determined to be 4.0 x 10^4 M^{-1} s^{-1}, which is ca. 4 times higher than the value of the dimethylstibanyl group.[25,36] The enhanced reactivity is probably due to the delocalization of the spin density to phenyl group at the transition state, thus, decreasing the activation energy. Because the faster DT leads to the formation of more controlled polymers with narrower MWD, **1a** is, in principle, better CTA than **1b**. However, the polymerization results contradict the kinetic data (Table 1). Therefore, the lower control of **1a** than **1b** must be due to the formation of the amount of dead polymers as revealed by the chain extension experiments

(Figure 2), though the origin of the increased formation of dead polymers needs further studies.

The rate constants k_d for the thermal dissociation was determined to be negligible ($\sim 0\ M^{-1}\ s^{-1}$) at 60 °C. However, since the polymerization of BA and styrene were carried out at 100 °C without radical initiators, thermal C-Sb bond homolysis should occur at high temperature.

Conclusions

We have demonstrated CTA **1a** serves as efficient CTA for the polymerization of BA and styrene, and that structurally well controlled PBA and polystyrene were formed, though **1a** could not control the polymerization of MMA. We also found that a binary system consisting of **1a** and tetraphenyldistibine was highly effective for the controlled polymerization of styrene and MMA. The kinetic study suggests that diphenylstibanyl group increases the rate of the degenerative transfer reaction and, in principle, exhibits the higher control of the polymerization than dimethylstibanyl group. However, since diphenylstibanyl group also increase the formation of dead polymers, the control of polymerization is determined by the contribution of these conflicting factors. This study would provide an important insight into the understanding of the factors that control the living radical polymerization.

Experimental Section

General. All reaction dealing with air- and moisture sensitive compounds were carried out in a dry reaction vessel under nitrogen atmosphere. ^1H and ^{13}C NMR (400 and 100 MHz, respectively) spectra were measured at ambient temperature in $CDCl_3$ as solvent and are reported in parts per million (δ) from internal tetramethylsilane or residual solvent peak. GPC was performed two linearly connected polystyrene mixed gel columns, which were calibrated with polystyrene or PMMA standards. IR spectra (absorption) are reported in cm^{-1}. High resolution mass spectra (HRMS) were obtained under electron impact ionization conditions.

Materials. Unless otherwise noted, reagents from suppliers were used as received. Styrene (99%, Wako), BA (99%, Wako), and MMA (99%, Wako) were washed with 5% aqueous sodium hydroxide solution and were distilled over calcium hydride under reduced pressure. AIBN (98%, Wako) was recrystallized from methanol. Diphenylstibanylbromide[30] and ethyl 2-dimethylstibanyl-2-methylpropionate (**1b**)[18] were prepared as reported.

2-Diphenylstibanyl-2-methylpropionitrile (1a). Isobutyronitrile (1.00 mL, 70.4 mmol) in

THF (30 mL) was added to a THF solution of lithium diisopropylamide, which was prepared by adding *n*-butyllithium (47.0 mL, 1.50 M in hexane, 70.4 mmol) to a solution of diisopropylamine (10.0 mL, 70.4 mmol) in THF (60 mL) at -78 °C, and the resulting solution was stirred at this temperature for 0.5 h. Diphenylstibanyl bromide (22.7 g, 64.0 mmol) in THF (50 mL) was added to this solution, and the resulting mixture was stirred for 0.5 h at this temperature. Water, which was deoxygenated by passing through a nitrogen gas for 0.5 h before use, was added to this solution, and the aqueous layer was separated under nitrogen atmosphere. The remaining organic phase was washed successively with deoxygenated saturated aqueous NH_4Cl solution and saturated aqueous NaCl solution, dried over $MgSO_4$, and filtered under nitrogen atmosphere. Solvent was removed under reduced pressure followed by distillation under reduced pressure (b.p. 155-158 °C/1.0-1.3 mmHg) to give a white solid. The solid was further purified by recrystallization from deoxygenated hexane under nitrogen atmosphere to give 6.01 g of **1a** as a white solid (38% yield). mp: 64.8-66.6 °C. ^{1}H NMR ($CDCl_3$, 400 MHz) 1.56 (s, 6H, $C(CH_3)_2$), 7.42-7.46 (m, 6H, *p*-H and *m*-H of $SbPh_2$), 7.66-7.69 (m, 4H, *o*-H of $SbPh_2$); ^{13}C NMR ($CDCl_3$, 100 MHz) 19.71, 25.39, 126.333, 129.17, 129.68, 135.95, 137.53; HRMS (EI) *m/z*: Calcd for $C_{16}H_{16}NSb$ $(M)^+$, 343.0321; Found 343.0298; IR ($CHCl_3$) 667, 760, 1211, 1431, 1520, 2399, 3019.

Tetraphenyldistibine.[18] Diphenylstibanyl bromide (11.5 g, 32.4 mmol) in THF (30 mL) was slowly added to a heterogeneous mixture of magnesium chips (0.39 g, 16.2 mmol) in THF (10 mL) over 1 h and the resulting solution was stirred at room temperature for 2 h. Water, which was deoxygenated by passing through a nitrogen gas for 0.5 h before use, was added to this solution, and the aqueous layer was separated under nitrogen atmosphere. The remaining organic phase was washed successively with deoxygenated saturated aqueous NH_4Cl solution and saturated aqueous NaCl solution, dried over Na_2SO_4, and filtered under nitrogen atmosphere. After removal of the solvent under reduced pressure, recrystallization of the residue from deoxygenated ether gave 1.97 g of tetraphenyldistibine as a pale yellow solid (24% yield). mp: 129.8-132.1 °C. ^{1}H NMR ($CDCl_3$, 400 MHz) 6.97-7.03 (m, 12H, *p*-H and *m*-H of $SbPh_2$), 7.51-7.56 (m, 8H, *o*-H of $SbPh_2$); ^{13}C NMR ($CDCl_3$, 100 MHz) 128.47, 129.19, 134.31, 137.93 ; HRMS (EI) *m/z*: Calcd for $C_{16}H_{16}NSb$ $(M)^+$, 551.9645; Found 551.9612; IR ($CHCl_3$) 812, 1161, 1329, 1452, 1618, 2274, 3235.

Typical experimental procedure for the polymerization of BA. A solution of **1a** (52.9 mg, 0.15 mmol), AIBN (2.5 mg, 0.015 mmol), and BA (2.2 mL, 15.4 mmol) was heated at 60 °C for 4.5 h under a nitrogen atmosphere in a glove box. A small portion of the reaction mixture was withdrawn and dissolved in $CDCl_3$. The conversion of monomer (87%) was determined by ^{1}H

NMR. After the volatile materials were removed under reduced pressure, the M_n (= 11000) and the MWD (M_w/M_n = 1.17) were determined by GPC calibrated with PMMA standards.

Typical experimental procedure for the polymerization of styrene. A solution of **1a** (35.1 mg, 0.10 mmol), AIBN (1.7 mg, 0.01 mmol), and St (1.20 mL, 10.2 mmol) was heated at 60 °C for 48 h under a nitrogen atmosphere in a glove box. A small portion of the reaction mixture was withdrawn and was dissolved in $CDCl_3$. The conversion of monomer (85%) was determined by ^1H NMR. The rest of the reaction mixture was dissolved in CHCl3 (5 mL) and poured into vigorously stirred methanol (200 mL). The precipitated polymer was collected by suction and was dried under vacuum at 40 °C to give polystyrene in 82% (0.89 g). Analytical GPC calibrated by polystyrene standards indicated that the polymer formed with M_n = 9,900 and M_w/M_n = 1.55.

Typical experimental procedure for the polymerization of MMA. A solution of **1a** (48.3 mg, 0.14 mmol), AIBN (2.3 mg, 0.014 mmol), tetraphenyldistibine (77.3 mg, 0.14 mmol), and MMA (1.5 mL, 14 mmol) was heated at 60 °C for 12 h under a nitrogen atmosphere in a glove box. A small portion of the reaction mixture was withdrawn and was dissolved in $CDCl_3$ (0.5 mL). Conversion of monomer (92%) was determined by ^1H NMR The rest of the reaction mixture was dissolved in $CHCl_3$ (5 mL) and poured into vigorously stirred hexane (200 mL). The precipitated polymer was collected by suction and was dried under vacuum at 40 °C to give PMMA in 91% (1.27 g). Analytical GPC calibrated by PMMA standards indicated that the polymer formed with M_n = 9,900 and M_w/M_n = 1.25.

General procedure for the chain extension test. A solution of styrene (0.38 mL, 3.3 mmol), **1a** (37.8 mg, 0.11 mmol) and AIBN (1.81 mg, 0.011 mmol) was heated at 60 °C for 36 h under a nitrogen atmosphere in a glove box. A small portion of the reaction mixture was extracted and dissolved in $CDCl_3$. The conversion of the monomer (81%) and M_n (= 2,400) and M_w/M_n (= 1.38) were determined by ^1H NMR and GPC, respectively. Styrene (2.52 mL, 22 mmol) was added to the reaction mixture, and the resulting mixture was stirred at 60 °C for 72 h under nitrogen atmosphere in a glove box. A small portion of the reaction mixture was withdrawn and dissolved in $CDCl_3$. The conversion of monomer (178%, total yield) was determined by ^1H NMR. The rest of the reaction mixture dissolved in $CHCl_3$ (10 mL) and was poured into a vigorously stirred MeOH (200 mL). The product was collected by filtration and dried under reduced pressure at 40 °C to give polystyrene in 75% (1.97 g). The resulting polystyrene possessed M_n of 18,400 and M_w/M_n of 1.51 as determined by GPC (Figure 2a). The amount of dead polymer (14%) was determined by the method reported by Fukuda. et. al.[29]

Preparation of macro CTA (2). A solution of styrene (4.78 mL, 41.7 mmol), **1a** (478 mg, 1.39 mmol), AIBN (22.8 mg, 0.14 mmol), and tetraphenyldistibine (27.8 mg, 0.03 mmol) was heated at 60 °C for 33 h. The resulting polystyrene was dissolved with 10 mL of $CHCl_3$, which was deoxygenated by bubbling nitrogen gas for 0.5 h before use, and was poured into vigorously stirred 200 mL of methanol, which was deoxygenated by bubbling nitrogen gas for 0.5 h before use, under nitrogen atmosphere in a glove box. The precipitated polymer was collected by filtration and was dried under reduced pressure to give 3.79 g of **2** (87 % yield). GPC analysis indicated the polymer formed with $M_n = 2{,}500$ and $M_w/M_n = 1.11$.

General procedure for the kinetic study. Peak resolution method for determining k_{act}.[7,35] Organostibine-mediated living radical polymerization by CTA **2a** possessing diphenylstibanyl substituents possibly includes reversible termination (RT : Figure 1c) and degenerative transfer (DT : Figure 1b) as the activation processes (Figure 1a). When both processes coexist, the pseudo-first-order activation rate constant k_{act} will take the form

$$k_{act} = k_t + k_{ex}[P\bullet]$$

in which k_t and k_{ex} are the rate constants for RT and DT, respectively.

The k_{act} was determined by the GPC peak resolution method. When P_0–$SbPh_2$ is activated, the released $P_0\bullet$ will propagate until it is deactivated to give a new adduct P_1–$SbPh_2$. (The subscripts 0 and 1 denote the number of activation.) Since P_0- $SbPh_2$ and P_1- $SbPh_2$ are generally different in chain length and its distribution, they may be distinguishable by GPC. By following the decay in [P_0–$SbPh_2$], k_{act} can be determined from the first-order plot

$$\ln([P_0\text{–}SbPh_2]_0/[P_0\text{–}SbPh_2]) = k_{act}t$$

in which $[P_0\text{–}SbPh_2]_0$ and $[P_0\text{–}SbPh_2]$ are the concentrations of **2a** at times zero and t, respectively.

The [P•] was determined monomer concentration [M] as a function of the added AIBN concentration

$$\ln([M]_0/[M]) = k_p\,[P\bullet]t$$

in which k_p are propagation rate constant of monomer

General procedure for determination of k_{act} at 60 °C for diphenylstibanyl-substituted polystyrene macro CTA 2a in styrene polymerization. A Schlenk flask was charged with the styrene solution (~ 1.5 mL) of **2a** (30 mM) and AIBN (0-20 mM) under nitrogen atmosphere in a glove box. The flask was equipped with stopcock, and was immersed in an oil bath at 60 °C with

magnetic stirring (t = 0 min). After a prescribed time t, an aliquot (0.1 mL) of the solution was taken out with a syringe, quenched in the air at room temperature, and then diluted with $CHCl_3$ to a known concentration to be analyzed by GPC. Figure 3 shows examples of time-dependent GPC chromatograms under $[\mathbf{2a}]_0$ = 30 mM and $[AIBN]_0$ = 10 mM in styrene. Figures 4 and 5 show the first-order plot of **2a** and monomer (M) concentrations ($[\mathbf{2a}]_0/[\mathbf{2a}]$ and $[M]_0/[M]$), respectively under various AIBN concentrations. In all examined cases, the plot is approximately linear, and the slopes of each line of Figures 4 and 5 give k_{act} and $k_p[P\bullet]$, respectively. Figure 6 shows plot of k_{act} vs. $k_p[P\cdot]$. The k_t (~ 0 s^{-1}) was determined from the intercept and the k_{ex} from the slope. With the known k_p (= 340 M^{-1} s^{-1}),[31] k_{ex} was calculated to be 4.0 x 10^4 M^{-1} s^{-1}.

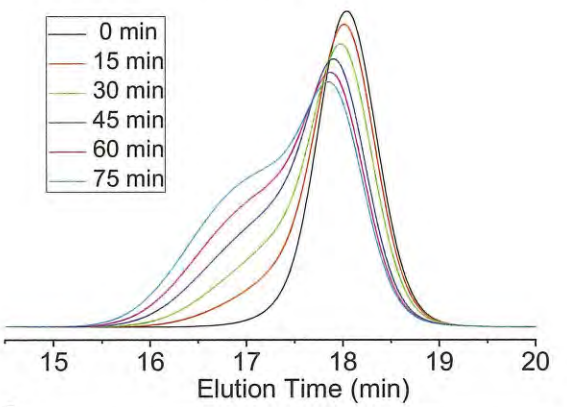

Figure 3. GPC traces for the polymerization of styrene in the presence of **2a** and AIBN at 60 °C: $[\mathbf{2a}]_0$ = 30 mM/$[AIBN]_0$ = 10 mM.

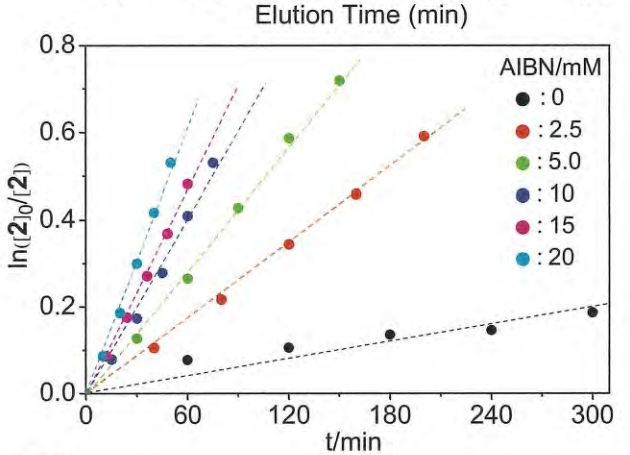

Figure 4. Plot of $\ln([\mathbf{2a}]_0/[\mathbf{2a}])$ vs. t for the polymerization of styrene in the presence of **2a** and AIBN at 60 °C: $[\mathbf{2a}]_0$ = 30 mM/$[AIBN]_0$ = 0–20 mM (as indicated in the figure).

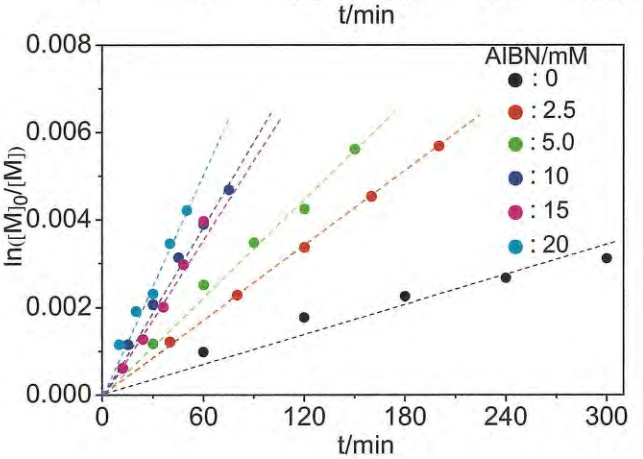

Figure 5. Plot of $\ln([M]_0/[M])$ vs. t for the polymerization of styrene in the presence of **2a** and AIBN at 60 °C: $[\mathbf{2a}]_0$ = 30 mM/$[AIBN]_0$ = 0–20 mM (as indicated in the figure).

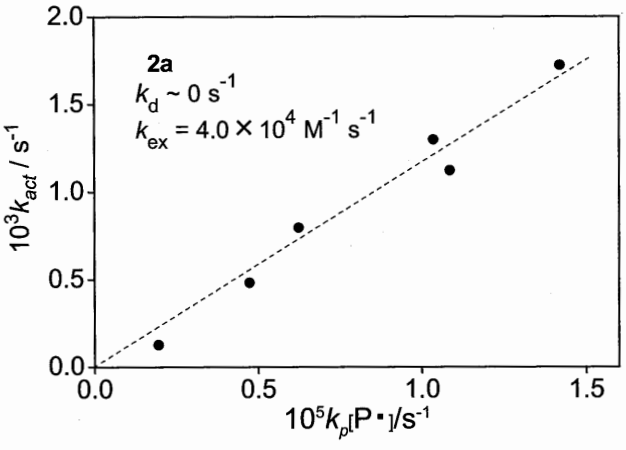

Figure 6. Plot of k_{act} vs. k_p[P•] for the polymerization of styrene in the presence of **2a** and AIBN at 60 °C: $[\mathbf{2a}]_0$ = 30 mM/$[AIBN]_0$ = 0–20 mM.

References

(1) *Handbook of Radical Polymerization*; Matyjaszewski, K.; Davis, T. P., Eds.; Wiley-Interscience: New York, 2002.

(2) Moad, G.; Solomon, D. H. *The Chemistry of Radical Polymerization*; Elsevier: Amsterdam, 2006.

(3) Lowe, A. B.; McCormick, C. L. *Prog. Polym. Sci.* **2007**, *32*, 283-351.

(4) Ouchi, M.; Terashima, T.; Sawamoto, M. *Chem. Rev.* **2009**, *109*, 4963-5050.

(5) Rosen, B. M.; Percec, V. *Chem. Rev.* **2009**, *109*, 5069-5119.

(6) Yamago, S. *Chem. Rev.* **2009**, *109*, 5051-5068.

(7) Goto, A.; Fukuda, T. *Prog. Polym. Sci.* **2004**, *29*, 329–385.

(8) Yamago, S.; Iida, K.; Yoshida, J. *J. Am. Chem. Soc.* **2002**, *124*, 2874-2875.

(9) Yamago, S.; Iida, K.; Yoshida, J. *J. Am. Chem. Soc.* **2002**, *124*, 13666-13667.

(10) Goto, A.; Kwak, Y.; Fukuda, T.; Yamago, S.; Iida, K.; Nakajima, M.; Yoshida, J. *J. Am. Chem. Soc.* **2003**, *125*, 8720-8721.

(11) Yamago, S.; Iida, K.; Nakajima, M.; Yoshida, J. *Macromolecules* **2003**, *36*, 3793-3796.

(12) Yusa, S.; Yamago, S.; Sugahara, M.; Morikawa, S.; Yamamoto, T.; Morishima, Y. *Macromolecules* **2007**, *40*, 5907-5915.

(13) Sugihara, Y.; Kagawa, Y.; Yamago, S.; Okubo, M. *Macromolecules* **2007**, *40*, 9208-9211.

(14) Kayahara, E.; Yamago, S.; Kwak, Y.; Gota, A.; Fukuda, T. *Macromolecules* **2008**, *41*, 527-529.

(15) Hasegawa, J.; Kanamori, K.; Nakanishi, K.; Hanada, T.; Yamago, S. *Macromolecules* **2009**, *42*, 1270-1277.

(16) Hasegawa, J.; Kanamori, K.; Nakanishi, K.; Hanada, T.; Yamago, S. *Macromol. Rapid Commun.* **2009**, *30*, 986-990.

(17) Yamago, S.; Ukai, Y.; Matsumoto, A.; Nakamura, Y. *J. Am. Chem. Soc.* **2009**, *131*, 2100-2101.

(18) Yamago, S.; Ray, B.; Iida, K.; Yoshida, J.; Tada, T.; Yoshizawa, K.; Kwak, Y.; Goto, A.; Fukuda, T. *J. Am. Chem. Soc.* **2004**, *126*, 13908-13909.

(19) Ray, B.; Kotani, M.; Yamago, S. *Macromolecules* **2006**, *39*, 5259-5265.

(20) Yamago, S.; Yamada, T.; Togai, M.; Ukai, Y.; Kayahara, E.; Pan, N. *Chem. Eur. J.* **2009**, *15*, 1018-1029.

(21) Yamago, S. *Chem. Rev.* **2009**, *109*, 5051-5068.

(22) Yamago, S. *Synlett* **2004**, 1875-1890.

(23) Yamago, S. *Proc. Jpn. Acad., Ser. B* **2005**, *81*, 117-128.

(24) Yamago, S. *J. Polym. Sci. Part A: Polym. Chem.* **2006**, *44*, 1-12.

(25) Kwak, Y.; Goto, A.; Fukuda, T.; Yamago, S.; Ray, B. *Zeit. Phys. Chem.* **2005**, *219*, 283-293.

(26) Kwak, Y.; Goto, A.; Fukuda, T.; Kobayashi, Y.; Yamago, S. *Macromolecules* **2006**, *39*, 4671-4679.

(27) Goto, A.; Ohno, K.; Fukuda, T. *Macromolecules* **1998**, *31*, 2809-2814.

(28) Alonzo, G.; Breunig, H. J.; Denker, M.; Ebert, K. H.; Offermann, W. *J. Organomet. Chem.* **1996**, *522*, 237-240.

(29) Goto, A.; Fukuda, T. *Macromolecules* **1997**, *30*, 5183-5186.

(30) Kajiwara, A.; Matyjaszewski, K. *Macromolecules* **1998**, *31*, 5695-5701.

(31) Yamago, S.; Yamada, T.; Togai, M.; Ukai, Y.; Kayahara, E.; Pan, N. *Chem. Eur. J.* **2009**, *15*, 1018-1029.

(32) Kwak, Y.; Tezuka, M.; Goto, A.; Fukuda, T.; Yamago, S. *Macromolecules* **2007**, *40*, 1881-1885.

(33) Barrett, A. G. M.; Melcher, L. M. *J. Am. Chem. Soc.* **1991**, *113*, 8177-8173.

(34) Goto, A.; Terauchi, T.; Fukuda, T.; Miyamoto, T. *Macromol. Rapid. Commun.* **1997**, *18*, 673-681.

(35) Goto, A.; Fukuda, T. *Prog. Polym. Sci.* **2004**, *29*, 329-385.

(36) Yamago, S.; Ray, B.; Iida, K.; Yoshida, J.; Tada, T.; Yoshizawa, K.; Kwak, Y.; Goto, A.; Fukuda, T. *J. Am. Chem. Soc.* **2004**, *126*, 13908-13909.

(37) Fukuda, T.; Goto, A.; Ohno, K. *Macromol. Rapid Commun.* **2000**, *21*, 151-165.

(38) Fukuda, T. *J. Polym. Sci. Part A* **2004**, *42*, 4743-4755.

(39) Gilbert, R. G. *Pure Appl. Chem.* **1996**, *68*, 1491-1494.

(40) We previously reported that 1-phenyltellanyl-1-phenylethane (A) was less efficient for PDI control than corresponding 1-methyltellanyl derivative in styrene polymerization (ref 14). However, the current results suggest that the previous results were affected by unexpected

factors presumably a small amount of impurities present in the transfer agent because of the difficulty to obtain pure A.

(41) Yamago, S.; Miyazoe, H.; Goto, R.; Hashidume, M.; Sawazaki, T.; Yoshida, J. *J. Am. Chem. Soc.* **2001**, *123*, 3697-3705.

(42) Kwak, Y.; Goto, A.; Fukuda, T.; Yamago, S.; Ray, B. *Z. Phys. Chem.* **2005**, *219*, 283-293.

(43) The k_d value is less accurate than the kex value because the former is more sensitive to the experimental error. Furthermore, as the kd values obtained this study were very small, we do not think that detailed comparison of the substituent effects on the k_d is significant.

(44) Yamago, S. *Jpn. Kokai Tokkyo Koho* **2005**, JP2005300277.

Chapter 3

Development of Organobismuthine-Mediated Living Radical Polymerization

Abstract

Methyl 2-dimethylbismuthanyl-2-methylpropionate (**1a**) are excellent precursors for carbon-centered radicals and promote highly controlled controlled/living radical polymerization. Both conjugated monomers,e.g., styrene, methyl methacrylate, *n*-butyl acrylate, and *N*-isopropyl acrylamide and nonconjugated monomers, e.g., *N*-vinylpyrrolidone were polymerized in a controlled manner to give well-defined polymers with predetermined molecular weights (M_ns) and narrow molecular weight distributions (MWDs). Although generation of carbon-centered radicals from organobismuthines has been reported, this is the first example for the use of them in synthetic radical chemistry. Kinetic experiments suggested that the current polymerization proceeded through two activation mechanisms, namely, thermal homolytic carbon-bismuth cleavage and degenerative group transfer mechanisms. The rate for the organobismutanyl group transfer reaction is the fastest among the group transfer and atom transfer reactions involving Group 15, 16, and 17 heteroatom compounds reported so far, indicating that organobismuthines are the most reactive toward GT reaction among their heteroatom compounds. The kinetic data are also consistent with the polymerization result that **1a** show higher MWD control than organotellurium, stibine, and iodine compounds.

Introduction

Synthetic radical chemistry of Group 16 and 17 heteroatom compounds, such as organoselenides, tellurides, bromides, and iodides, has been the subject of intensive research because of their ability to generate carbon-centered radicals under mild conditions.[1-4] In contrast, the synthetic radical chemistry of Group 15 heteroatom compounds is virtually unknown. We recently reported that organostibines are excellent precursors for carbon-centered radicals and promote highly controlled living radical polymerization.[5-11] The results prompted us to examine radical reactions involving Group 15 heteroatom compounds other than organostibines.

The key feature of organostibines in radical chemistry is their ability to undergo organostibanyl group-transfer (GT) reactions with radicals to generate new carbon-centered radicals. Although organotellurides and iodides have been reported as being the most reactive heteroatoms towards the GT and atom-transfer (AT) reactions so far,[12-17] our results show that organostibines are more reactive than these heteroatom compounds. The superior transfer ability leads to higher reaction efficiencies and controls in GT and AT additions to alkynes and alkenes,[12] such as living radical polymerization.[18,19] Furthermore, GT and AT reactions are faster with heteroatoms lower on the periodic table. Therefore, we have been interested in the reactivity of organobismuthines. We report herein that organobismuthines are indeed excellent precursors for carbon-centered radicals and promote highly controlled living radical polymerization; the level of control in organobismuthine-mediated living radical polymerization (BIRP) (Scheme 1) is considerably higher than that in organostibine-, tellurium-, and iodine-mediated radical polymerizations (SBRP,[5-7] TERP,[20-22] and IRP,[23-25] respectively). Although several examples involving the generation of radicals from organobismuthines have been reported,[26-29] this is the first example of the use of them in synthetic radical chemistry.

Scheme 1. Organo*bis*muthine-mediated living *r*adical *p*olymerization (BIRP)

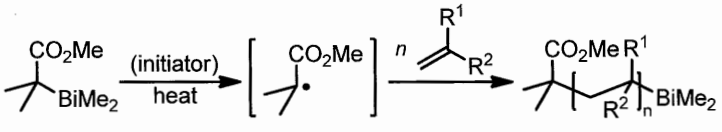

Results and Discussion

Preparation of CTA 1. Methyl 2-dimethylbismuthanyl-2-methylpropionate **1a** and 2-diphenylbismuthanyl-2-methylpropionitrile **1b** were synthesized by the analogous method for the synthesis of organostibine[5] chain transfer agents (Scheme 2). Thus, methyl isobutyrate and isobutyronitrile were treated with lithium diisopropylamide in THF at -78 °C, and the resulting anions were quenched by dimethyl- and diphenyl- bismuthanyl bromide,[30] respectively. After aqueous work up under nitrogen atmosphere, **1a** and **1b** were isolated in 47 and 51% yield as an slightly yellow oil and a pale yellow crystals by distillation and by recrystallization from diethyl ether, respectively. These compounds were easily oxidized in air but were stored for long period (> 1 year) under nitrogen atmosphere and were routinely treated in globe box.

Scheme 2. Synthesis of organobismuthine CTAs **1a** and **1b**.

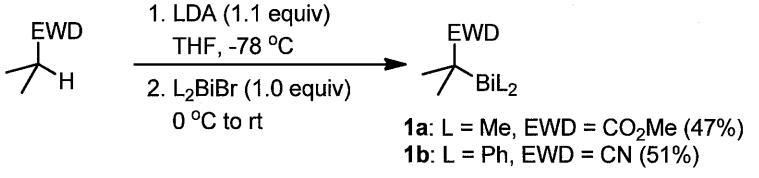

Radical mediated reaction. Generation of a carbon-centered radical from **1a** was confirmed by a tributyltin hydride mediated reduction, which was performed at 80 °C for 1 hour to give methyl 2-methylpropionate in quantitative yield (Scheme 3). When tributyltin deuteride was used, the corresponding deuterated product was formed. The rates of the reduction were not affected much by the presence of 0.1 equivalent of 2,2'-azobisisobutyronitrile (AIBN, a radical initiator) or 2,2,6,6-tetramethylpiperidinyloxy free radical (TEMPO, a radical inhibitor). When a stoichiometric amount of TEMPO was used, the corresponding TEMPO adduct **2** was obtained in 83% yield. Methyl methacryalte **3** was also obtained in 7% as byproducts with recovery of 10% of **1a**. **3** would be formed by irreversible abstraction of α-proton of carbon-centered radical generated from **1a** with TEMPO. These results indicate that the corresponding carbon-centered radical is generated from **1a** by C-Bi bond homolysis under mild thermal conditions and **1a** serve as efficient precursor of carbon-centered radical.

Scheme 3. Radical mediated reactions by using organobismuthine **1a**.

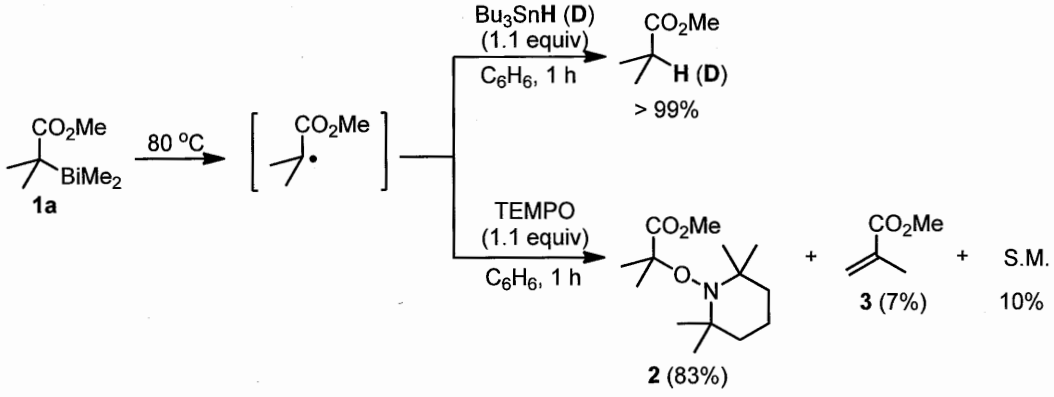

Polymerization of styrene. The bulk polymerization of styrene using **1a** as chain transfer agent (CTA) was next examined. Thus, a solution of **1a** and styrene (100 equiv) was heated at 100 °C for 4 hours. The polymerization proceeded smoothly and the number average molecular weight (M_n) increased linearly with the conversion of styrene, the values of which were very close to the theoretically calculated values from the ratio of styrene/**1a** (Table 1 and Figure 1). Furthermore, the relatively narrow molecular weight distributions (MWDs, $M_w/M_n < 1.25$) were observed from the beginning of polymerization reaction. Consequently, the polymerization was completed in 4 hours, and polystyrene with [M_n (exp) = 10500, M_n (theo) = 10100 from the ratio of styrene/**1a**)] and a narrow MWD (M_w/M_n =1.07) was obtained in quantitative yield. This result is in sharp contrast to those of TERP[20] and SBRP[5], which require 15–48 h at 100–110 °C and give MWD of 1.14–1.15

Table 1. Polymerization of styrene in the presence of organobismutine **1a**.

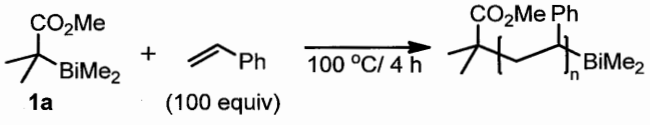

Time (h)	Conv. (%) [a]	M_n (theo)	M_n (exp) [b]	M_w/M_n [b]
0.5	18	1,900	1,200	1.24
1	31	3,200	2,900	1.14
2	60	6,200	6,700	1.09
3	80	8,300	8,000	1.10
4	99	10,100	10,500	1.07

[a]Monomer conversion was determined by ^{1}H NMR. [b]Number-average molecular weight (M_n) and molecular weight distribution (MWD = M_w/M_n) were obtained by size exclusion chromatography calibrated by polystyrene standards using $CHCl_3$ as eluent.

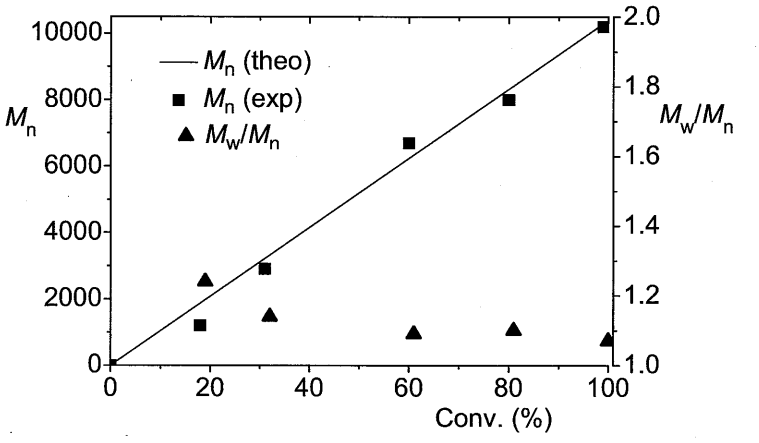

Figure 1. Correlation between monomer conversion *vs.* M_n and M_w/M_n in the polymerization of 100 equiv of styrene at 100 °C in the presence of **1a**.

Table 2. Polymerization of styrene in the presence of organobismutine **1a**.

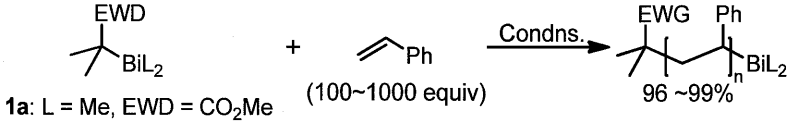

1a: L = Me, EWD = CO_2Me
1b: L = Ph, EWD = CN

(100~1000 equiv)

96 ~99%

Entry	CTA	Styrene (equiv)	Conditions (°C/h)	Conv.[a] (%)	M_n (theo)	M_n (exp)[b]	M_w/M_n[b]
1	**1a**	100	100/ 4	99	10,300	10,500	1.07
2	**1a**	200	100/ 8	96	20,000	20,100	1.09
3	**1a**	500	100/ 16	97	50,400	49,500	1.12
4	**1a**	1000	100/ 24	98	100,000	86,900	1.21
5	**1a**	1500	100/ 32	91	142,000	130,000	1.49
6[c]	**1a**	100	60/ 18	100	10,400	10,500	1.09
7	**1b**	100	100/2.5	76	8,000	18,600	1.15

[a]Monomer conversion was determined by ^1H NMR. [b]Number-average molecular weight (M_n) and molecular weight distribution (MWD = M_w/M_n) were obtained by size exclusion chromatography calibrated by polystyrene standards using $CHCl_3$ as eluent. [c]0.2 equiv of AIBN was added.

Moreover, the M_n value of polystyrene increased linearly with an increase of the styrene/**1a** ratio, and the desired high-M_n polystyrenes with narrow MWD values were obtained in all cases (Table 2, entries 1-5, and Figure 2). Although the M_n value deviated slightly from the theoretical value and the MWD value increased as the targeted M_n value

increased, a sufficiently high level of control was obtained. These results strongly support the living character of the current polymerization. Polymerization also occurred at 60 °C in the presence of AIBN (0.2 equiv) to give well-controlled polystyrene (entry 6). The styrene polymerization using **1b** as CTA also sufficiently controlled the polymerization (entry 7).

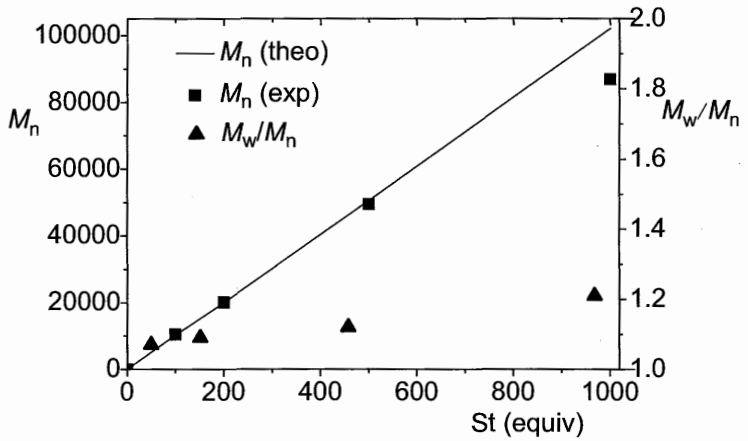

Figure 2. Correlation between the amount of styrene *vs.* M_n and M_w/M_n of the resulting polystyrene in the polymerization of styrene at 100 °C in the presence of **1a**.

Synthetic Scope. The synthetic scope of the current polymerization reaction was examined with various vinyl monomers (Table 3). Organobismuthine CTA **1a** were highly versatile and promoted controlled polymerization of both conjugated monomers, e.g., methyl methacrylate (MMA, entries 1-3), *n*-butyl acrylate (BA, entries 4–6), and *N*-isopropyl acrylamide (NIPAM, entries 7-9) and nonconjugated monomers,e.g., *N*-vinylpyrrolidone (NVP, entries 10 and 11). In all cases, the desired polymers formed with high monomer conversion and excellent control of the M_n and MWD, the level of which was considerably higher than with SBRP, TERP, and IRP. High-M_n polymers (M_n ~ 100,000) were synthesized in a controlled manner in all cases (entries 3, 6, and 9). Polymerization of BA, NIPAM, and NVP proceeded smoothly at 60 °C in the presence of AIBN (0.2 equiv), whereas it did not proceed efficiently without AIBN at 100 °C (entries 4-11).[15] This result is attributed to the strong C-Bi bond of the corresponding dormant polymer species,[31,20] from which the radical was not generated efficiently at this temperature.

Table 3. Polymerization of vinyl monomer in the presence of organobismutine **1a**.

Entry	Monomer[a] (equiv)	Conditions (°C/h)	Conv.[b] (%)	M_n (theo)	M_n (exp)[c]	M_w/M_n[c]
1	MMA (100)	100/3	99	9,900	10,800	1.10
2	MMA (500)	100/4	93	46,500	54,300	1.11
3	MMA (1000)	100/5	100	100,000	107,200	1.14
4	BA (100)	60/3[d]	97	12,400	11,000	1.10
5	BA (500)	60/8[d]	95	60,800	52,000	1.11
6	BA (1000)	60/8[d]	98	125,000	121,900	1.20
7	NIPAM (100)	60/2[def]	94	10,600	12,200	1.10
8	NIPAM (500)	60/8[d,e]	94	53,200	62,000	1.10
9	NIPAM (1000)	60/16[d,e]	93	105,000	98,700	1.15
10	NVP (100)	60/1[d]	94	10,500	11,100	1.06
11	NVP (500)	60/2[d]	100	55,600	60,000	1.12

[a]St = styrene, MMA = methyl methacrylate, BA = *n*-butyl acrylate, NIPAM = *n*-isopropyl acylamide, NVP = *N*-vinylpyrrolidone. [b]Monomer conversion was determined by ^{1}H NMR. [c] Number-average molecular weight (M_n) and molecular weight distribution (MWD = M_w/M_n) were obtained by size exclution chromatography calibrated by polystyrene standards for runs 1-3 and poly(mehyl methacrylate) standards for other entries. [d]AIBN (0.2 equiv) was added. [e]Reaction was carried out in DMF.

Confirmation of living character. The living character of the current polymerization was confirmed unambiguously by several control experiments. First, The living character was suggested by the linear increase of Mn upon conversion of monomers and monomer/**1a** ratio, as shown in the previous section.

The existence of "living" organobismuth group at the ω-polymer end was clarified by deuterium labeling experiments. Thus, polystyrene **4** (M_n = 2,900 and M_w/M_n = 1.09) bearing a dimethylbismuthanyl group at the ω-end of the polymer, was prepared in 100% yield from **1a** and styrene (30 equiv) by heating at 100 °C for 3 h. It was treated with 1.1 equiv of tributyltin deuteride at 80 °C for 1 h in the presence of AIBN (0.1 equiv) to give the ω-end deuterated polystyrene **5** (Scheme 4). Furthermore, matrix-assisted laser-desorption ionization time-of-flight mass

(MALDI-TOF MS) analysis of **5** showed the series of peaks corresponding to the molecular ion masses of **5** were observed (Figure 3).

Scheme 4. Deuterium-labeling experiment of ω-bismuthanyl group of polystyrene.

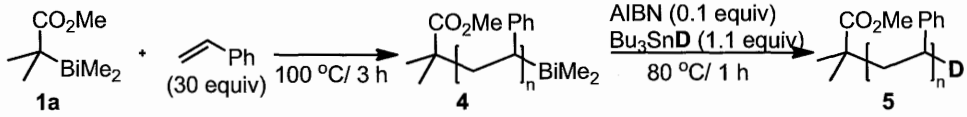

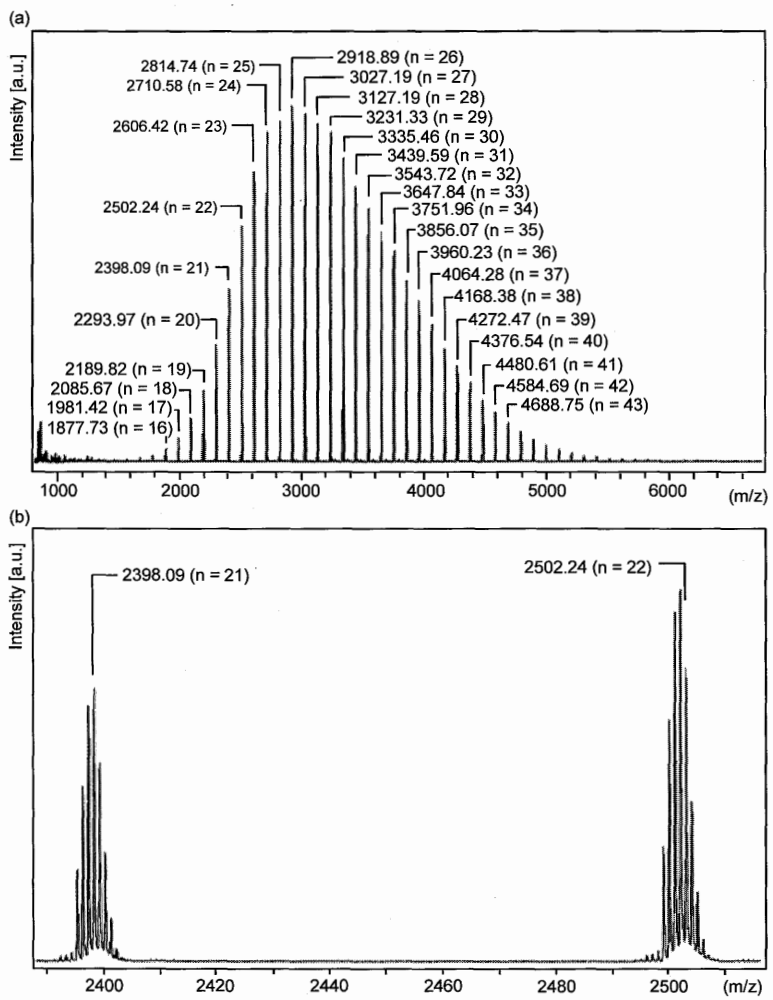

Figure 3. Full (a) and enlarged (b) TOF-MS spectra of end-deuterated polystyrene. The molecular ions were observed as silver ion adducts [$m/z = (M + Ag)^+$]. Molecular weight (M_n) and molecular weight distribution (MWD = M_w/M_n) were directly obtained by MS spectra.

Synthesis of block copolymers. Furthermore, A block copolymer, poly(styrene-*block*-NVP), was successfully synthesized by using the living polystyrene polymer end (Scheme 5). Thus, the treatment of a polystyrene macro-CTA (**4**, M_n = 6000, M_w/M_n = 1.07), which was prepared by heating the mixture of 1a and styrene (50 equiv), with NVP (100 equiv) in the presence of AIBN (0.2 equiv) in DMF at 60 °C for 18 h afforded the corresponding diblock copolymer **6** in 93% yield (M_n =15,100, M_w/M_n = 1.16). The GPC analysis of the obtained polymer revealed the disappearance of macro-CTA and the clean formation of the desired diblock copolymer (Figure 4). Since these block copolymers consist of nonpolar polystyrene segment and polar polyNVP segment, their physical properties would be of great interest.

Scheme 5. Synthesis of block copolymer.

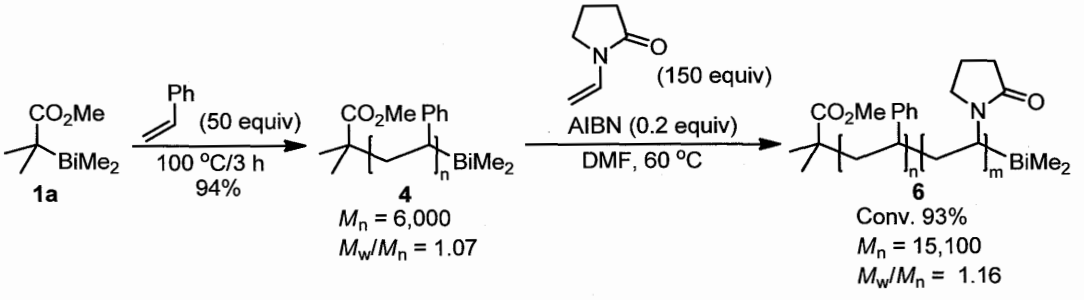

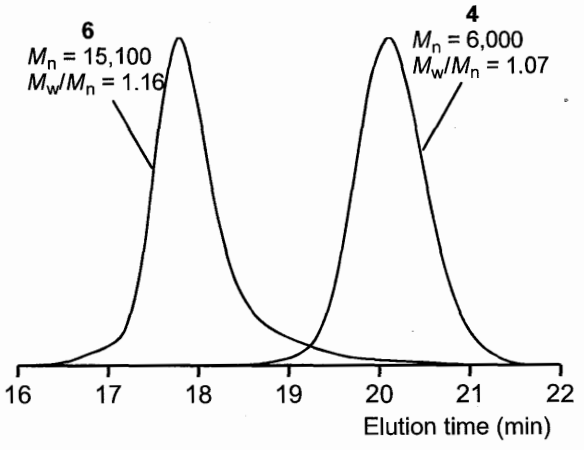

Figure 4. GPC traces of polystyrene **4** and poly(styrene-*block*-NVP) **6**.

Mechanistic studies. Kinetic experiments[32] were carried out to clarify the mechanism of BIRP. The contribution of the thermal carbon-bismuth cleavage and the degenerative chain transfer was determined in styrene polymerization according to the method previously mentioned in Chapters 1 and 2 (Scheme 6).

Scheme 6. Mechanism for BIRP.

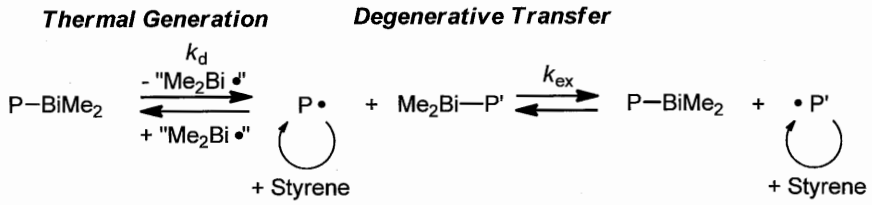

The rate constant k_{ex} for dimethylbismutanyl GT in styrene polymerization at 100 °C was determined to be 4.6 x 10^4 M^{-1} s^{-1}, which is around 2, 3, and 12 times faster than dimethylstibanyl GT, methyltellanyl GT, and iodine AT reactions, respectively. As the faster degenerative transfer leads to greater MWD control,[18,33] the kinetic data are consistent with the polymerization results. Because the organobismutanyl GT reaction is the fastest among the GT and AT reactions involving Group 15, 16, and 17 heteroatoms reported so far, BIRP has, in principle, the best MWD control among the living radical polymerization methods using heteroatom compounds.

The rate constant k_d for the thermal dissociation was determined to be 1.2 x 10^{-4} M^{-1} s^{-1} (100 °C), which is at least 2 times faster than that in SBRP, TERP, and IRP. The result indicates that organobismuthines are also the best radical initiators among the heteroatom compounds. Azo initiators cause the formation of the corresponding radical-initiated polymer upon its consumption and increase the formation of "dead" polymers. Therefore, the controllability of the polymerization decreases in the presence of azo initiators. In this respect, efficient thermal generation contributed considerably to the precise control in styrene and MMA polymerizations.

Conclusions

We have demonstrated that organobismuthines are excellent initiators and mediators for the highly controlled living radical polymerization. Both various conjugated and unconjugated vinyl monomers could be polymerized efficiently, to give the corresponding polymers with predetermined molecular weight and narrow molecular weight distribution. The high level of fidelity of organobismuthine polymer end group was unambiguously confirmed by block copolymer synthesis and labeling experiments. The results clearly open the possibility of the use of organobismuthines in controlled radical reactions. The excellent controllability and versatility of BIRP would be highly attractive for the precision synthesis of a variety of functional polymers.

Experimental Section

General. All reaction conditions dealing with air- and moisture sensitive compounds were carried out in a dry reaction vessel under nitrogen or argon atmosphere. ^{1}H NMR (400 MHz) and ^{13}C NMR (100 MHz) spectra were measured for a $CDCl_3$ or DMSO-d_6 solution of a sample. ^{1}H NMR spectra are reported in parts per million (δ) from internal tetramethylsilane or residual solvent peak, and ^{13}C NMR from solvent peak. IR spectra (absorption) are reported in cm^{-1}. High resolution mass spectra (HRMS) were obtained under electron impact ionization conditions. MALDI-TOF mass spectra were obtained in the reflection mode and at 20 kV acceleration voltage. Samples were prepared from a tetrahydrofuran (THF) solution by mixing sample (1 mg/mL), dithranol (10 mg/mL), and sodium trifluoroacetate (1 mg/mL) in a ratio of 5:1:1. The gel permeation chromatography (GPC) was performed two linearly connected polystyrene mixed gel columns, which were calibrated with polystyrene and poly(methyl methacrylate) standards. Chloroform was used as an eluant for polystyrene (PSt), poly(methyl methacrylate) (PMMA), and poly(butyl acrylate) samples, and 0.01 mol L^{-1} lithium chloride solution of DMF for poly(*N*-isopropyl acrylamide) and poly(*N*-vinylpyrroridone) samples.

Materials. Unless otherwise noted, materials were obtained from commercial suppliers and were used as received. Styrene, methyl methacrylate, butyl acrylate, and *N*-vinylpyrrolidone were washed with 5% aqueous sodium hydroxide solution and were distilled over calcium hydride under reduced pressure and stored under nitrogen atmosphere. *N*-isopropyl acrylamide was recrystalized from hexane and stored in a refrigerator. Azobis(isobutyronitrile) (AIBN) was recrystallized from methanol and stored in a refrigerator. DMF was distilled from CaH_2 and stored under nitrogen atmosphere.

Preparation of methyl 2-dimethylbismuthanyl-2-methylpropionate (1a). Lithium diisopropylamide (14.0 mL, 2.0 M solution in heptane, THF, and ethylbenzene, 28 mmol) was slowly added to a solution of methyl isobutyrate (2.86 g, 28 mmol) in THF (25 mL) at –78 °C. The resulting mixture was stirred for 10 min at this temperature, and was slowly warmed to –30 °C over 1 h. Dimethylbismuthanyl bromide[1] (8.9 g) in THF (25 mL) was added to the reaction mixture at this temperature, and the solution was slowly warmed to 0 °C over 1 h. The precipitate was filtrated off by passing through a glass wool under a nitrogen atmosphere, and the resulting solution was evaporated under reduced pressure followed by distillation under reduced pressure (b.p. 32 °C/1.5 mmHg) to give the title compound as an slightly yellow oil (4.45 g, 47%). ^{1}H NMR (400 MHz,

$CDCl_3$) 1.08 (s, 6H, $Bi(CH_3)_2$), 1.77 (s, 6H, $C(CH_3)_2$), 3.72 (s, 3H, OCH_3); ^{13}C NMR (100 MHz, $CDCl_3$) 10.12, 21.84, 24.12, 50.68, 178.28; HRMS (EI) *m/z*: Calcd for $C_7H_{15}O_2Bi$ $(M)^+$, 340.0875; Found 340.0871; IR (neat) 815, 1135, 1185, 1270, 1460, 1695, 2940.

Preparation of 2-diphenylbismuthanyl-2-methylpropionitrile (1b). Isobutyronitrile (1.1 mL, 12 mmol) in THF (10 mL) was added to a solution of lithium diisopropylamide, which was prepared by adding *n*-butyllithium (8.1 mL, 1.49 M in hexane, 12 mmol) to a solution of diisopropylamine (1.7 mL, 12 mmol) in THF (10 mL) at -78 °C, and the resulting solution was stirred at this temperature for 0.5 h. Diphenylbismuthanyl bromide[2] (4.43 g, 10 mmol) in THF (50 mL) was added to this solution, and the resulting mixture was stirred for 0.5 h at this temperature. The reaction was quenched by addition of saturated and degassed brine, and water layer was extracted by syringe. The resulting organic phase was dried by addition of magnesium sulfate, and passed through a pad of Celite under a nitrogen atmosphere. After removal of the solvent under reduced pressure, the residue was purified by recrystallization from diethyl ether to afford the titled product as pale yellow crystals (2.20 g, 51%). ^1H NMR (DMSO-d_6, 400 MHz) 1.86 (s, 6H, Bi*CH*$_3$), 7.39 (tt, J = 1.2 Hz, 7.4 Hz, 2H, ArH), 7.55 (tt, J = 1.2 Hz, 7.4 Hz, 4H, ArH), 7.90 (dt, J = 1.2 Hz, 7.4 Hz, 2H, ArH); ^{13}C NMR (DMSO-d_6, 100 MHz) 24.66, 27.33, 127.71, 128.04, 130.55, 136.34, 164.73; HRMS (EI) *m/z*: Calcd for $C_{16}H_{16}NBi$ $(M)^+$, 431.1086; Found 431.1058; IR (C_6H_6) 703, 1617, 1807, 1822, 2210, 3013, 3100.

Tributyltin hydride reduction of 1a. A solution of **1a** (34.0 mg, 0.10 mmol), tributyltin hydride (32.1 mg, 0.11 mmol), AIBN (1.6 mg, 0.01 mmol), and 5 μl tetrachloroethane (as internal standard) in 0.6 ml C_6D_6 in a sealed NMR tube was heated at 80 °C for 1 h. The ^1H NMR spectra, taken before and after heating, indicated that **1a** quantitatively converted into the methyl isobutyrate [^1H NMR (400 MHz) 1.01 (d, J = 6.8 Hz, 6 H), 2.31 (sept, J = 6.9 Hz, 1 H), 3.32 (s, 3 H)]. The addition of commercially available methyl isobutyrate (ca. 0.3 mmol) to the unsealed NMR tube increased the peak intensity of its all characteristic peaks. No appearance of the methyne proton at 2.40 ppm was observed when tributyltin deuterated was used instead of tributyltin hydride.

Reaction of 1a with TEMPO. A solution of **1a** (34 mg, 0.10 mmol) and TEMPO (18.75 mg, 0.12 mmol) in 0.6 mL C_6D_6 in a sealed NMR tube was heated at 80 °C for 1 h. The ^1H NMR spectra indicated 83 % formation of TEMPO-adduct **2**[3] and 7 % of methyl methacrylate **3** together with 10 % of unreacted **1a**. Pure **2** was isolated by preparative GPC. ^1H NMR (400 MHz, $CDCl_3$) 0.99 (s, 6H), 1.14 (s, 6H), 1.23-1.5 (m, 6H), 1.47 (s, 6H), 3.72 (s, 3H); ^{13}C NMR (100 MHz, $CDCl_3$)

17.07, 20.43, 24.46, 33.37, 40.58, 51.75, 59.53, 81.12, 176.53; HRMS (EI) *m/z*: Calcd for $C_7H_{15}O_2Bi$ $(M)^+$, 257.1991; Found 257.1994.

Typical procedure of polymerization of styrene. A solution of styrene (1.04 g, 10 mmol) and **1a** (41 μL, 0.10 mmol) was heated at 100 °C for 4 h with stirring under nitrogen atmosphere in a glove box. A small portion of the reaction mixture was taken and dissolved in $CDCl_3$. The conversion of monomer (96%) was determined by ^1H NMR. The rest of reaction mixture was dissolved in $CHCl_3$ (4 mL) and poured into a vigorously stirred methanol (200 mL). The product was collected by filtration and dried under reduced pressure at 40 °C to give 1.013 g of polystyrene. GPC analysis calibrated with polystyrene standards indicated the polymer formed with M_n = 10,500 and M_w/M_n = 1.07.

GPC traces of each experiments using **1a** by changing styrene/**1a** ratio are shown (Figure 5).

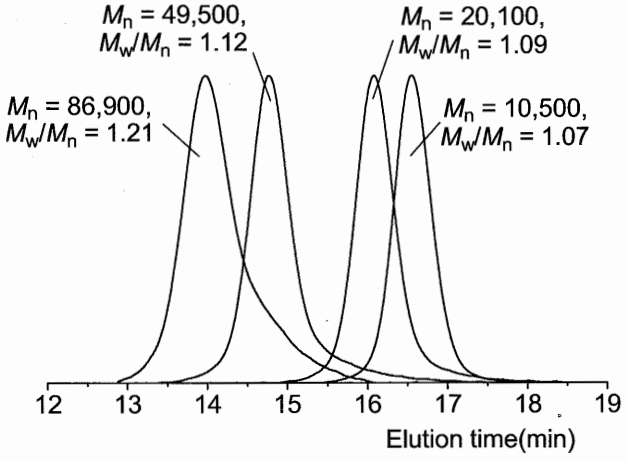

Figure 5. GPC traces of polystyrene samples prepared by varying styrene/**1a** ratio

Typical procedure of polymerization of methyl methacrylate. A solution of methyl methacrylate (1.00 g, 10 mmol) and **1a** (41 μL, 0.10 mmol) was heated at 100 °C 3 h with stirring under nitrogen atmosphere in a glove box. A small portion of the reaction mixture was withdrawn and dissolved in $CDCl_3$. The conversion of monomer (94%) was determined by ^1H NMR. The rest of reaction mixture was dissolved in $CHCl_3$ (4 mL) and poured into a vigorously stirred hexane (200 mL). The product was collected by filtration and dried under reduced pressure at 40 °C. GPC analysis calibrated with poly(methyl methacrylate) standards indicated the polymer formed with M_n = 9,900 and M_w/M_n = 1.13.

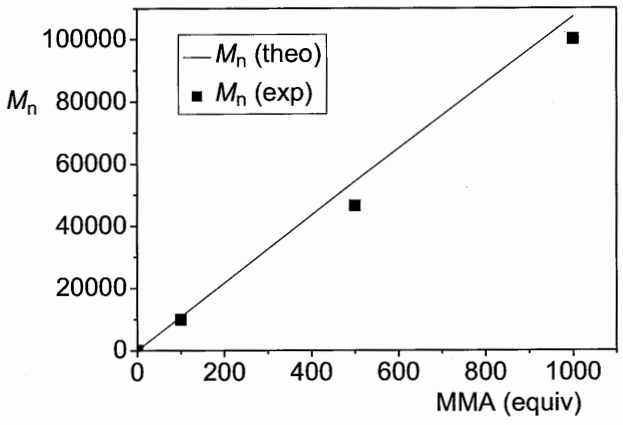

Figure 6. Correlation of experimental and theoretical molecular weight (M_n) of poly(methyl methacrylate) in the bulk polymerization of methyl methacrylate with **1a** as a function of the amount of methyl methacrylate used (100–1000 equiv).

Typical procedure of polymerization of *n*-butyl acrylate. A solution of *n*-butyl acrylate (1.28 g, 10 mmol), mediator **1a** (41 μL, 0.10 mmol), and AIBN (3.2 mg, 0.02 mmol) was heated at 60 °C for 3 h with stirring under nitrogen atmosphere in a glove box. A small portion of the reaction mixture was withdrawn and dissolved in $CDCl_3$. The conversion (97%) of monomer was determined by ^1H NMR. After the volatile materials were removed under reduced pressure, GPC analysis calibrated with poly(methyl methacrylate) standards indicated the polymer formed with M_n = 11,100 and M_w/M_n = 1.10.

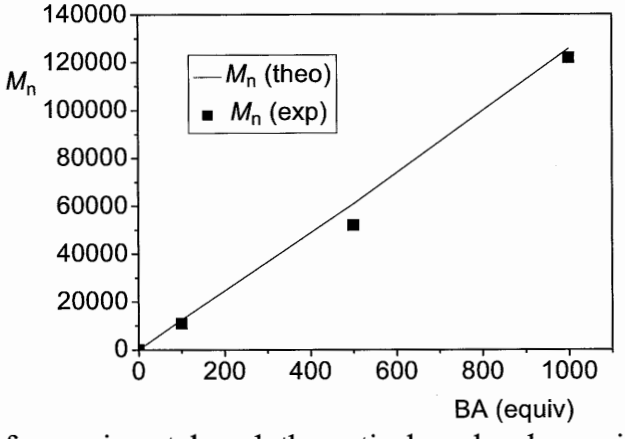

Figure 7. Correlation of experimental and theoretical molecular weight (M_n) of poly(*n*-butyl acrylate) in the bulk polymerization of *n*-butyl acrylate with **1a** as a function of the amount of *n*-butyl acrylate used (100–1000 equiv).

Typical procedure of polymerization of *N*-isopropylacrylamide. A solution of *N*-isopropylacrylamide (0.566 g, 5 mmol), mediator **1a** (21 mL, 0.05 mmol), and AIBN (1.6 mg,

0.01 mmol) in DMF (0.5 mL) was heated at 60 °C for 2 h with stirring under nitrogen atmosphere in a glove box. A small portion of the reaction mixture was withdrawn and dissolved in $CDCl_3$. The conversion of monomer (94%) was determined by ^1H NMR. The rest of reaction mixture was dissolved in $CHCl_3$ (4 mL) and poured into a vigorously stirred hexane (200 mL). The product was collected by filtration and dried under reduced pressure at 40 °C. GPC analysis calibrated with poly(methyl methacrylate) standards indicated the polymer formed with M_n = 14,400 and M_w/M_n = 1.04.

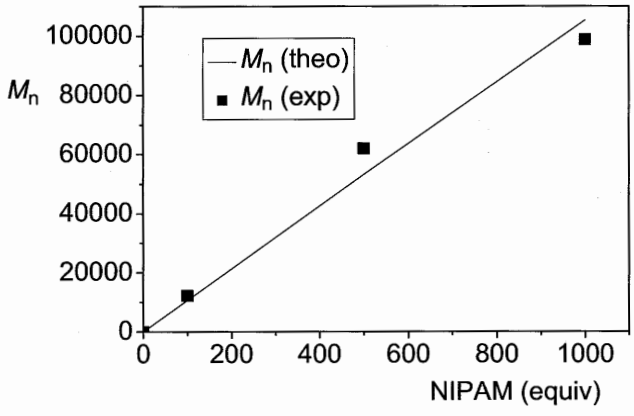

Figure 8. Correlation of experimental and theoretical molecular weight (M_n) of poly(*N*-isopropylacrylamide) in the bulk polymerization of *N*-isopropylacrylamide with **1a** as a function of the amount of *N*-isopropylacrylamide used (100–1000 equiv).

Typical procedure of polymerization of *N*-vinylpyrrolidinone. A solution of *N*-vinylpyrrolidinone (1.11 g, 10 mmol), mediator **1a** (41 μL, 0.10 mmol), and AIBN (3.3 mg, 0.02 mmol) was heated at 60 °C for 3 h with stirring under nitrogen atmosphere in a glove box. A small portion of the reaction mixture was withdrawn and dissolved in $CDCl_3$. The conversion of monomer (94%) was determined by ^1H NMR. The rest of reaction mixture was dissolved in $CHCl_3$ (4 mL) and poured into a vigorously stirred hexane (200 mL). The product was collected by filtration and dried under reduced pressure at 40 °C. GPC analysis calibrated with poly(methyl methacrylate) standards indicated the polymer formed with M_n = 11,100 and M_w/M_n = 1.06.

End-deuteration; Synthesis of polyStyrene-D (5). A solution of styrene (1.04 g, 10 mmol) and **1a** (65 μL, 0.33 mmol) was heated at 100 °C for 3 h with stirring under nitrogen atmosphere in a glove box. The resulting solid was dissolved by adding α,α,α-trifluoromethylbenzene (4 mL) at room temperature. Tributyltin deuteride (134 μL, 0.45mmol) and AIBN (5.42 mg, 0.03 mmol) was added, and the resulting mixture was stirred at 80 °C for 1 h. The reaction mixture was poured into a

vigorously stirred methanol (200 mL). The product was collected by filtration and dried under reduced pressure at 40 °C to give 1.06 g of polystyrene (100% yield). Analytical GPC indicated that the polymer formed with M_n = 2900 and M_w/M_n = 1.09. The polymer was further purified by preparative GPC (to remove residual tin compounds) for MALDI-TOF MS analysis The MS analysis indicated that the polymer formed with M_n = 3420 and M_w/M_n = 1.03.

Preparation of polystyrene macro chain transfer agent (4). A mixture of mediator **1a** (38 μL, 0.20 mmol) and styrene (0.57 mL, 10 mmol) was heated to 100 °C for 3 h with stirring under nitrogen atmosphere in a grove box. A small portion of the reaction mixture was withdrawn and dissolved in $CDCl_3$. The conversion of monomer (94%) was determined by ^1H NMR. The rest of reaction mixture was dissolved in $CHCl_3$ (4 mL) and poured into a vigorously stirred methanol (200 mL) under nitrogen atmosphere in a glove box. The product was collected by filtration in the glove box and dried under reduced pressure at room temperature. The number averaged molecular weight (M_n = 6000) and the polydispersity index (M_w/M_n = 1.07) were determined by GPC calibrated with polystyrene standard.

Synthesis of PSt-*b*-PVP block copolymer (6). A mixture of polystyrene macro chain transfer agent **4** (0.62 g, 0.10 mmol, M_n = 6000, M_w/M_n = 1.07), AIBN (3.3 mg, 0.02 mmol), and *N*-vinylpyrrolidone (1.06 mL, 10 mmol) in DMF (1.0 mL) was heated to 60 °C for 16 h with stirring under nitrogen atmosphere in a glove box. A small portion of the reaction mixture was withdrawn and dissolved in $CDCl_3$. The conversion of monomer (93%) was determined by ^1H NMR. The rest of mixture dissolved in $CHCl_3$ and was poured into a vigorously stirred hexane (200 mL). The product was collected by filtration and dried under reduced pressure at 40 °C. The number averaged molecular weight (M_n = 15100) and the polydispersity index (M_w/M_n = 1,16) were determined by GPC calibrated with poly(methyl methacrylate) standards.

References

(1) Curran, D. P. *Compreensive Organic Synthesis*; Pergamon: Oxford, 1991; Vol. 4.

(2) *Radicals in Organic Synthesis*; Renaud, P.; Sibi, M., Eds.; Wiley-VCH: Weinheim, 2000.

(3) Curran, D. P. *Aldrichimica Acta* **2000**, *33*, 104-110.

(4) Yamago, S. *Synlett* **2004**, 1875-1890.

(5) Yamago, S.; Ray, B.; Iida, K.; Yoshida, J.; Tada, T.; Yoshizawa, K.; Kwak, Y.; Goto, A.; Fukuda, T. *J. Am. Chem. Soc.* **2004**, *126*, 13908-13909.

(6) Kwak, Y.; Goto, A.; Fukuda, T.; Yamago, S.; Ray, B. *Z. Phys. Chem.* **2005**, *219*, 283-293.

(7) Ray, B.; Kotani, M.; Yamago, S. *Macromolecules* **2006**, *39*, 5259-5265.
(8) Yamago, S. *Proc. Jpn. Acad., Ser. B* **2005**, *81*, 117-128.
(9) Yamago, S. *J. Polym. Sci. Part A: Polym. Chem.* **2006**, *44*, 1-12.
(10) Moad, G.; Solomon, D. H. *The Chemistry of Radical Polymerization*; Elsevier: Amsterdam, 2006.
(11) *Handbook of Radical Polymerization*; Matyjaszewski, K.; Davis, T. P., Eds.; Wiley-Interscience: New York, 2002.
(12) Curran, D. P.; Bosch, E.; Kaplan, J.; Newcomb, M. *J. Org. Chem.* **1989**, *54*, 1826-1831.
(13) Curran, D. P.; Martin-Esker, A. A.; Ko, S. B.; Newcomb, M. *J. Org. Chem.* **1993**, *58*, 4691-4695.
(14) Benjamin, L. J.; Schiesser, C. H.; Sutej, K. *Tetrahedron* **1993**, *49*, 2557-2566.
(15) Goto, A.; Kwak, Y.; Fukuda, T.; Yamago, S.; Iida, K.; Nakajima, M.; Yoshida, J. *J. Am. Chem. Soc.* **2003**, *125*, 8720-8721.
(16) Kwak, Y.; Goto, A.; Fukuda, T.; Kobayashi, Y.; Yamago, S. *Macromolecules* **2006**, *39*, 4671-4679.
(17) Goto, A.; Ohno, K.; Fukuda, T. *Macromolecules* **1998**, *31*, 2809-2814.
(18) Fukuda, T. *J. Polym. Sci. Part A* **2004**, *42*, 4743-4755.
(19) Goto, A.; Fukuda, T. *Prog. Polym. Sci.* **2004**, *29*, 329-385.
(20) Yamago, S.; Iida, K.; Yoshida, J. *J. Am. Chem. Soc.* **2002**, *124*, 2874-2875.
(21) Yamago, S.; Iida, K.; Yoshida, J. *J. Am. Chem. Soc.* **2002**, *124*, 13666-13667.
(22) Yamago, S.; Iida, K.; Nakajima, M.; Yoshida, J. *Macromolecules* **2003**, *36*, 3793-3796.
(23) Oka, M.; Tatemoto, M. *Contemporary Topics in Polymer Science*; Plenum: New York, 1984.
(24) Matyjaszewski, K.; Gaynor, S.; Wang, J.-S. *Macromolecules* **1995**, *28*, 2093-2095.
(25) David, G.; Boyer, C.; Tonnar, J.; Ameduri, B.; Lacroix-Desmazes, P.; Boutevin, B. *Chem. Rev.* **2006**, *106*, 3936-3962.
(26) Hey, D. H.; Shingleton, D. A.; Williams, G. H. *J. Chem. Soc.* **1963**, 1958-1967.
(27) Davies, A. G.; Hook, S. C. W. *J. Chem. Soc. B.* **1970**, 735-737.
(28) Davies, A. G.; Griller, D.; Roberts, B. P. *J. Chem. Soc. B.* **1971**, 1823-1829.
(29) Barton, D. H. R.; Bridon, D.; Zard, S. Z. *Tetrahedron* **1989**, *45*, 2615-2626.
(30) Alonzo, G.; Breunig, H. J.; Denker, M.; Ebert, K. H.; Offermann, W. *J. Organomet. Chem.* **1996**, *522*, 237-240.
(31) Hawker, C. J. *Acc. Chem. Res.* **1997**, *30*, 373-382.
(32) Goto, A.; Terauchi, T.; Fukuda, T.; Miyamoto, T. *Macromol. Rapid. Commun.* **1997**, *18*, 673-681.
(33) Fukuda, T.; Goto, A.; Ohno, K. *Macromol. Rapid Commun.* **2000**, *21*, 151-165.

Chapter 4

Development of an Arylthiobismuthine Cocatalyst for Precision Control of Organobismuthine-Mediated Living Radical Polymerization

Abstract

Diphenyl(2,6-dimesitylphenylthio)bismuthine (**1a**) serves as an excellent cocatalyst in organobismuthine-mediated living radical polymerization (BIRP). Both low and high molecular weight polystyrenes and poly(butyl acrylate)s (PBAs) with controlled molecular weights and low polydispersity indices (PDIs) were synthesized by the addition of a catalytic amount of **1a** to an organobismuthine chain transfer agent, methyl 2-dimethylbismuthanyl-2-methylpropionate (**3**). The number-average molecular weight (M_n) of the resulting polymers increases linearly with the monomer/**3** ratio. Structurally well-defined polystyrenes with M_ns in the range of $1.0 \times 10^4 \sim 2.0 \times 10^5$ and PDIs of 1.07 ~ 1.15 and PBAs with M_ns in the range of $1.2 \times 10^4 \sim 2.8 \times 10^6$ and PDIs of 1.06 ~ 1.43 were successfully prepared under mild thermal conditions. Control experiments suggested that **1a** reversibly reacts with the polymer end radical to generate an organobismuthine dormant species and 2,6-dimesitylphenylthiyl radical (**2a**). This reaction avoids the occurrence of chain termination reactions involving the polymer end radicals and avoids undesired loss of the bismuthanyl polymer end group. The bulky 2,6-dimesitylphenyl group attached to the sulfur atom may prevent the addition of thiyl radicals to the vinyl monomers generating a new polymer chain.

Introduction

Living radical polymerization (LRP) has become an indispensable method for the synthesis of well-defined, advanced polymeric materials, because it allows the polymerization of a variety of functional vinyl monomers to give products with well-controlled molecular weights and molecular weight distributions.[1-3] LRPs that have been widely used include nitroxide-mediated radical polymerization,[4] atom transfer radical polymerization (ATRP),[5-7] and reversible addition-fragmentation chain-transfer radical polymerization (RAFT).[8,9] We have also developed organotellurium-,[10-13] organostibine-,[14-16] and organobismuthine-mediated[17] LRP (TERP, SBRP, and BIRP, respectively), which have proved to be powerful methods.[18,19] New variants of LRP have also emerged, such as cobalt-mediated polymerization,[20-26] single-electron transfer (SET) LRP,[27-30] titanium-catalyzed polymerization,[31] and reversible chain-transfer catalyzed polymerization.[32,33]

Despite these developments, a significant drawback of LRP is the synthesis of high molecular weight polymers. Because the polymer-end radical is always subject to irreversible termination reactions,[34] dead polymers accumulate in the reaction mixture as the targeted molecular weight increases. Nevertheless, a few examples of the synthesis of high molecular weight polyacrylates and polymethacrylates have been reported, with number-average molecular weights (M_ns) sometimes exceeding 1 x 10^6, which usually correspond to degree of polymerization of more than 10^4. For example, ultra-high molecular weight poly(methyl methacrylate), with M_ns in the range 1.3 - 3.6 x 10^6 and narrower molecular weight distributions (MWDs) of less than 1.3, have been prepared by RAFT[35] and ATRP[36,37] under high pressure conditions. However, this method requires special apparatus and is hence synthetically unattractive. The only examples thus far reported under ambient conditions are the synthesis of poly[2-(dimethylamino)ethyl methacrylate] with M_n = 8.5 x 10^5 by ATRP,[38] poly(methyl acrylate) with M_n = 1.4 x 10^6 by SET LRP using a copper catalyst,[28] and poly(butyl methacrylate) with M_n = 1.0 x 10^6 by ATRP under miniemulsion conditions.[39] The synthesis of high molecular weight polystyrene is more difficult than that of poly(meth)acrylates because of the existence of autoinitiation and the slow propagation rate. The synthesis of polystyrene by RAFT with an M_n of 2 x 10^5 and a MWD of 1.12 has been reported, but under high pressure conditions.[40] Ultrahigh molecular weight poly(meth)acrylates and polystyrenes with M_ns exceeds 10^7 were synthesized by plasma initiated polymerization, but its synthetic efficiency and generality were quite limited.[41] Therefore, the development of a new method that allows the synthesis of high molecular weight polymers under ambient conditions is desirable, but is also a significant challenge.

In chapter 3, we found that BIRP allows better control of MWD than TERP and SBRP for the synthesis of low molecular weight polymers (M_n < 1 x 10^5). However, when the target molecular weight of the polymers synthesized by BIRP was increased, we observed an apparent loss of MWD control. We also observed the precipitation of black particles, presumably bismuth metal, indicating the loss of the organobismuthine polymer-end group. Therefore, if the loss of this polymer-end group could be avoided, BIRP would be suitable for the synthesis of high molecular weight polymers in a controlled manner.

We have already reported that the addition of ditellurides[11] and distibines[16] effectively increases the MWD control that can be achieved in TERP and SBRP, respectively, for the polymerization of styrene and methyl methacrylate (MMA). Kinetic studies of the effect of ditelluride revealed that it acts as a capping reagent for the polymer-end radical (P•) through a homolytic substitution reaction, forming a dormant species P-TeR (Scheme 1a).[42] The liberated tellanyl radical (RTe•) is essentially inert towards the monomers but reacts with the organotellurium dormant species to regenerate the polymer-end radical and the ditelluride. In contrast, deactivation of the polymer end radical to the dormant species in the absence of ditelluride proceeds by a homolytic substitution reaction with the organotellurium dormant species, that is, a degenerative transfer reaction (Scheme 1b).[43,44] In the case of the methyltellanyl group (X = TeMe), the rate of deactivation by the ditelluride is approximately 100 times faster than that by the organotellurium dormant species in the polymerization of styrene, and this is the origin of the increased MWD control achieved by the addition of ditellurides. We envisioned that faster deactivation would decrease the occurrence of undesired termination reaction of the polymer end radicals, and that this type of diheteroatom compound is thus potentially useful as a cocatalyst for the synthesis of high molecular weight polymers.

Scheme 1. Mechanisms of activation/deactivation of polymer-end radical P· by (a) ditelluride $(TeR)_2$ and distibine $(SbR_2)_2$, and (b) organotellurium (P-TeR), organostibine ($P\text{-}SbR_2$), and organobismuthine ($P\text{-}BiR_2$) dormant species.

(a) Deactivation by ditelluride or distibine

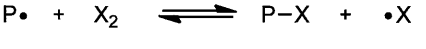

X = TeR, SbR_2

(b) Deactivation by tellurium, stibine, and bismuthine dormant species

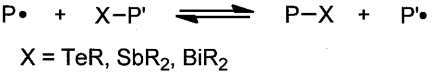

X = TeR, SbR_2, BiR_2

By analogy with the effects of ditellurides and distibines, dibismuthines would be a formidable cocatalyst for BIRP. However, these compounds are thermally labile. For example, tetramethyldibismuthine decomposes even at room temperature,[45] and thus dibismuthines cannot be used as cocatalysts in this process. We focused on arylthiobismuthine **1** as a potential cocatalyst (Scheme 2). Barton and coworkers have already reported that tris(phenylthio)bismuthine generates a benzenethiyl radical upon reaction with carbon-centered radicals.[46] Therefore, we expected that **1** should react with polymer-end radicals to form an organobismuthine dormant species and an arylthiyl radical **2**. We have recently found that arylthiyl radicals are highly reactive towards organobismuthines to generate carbon-centered radicals through homolytic substitution reactions.[47] Therefore, radical **2** should react with the organobismuthine dormant species to regenerate the polymer-end radical (P·) and **1**. Thiyl radicals are also reactive towards alkenes, [48] and the degree of control over the LRP would diminish if **2** were to react with the monomers. Therefore, we decided to use an arylthiyl radical bearing the sterically bulky mestyl group (Mes = 2,4,6-$Me_3C_6H_2$) at both the 2- and 6-positions. We chose this substituent because of its well known steric shielding effect and also ease of availability of the precursor of **1a** (R^1 = Ph, R^2 = Mes), namely 2,6-dimesitylbenzenethiol.[49,50]

Scheme 2. Hypothetical reaction of arylthiobismuthines with a polymer-end radical P

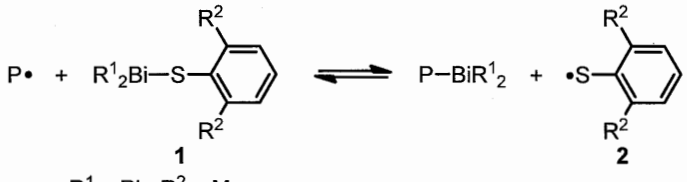

a: R^1 = Ph, R^2 = Mes
b: R^1 = Ph, R^2 = H
c: R^1 = Me, R^2 = Mes

We report here on the synthesis of arylthiobismuthine cocatalyst **1** and its effect on BIRP. We show that BIRP becomes more controllable in the presence of a catalytic amount of **1a** (R^1 = Ph, R^2 = Mes), allowing the synthesis of high molecular weight polystyrenes ($M_n \sim 2 \times 10^5$) and ultra-high molecular weight polyacrylates ($M_n \sim 3 \times 10^6$) with well-controlled molecular weight distributions, starting from monofunctional organobismuthine chain transfer agents, such as **3** (eq 1). This is the first example in which the synthetic utility of thiobismuthines in controlling radical reactions and radical polymerization has been demonstrated. We also propose a mechanism shown in Scheme 2 for the action of **1** based on several control experiments. This new deactivation mechanism of

polymer end radicals in addition to the conventional degenerative transfer of organobismuthines (Scheme 1b, X = BiR_2) should be responsible for the successful synthesis of ultrahigh molecular polymers.

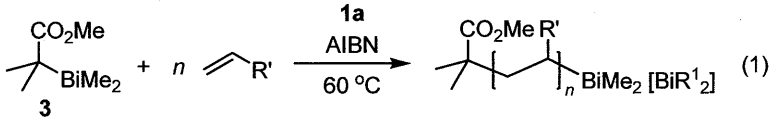

Results and Discussion

Synthesis of arylthiobismthine 1. 2,6-Dimesitylbenzenethiol[50] was treated with *n*-butyl lithium (1.1 equiv) in THF at -78 °C, followed by diphenylbismuthanyl bromide[51] (Scheme 3). The desired thiobismuthine **1a** was isolated in 69% yield by silica gel chromatography followed by recrystallization as a yellow crystal stable towards air and moisture. Diphenyl(phenylthio)bismuthine (**1b**), which has no sterically bulky substituents on the arylthiyl group, was prepared in 75% yield starting from benzenethiol. Synthesized dimethyl(2,6-dimesitylphenylthio)bismuthine (**1c**) was also carried out. Though **1c** was obtained as a major component as an air-sensitive amorphous, some impurities could not be completely removed. Therefore, we used **1c** only for mechanistic studies, because the degree of control achievable in LRP is sometimes strongly influenced by a small amount of an impurity.

Scheme 3. Synthesis of arylthiobismuthine derivatives

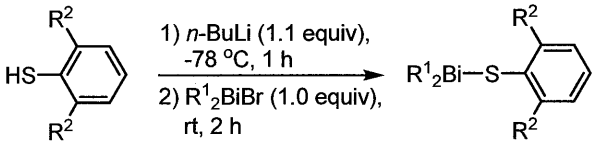

1a: R^1 = Ph, R^2 = Mes (69%)
1b: R^1 = Ph, R^2 = H (75%)
1c: R^1 = Me, R^2 = Mes (82%)

Effect of 1 on polymerization of styrene by BIRP. We first examined the effects of **1a** on the polymerization of styrene using organobismuthine **3** as a chain transfer agent (Table 1). When a mixture of **3**, 2,2'-azobis-isobutyronitrile (AIBN) (0.2 equiv), **1a** (0.2 equiv), and styrene (1000 equiv) was heated at 60 °C under a nitrogen atmosphere in a glove box, polystyrene formed with quantitative monomer conversion as judged by ^{1}H NMR spectroscopy (Table 1, entry 1). The slightly yellowish crude product (Figure 1a) was dissolved in chloroform, and precipitation from

methanol gave polystyrene as a white powder. Analysis by gel permeation chromatography (GPC) indicated the formation of highly-controlled polystyrene with the M_n close to that calculated from the monomer/**3** ratio [M_n(exp) = 103,000] and with a narrow MWD (M_w/M_n = 1.11). When the amount of **1a** was increased to 0.5 and 1.0 equiv, we also obtained highly-controlled polystyrenes with narrow MWDs (M_w/M_n = 1.13–1.14) as colorless products (Table 1, entries 2 and 3). However, the degree of control achieved, as indicated by the M_n and MWD, was slightly lower than that attained in the presence of 0.2 equiv of **1a**.

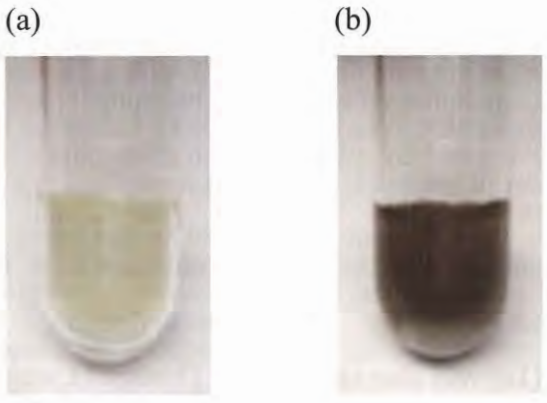

Figure 1. Effects of **1a** on color of polystyrene crude product prepared (a) in the presence of **1a** (Table 1, entry 1) and (b) in the absence (Table 1, entry 6)

The addition of 0.2 equiv of **1b** also resulted in the formation of a colorless product, but the polymerization was less controlled than that in the presence of **1a** in terms of both M_n and PDI (Table 1, entry 4). This result clearly indicates the importance of using a sterically bulky mesityl group. Polymerization under the same reaction conditions without the addition of **1a** resulted in a high monomer conversion (86%), but a black precipitate appeared in the reaction mixture (Figure 1b). Furthermore, the M_n of the resulting polymer was approximately 20% lower than the theoretical value, and the MWD was broader than that of the product formed in the presence of **1a** (Table 1, entry 5). The effects of tetraphenyldibismuthine, which is thermally more stable than tetramethyl derivative,[41] were also investigated. However, the reaction mixture became black, and no improvement of the MWD control was observed (entry 6). These results clearly indicate that the addition of **1a** considerably suppresses the loss of the organobismuthanyl polymer-end and increases the control over the M_n and MWD of the products.

The effects of **1a** were further investigated by carrying out the polymerization of 2000 equiv of styrene (Table 1, entries 7-10). Polymerization in the presence of **1a** (0.2-1.0 equiv) resulted in high monomer conversions and gave colorless polymers in all cases (Table 1, entries 7–9). Highly controlled polystyrenes with narrow MWDs and M_ns close to the theoretical values were obtained in all cases. The use of 0.2 equiv of **1a** was most effective in attaining a high monomer conversion, a high degree of control of the M_n and a narrow MWD. Polystyrene with M_n of 2.0×10^5 and MWD of 1.15 was obtained under optimized conditions (entry 7). In contrast, polymerization carried out in the absence of **1a** did not reach a high monomer conversion after 96 h, and afforded polystyrene with a rather broad MWD of 1.34. The formation of a black precipitate was also observed in the reaction mixture (Table 1, entry 10).

The M_n of the polystyrene could be controlled by the styrene/**3** ratio but not by the styrene/**1a** ratio, and thus both low molecular weight ($M_n \sim 10{,}000$) and high molecular weight polystyrenes could be selectively synthesized by varying the styrene/**3** ratio in the presence of 0.2 equiv of **1a** (Table 1, entries 11-15 and Figure 2). These results clearly indicate that **1a** does not initiate the polymerization. The effect of **1a** on the M_n and MWD of the product was marginal for the synthesis of low molecular weight polystyrenes ($M_n < 50{,}000$), but it became more significant as the targeted molecular weight increased ($M_n > 50{,}000$). The M_ns for polystyrene prepared in the presence of **1a** linearly increased with the amount of styrene used, as shown by the filled squares in Figure 2, and were all close to the corresponding theoretical values. This linear correlation is consistent with the living character of the polymerization. GPC traces of the polystyrenes were unimodal in all cases, and the peak maxima shifted towards higher molecular weight as the styrene/**3** ratio increased (Figure 3).

Table 1. Effect of arylthiobismuthine **1** on polymerization of styrene[a]

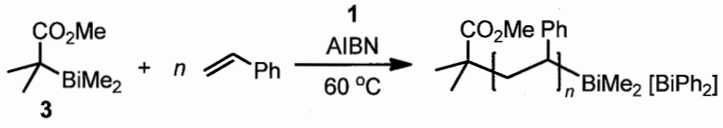

Entry	Equiv	**1** (equiv)	Time (h)	Conv. (%)[b]	M_n (theo)	M_n (exp)[c]	M_w/M_n[c]
1	1,000	**1a** (0.2)	84	98	102,000	103,000	1.11
2	1,000	**1a** (0.5)	84	83	86,400	85,500	1.13
3	1,000	**1a** (1.0)	84	82	85,400	80,500	1.17
4	1,000	**1b** (0.2)	84	88	91,500	90,200	1.27
5	1,000	$(Ph_2Bi)_2$ (0.2)[d]	84	75	78,100	69,200	1.31
6	1,000	None	84	96	99,800	81,900	1.21
7	2,000	**1a** (0.2)	96	94	196,000	198,000	1.15
8	2,000	**1a** (0.5)	96	94	167,000	147,000	1.15
9	2,000	**1a** (1.0)	96	81	169,000	130,000	1.22
10	2,000	None	96	55	115,000	107,000	1.34
11	100	**1a** (0.2)	24	96	10,000	10,900	1.07
12	200	**1a** (0.2)	32	99	20,600	24,700	1.09
13	500	**1a** (0.2)	60	99	51,600	55,500	1.10
14	700	**1a** (0.2)	65	100	72,800	79,500	1.11
15	1,500	**1a** (0.2)	90	96	150,000	139,000	1.13
16	100	**1b** (0.2)	24	100	10,400	13,600	1.13
17	500	**1b** (0.2)	60	100	52,000	54,700	1.18
18	1000	**1a** (0.2)	84	86	89,600	84,600	1.13

[a]A mixture of **3**, **1** (0-1.0 equiv), AIBN (0.2 equiv), and styrene was heated under a nitrogen atmosphere. [b]Monomer conversion was determined by ^{1}H NMR. [c]Number-average molecular weight (M_n) and molecular weight distribution (MWD = M_w/M_n) were obtained by size exclusion chromatography, which was calibrated using polystyrene standards, using $CHCl_3$ as the eluent. [d]Tetraphenyldibismuthine was added instead of **1**.

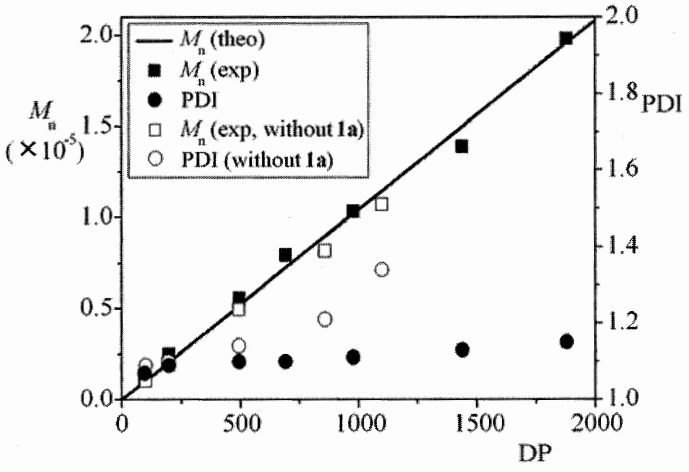

Figure 2. Correlation between the degree of polymerization (DP) of styrene and the number-average molecular weight (M_n) and molecular weight distribution (MWD = M_w/M_n) of the resulting polystyrenes, for the bulk polymerization of styrene with **3** at 60 °C in the presence or absence of **1a**.

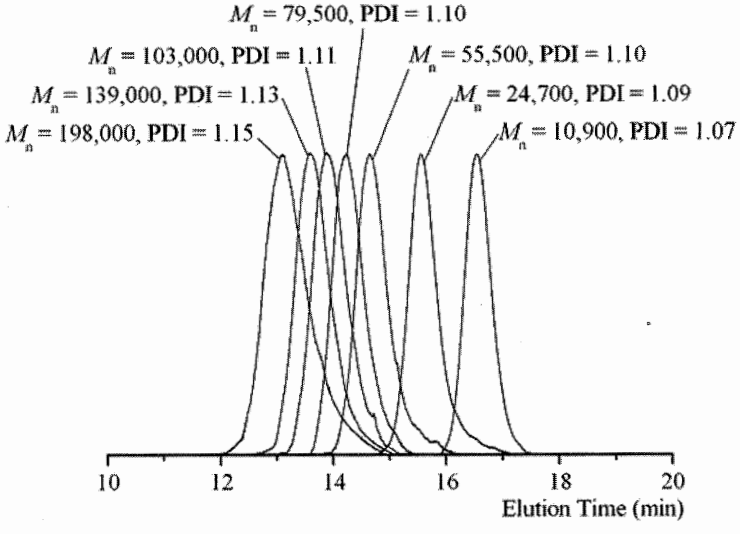

Figure 3. GPC traces of polystyrenes synthesized by varying the styrene/**3** ratio

The living character of the polymerization was further confirmed by control experiments. At first, kinetic studies were carried out by using 100 equiv of styrene. The plot of monomer conversion versus time shown in Figure 4a indicates that pseudo-first-order kinetics with respect to the monomer were followed, implying that the concentration of the radical species remained constant during the polymerization. The apparent rate constant (k_p^{app}) was determined to be 0.11 h^{-1}. A linear correlation was observed between the M_n of the polystyrene and the monomer conversion (Figure 4b). The MWD was rather high at low monomer conversion (M_w/M_n = 1.23 at 24%

conversion), but it decreased as the polymerization progressed (M_w/M_n = 1.08 at 95% conversion). Second, a chain extension experiment was examined. Thus, polystyrene (M_n = 8,200, M_w/M_n = 1.09) was prepared from **3** and 100 equiv of styrene in the presence of 0.2 equiv of **1a** and AIBN at 60 °C in 85% monomer conversion, and styrene (100 equiv) was added to the crude reaction mixture. After being heated at 60 °C for 18 h, we obtained the chain extended polystyrene with M_n = 19,600 and M_w/M_n = 1.12. GPC traces clearly revealed that the initially formed polystyrene was completely converted. All of these results are consistent with the living character of the polymerization under the current conditions.

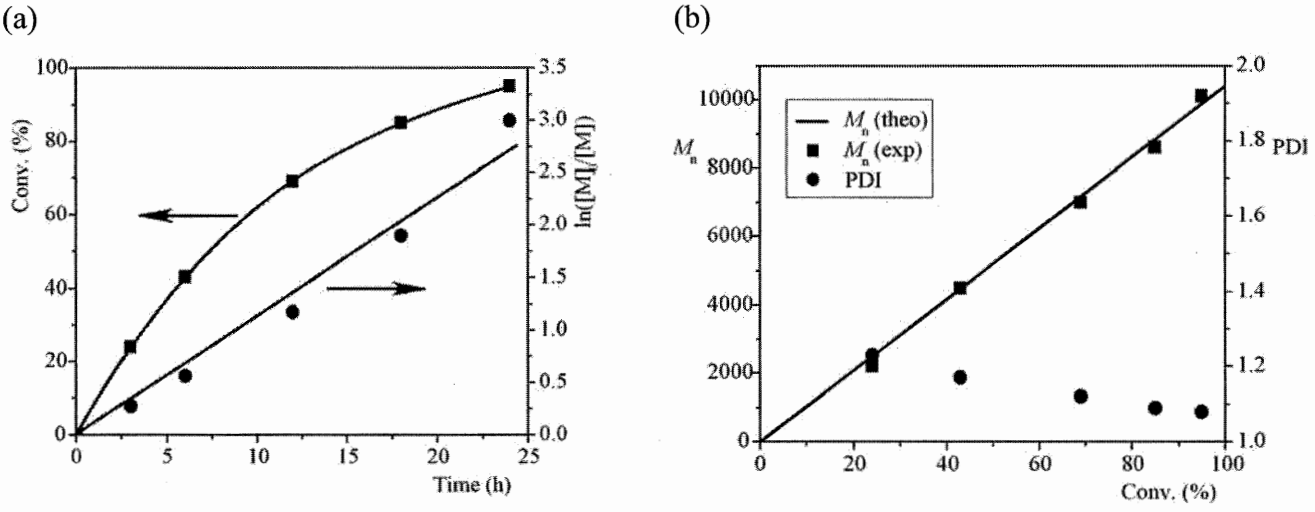

Figure 4. (a) First-order plot of monomer conversion *vs* time and (b) correlation of M_n and MWD on monomer conversion for the bulk polymerization of styrene (100 equiv) at 60 °C in the presence of **3** and **1a**

Polymerization of *n*-butyl acrylate by BIRP in the presence of a cocatalyst We next studied the polymerization of *n*-butyl acrylate (BA, 100 equiv) by BIRP using chain transfer agent **3** and AIBN (0.2 equiv) in the presence of **1a** (0.2 equiv) at 60 °C. The polymerization was complete within 0.5 h, and the desired poly(butyl acrylate) (PBA) was obtained in 82% yield. The M_n of 11,600 was close to the theoretical value calculated from the BA/**2** ratio and the MWD was 1.06 (Table 2, entry 1). The rate of polymerization followed first-order kinetics to the monomer and M_n increased linearly with the monomer conversion. These results are again consistent with the living character of the polymerization.

We also examined the synthesis of high and ultrahigh molecular weight PBAs by increasing the BA/**3** ratio from 500 to 50,000 in the presence of 0.2 equiv of **1a** (Table 2, entries 2–8). The range of M_ns obtained for the resulting PBAs was so wide that two sets of GPC columns were

necessary for the analysis: the exclusion limit of the first system was M_n = 2 x 10^6 and that of the second was 2 x 10^7. We found that the M_n increased linearly with the BA/**3** ratio, although the monomer conversion decreased due to the increase of viscosity of the reaction mixture. Highly controlled PBAs with narrow MWDs and M_ns close to their theoretical values were obtained in all cases. The GPC traces of all the PBAs were unimodal, and the peak maxima shifted to higher molecular weight as the targeted molecular weight increased (Figure 5). It is worth noting that a PBA with an M_n of 1.4 x 10^6 and a MWD of 1.22 was obtained at 47% monomer conversion when 20,000 equiv of BA was employed (Table 2, entry 7). Moreover, a PBA with an M_n of 2.8 x 10^6 was obtained at 41% monomer conversion when 50,000 equiv of BA was employed (Table 2, entry 8).

Table 2. Organobismuthine-mediated living radical polymerization of *n*-butyl acrylate (BA) in the presence of co-catalyst **1a**[a]

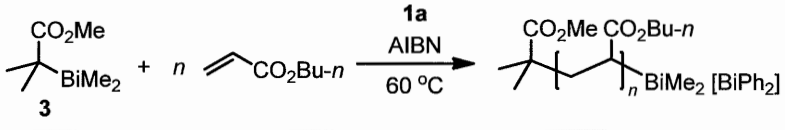

Entry	equiv	Time (h)	Conv. (%)[b]	M_n (theo)	M_n(exp)[c]	M_w/M_n[c]
1	100	0.5	82	10,500	11,600	1.06
2	500	1.5	85	54,400	45,400	1.08
3	1,000	2	82	105,000	131,000	1.12
4	4,000	4	72	369,000	295,000	1.18
5	8,000	5	63	646,000	528,000	1.19
					(491,000)	(1.18)
6	10,000	6	58	743,000	735,000	1.20
					(701,000)	(1.21)
7	20,000	7	47	1,200,000	1,370,000	1.22
8	50,000	9	41	2,630,000	2,820,000	1.43

[a]A mixture of **3**, **1a** (0.2 equiv), AIBN (0.2 equiv), and BA was heated under a nitrogen atmosphere. [b]Monomer conversion was determined by ^{1}H NMR. [c]Number-average molecular weight (M_n) and molecular weight distribution (MWD = M_w/M_n) were obtained by size exclusion chromatography, which was calibrated using polyMMA standards. Two linearly connected columns with exclusion limit = 2 x 10^6 using $CHCl_3$ as the eluent were used for runs 1-6, and a similar setup with exclusion limit = 2 x 10^7 using THF as the eluent was used for runs 5-8. The data obtained from the THF system are shown in parenthesis for runs 5 and 6.

Although the MWD of the latter product was slightly broader (M_w/M_n = 1.43) than those of the smaller molecular weight polymers, it is still acceptable. This product represents the highest molecular weight polyacrylate thus far synthesized under a controlled manner by LRP from a monofunctional chain transfer agent and under ambient conditions.

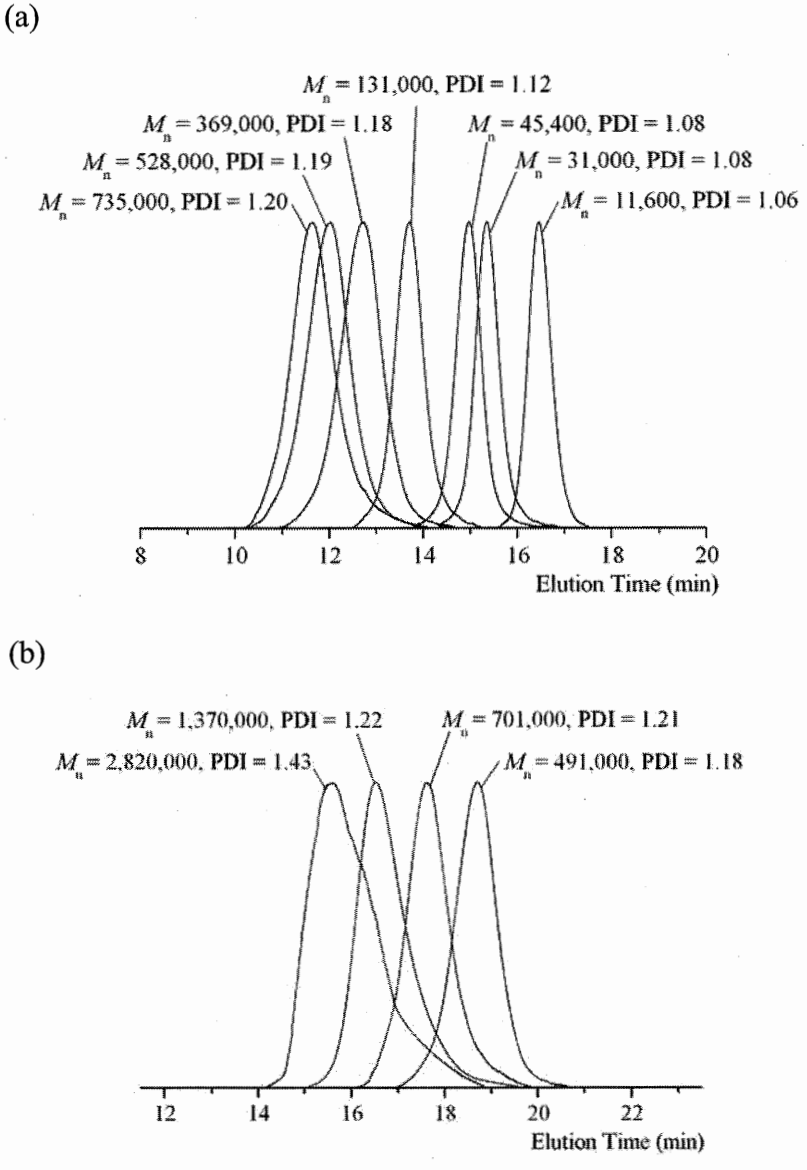

Figure 5. GPC traces of PBA samples prepared by varying the BA/**3** ratio measured by GPC columns with (a) exclusion limit = 2 x 10^6 and (b) exclusion limit = 2 x 10^7

Mechanism of action of the cocatalyst. The role of cocatalyst **1** was examined. First, a 1:1 mixture of organobismuthine chain transfer agent **4** and thiobismuthine **1a** was heated in the presence of AIBN (0.1 equiv) in THF-d_8 at 80 °C in an NMR tube, and the reaction mixture was

monitored by ^{1}H NMR (Scheme 4). Equal amounts of **4** and **1a** were slowly consumed and a new set of signals corresponding to organobismuthine **5** and thiobismuthine **1c** appeared. The reaction reached to an 8:2 mixture of **4** (or **1a**) to **5** (or **1c**) after 3 h, and the ratio did not change further on prolonged heating. Next, the reverse reaction starting from a mixture of **5** and **1c** was examined at 80 °C in the presence of 0.1 equiv of AIBN. Although the reaction was slow and further addition of AIBN was required (0.1 equiv at 3, 6, and 9 h), a mixture of **4** (or **1a**) and **5** (or **1c**) in the ratio 8:2 was eventually reached after 11h. These results indicate that equilibrium was reached in both cases.

Scheme 4. Bismuthanyl group exchange reaction between organobismuthine and thiobismuthine

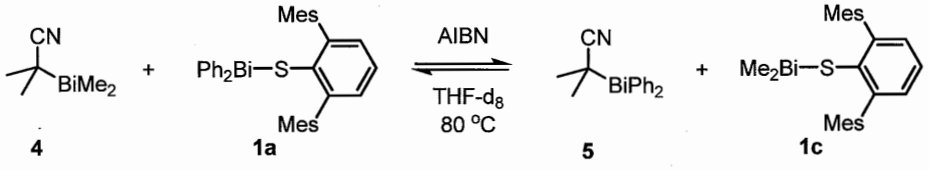

A plausible mechanism to account for this exchange reaction is shown in Scheme 5. The carbon-centered radical **6** generated from AIBN reacts with **1a** or **1c** to give **4** or **5**, respectively, and 2,6-dimesitylphenylthiyl radical (**2a**). This thiyl radical then reacts with **4** or **5** to regenerate **6** and **1a** or **1c**. Both the reaction of **6** with **1** and of **2a** with **4** or **5** took place unselectively regardless of the substituent on the bismuth atom (R^1 = Ph or Me). Therefore, the reaction eventually reached equilibrium giving a statistical mixture of compounds.

Scheme 5. Radical-mediated exchange reaction of bismuthanyl groups

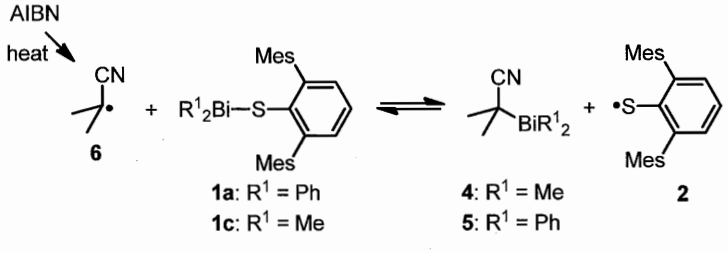

These results also imply that the homolytic substitution reaction of the polymer-end radical with **1a** occurs as shown in Scheme 2. This effective deactivation of the polymer-end radical must be responsible for the increased control of the PDI and for the successful synthesis of high molecular weight polymers that are possible in the presence of **1a**. The results may be also explained by the formation of a stable (but not persistent) hypervalent bismuthanyl radical by the

reaction of the polymer-end radical with **1a**. However, this scenario is less likely, because, if such a radical formed, the rate retardation of the polymerization would be observed due to the occurrence of chain-breaking termination reactions, as observed in RAFT polymerization.[52-56]

Conclusions

We have shown that highly-controlled BIRP is possible by carrying out the polymerization in the presence of a newly designed arylthiobismuthine cocatalyst **1a**. High molecular weight polystyrenes and ultra-high molecular weight poly(butyl acrylate)s have been synthesized in a controlled manner in the presence of this cocatalyst. In addition to its synthetic utility, this work also provides insight into the fundamental reactivities of diheteroatom compounds in radical reactions. The reactivity of the Bi-S s bond towards carbon-centered radicals and the presence of a sterically bulky aryl group on the sulfur atom of the cocatalyst are responsible for the success in the synthesis of high molecular weight polymers. It is our hope that this work will inspire renewed interest in the use of heteroatom-heteroatom s bonds as heteroatom compounds for the precision control of radical reaction.

Experimental Section

General. All reaction conditions dealing with air- and moisture sensitive compounds were carried out in a dry reaction vessel under nitrogen atmosphere. ^{1}H NMR (400 MHz) and ^{13}C NMR (100 MHz) spectra were measured for a $CDCl_3$ solution of a sample. ^{1}H NMR spectra are reported in parts per million (δ) from internal tetramethylsilane or residual solvent peak, and ^{13}C NMR from solvent peak. IR spectra (absorption) are reported in cm^{-1}. High resolution mass spectra (HRMS) were obtained under electron impact ionization conditions. Gel permeation chromatography (GPC) was performed on a liquid chromatography equipped with two linearly connected polystyrene mixed gel columns (exclusion limit = 2 x 10^6 [Shodex LF-604] or exclusion limit = 2 x 10^7 [Shodex KF-806]), which were calibrated against polystyrene or poly(methyl methacrylate) standards using chloroform or THF as an eluant. Detection was made by a refractive-index (RI) at 40 °C.

Materials. Unless otherwise noted, materials obtained from commercial suppliers were used as received. Styrene and butyl acrylate were washed with 5% aqueous sodium hydroxide solution and were distilled over calcium hydride under reduced pressure and stored in a refrigerator under nitrogen atmosphere. Azobis(isobutyronitrile) (AIBN) was recrystallized from methanol and stored

in a refrigerator. Diphenylbismuthanyl bromide,[1] dimehylbismuthanyl bromide[1] and 2,6-dimesitylbenzenethiol[2] were prepared according to the literature procedure. Methyl 2-dimethylbismuthanyl-2-methylpropionate (**3**) and 2-diphenylbismuthanyl-2-methylpropionitrile (**5**) was prepared as reported.[3]

Preparation of diphenyl(2,6-dimesitylphenylthio)bismthine (1a). *n*-Butyllithium (11.0 mL, 1.55 M solution in hexane, 17 mmol) was slowly added to a solution of 2,6-dimesitylbenzenethiol[50] (5.89 g, 17 mmol) in ether (30 mL) at –78 °C. The resulting mixture was stirred for 1 h at this temperature, and was slowly warmed to room temperature over 1 h. Diphenylbismuthanyl bromide[51] (6.65 g, 15 mmol) was added to the reaction mixture at 0 °C, which was then stirred for 2 h at room temperature. Water was added, and the organic phase was separated. The organic phase was successively washed with saturated aqueous NH_4Cl solution and saturated aqueous NaCl solution, dried over $MgSO_4$, and was then passed through a pad of Celite. Removal of the solvent under reduced pressure, and recrystallization of the residue from chloroform/hexane gave 7.32 g of **1a** as pale yellow crystals (69% yield). mp: 140.0-142.4 °C. ^{1}H NMR (400 MHz, $CDCl_3$) 2.03 (s, 12H, *o*-CH_3 of mesityl), 2.30 (s, 6H, *p*-CH_3 of mesityl), 6.87 (s, 4H, *m*-H of mesityl), 7.13 (d, J = 7.6 Hz, 2H, *m*-H of SAr), 7.20 (tt, , J = 7.6, 1.2 Hz, 2H, *p*-H of $BiPh_2$), 7.26-7.32 (m, 1H, *p*-H of SAr, 4H, *m*-H of $BiPh_2$), 7.44 (dt, J = 6.8, 1.2 Hz, 4H, *o*-H of $BiPh_2$); ^{13}C NMR (100 MHz, $CDCl_3$) 21.00, 21.12, 127.19, 127.55, 128.28, 128.82, 130.65, 133.84, 135.79, 136.46, 136.92, 139.37, 146.63, 165.51; HRMS (EI) *m/z*: Calcd for $C_{36}H_{35}SBi$ $(M)^+$, 708.2262; Found 708.2263; IR (neat) 815, 1135, 1185, 1270, 1460, 1695, 2940.

Diphenyl(phenylthio)bismuthine (1b). *n*-Butyllithium (19.5 mL, 1.46 M solution in hexane, 28 mmol) was slowly added to a solution of benzenethiol (2.80 mL, 28 mmol) in THF (30 mL) at –78 °C. The resulting mixture was stirred for 1 h at this temperature, and was slowly warmed to room temperature over 1 h. Diphenylbismuthanyl bromide (11.1 g, 25 mmol) was added at 0 °C, and the resulting mixture was stirred for 2 h at room temperature. Water was added, and organic phase was separated. The organic phase was successively washed with saturated aqueous NH_4Cl solution and saturated aqueous NaCl solution, dried over $MgSO_4$, and was passed through a pad of Celite. After removal of the solvent under reduced pressure, recrystallization of the residue from ether gave 8.88 g of **1b** as a yellow solid (75% yield). mp: 91.7-92.7 °C. ^{1}H NMR (400 MHz, $CDCl_3$) 7.03-7.07 (m, 1H, *p*-H of SPh), 7.09- 7.14 (m, 2H, *m*-H of SPh), 7.30-7.34 (m, 2H, *o*-H of SPh, 2H, *p*-H of $BiPh_2$), 7.50 (t, J = 7.6 Hz, 4H, *m*-H of $BiPh_2$), 8.03 (dd, J = 8.0, 1.2 Hz, 4H, *o*-H of $BiPh_2$); ^{13}C NMR (100 MHz, $CDCl_3$) 126.41, 128.33, 128.50, 131.39, 134.64, 135.47, 137.22,

167.22; HRMS (EI) *m/z*: Calcd for $C_{36}H_{35}SBi$ $(M)^+$, 472.0698; Found 472.0700; IR (KBr) 692, 923, 991, 1016, 1114, 1369, 1435, 1473, 1574, 1709, 2220, 2251, 2924, 2964, 3057.

Dimethyl(2,6-dimesitylphenylthio)bismuthine (1c). *n*-Butyllithium (5.80 mL, 1.55 M solution in hexane, 9.0 mmol) was slowly added to a solution of 2,6-dimesitylbenzenethiol (2.77 g, 8.0 mmol) in THF (30 mL) at –78 °C. The resulting mixture was stirred for 1 h at this temperature, and was slowly warmed to room temperature over 1 h. Dimethylbismuthanyl bromide (2.55 g, 8.0 mmol) was added at 0 °C, and the resulting mixture was stirred for 2 h at room temperature. Volatile materials were removed under reduced pressure, and deoxygenated hexane (30 mL) was introduced. The insoluble precipitate (LiBr) was filtered through a pad of Celite under nitrogen atmosphere, and hexane was removed up to the first appearance of particle under reduced pressure. The cooling of the solution gave 3.84 g of as a yellow crystal, which was predominantly consisted of **1c**. Several attempts to increase the purity were so far unsuccessful. mp: 67.0-68.7 °C. ^{1}H NMR (400 MHz, C_6D_6) 0.98 (s, 6H, $BiMe_2$), 2.06 (s, 12H, *o*-CH_3 of mesityl), 2.33 (s, 6H, *p*-CH_3 of mesityl), 6.92 (s, 4H, *m*-H of mesityl), 7.03 (d, J = 7.2 Hz, 2H, *m*-H of SAr), 7.21 (t, J = 7.2 Hz, 1H, *p*-H of SAr); ^{13}C NMR (100 MHz, C_6D_6) 15.96, 21.20, 21.23, 126.27, 128.60, 129.13, 136.09, 136.40, 136.62, 140.09, 145.76; HRMS (EI) *m/z*: Calcd for $C_{26}H_{31}SBi$ $(M)^+$, 584.1950; Found 584.1954. IR (C_6H_6) 689, 721, 733, 955, 1012, 1055, 1078, 1431, 1471, 1570, 3037.

2-Dimethylbismuthanyl-2-methylpropionitrile (4) Isobutyronitrile (1.00 mL, 11.0 mmol) in THF (10 mL) was added to a THF solution of lithium diisopropylamide, which was prepared by adding *n*-butyllithium (7.72 mL, 1.47 M in hexane, 11.5 mmol) to a solution of diisopropylamine (1.54 mL, 11.0 mmol) in THF (10 mL) at -78 °C, and the resulting solution was stirred at this temperature for 0.5 h. Dimethylbismuthanyl bromide[1] (3.19 g, 10.0 mmol) in THF (50 mL) was added to this solution, and the resulting mixture was stirred for 0.5 h at this temperature. The reaction was quenched by addition of saturated sodium chloride solution, which was deoxygenated by passing through a nitrogen gas for 0.5 h before use. After the water phase was separated, magnesium sulfate was added to the organic phase under a nitrogen atmosphere, and the resulting solution was passed through a pad of Celite under a nitrogen atmosphere. After removal of the solvent under reduced pressure, recrystallization of the residue from deoxygenated diethyl ether gave 1.88g of **4** as a white solid (61% yield). mp: 58.6-59.8 °C. ^{1}H NMR ($CDCl_3$, 400 MHz) 1.29 (s, 6H, $BiCH_3$), 1.79 (s, 6H, $C(CH_3)_2$); ^{13}C NMR ($CDCl_3$, 100 MHz) 11.67, 24.78, 25.79, 128.24; HRMS (EI) *m/z*: Calcd for $C_{16}H_{16}NBi$ $(M)^+$, 307.0774; Found 307.0764; IR ($CHCl_3$) 667, 725, 790, 929, 1207, 1222, 1421, 1520, 2198, 2399, 3019.

Typical procedure for polymerization of styrene. A solution of styrene (1.15 mL, 10.0 mmol), **1a** (14.2 mg, 0.020 mmol), AIBN (3.28 mg, 0.020 mmol) and **3**[17] (18.28 μL, 0.10 mmol) was heated at 60 °C for 24 h with stirring under a nitrogen atmosphere in a glove box. A small portion of the reaction mixture was extracted and dissolved in $CDCl_3$. The conversion of the monomer (96%) was determined by ^1H NMR. The rest of the reaction mixture was dissolved in a 10 mM TEMPO/$CHCl_3$ solution (4 mL) and poured into vigorously stirred methanol (200 mL). The product was collected by filtration and dried under reduced pressure at 40 °C to give 0.99 g of polystyrene. The number-averaged molecular weight (M_n = 10,900) and the MWD (M_w/M_n = 1.07) were determined by GPC calibrated using polystyrene standards.

Typical procedure of polymerization of *n*-butyl acrylate. A solution of *n*-butyl acrylate (1.43 mL, 10.0 mmol), **1a** (14.2 mg, 0.02 mmol), AIBN (3.28 mg, 0.02 mmol) and **3** (18.3 μL, 0.10 mmol) was heated at 60 °C for 0.5 h with stirring under nitrogen atmosphere in a glove box. A small portion of the reaction mixture was taken and dissolved in $CDCl_3$. The conversion of monomer (82%) was determined by ^1H NMR. After the volatile materials were removed under reduced pressure, the number averaged molecular weight (M_n = 11600) and the MWD (M_w/M_n = 1.06) were determined by GPC calibrated with poly(methyl methacrylate) standards. Figure 6 (a) and (b) show the plot of monomer conversion vs *t* and correlation between M_n and PDI *vs.*

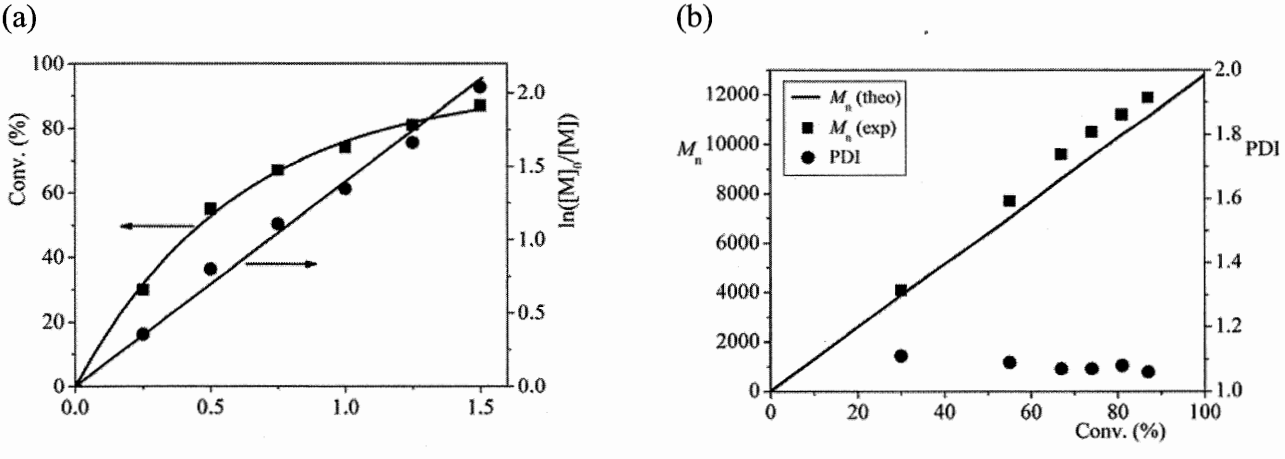

Figure 6. (a) First-order plot of monomer conversion *vs* time and (b) correlation of M_n and PDI on monomer conversion for the bulk polymerization of butyl acrylate (100 equiv) at 60 °C in the presence of **3**, **1a**, and AIBN.

monomer conversion of the resulting poly(*n*-butyl acrylate) for the polymerization of 100 equiv of *n*-butyl acrylate in the presence of in the presence of **3**, **1a**, and AIBN (0.1 equiv), respectively. The apparent rate constant (k_p^{app}) was determined to be 1.44 h^{-1}.

Chain extension experiment. A solution of styrene (1.15 mL, 10.0 mmol), **1a** (14.2 mg, 0.020 mmol), AIBN (3.28 mg, 0.020 mmol) and **3** (18.28 μL, 0.10 mmol) was heated at 60 °C for 18 h with stirring under a nitrogen atmosphere in a glove box. A small portion of the reaction mixture was extracted and dissolved in $CDCl_3$. The conversion of the monomer (85%) was determined by ^1H NMR, and M_n (= 8,200) and M_w/M_n (= 1.09) were determined by GPC. The rest of reaction mixture was dissolved in styrene (1.15 mL, 10.0 mmol) and was heated at 60 °C for 18 h with stirring under nitrogen atmosphere in a glove box. A small portion of the reaction mixture was withdrawn and dissolved in $CDCl_3$. The conversion of monomer (191%, total yield) was determined by ^1H NMR. The rest of mixture dissolved in $CHCl_3$ and was poured into a vigorously stirred MeOH (200 mL). The product was collected by filtration and dried under reduced pressure at 40 °C. The resulting polystyrene possessed M_n of 19,600 and M_w/M_n of 1,12 as determined by GPC (Figure 7).

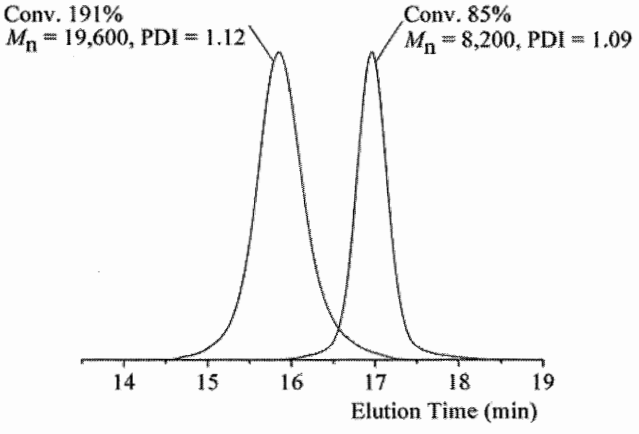

Figure 7. GPC traces of polystyrene samples before and after the chain extension

References

(1) *Handbook of Radical Polymerization*; Matyjaszewski, K.; Davis, T. P., Eds.; Wiley-Interscience: New York, 2002.

(2) Moad, G.; Solomon, D. H. *The Chemistry of Radical Polymerization*; Elsevier: Amsterdam, 2006.

(3) Braunecker, W. A.; Matyjaszewski, K. *Prog. Polym. Sci.* **2007**, *2007*, 93-146.

(4) Hawker, C. J.; Bosman, A. W.; Harth, E. *Chem. Rev.* **2001**, *101*, 3661-3688.
(5) Matyjaszewski, K.; Xia, J. *Chem. Rev.* **2001**, *101*, 2921-2990.
(6) Ouchi, M.; Terashima, T.; Sawamoto, M. *Acc. Chem. Res.* **2008**, *41*, 1120-1132.
(7) Kamigaito, M.; Ando, T.; Sawamoto, M. *Chem. Rev.* **2001**, *101*, 3689-3746.
(8) Moad, G.; Rizzardo, E.; Thang, S. H. *Polymer* **2008**, *49*, 1079-1131.
(9) Lowe, A. B.; McCormick, C. L. *Prog. Polym. Sci.* **2007**, *32*, 283-351.
(10) Yamago, S.; Iida, K.; Yoshida, J. *J. Am. Chem. Soc.* **2002**, *124*, 2874-2875.
(11) Yamago, S.; Iida, K.; Yoshida, J. *J. Am. Chem. Soc.* **2002**, *124*, 13666-13667.
(12) Yusa, S.; Yamago, S.; Sugahara, M.; Morikawa, S.; Yamamoto, T.; Morishima, Y. *Macromolecules* **2007**, *40*, 5907-5915.
(13) Sugihara, Y.; Kagawa, Y.; Yamago, S.; Okubo, M. *Macromolecules* **2007**, *40*, 9208-9211.
(14) Yamago, S.; Ray, B.; Iida, K.; Yoshida, J.; Tada, T.; Yoshizawa, K.; Kwak, Y.; Goto, A.; Fukuda, T. *J. Am. Chem. Soc.* **2004**, *126*, 13908-13909.
(15) Ray, B.; Kotani, M.; Yamago, S. *Macromolecules* **2006**, *39*, 5259-5265.
(16) Yamago, S.; Yamada, T.; Togai, M.; Ukai, Y.; Kayahara, E.; Pan, N. *Chem. Eur. J.* **2009**, *15*, 1018-1029.
(17) Yamago, S.; Kayahara, E.; Kotani, M.; Ray, B.; Kwak, Y.; Goto, A.; Fukuda, T. *Angew. Chem. Int. Ed.* **2007**, *46*, 1304-1306.
(18) Yamago, S. *J. Polym. Sci., Part A: Polym. Chem.* **2005**, *44*, 1-12.
(19) Yamago, S. *Proc. Jpn. Acad., Series B: Phys. Biol. Sci.* **2005**, *81*, 117-128.
(20) Gridnev, A. A.; Ittel, S. D. *Chem. Rev.* **2001**, *101*, 3611-3660.
(21) Wayland, B. B.; Poszmik, G.; Mukerjee, S. L. *J. Am. Chem. Soc.* **1994**, *116*, 7943-7944.
(22) Debuigne, A.; Caille, J.-R.; Jérôme, R. *Angew. Chem. Int. Ed.***2005**, *44*, 1101-1104.
(23) Debuigne, A.; Caille, J.-R.; Jérôme, R. *Macromolecules* **2005**, *38*, 5452-5458.
(24) Debuigne, A.; Caille, J.-R.; Willet, N.; Jérôme, R. *Macromolecules* **2005**, *38*, 9488-9496.
(25) Bryaskova, R.; Detrembleur, C.; Debuigne, A.; Jérôme, R. *Macromolecules* **2006**, *39*, 8263-8268.
(26) Debuigne, A.; Willet, N.; Jérôme, R.; Detrembleur, C. *Macromolecules* **2007**, *40*, 7111-7118.
(27) Percec, V.; Popov, A. V.; Ramirez-Castillo, E.; Monteiro, M.; Barboiu, B.; Weichold, O.; Asandei, A. D.; Mitchell, C. M. *J. Am. Chem. Soc.* **2002**, *124*, 4940-4941.
(28) Percec, V.; Guliashvili, T.; Ladislaw, J. S.; Wistrand, A.; Stjemdahl, A.; Sienkowska, M. J.; Monteiro, M.; Sahoo, S. *J. Am. Chem. Soc.* **2006**, *128*, 14156-14165.
(29) Lligadas, G.; Rosen, B. M.; Monteiro, M. J.; Percec, V. *Macromolecules* **2008**, *41*, 8360-8364.
(30) Lligadas, G.; Rosen, B. M.; Bell, C. A.; Monteiro, M. J.; Percec, V. *Macromolecules* **2008**, *41*, 8365-8371.

(31) Asandei, A. D.; Moran, I. W. *J. Am. Chem. Soc.* **2002**, *126*, 15932-15933.

(32) Goto, A. Z., H.; Hirai, N.; Wakada, T.; Tsujii, Y.; Fukuda, T. *J. Am. Chem. Soc.* **2007**, *129*, 13348-13354.

(33) Goto, A.; Hirai, N.; Wakada, T.; Nagasawa, K.; Tsujii, Y.; Fukuda, T. *Macromolecules* **2008**, *41*, 6261-6264.

(34) Fukuda, T.; Terauchi, T.; Goto, A.; Ohno, K.; Tsujii, Y.; Miyamoto, M.; Kobatake, S.; Yamada, B. *Macromolecules* **1996**, *29*, 6393-6398.

(35) Rzayev, J.; Penelle, J. *Angew. Chem. Int. Ed.* **2004**, *43*, 1691-1694.

(36) Kwiatkowski, P.; Jurczak, J.; Pietrasik, J.; Jakubowski, W.; Mueller, L.; Matyjaszewski, K. *Macromolecules* **2008**, *41*, 1067-1069.

(37) Arita, T.; Kayama, Y.; Ohno, K.; Tsujii, Y.; Fukuda, T. *Polymer* **2008**, *49*, 2426-2429.

(38) Mao, B. W.; Gan, L. H.; Gan, Y. Y. *Polymer* **2006**, *47*, 3017-3020.

(39) Simms, R. W.; Cunningham, M. F. *Macromolecules* **2007**, *40*, 860-866.

(40) Arita, T.; Buback, M.; Janssen, O.; Vana, P. *Macromol. Rapid Commun.* **2004**, *25*, 1376-1381.

(41) Simionescu, C. I.; Simionescu, B. C. *Pure. Appl. Chem.* **1984**, *1984*, 427-438.

(42) Kwak, Y.; Tezuka, M.; Goto, A.; Fukuda, T.; Yamago, S. *Macromolecules* **2007**, *40*, 1881-1885.

(43) Goto, A.; Kwak, Y.; Fukuda, T.; Yamago, S.; Iida, K.; Nakajima, M.; Yoshida, J. *J. Am. Chem. Soc.* **2003**, *125*, 8720-8721.

(44) Kwak, Y.; Goto, A.; Fukuda, T.; Kobayashi, Y.; Yamago, S. *Macromolecules* **2006**, *39*, 4671-4679.

(45) Ashe III, A. J.; Ludwig Jr., E. G.; Oleksyszyn, J. *Organometallics* **1983**, *2*, 1859-1866.

(46) Barton, D. H. R.; Bridon, D.; Zard, S. Z. *Tetrahedron* **1989**, *45*, 2615-2626.

(47) Yamago, S.; Matsumoto, A. *J. Org. Chem.* **2008**, *73*, 7300-7304.

(48) *Sulfur-Centered Radicals*; Bertrand, M. P.; Ferreri, C., Eds.; WILEY-VCH: Weinheim, 2001; Vol. 2.

(49) Power, P. P. *J. Organomet. Chem.* **2004**, *689*, 3904-3919.

(50) Ellison, J. J.; Ruhlandt-Senge, K.; Power, P. P. *Angew. Chem. Int. Ed.* **1994**, *33*, 1178-1180.

(51) Clegg, W.; Errington, R. J.; Fisher, G. A.; Hockless, D. C. R.; Norman, N. C.; Orpen, A. G.; Stratford, S. E. *J. Chem. Soc. Dalton Trans.* **1992**, 1967-1974.

(52) Monteiro, M.; de Brouwer, H. *Macromolecules* **2001**, *34*, 349-352.

(53) Kwak, Y. G., A.; Tsujii, Y.; Murata, Y.; Komatsu, K.; Fukuda, T. *Macromolecules* **2002**, *35*, 3026-3029.

(54) Calitz, F. M.; McLeary, J. B.; McKenzie, J. M.; Tonge, M. P.; Klumperman, B.; Sanderson, R. D. *Macromolecules* **2003**, *36*, 9687-9690.

(55) Kwak, Y.; Goto, A.; Komatsu, M.; Sugiura, Y.; Fukuda, T. *Macromolecules* **2004**, *37*, 4434-4440.

(56) Feldermann, A.; Coote, M. L.; Stenzel, M. H.; Davis, T. P.; Barner-Kowollik, C. *J. Am. Chem. Soc.* **2004**, *126*, 15915-15923.

Chapter 5

Synthesis of Structurally Well-controlled ω-Vinylidene Functionalized Poly(alkyl methacrylate)s and Polymethacrylonitrile by Organotellurium, Organostibine, Organobismuthine-Mediated Living Radical Polymerization

Abstract

The reaction of poly(methyl methacrylate) (PMMA), poly(*i*-butyl methacrylate), poly(2-hydroxyethyl methacrylate), and polymethacrylonitrile bearing organotellurium, organostibine, and organobismuthine ω-living polymer end groups with 2,2,6,6-tetramethylpiperidine 1-oxy (TEMPO) under thermal or photochemical conditions gave the corresponding ω-vinylidene functionalized polymethacrylates and polymethacrylonitrile with high end group fidelity. Treatment of the PMMA with ethyl 2-[(tributylstannyl)methyl]acrylate also gave a PMMA bearing the same ω-vinylidene end functionality. ^{1}H NMR, GPC, MALDI TOF MS, and thermogravimetric analyses revealed the highly controlled and defined structure of poly(alkyl methacrylate)s and polymethacrylonitrile in terms of molecular weight, molecular weight distribution, and the ω-polymer end structure.

Introduction

There has been growing interest on new synthetic methods for the preparation of structurally well-defined polymers with controlled chain-end functional groups.[1,2] Among various end-functionalized polymers, ω-vinylidene functionalized polymethacrylates of general structure **1** (Chart 1) have been regarded as important precursors of copolymers[3] and block copolymers[4] and as chain transfer agents.[5,6] They were usually prepared by the catalytic chain transfer polymerization of methacrylate monomers using cobalt catalysts[7,8] and by radical copolymerization of methacrylates with α-thioalkoxymethacrylates[9-11] or an α-bromomethacrylate.[12] Although these methods provided the desired polymers with high ω-end group fidelity, control of macromolecular structure in terms of molecular weight and molecular weight distribution (MWD) was difficult so far due to the occurrence of chain transfer and termination reactions.

Chart 1. Structure of ω-vinylidene functionalized polymethacrylates.

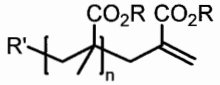

1

An alternative and attractive synthetic route for structurally well-defined **1** would be the use of living radical polymerization, which has been recognized as one of the most efficient methods for the precision synthesis of macromolecules possessing a variety of polar functional groups.[13,14] Indeed, Sawamoto[15] and Haddleton[16] reported that the reaction of poly(methyl methacrylate)s (PMMAs) possessing halogen ω-polymer end group, which was synthesized by ruthenium and copper catalyzed living radical polymerization, with 2,2,6,6-tetramethylpiperine 1-oxyl (TEMPO) gave the corresponding ω-vinylidene functionalized PMMAs. However, though high control of molecular weights and MWDs was achieved under these conditions, efficiency of the end group transformation was rather unsatisfactory (~80%).

We have already reported new living radical polymerization methods using organotellurium, organostibine, and organobismuthine compounds,[17-19] which are designated as TERP,[20-26] SBRP,[27-29] and BIRP,[30,31] respectively. These methods are highly versatile in polymerizing different families of monomers possessing varieties of polar functional groups. Furthermore, the heteroatomic polymer ends are efficiently converted to varieties of functional groups under radical and ionic conditions.[20,29,32,33] As shown in chapter 3, we already found that organobismuthine chain

transfer agent **2a** reacted with TEMPO at 80 °C to give the corresponding TEMPO adduct **3** in good yield (Scheme 1a).[30] This result prompted us to investigate the reaction of living polymer **4** prepared by BIRP, SBRP, and TERP with TEMPO.

In this chapter, we report the synthesis of ω-vinylidene functionalized polymethacrylates **5** by the reaction of **4** and TEMPO (Scheme 1b). The end group transformation proceeded in quantitatively and afforded the desired **5** as a sole product. We also report an alternative synthetic route to ω-vinylidene functionalized polymethacrylate **6** by the reaction of **4** with ethyl 2-[(tributylstannyl)methyl]acrylate (Scheme 1c). This is the first report on the controlled synthesis of ω-vinylidene functionalized polymethacrylates in terms of molecular weight, molecular weight distribution, and end group functionality.

Scheme 1. TEMPO-mediated transformations of organoheteroatomic chain transfer agents and living polymers.

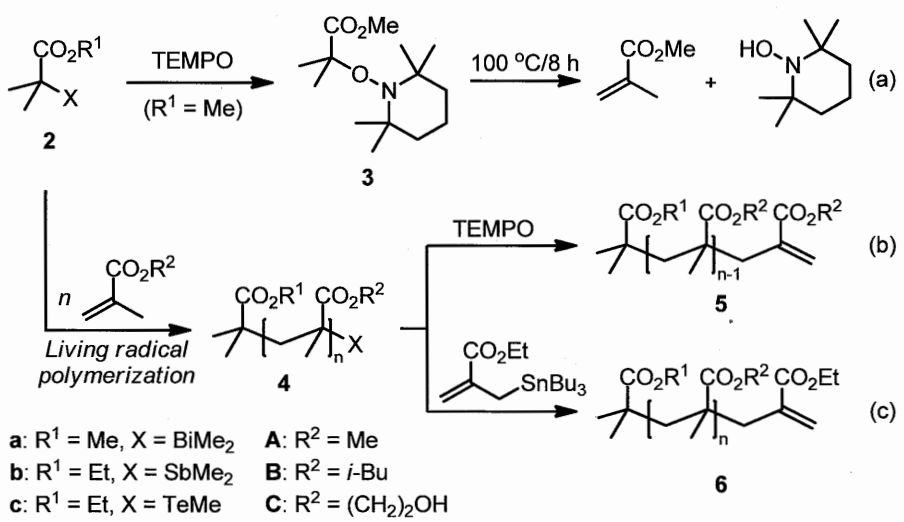

It has been reported that structure of the ω-polymer end group in PMMA are known to affect its thermal stability, and ω-vinylidene PMMA, such as **5A** (R^2 = Me), degrades much lower temperature than ω- saturated PMMA.[34-36] As a part of structural determination of the ω-end group, we also examined the thermal properties of the synthesized PMMAs.

Results and discussions

Synthesis of ω-vinylidene functionalized polymethacrylates and polymethacrylonitrile. The reaction of PMMA **4aA** (R^1, R^2 = Me) possessing dimethylbismuthanyl group at ω-polymer

end was initially examined. Thus, **4aA** (M_n = 3,300, M_w/M_n = 1.12, where M_n and M_w are the number-average and weight average molecular weight, respectively, and M_w/M_n represents molecular weight distribution), which was prepared in 98% yield from **2a** and MMA (30 equiv) by heating at 100 °C for 3 h, was dissolved in trifluoromethylbenzene and was treated with 1.2 equiv of TEMPO at 80 °C for 1 h. Precipitation from hexane gave the desired ω-vinylidene functionalized PMMA **5A** (R^1, R^2 = Me) as a white powder. Gel permeation chromatography indicated that **5A**

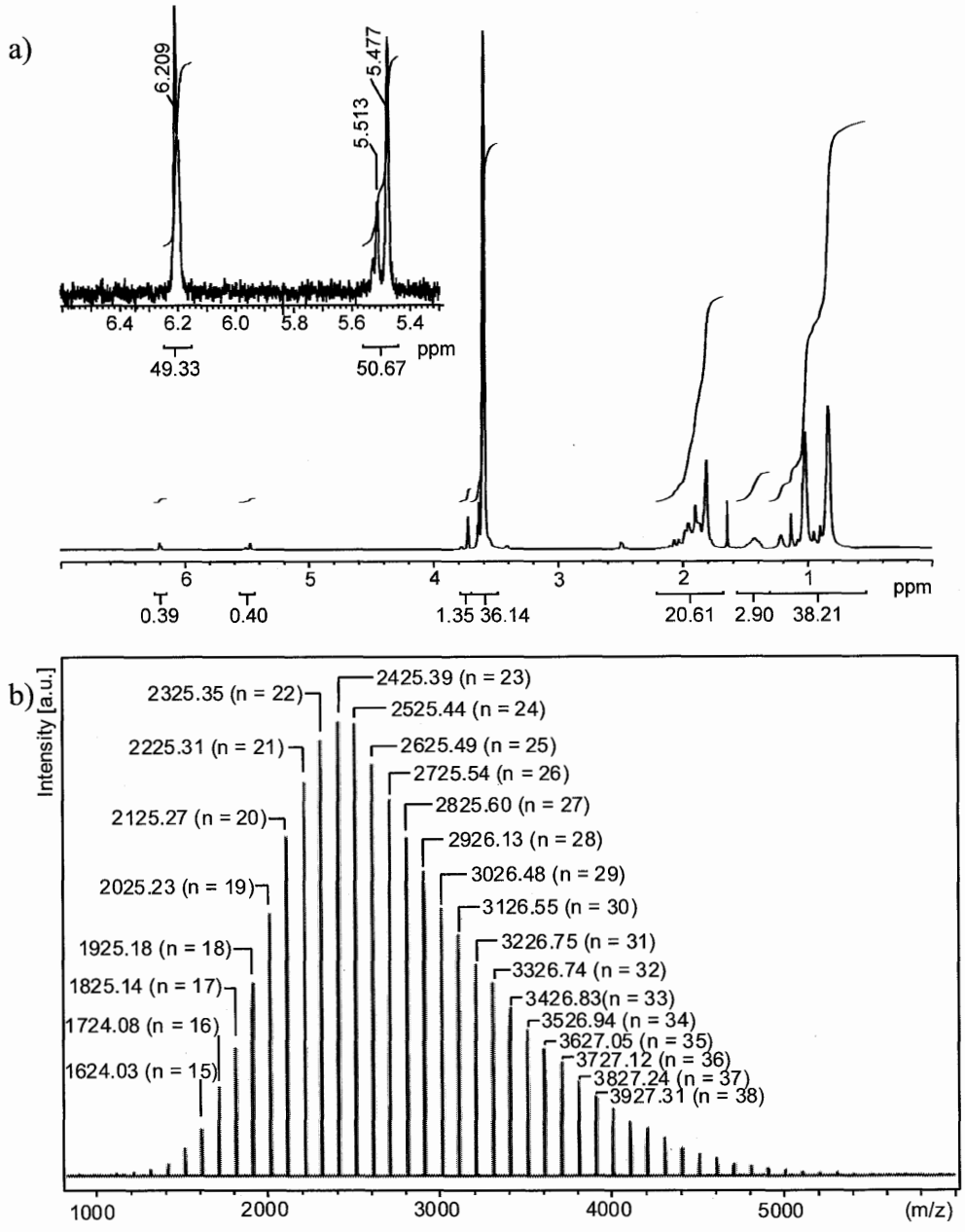

Figure 1. a) ^{1}H NMR and b) MALDI TOF MS spectra of ω-vinylidene PMMA **5A** (R^1, R^2 = Me). A major series of peaks as indicated by average mass number in TOF MS spectrum are observed as sodium ion adduct $(M + Na)^+$.

possessed virtually identical M_n and MWD to **4aA**, indicating no degradation occurred during the transformation. The ^{1}H NMR analysis revealed the existence of an exomethylene functionality as judged by the signals at δ = 5.44~5.56 and 6.16~6.24 ppm (Figure 1a). A comparison of the integrals of these olefinic protons with those of methoxy protons revealed a nearly quantitative conversion of the dimethylbismuthanyl group to the vinylidene group. The high end group fidelity was further confirmed by matrix assisted laser desorption ionization time of flight mass (MALDI-TOF MS) spectroscopy analysis by observing the series of peaks possessing the molecular masses of **5A** (Figure 1b). All these results clearly revealed the selective formation of **5A** from **4aA**.ω-Dimethylbismuthanyl-substituted PMMAs with M_n of 5,900 and M_w/M_n of 1.21 and M_n of 13,000 and M_w/M_n of 1.17 were also converted to the corresponding **5A** under the same conditions. The desired high molecular weight ω-vinylidene PMMAs were formed with quantitative end-group conversions in all cases (entries 2 and 3). The high efficiency of the transformation must be attributed to the highly effective radical generation from **4aA** by direct carbon-bismuth bond homolysis under the reaction conditions.[30]

Formation of **5** can be explained by irreversible abstraction of α-proton of polymer end radical **7** generated thermally from **4** with TEMPO (Scheme 2a). Coupling reaction of **7** with TEMPO may also occur to give PMMA-TEMPO adduct **8** (Scheme 2b), but it regenerates **7** under the reaction conditions. Therefore, the irreversible reaction shifts the equilibrium and leads to the exclusive formation of **5**. This mechanism is supported by the selective and quantitative transformation of isolated **3** to MMA and 2,2,6,6-tetramethylpiperidine 1-ol after heating **3** at 100 °C for 8 h. The different reactivity between **3** and **8** must be attributed to the "polymer effects" on the radical generation from the dormant species;[37] higher reactivity of macroinitiators than monomeric initiators with the same polymer end group structure towards radical generation was reported in nitroxide-mediated radical polymerization,[38,39] atom transfer radical polymerization,[40-42] and reversible addition-fragmentation chain-transfer polymerization.[43,44]

Scheme 2. Mechanism for the formation of **5**.

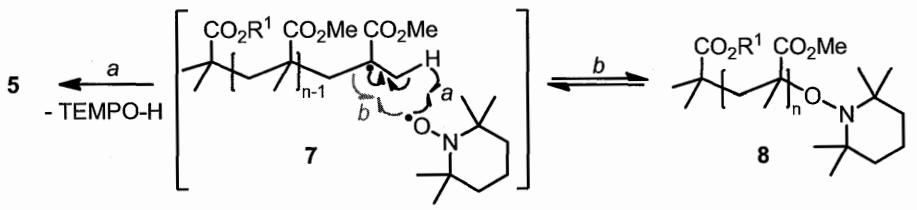

Table 1. Synthesis of ω-vinylidene functionalized poly(alkyl methacrylate)s and polymethacrylonitrile.

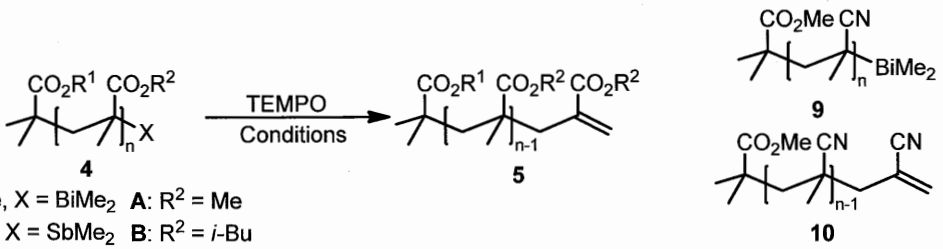

4 5

a: R^1 = Me, X = $BiMe_2$ **A**: R^2 = Me
b: R^1 = Et, X = $SbMe_2$ **B**: R^2 = *i*-Bu
c: R^1 = Et, X = TeMe **C**: R^2 = $(CH_2)_2OH$

entry	Polymer[a] (M_n/MWD)	TEMPO (equiv)	Conditions (°C/h)	Product	Conv.[b] (%)	M_n/MWD[c]
1	**4aA** (3,300/1.20)	1.2	80/1	**5A** (R^1 = Me)	98	3,300/1.19
2	**4aA** (5,900/1.21)	1.2	80/1	**5A** (R^1 = Me)	95	5,700/1.18
3	**4aA** (13,000/1.17)	1.2	80/1	**5A** (R^1 = Me)	95	10,900/1.17
4	**4bA** (3,600/1.35)	1.2	100/15	**5A'** (R^1 = Et)	60	3,500/1.29
5	**4bA** (3,800/1.31)	3	100/0.25	**5A'** (R^1 = Et)	94	3,600/1.32
6	**4cA** (3,500/1.25)	1.2	100/24	**5A'** (R^1 = Et)	75	3,500/1.28
7	**4cA** (3,700/1.26)	3	100/24	**5A'** (R^1 = Et)	98	3,600/1.25
8	**4cA** (2,900/1.25)	1.2	rt (*hv*)[d]/3	**5A'** (R^1 = Et)	80	3,500/1.28
9	**4cA** (3,600/1.31)	3	50 (*hv*)[d]/3	**5A'** (R^1 = Et)	99	3,700/1.32
10	**4aB** (4,300/1.13)	1.2	80/1	**5B** (R^1 = Me)	98	4,100/1.14
11	**9** (3,300/1.23)	3	100/2	**10**	92	3,200/1.23
12	**4cC** (3,900/1.17)	3	50 (*hv*)[d]/9	**5C** (R^1 = Et)	91	3,900/1.19

[a]See Table 2 in the experimental section for the synthesis. [b]Conversion ratio of ω-polymer end group determined by ^{1}H NMR. [c]Number-average molecular weight (M_n) and molecular weight distribution (MWD = M_w/M_n) were obtained by size exclusion chromatography calibrated by PMMA standards. [d]The reaction mixture was irradiated by 500W Hg lamp through a low frequency cut filter (>470 nm).

We next examined the synthesis of **5A'** (R^1 = Et, R^2 = Me) starting from dimethylstibanyl substituted **4bA** and methyltellanyl substituted **4cA** with TEMPO (entries 4~7). The reactions were slow even at 100 °C, but **4bA** and **4cA** were eventually converted to **5A'** in nearly quantitative yields after heating at 100 °C for 1 day in the presence of 3 equiv of TEMPO (entries 5 and 7). The results can be explained by considering the strength of carbon-heteroatom bond; carbon-stibine and carbon-tellurium bonds are much stronger than carbon-bismuth bond.[30,45,46] Therefore, thermal generation of polymer-end radicals from **4bA** and **4cA** must be considerably slower than that from

4aA. It is worth noting that highly efficient end group transformations were achieved under such harsh conditions.

We have already found that carbon-tellurium bond can be effectively activated under photo irradiation even at low temperature.[47-49] Therefore, we next examined the photolysis of **4cA** in the presence of TEMPO at room temperature. PMMA **4cA** was completely consumed within 3 h by irradiation of UV-vis light (500 W high pressure mercury lamp through a short wave length cut off filter [<470 nm][49]) at room temperature, but the efficiency of the conversion to **5A'** was about 80% (entry 8). An uncharacterized compound was detected by ^{1}H NMR analysis of the crude reaction mixture. We assumed this compound as a PMMA-TEMPO adduct **8'** (R^1 = Et), and we envisioned that **8'** would be converted to **5A'** at higher temperature. Indeed, the photolysis of **4cA** at 50 °C for 3 h selectively gave **5A'** in quantitative yield (entry 9).

This protocol is not limited to the synthesis of PMMA derivatives. For example, treatment of poly(*i*-butyl methacrylate) **4aB** (R^1 = Me, R^2 = *i*-Bu, M_n = 4,300, M_w/M_n = 1.13) and polymethacrylonitrile **9** (M_n = 3,300, M_w/M_n = 1.23) bearing dimethylbismuthanyl ω-end with TEMPO at 80 or 100 °C gave **5B** (R^1 = Me, R^2 = *i*-Bu) and **10** in high end group conversions (entries 10 and 11). Poly(2-hydroxyethyl methacrylate) **4cC** [R^1 = Et, R^2 = $(CH_2)_2OH$, M_n = 3,900, M_w/M_n = 1.17] bearing methyltellanyl ω-end group was also completely converted to **5C'** [R^1 = Et, R^2 = $(CH_2)_2OH$] upon treatment with TEMPO under photo irradiation (entry 12). Molecular weights and MWDs of the starting living polymers **4** and **9** were retained to **5** and **10** in all cases. Therefore, structurally highly controlled polymethacrylates and polymethacrylonitrile with respect to molecular weight and MWD with defined ω-polymer end structure were successfully synthesized. These compounds would be also useful for the synthesis of copolymers.[3,4]

We next examined the reaction of **4** with ethyl 2-[(tributylstannyl)methyl]acrylate, as we have already demonstrated that the allylstannane is highly useful reagent for the selective transformation of polystyrenes bearing tellanyl and stibanyl groups as the ω-end group.[20,29] We were pleased to find that the reaction of PMMA **4aA** and ethyl 2-[(tributylstannyl)methyl]acrylate occurred smoothly at 80 °C for 1 h and gave **6A** (R^1, R^2 = Me) (Scheme 1c). The ^{1}H NMR analysis indicated the virtually complete transformation of the dimethylbismuthanyl group to the ω-vinylidene group.

Effects of end group structure on thermal stability of PMMA. Thermal degradation of ω-vinylidene PMMA **5A** (M_n = 3,300, M_w/M_n = 1.19) was analyzed by using combined differential scanning calorimetry and thermogravimetric analysis (TGA, heating rate = 10 °C/min).

ω-Protonated PMMA **11** (M_n = 4,100, M_w/M_n = 1.22), which was prepared by tributyltin hydride reduction of **4cA**,[21] was also analyzed as a reference.

Chart 2. Structure of ω-Protonated PMMA **11**.

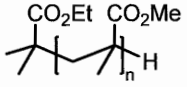

11

ω-Protonated PMMA **11** started to degrade at approximately 370 °C and all the polymer completely degraded around 450 °C (Figure 2a). Degradation of ω-vinylidene PMMA **5A**, on the other hand, began at approximately 270 °C and ended about at 340 °C (Figure 2b). Virtually identical thermograms were obtained under a nitrogen or an air flow. The clean single step decomposition of each PMM sample is consistent with the defined polymer end structure. Although the relative stability of these PMMAs is similar to the previous reports, absolute temperatures of the degradation as well as the TGA profiles were considerably different from the previous reports, especially in ω-vinylidene PMMA. For example, Manring reported that degradation of ω-vinylidene PMMA sample started from about 130 °C and completed at around 420 °C.[35] This is presumably due to the difference of sample conditions, such as powder or film, impurities in the sample, and also the rate of heating. Since our measurements were done using samples with virtually complete end group fidelity, we believe that our results provide more accurate data on the thermal properties of PMMAs.

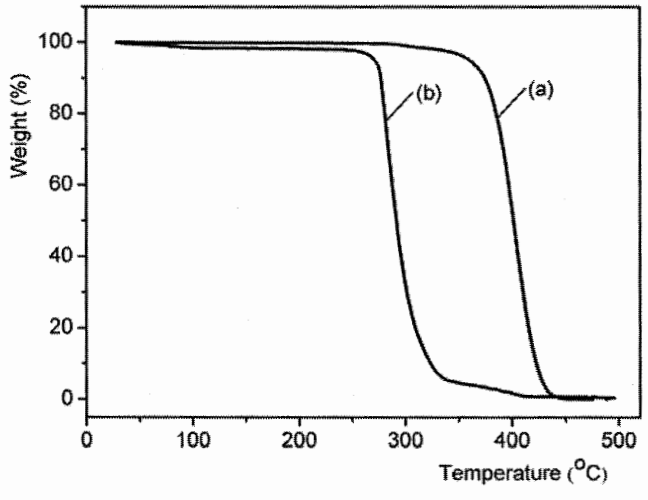

Figure 2. TGA thermograms of (a) ω-protonated PMMA **11** (M_n = 4,100, M_w/M_n = 1.22), and (b) ω-vinylidene PMMA **5A** (M_n = 3,300, M_w/M_n = 1.19). The measurement was carried out by heating

a PMMA sample from room temperature to 500 °C under a nitrogen flow with heating rate of 10 °C/min.

Conclusions

We have demonstrated that the reactions of TEMPO and poly(alkyl methacrylate)s and polymethacrylonitrile bearing organobismuthine, organostibine, and organotellurium ω-polymer end groups proceed quantitatively under thermal or photochemical conditions. The high efficiency of the transformation combined with the well controlled macromolecular structure of the starting heteroatom-substituted living polymers lead to the successful synthesis of structurally well controlled poly(alkyl methacrylate)s and polymethacrylonitrile with defined ω-vinylidene group functionality. The same type of polymer was also synthesized under the controlled manner by the reaction of the heteroatom-substituted living polymers with ethyl 2-[(tributylstannyl)methyl]acrylate. This route would be synthetically more versatile than the first route using TEMPO. TGA analysis revealed that the polymers with defined ω-end group degraded in one step, indicating the importance of controlled end group structures for polymer properties.

Experimental Section

General. All reaction conditions dealing with air- and moisture sensitive compounds were carried out in a dry reaction vessel under nitrogen atmosphere. ^{1}H NMR (400 MHz) spectra were measured for a $CDCl_3$, CD_3OD, or DMF-d_7 solution of a sample and are reported in parts per million (δ) from internal tetramethylsilane or residual solvent peak. MALDI TOF MS spectra were obtained in the reflection mode and at 20 kV acceleration voltage. Samples were prepared from a tetrahydrofuran (THF) solution by mixing sample (10 mg/mL), dithranol (10 mg/mL), and sodium trifluoroacetate (5 mg/mL) in a ratio of 1:1:1. GPC was performed two linearly connected polystyrene mixed gel columns, which were calibrated with PMMA standards. Analyses were made using chloroform or 0.1 mol/l LiBr solution of DMF as an eluant with a flow rate of 1.0 mL/min with a refractive-index (RI) detector at 40 °C. Differential scanning calorimetry and TGA was performed from room temperature to 500°C under a nitrogen or an air flow with heating rate of 10 °C/ min. A lamp housing equipped with a 500 W high pressure mercury lamp (500W) was used for photochemical reaction. A short wave length cut filter (>470 nm, Asahi Techno Glass) was employed to control the light.

Materials. Unless otherwise noted, materials were obtained from commercial suppliers and were used as received. Isobutyl methacrylate was a gift from Sekisui Chemical Co. Methyl methacrylate, isobutyl methacrylate and methacrylonitrile were washed with 5% aqueous sodium hydroxide solution and were distilled over calcium hydride under reduced pressure and stored under a nitrogen atmosphere. 2-Hydroxyethyl methacrylate was distilled under reduced pressure and stored under nitrogen atmosphere. Trifluoromethylbenzene was distilled from CaH_2 and stored under nitrogen atmosphere. 2,2'-Azobisisobutyronitrile (AIBN) was recrystallized from methanol and stored in a refrigerator. Methyl 2-dimethylbismuthanyl-2-methylpropionate (**2a**),[30] ethyl 2-dimethylstibanyl-2-methylpropionate (**2b**),[28] ethyl 2-methyl-2-methyltellanylpropionate (**2c**),[20, 21] dimethylditelluride,[21] and ethyl 2-[(tributylstannyl)methyl]acrylate[50] were prepared as reported. End-protonated PMMA **11** was prepared from **2c** and MMA in the presence of dimethyl ditelluride followed by tributyltin hydride reduction.[21]

Typical Procedure of Preparation of ω-vinylidene functionalized PMMA 5A from 4aA. A solution of MMA (0.30 mL, 3.00 mmol) and **2a** (18.3 μL, 0.10 mmol) was heated at 100 °C with stirring for 3 h under a nitrogen atmosphere in a glove box. A small portion of the reaction mixture was taken and dissolved in $CDCl_3$. The conversion of monomer (98%) was determined by the ^1H NMR analysis, and number averaged molecular weight (M_n = 3,300) and M_w/M_n (= 1.20) were determined by the GPC analysis (Table 2, entry 1). The resulting mixture was dissolved in 3 mL of trifluoromethylbenzene, and TEMPO (18.9 mg, 0.12 mmol) was added to this mixture. After the resulting solution was heated at 80 °C for 1 h, it was poured into a vigorously stirred hexane (100 mL). The product was collected by filtration and dried under reduced pressure at 40 °C to give 0.27 g of **5A** (87% yield) with M_n of 3,300 and M_w/M_n of 1.19. ^1H NMR analysis revealed the existence of characteristic signal at 5.44~5.56 and 6.16~6.24 ppm (Figure 1a). A comparison of the integrals of these olefinic protons with those of methoxy protons revealed 98% efficiency of the transformation. MALDI TOF MS analysis also indicated the selective formation of **5A** (Figure 1b). The TGA analysis of the polymer indicated a single step of weight loss from around 270 °C to 340 °C (Figure 2b).

Reaction conditions for the synthesis of PMMA samples **4aA** and **5A** with M_n of 5,700 and 10,900 were shown in entries 2 and 3 of Table 1 and 2, respectively.

Synthesis of 5A' from 4bA. A solution of MMA (3.20 mL, 30 mmol), AIBN (32.8 mg, 0.20 mmol), and **2b** (0.21 mL, 1.00 mmol) was stirred at 60 °C for 6 h under a nitrogen atmosphere in a glove box. A small portion of the reaction mixture was taken and dissolved in $CDCl_3$. The

conversion of monomer (95%) was determined by ^{1}H NMR, and M_n (= 3,800) and M_w/M_n (= 1.31) were determined by GPC analysis (Table 2, entry 5). The remaining polymer mixture was dissolved in 10 mL of trifluoromethylbenzene, and TEMPO (0.47 g, 3.00 mmol) was added. The resulting solution was heated at 100 °C for 0.25 h, and was poured into a vigorously stirred hexane (1.8 L). The product was collected by filtration and dried under reduced pressure at 40 °C to give **5A'** in 98% yield (3.05 g) with M_n of 3,600 and M_w/M_n of 1.32. The conversion efficiency of ω-polymer end group was determined to be 94% by the ^{1}H NMR analysis.

Synthesis of 5A' from 4cA. A solution of MMA (3.20 mL, 30 mmol), **2c** (0.18 mL, 1.00 mmol), and dimethylditelluride (0.11 mL, 1.00 mmol) was heated at 80 °C with stirring for 12 h under a nitrogen atmosphere in a glove box. A small portion of the reaction mixture was taken and dissolved in $CDCl_3$. The conversion of monomer (95%) was determined by the ^{1}H NMR analysis. M_n of 3,600 and M_w/M_n of 1.31 were determined by the GPC analysis (Table 2, entry 9). The remaining polymer mixture was dissolved in 10 mL of trifluoromethylbenzene, and TEMPO (0.47 g, 3.00 mmol) was added. The resulting solution was irradiated through a low frequency cut-off filter (>470 nm) at 50°C for 3 h, and was poured into a vigorously stirred hexane (1.0 L). The product was collected by filtration and dried under reduced pressure at 40 °C to give 3.01 g of **5A'** (97% yield) with M_n of 3,700 and M_w/M_n of 1.32. The conversion efficiency of ω-polymer end group was determined to be 99% by the ^{1}H NMR analysis.

Synthesis of 5B from 4aB. A solution of isobutyl methacrylate (0.34 mL, 2.14 mmol) and **2a** (13.0 μL, 0.071 mmol) was heated at 100 °C with stirring for 1 h under a nitrogen atmosphere in a glove box. A small portion of the reaction mixture was taken and dissolved in $CDCl_3$. The conversion of monomer (94%) was determined by ^{1}H NMR, and M_n (= 4,300) and M_w/M_n (= 1.13) were determined by the GPC analysis. The remaining mixture was dissolved in 1 mL of trifluoromethylbenzene. TEMPO (13.4 mg, 0.086 mmol) was added, and the resulting solution was heated at 80 °C for 1 h. Solvent was removed, and the resulting crude mixture was purified by preparative GPC using chloroform as an eluent. The product was dried under reduced pressure at 40 °C to give 0.27 g of **5B** (89% yield) with M_n of 4,100 and M_w/M_n of 1.14. The ^{1}H NMR analysis revealed the existence of characteristic signal at 5.44~5.56 and 6.16~6.24 ppm (Figure 3a). A comparison of the integrals of these olefinic protons with those of ester methylene protons of isobutyl group (δ = 3.60-3.85) revealed 98% efficiency of the ω-end group transformation. MALDI TOF MS analysis also indicated the selective formation of **5B** (Figure 3b).

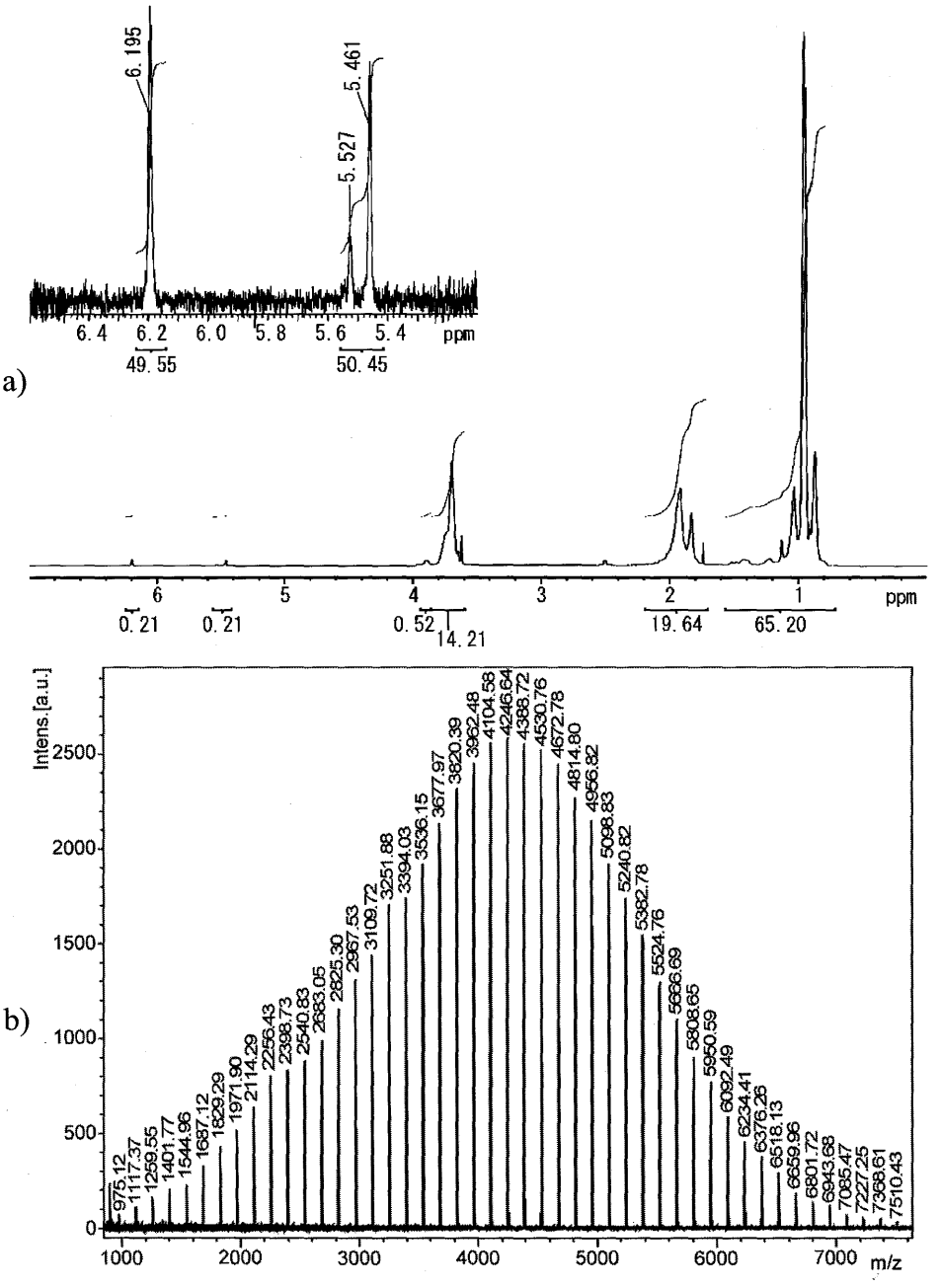

Figure 3. a) ^{1}H NMR and b) MALDI TOF MS spectra of poly(*i*-butyl methacrylate) **5B**. A major series of peaks as indicated by average mass number in TOF MS spectrum are observed as sodium ion adduct $(M + Na)^+$.

Synthesis of 10 from 9. A solution of methacrylonitrile (0.252 mL, 3.0 mmol) and **2a** (18.3 μL, 0.10 mmol) in DMF (1.0 mL) was heated at 80 °C with stirring for 3 h under a nitrogen atmosphere in a glove box. A small portion of the reaction mixture was taken and dissolved in $CDCl_3$. The conversion of monomer (91%) was determined by the ^{1}H NMR analysis, and M_n (=

3,300) and M_w/M_n (= 1.23) were determined by the GPC analysis (Table 2, entry 11). TEMPO (46.9 mg, 0.30 mmol) was added, and the resulting solution was heated at 100 °C for 2 h. Solvent and residual monomer were removed under reduced pressure (<0.1 mmHg) at 80 °C for 3 h. The remaining crude mixture was dissolved in acetone (1.0 mL) and poured into a vigorously stirred hexane (200 mL). The product was collected by filtration and dried under reduced pressure at 40 °C to give **10** in 92% yield (185 mg) with M_n of 3,200 and M_w/M_n of 1.23. The ^{1}H NMR analysis in DMF-d_7 revealed the existence of characteristic signal at 6.24~6.34 and 6.38~6.46 ppm (Figure 4). A comparison of the integrals of these olefinic protons with those of methyl ester moiety at the α-polymer end (δ = 3.70) and methylene protons in a polymer chain (δ = 2.05~2.70) revealed 92% efficiency of the ω-end group transformation.

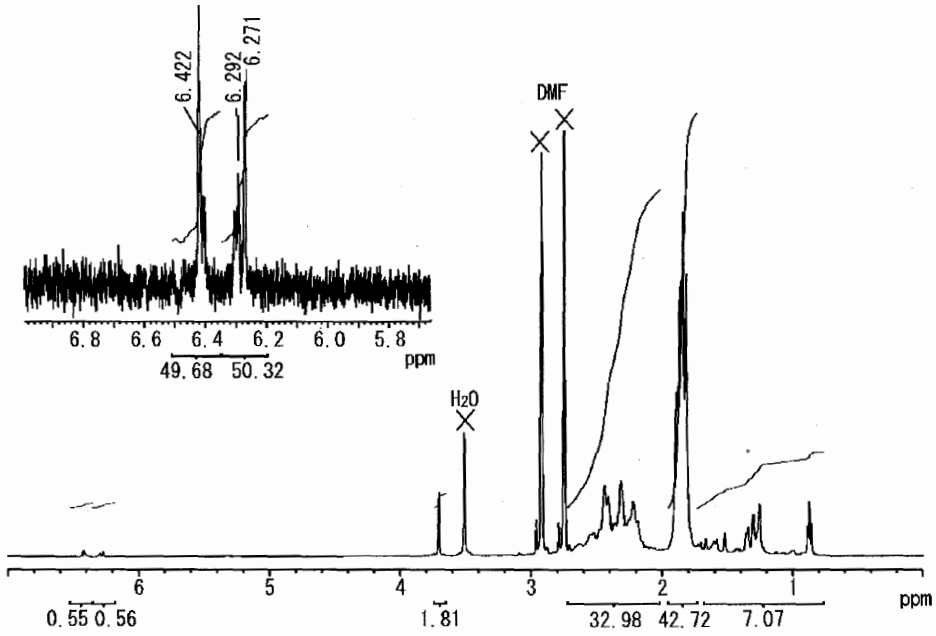

Figure 4 . ^{1}H NMR spectra of ω-vinylidene polymethacrylonitrile **10**

Synthesis of 5C from 4cC. A solution of 2-hydroxyethyl methacrylate (0.364 mL, 3.0 mmol), **2c** (17.5 μL, 0.1 mmol), and dimethyl ditelluride (10.6 μL, 1.0 mmol) in DMF (1.0 mL) was heated at 80 °C with stirring for 16 h under a nitrogen atmosphere in a glove box. A small portion of the reaction mixture was taken and dissolved in CD_3OD. The conversion of monomer (97%) was determined by the ^{1}H NMR analysis, and M_n (= 3,900) and M_w/M_n (= 1.17) were determined by the GPC analysis. TEMPO (47 mg, 0.30 mmol) was added, and the resulting solution was irradiated through a low frequency cut-off filter (>470 nm) at 50°C for 9 h. Solvent and residual monomer were removed under reduced pressure (<0.1 mmHg) at 80 °C for 3 h. The remaining crude mixture

was dissolved in acetone (1.0 mL) and poured into a vigorously stirred hexane (200 mL). The product was collected by filtration and dried under reduced pressure at 40 °C to give **5C** in 89% yield (0.26 g) with M_n of 3,900 and M_w/M_n of 1.19. The ^{1}H NMR analysis in CD_3OD revealed the existence of characteristic signal at 5.58~5.72 and 6.22~6.38 ppm (Figure 5). A comparison of the integrals of these olefinic protons with those of two sets of ester methylene protons (δ = 3.60~3.90 and 3.90~4.12) and methyl ester protons derived from α-polymer end (δ = 4.12~4.28) revealed 91% efficiency of the ω-end group transformation.

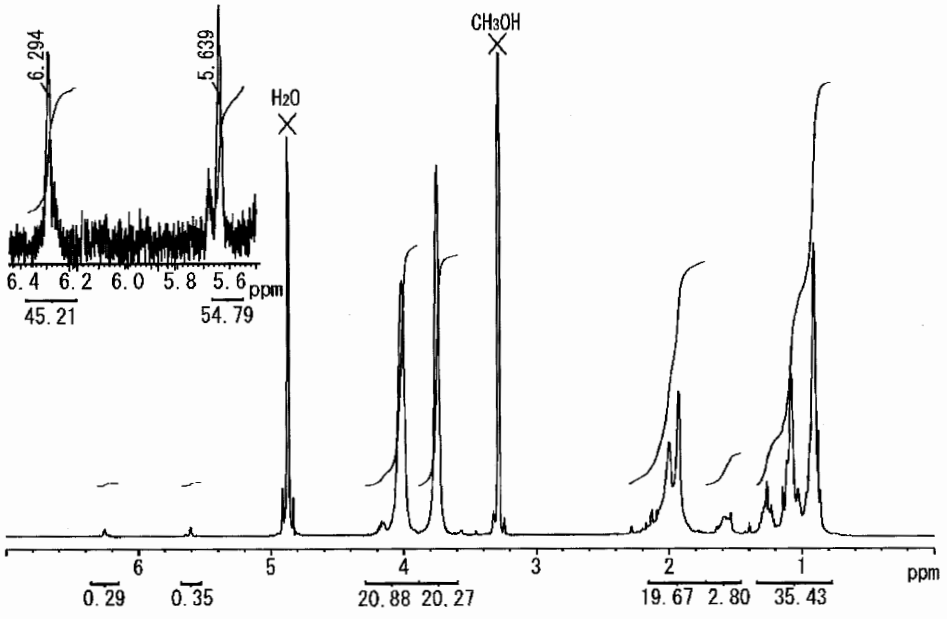

Figure 5 . ^{1}H NMR spectra of ω-vinylidene poly(2-hydroxyethyl methacrylate) **5C** and 3.90~4.12) and methyl ester protons derived from α-polymer end (δ = 4.12~4.28) revealed 91% efficiency of the ω-end group transformation.

Synthesis of 6A from 4aA. A solution of MMA (0.32 mL, 3.00 mmol) and **2a** (18.3 μL, 0.10 mmol) was stirred at 100 °C for 3 h under a nitrogen atmosphere in a glove-box. A small portion of the reaction mixture was taken and dissolved in $CDCl_3$. The conversion of monomer (99%) was determined by ^{1}H NMR, and M_n (= 3,100) and M_w/M_n (= 1.23) were determined by the GPC analysis. The remaining mixture was dissolved in 1.5 mL of trifluoromethylbenzene. Ethyl 2-[(tributylstannyl)methyl]acrylate (44.0 μL, 0.12 mmol) and AIBN (1.6 mg, 0.01 mmol) were added, and the resulting solution was heated at 80 °C for 1 h. The reaction mixture was poured into a vigorously stirred hexane (200 mL). The product was collected by filtration and dried under

reduced pressure at 40 °C to give **6A** in 87% yield (0.26 g) with M_n of 2,900 and M_w/M_n of 1.22. The ^{1}H NMR analysis revealed the existence of characteristic signal at 5.44~5.56 and 6.16~6.24 ppm (Figure 6). The analysis also revealed the conversion efficiency of ω-polymer end group was 95%.

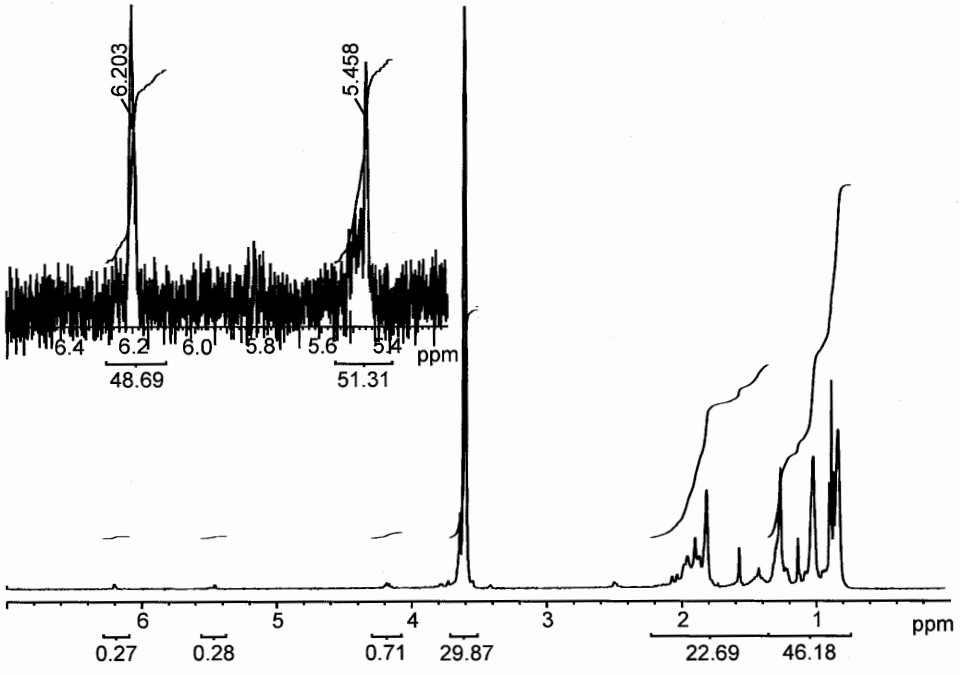

Figure 6. ^{1}H NMR spectra of ω-vinylidene PMMA **6A.**

Table 2. Synthesis of poly(alkyl methacrylate)s **4** and methacrylonitrile **9** by TERP, SBRP, or BIRP.

Entry	**2**	Monomer[a] (equiv)	Conditions (°C/h)	**4** or **9** Conv.[b] (%)	M_n/MWD[c]
1	**2a**	MMA (30)	100/1	98	3,300/1.20
2	**2a**	MMA (50)	100/3	96	5,900/1.21
3	**2a**	MMA(100)	100/3	91	13,000/1.17
4	**2b**	MMA (30)	60/6[d]	93	3,600/1.35
5	**2b**	MMA (30)	60/6[d]	95	3,800/1.31
6	**2c**	MMA (30)	80/12[e]	94	3,500/1.25
7	**2c**	MMA (30)	80/12[e]	93	3,700/1.26
8	**2c**	MMA (30)	80/12[e]	95	2,900/1.25
9	**2c**	MMA (30)	80/12[e]	95	3,600/1.31

Entry	**2**	Monomer[a] (equiv)	Conditions (°C/h)	**4** or **9** Conv.[b] (%)	M_n/MWD[c]
10	**2a**	BMA (30)	100/1	94	4,300/1.13
11	**2a**	MAN (30)	80/3	91	3,300/1.23
12	**2c**	HEMA (30)	80/16[e]	97	3,900/1.17

[a]Abbreviation: MMA = methyl methacrylate, BMA = *i*-butyl methacrylate, MAN = methacrylonitrile, HEMA = 2-hydroxyethyl methacrylate. [b]Monomer conversion was determined by ^{1}H NMR. [c]Number-average molecular weight (M_n) and molecular weight distribution (MWD = M_w/M_n) were obtained by size exclusion chromatography calibrated by polyMMA standards. ^{1}H NMR. [d]0.2 equiv of AIBN was added. [e]1.0 equiv of $(TeMe)_2$ was added.

References

(1) Matyjaszewski, K.; Gnanou, Y.; Leibler, L. *Macromolecular Engineering*; Wiley-VCH: Weinheim, 2007.

(2) Boutevin, B.; David, G.; Boyer, C. *Adv. Polym. Sci.* **2007**, *206*, 31-135.

(3) Cacioli, P.; Hawthorne, D. G.; Laslett, R. L.; Rizzardo, E.; Solomon, D. H. *J. Macromol. Sci. Chem. A* **1986**, *23*, 839 - 852.

(4) Krstina, J.; Moad, G.; Rizzardo, E.; Winzor, C. L.; Berge, C. T.; Fryd, M. *Macromolecules* **1995**, *28*, 5381-5385.

(5) Moad, C. L.; Moad, G.; Rizzardo, E.; Thang, S. H. *Macromolecules* **1996**, *29*, 7717-7726.

(6) Miyake, K.; Zetterlund, P. B.; Yamada, B. *Macromol. Rapid Commun.* **2004**, *25*, 1905-1911.

(7) Gridnev, A. A.; Ittel, S. D. *Chem. Rev.* **2001**, *101*, 3611-3660.

(8) M. Muratore, L.; Steinhoff, K.; P. Davis, T. *J. Mater. Chem.* **1999**, *9*, 1687-1691.

(9) Meijs, G. F.; Rizzardo, E.; Thang, S. H. *Macromolecules* **1988**, *21*, 3122-3124.

(10) Meijs, G. F.; Morton, T. C.; Rizzardo, E.; Thang, S. H. *Macromolecules* **1991**, *24*, 3689-3695.

(11) Meijs, G. F.; Rizzardo, E.; Thang, S. H. *Polym. Bull.* **1990**, *24*, 501-505.

(12) Yamada, B.; Kobatake, S.; Otsu, T. *Polym. J.* **1992**, *24*, 281-290.

(13) *Handbook of Radical Polymerization*; Matyjaszewski, K.; Davis, T. P., Eds.; Wiley-Interscience: New York, 2002.

(14) Moad, G.; Solomon, D. H. *The Chemistry of Radical Polymerization*; Elsevier: Amsterdam, 2006.

(15) Nishikawa, T.; Ando, T.; Kamigaito, M.; Sawamoto, M. *Macromolecules* **1997**, *30*, 2244-2248.

(16) Bon, S. A. F.; Steward, A. G.; Haddleton, D. M. *J. Polym. Sci. Part A* **2000**, *38*, 2678-2686.

(17) Yamago, S. *Synlett* **2004**, 1875-1890.

(18) Yamago, S. *J. Polym. Sci. Part A: Polym. Chem.* **2006**, *44*, 1-12.

(19) Yamago, S. *Proc. Jpn. Acad., Ser. B* **2005**, *81*, 117-128.

(20) Yamago, S.; Iida, K.; Yoshida, J. *J. Am. Chem. Soc.* **2002**, *124*, 2874-2875.

(21) Yamago, S.; Iida, K.; Yoshida, J. *J. Am. Chem. Soc.* **2002**, *124*, 13666-13667.

(22) Goto, A.; Kwak, Y.; Fukuda, T.; Yamago, S.; Iida, K.; Nakajima, M.; Yoshida, J. *J. Am. Chem. Soc.* **2003**, *125*, 8720-8721.

(23) Yamago, S.; Iida, K.; Nakajima, M.; Yoshida, J. *Macromolecules* **2003**, *36*, 3793-3796.

(24) Sugihara, Y.; Kagawa, Y.; Yamago, S.; Okubo, M. *Macromolecules* **2007**, *40*, 9208-9211.

(25) Yusa, S.; Yamago, S.; Sugahara, M.; Morikawa, S.; Yamamoto, T.; Morishima, Y. *Macromolecules* **2007**, *40*, 5907-5915.

(26) Kayahara, E.; Yamago, S.; Kwak, Y.; Gota, A.; Fukuda, T. *Macromolecules* **2008**, *41*, 527-529.

(27) Yamago, S.; Ray, B.; Iida, K.; Yoshida, J.; Tada, T.; Yoshizawa, K.; Kwak, Y.; Goto, A.; Fukuda, T. *J. Am. Chem. Soc.* **2004**, *126*, 13908-13909.

(28) Ray, B.; Kotani, M.; Yamago, S. *Macromolecules* **2006**, *39*, 5259-5265.

(29) Yamago, S.; Yamada, T.; Togai, M.; Ukai, Y.; Kayahara, E.; Pan, N. *Chem. Eur. J.* **2009**, *15*, 1018-1029.

(30) Yamago, S.; Kayahara, E.; Kotani, M.; Ray, B.; Kwak, Y.; Goto, A.; Fukuda, T. *Angew. Chem. Int. Ed.* **2007**, *46*, 1304-1306.

(31) Kayahara, E.; Yamago, S. *J. Am. Chem. Soc.* **2009**, *131*, 2508-2513.

(32) Yamada, T.; Mishima, E.; Ueki, K.; Yamago, S. *Chem. Lett.* **2008**, *37*, 650-651.

(33) Yamago, S.; Matsumoto, A. *J. Org. Chem.* **2008**, *73*, 7300-7304.

(34) Kashiwagi, T.; Inaba, A.; Brown, J. E.; Hatada, K.; Kitayama, T.; Masuda, E. *Macromolecules* **1986**, *19*, 2160-2168.

(35) Manring, L. E. *Macromolecules* **1988**, *21*, 528-530.

(36) Manring, L. E. *Macromolecules* **1989**, *22*, 2673-2677.

(37) Goto, A.; Fukuda, T. *Prog. Polym. Sci.* **2004**, *29*, 329-385.

(38) Marque, S.; Le Mercier, C.; Tordo, P.; Fischer, H. *Macromolecules* **2000**, *33*, 4403-4410.

(39) Goto, A.; Terauchi, T.; Fukuda, T.; Miyamoto, T. *Macromol. Rapid. Commun.* **1997**, *18*, 673-681.

(40) Wang, J.-S.; Matyjaszewski, K. *Macromolecules* **1995**, *28*, 7901-7910.

Chapter 6

Generation of Carboanions via Stibine-Metal and Bismuth-Metal Exchange Reactions and Its Applications to the Precision Synthesis of ω-End Functionalized Polymers

Abstract

Generation of carboanions from organostibines and organobismuthines via heteroatom-metal exchange reactions was examined from synthetic and mechanistic viewpoints. The exchange reaction proceeded spontaneously upon treatment with various organometallic reagents, such as alkyl lithiums, alkyl magnesium halides, and tetraalkyl zincates, to afford the corresponding carboanions quantitatively. Due to the high reactivity of these heteroatom compounds, the exchange reactions exclusively took place even in the presence of various polar functional groups, which potentially react with organometallic species. The advantage of this method was exemplified by the end group transformation of living polymers bearing these heteroatom species at the ω-polymer end, prepared by using organostibine and bismuthine-mediated living radical polymerizations. Various polymers bearing polar functional groups and an acidic hydrogen e.g. poly(methyl methacrylate), poly(butyl acrylate), poly(*N*-isopropyl acrylamide), and poly(2-hydroxyethyl methacrylate), could be used in the exchange reactions, and subsequent trapping with electrophiles afforded the corresponding polymers with controlled molecular weights, molecular weight distributions, and end group functionalities. Competition experiments showed that organostibines and organobismuthines were among the most reactive heteroatom compounds towards organometallic reagents and that their high reactivity was responsible for the high chemoselectivity in the exchange reaction.

(41) Matyjaszewski, K.; Paik, H.-j.; Zhou, P.; Diamanti, S. J. *Macromolecules* **2001**, *34*, 5125-5131.

(42) Ohno, K.; Goto, A.; Fukuda, T.; Xia, J.; Matyjaszewski, K. *Macromolecules* **1998**, *31*, 2699-2701.

(43) Chong, Y. K.; Krstina, J.; Le, T. P. T.; Moad, G.; Postma, A.; Rizzardo, E.; Thang, S. H. *Macromolecules* **2003**, *36*, 2256-2272.

(44) Goto, A.; Sato, K.; Tsujii, Y.; Fukuda, T.; Moad, G.; Rizzardo, E.; Thang, S. H. *Macromolecules* **2001**, *34*, 402-408.

(45) Kwak, Y.; Goto, A.; Fukuda, T.; Yamago, S.; Ray, B. *Z. Phys. Chem.* **2005**, *219*, 283-293.

(46) Kwak, Y.; Goto, A.; Fukuda, T.; Kobayashi, Y.; Yamago, S. *Macromolecules* **2006**, *39*, 4671-4679.

(47) Yamago, S.; Miyazoe, H.; Yoshida, J. I. *Tetrahedron. Lett.* **1999**, *40*, 2339-2342.

(48) Yamago, S.; Miyazoe, H.; Goto, R.; Hashidume, M.; Sawazaki, T.; Yoshida, J. *J. Am. Chem. Soc.* **2001**, *123*, 3697-3705.

(49) Yamago, S.; Ukai, Y.; Matsumoto, A.; Nakamura, Y. *J. Am. Chem. Soc.* **2009**, *131*, 2100-2101.

(50) Baldwin, J. E.; Adlington, R. M.; Birch, D. J.; Crawford, J. A.; Sweeney, J. B. *J. Chem. Soc. Chem. Commun.* **1986**, 1339-1340.

Chapter 6

Generation of Carboanions via Stibine-Metal and Bismuth-Metal Exchange Reactions and Its Applications to the Precision Synthesis of ω-End Functionalized Polymers

Abstract

Generation of carboanions from organostibines and organobismuthines via heteroatom-metal exchange reactions was examined from synthetic and mechanistic viewpoints. The exchange reaction proceeded spontaneously upon treatment with various organometallic reagents, such as alkyl lithiums, alkyl magnesium halides, and tetraalkyl zincates, to afford the corresponding carboanions quantitatively. Due to the high reactivity of these heteroatom compounds, the exchange reactions exclusively took place even in the presence of various polar functional groups, which potentially react with organometallic species. The advantage of this method was exemplified by the end group transformation of living polymers bearing these heteroatom species at the ω-polymer end, prepared by using organostibine and bismuthine-mediated living radical polymerizations. Various polymers bearing polar functional groups and an acidic hydrogen e.g. poly(methyl methacrylate), poly(butyl acrylate), poly(*N*-isopropyl acrylamide), and poly(2-hydroxyethyl methacrylate), could be used in the exchange reactions, and subsequent trapping with electrophiles afforded the corresponding polymers with controlled molecular weights, molecular weight distributions, and end group functionalities. Competition experiments showed that organostibines and organobismuthines were among the most reactive heteroatom compounds towards organometallic reagents and that their high reactivity was responsible for the high chemoselectivity in the exchange reaction.

Introduction

Carbanions occupy a central position in organic synthesis.[1,2] Manyh methods have been developed for the generation of them, and the reaction of them with electrophiles is one of the most reliable methods in forming new carbon-carbon bonds.. Heteroatom-metal exchange reactions, which are also called transmetallation reactions, have been widely used for the generation because of the ease of availability of starting heteroatom compounds and their high efficiency in generating carbanions (Scheme 1).[3-12] Heavier organoheteroatom compounds of group 14, 16, and 17 elements in the periodic table, i.e., organostannanes, -selenides, -tellurides, -bromides, and -iodides, have been widely employed as precursors for carbanions, and their exchange reactions with various organometallic reagents, e.g., organolithium, -magnesium, -aluminium, -zinc, and -copper reagents give the corresponding organometallic species. On the other hand, although heteroatom-lithium exchange reactions of heavier group 15 elements, i.e., organostibines and -bismuthines, have been known for over 70 years,[13-18] their reactivities and synthetic efficiencies remain elusive.

Scheme 1. Generation of carbanions via heteroatom-metal exchange reactions and subsequent reactions with electrophiles. R = alkyl, aryl, alkynyl, or vinyl; R' = alkyl; X = heteroatom; M = metal; El^+ = electrophile.

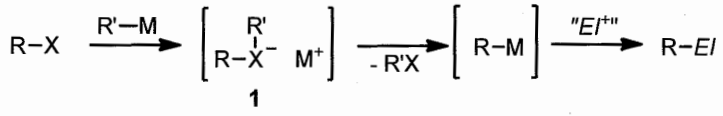

In addition, despite the numerous synthetic applications, little is known about the differences in reactivity of the heteroatom species towards generating carbanion species. Reich and coworkers reported that phenyliodideis slightly more reactive than diphenyltelluride when phenyl or *p*-tolyl lithium was employed.[19,20] Although organostibines have been thought to be more reactive than organoiodides, no quantitative data have been obtained.[20] Sonoda and coworkers have performed competition experiments on the exchange reactions of phenyl-substituted heteroatom compounds with butyl lithium generating phenyl lithium.[21] The results showed that iphenyliodide is the most reactive, followed by butylphenyltelluride, and then tributylphenylstannane in a ratio of 76:23:1 among heteroatom compounds comprised of fifth-row elements in the periodic table. Heteroatom compounds in the fourth row, such as butylphenylselenide and phenylbromide, are ~1000 times less reactive than phenyliodide.

The exchange reaction proceeds exclusively through ate complex **1** when heteroatom compounds comprised of fourth- and fifth-row elements are used,[22-25] whereas when heteroatom compounds with lighter atoms are used, minor pathways, such as a single electron transfer pathway, an S_N2 process, and a four center process,[26] also compete. Because the reactivity of the exchange reaction corresponds to the ease of formation of an ate complex, it is understandable that the heteroatom compounds with lighter elements are less reactive than those of heavier heteroatom compounds.[27] On the other hand, Reich and coworkers have reported that organoleads and organobismuthines, which are sixth-row elements, are less reactive than organostannanes and organostibines for the exchange reaction.[20] Therefore, there are no clear explanations or distinct evidence to explain the differences in reactivity among heteroatom compounds.

While developing living radical polymerization utilizing organostibine[28-30] and organobismuthine[31,32] compounds, we became interested in the possibility to generate carbanions via heteroatom-metal exchange reactions from organostibanyl and organobismuthanyl groups at the polymer ends (Scheme 2). The resulting carbanions would be synthetically useful to introduce various functional groups to the polymer ends, which cannot be made by other methods, such as radical- or carbocation-mediated transformation reactions. Such functionalization of the polymer end groups would add new functionalities and properties producing new functional polymeric materials with new or improved properties.[33-37] We have already reported that a methyltellanyl ω-end group in a polystyrene prepared by organotellurium-mediated living radical polymerization[38-46] can be transferred to styryl lithium by a tellurium-lithium exchange reaction,[47-51] and the reaction of the anion with carbon dioxide, gave ω-carboxylic acid polystyrene.[52] However, it is unclear whether this protocol is applicable to the end group of living polymers possessing polar functional groups. Since the high compatibility of polar functional groups is one of the most characteristic features of living radical polymerization, direct end-group functionalization of the functionalized polymers via carbanions is a major challenge in synthetic polymer chemistry.

Scheme 2. Synthesis of ω-functionalized poly(meth)acrylate through polymer-end anionic species.

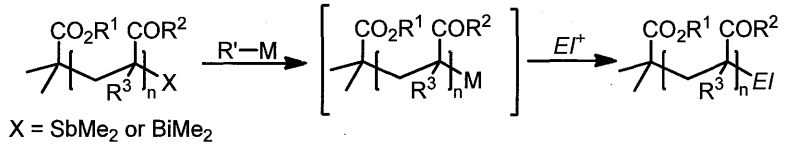

X = $SbMe_2$ or $BiMe_2$

We report here the generation of carbanions from organostibines and organobismuthines by heteroatom-metal exchange reactions. Generation of the carbanions occurs very rapidly and efficiently when stabilized carbanions, namely benzilic anions and enolate derivatives, are liberated. Since the reactivities of organostibines and organobismuthines are extremely high, the exchange reaction occurred exclusively at the polymer end even in the presence of polar functional groups in the polymer mainchains. Subsequent reactions with electrophiles gave ω-end functionalized polymers with highly controlled and defined structures in terms of molecular weights, molecular weight distributions, and end group functionalities. In addition, the reactivities of the heteroatom compounds towards the exchange reaction were examined. Competition experiments showed organostibines and organobismuthines were among the most reactive heteroatom compounds.

Results and Discussion

Generation of carboanions by stibine-metal and bismutine-metal exchange reactions. We initially examined stibine-metal exchange reactions by using ethyl 2-dimethylstibanyl-2-methylpropionate (**2a**) as a model substrate of polymethacrylate polymer-end groups (Table 1). **2a** was treated with BuLi (1.1 equiv) in THF at –78 °C for 0.5 h, and the generated anion, namely the lithium enolate of ethyl 2-methylpropionate, was treated with benzaldehyde (1.1 equiv) for 0.5 h at –78 °C to room temperature. Workup provided the desired alcohol **2A** in 97% yield (Table 1, entry 1). The exchange reaction occurred exclusively, and side products, such as an alcohol derived from the direct addition of BuLi to the ester, were not detected, indicating the high reactivity of organostibanyl groups. Me_4ZnLi_2,[53-55] *t*-Bu_4ZnLi_2,[56-58] and *i*-PrMgCl·LiCl,[59,60] which exhibit high functional group compatibility, were also effective for the exchange reaction, and **2A** was selectively obtained in nearly quantitative yield after the reaction with benzaldehyde in all cases (entries 2–4). Although a methyl anion can be generated upon the exchange reaction with **2a** via Sb-CH_3 bond cleavage, no such product was detected. In other words, only the most stable anion is liberated from **2a**. Methyl 2-dimethylbismuthanyl-2-methylpropionate (**3b**) and 2-diphenylbismuthanyl-2-methyl -propionitrile (**4c**) reacted with BuLi, Me_4ZnLi_2, *t*-Bu_4ZnLi_2, and *i*-PrMgCl·LiCl to afford **3A** and **4A**, respectively, in excellent yield in all cases after treatment of the generated carbanions with benzaldehyde (entries 5-12). Moreover, the ester and cyano groups remained intact in all cases, revealing the high reactivity of organostibanyl and organobismuthanyl groups towards organometallic reagents.

Table 1. Stibine-metal and Bismutine-metal Exchange Reactions.[a]

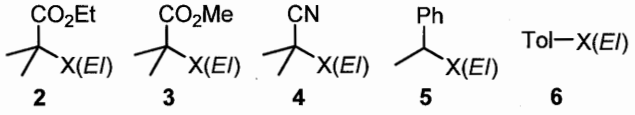

2 **3** **4** **5** **6**

a: X = $SbMe_2$, **b**: X = $BiMe_2$, **c**: X = $BiPh_2$, **d**: X= $SbTol_2$, **e**: X = $BiTol_2$
A: *El* = CH(OH)Ph, **B**: *El* = C(OH)Ph_2

Entry	Substrate	R'-M	Electrophile	Product	Yield (%)[b]
1	**2a**	BuLi	PhCHO	**2A**	97
2	**2a**	Me_4ZnLi_2	PhCHO	**2A**	99
3	**2a**	*t*-Bu_4ZnLi_2	PhCHO	**2A**	95
4	**2a**	*i*-PrMgCl·LiCl[c]	PhCHO	**2A**	93
5	**3b**	BuLi	PhCHO	**3A**	95
6	**3b**	Me_4ZnLi_2	PhCHO	**3A**	97
7	**3b**	*t*-Bu_4ZnLi_2	PhCHO	**3A**	98
8	**3b**	*i*-PrMgCl·LiCl[c]	PhCHO	**3A**	89
9	**4c**	BuLi	PhCHO	**4A**	88
10	**4c**	Me_4ZnLi_2	PhCHO	**4A**	97
11	**4c**	*t*-Bu_4ZnLi_2	PhCHO	**4A**	98
12	**4c**	*i*-PrMgCl·LiCl	PhCHO	**4A**	82
13	**5a**	BuLi	PhCOPh	**5B**	82
14	**5a**	Me_4ZnLi_2	PhCOPh	**5B**	98
15	**5a**	*t*-Bu_4ZnLi_2	PhCOPh	**5B**	95
16	**5a**	*i*-PrMgCl·LiCl	PhCOPh	**5B**	84
17	**6d**	BuLi	PhCHO	**6A**	75
18	**6d**	Me_4ZnLi_2	PhCHO	**6A**	75
19	**6d**	*t*-Bu_4ZnLi_2	PhCHO	**6A**	81
20	**6d**	*i*-PrMgCl·LiCl[c]	PhCHO	**6A**	86
21	**6e**	BuLi	PhCHO	**6A**	74
22	**6e**	Me_4ZnLi_2	PhCHO	**6A**	79
23	**6e**	*t*-Bu_4ZnLi_2	PhCHO	**6A**	80
24	**6e**	*i*-PrMgCl·LiCl[c]	PhCHO	**6A**	84

[a]Unless otherwise noted, the exchange reaction was carried out using R'-M (1.1 equiv) and substrate (1.0 equiv) in THF at –78 °C for 0.5 h, and the resultant metallated intermediate was treated with electrophiles (1.1 equiv) at –78 °C to rt for 0.5 h. [b]Determined by ^{1}H NMR with pyrazine as an internal standard. [c]The exchange reaction was carried out at 0 °C for 1 h, and the resultant metallated intermediate was treated with electrophile (1.1 equiv) at 0 °C to rt for 0.5 h.

The exchange reaction was further investigated with 1-dimethylstibanyl-1-phenylethane (**5a**), which mimics the polystyrene end group. After exchange reactions with BuLi, Me_4ZnLi_2, *t*-Bu_4ZnLi_2, and *i*-PrMgCl·LiCl, the resulting anionic species were treated with benzophenone, giving **5B** in excellent yields (entries 13–16). Exchange reactions of aryl-substituted substrates, such as tris(*p*-tolyl)stibine **6d** and -bismuthine **6e** with the lithium, zincate, and magnesium reagents proceeded smoothly to give the desired product **6A** in high yields (entries 17–24).

Application of the exchange reaction to carbon-carbon bond formation reactions. We next investigated carbon-carbon bond formation between the anionic species generated from **2a** and **3b** and various electrophiles (Table 2). We focused on the reaction of zincate derivatives because, to the best of our knowledge, there are no reports on reactions involving zincate enolates.[61] The reactions of lithium enolates generated from **2a** and **3b** were examined as references, and the results are summarized in the Experimental Section (Table 6). The zincate enolate generated from **2a** and **3b** with Me_4ZnLi_2 reacted with benzophenone (1.1 equiv) to give β-lactone **7** in moderate yield (Table 2, entries 1 and 2). No β-hydroxy ester products were detected. Since many metal enolates are inert to ketones, this is an advantage of the zincate species. The reaction of the zincate enolate generated from **2a** and Me_4ZnLi_2 or *t*-Bu_4ZnLi_2 with benzoyl chloride and carbon dioxide took place efficiently giving α-keto and α-carboxylic esters in nearly quantitative yields in all cases (entries 3, 4, 6 and 7). The enolate generated from **3b** and *t*-Bu_4ZnLi_2 showed the same reactivities and gave desired products in excellent yields (entries 5 and 8).

Moreover, zincate enolates were effective for allylation reactions when allyl iodide was used (entries 9–11). Arylation of the zincate enolate with phenyliodide in the presence of $Pd(PPh_3)_4$ gave the α-phenyl ester in moderate yields (entries 12 and 13), and the yields did not improve when other metal catalysts and/or ligands were employed.[62] Since arylation of the lithium enolate generated from **2a** and **3b** also gave similar results (Table S1), the low yields may be due to the existence of stoichiometric amounts of dimethylbutylstibine and -bisumuthine generated by the exchange reaction, which may influence the activity of the palladium catalysts.

Table 2. Reaction of "Zincate Enolate" with Electrophiles.[a]

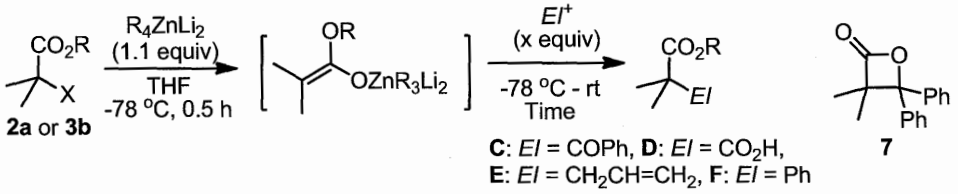

C: *El* = COPh, **D**: *El* = CO_2H, **E**: *El* = $CH_2CH{=}CH_2$, **F**: *El* = Ph

Entry	Substrate	Zincate	Electrophile (equiv)	Time (h)	Product	Yield (%)[a]
1	**2a**	Me_4ZnLi_2	PhCOPh (1.1)	3.0	**7**	61 (58)
2	**3b**	Me_4ZnLi_2	PhCOPh (1.1)	3.0	**7**	61
3	**2a**	Me_4ZnLi_2	PhCOCl (5.0)	1.0	**2C**	97 (97)
4	**2a**	*t*-Bu_4ZnLi_2	PhCOCl (5.0)	1.0	**2C**	99
5	**3b**	*t*-Bu_4ZnLi_2	PhCOCl (5.0)	1.0	**3C**	99 (95)
6	**2a**	Me_4ZnLi_2	CO_2 (excess)	2.0	**2D**	92 (91)
7	**2a**	*t*-Bu_4ZnLi_2	CO_2 (excess)	2.0	**2D**	90
8	**3b**	*t*-Bu_4ZnLi_2	CO_2 (excess)	2.0	**3D**	95 (91)
9	**2a**	Me_4ZnLi_2	Allyl Iodide (5.0)	5.0	**2E**	85 (82)
10	**2a**	*t*-Bu_4ZnLi_2	Allyl Iodide (5.0)	3.0	**2E**	94
11	**3b**	*t*-Bu_4ZnLi_2	Allyl Iodide (5.0)	3.0	**3E**	92 (92)
12	**2a**	Me_4ZnLi_2	PhI[b](2.0)	24	**2F**	59 (58)
13	**3b**	Me_4ZnLi_2	PhI[b](2.0)	24	**3F**	53 (48)

[a]Crude yield, which was determined by ^{1}H NMR with pyrazine as an internal standard. The number in parentheses is the isolated yield. [b]5 mol% $Pd(PPh_3)_4$ was added as a metal catalyst.

Generation of carboanions at ω-polymer end groups and their application to the synthesis of ω-functionalized polymers. The synthetic utility of the exchange reaction was further examined in the transformation of organostibine and -bismuthine polymer end groups of poly(meth)acrylate derivatives. Poly(methyl methacrylate) (PMMA) **8a** with a dimethylstibanyl group at the ω-end of the polymer (M_n = 3000, M_w/M_n = 1.21, where M_n and M_w are the number average and weight average molecular weights, respectively, and M_w/M_n is the molecular weight distribution) was prepared in 97% yield by heating **3a** and MMA (30 equiv) in the presence of dimethyl 2,2'-azobis(2-methylpropionate) (V-601) at 60 °C for 3 h.[28] It was dissolved in THF and treated with 1.1 equiv of BuLi at –78 °C for 0.5 h. The reaction was quenched by adding DCl (2.0

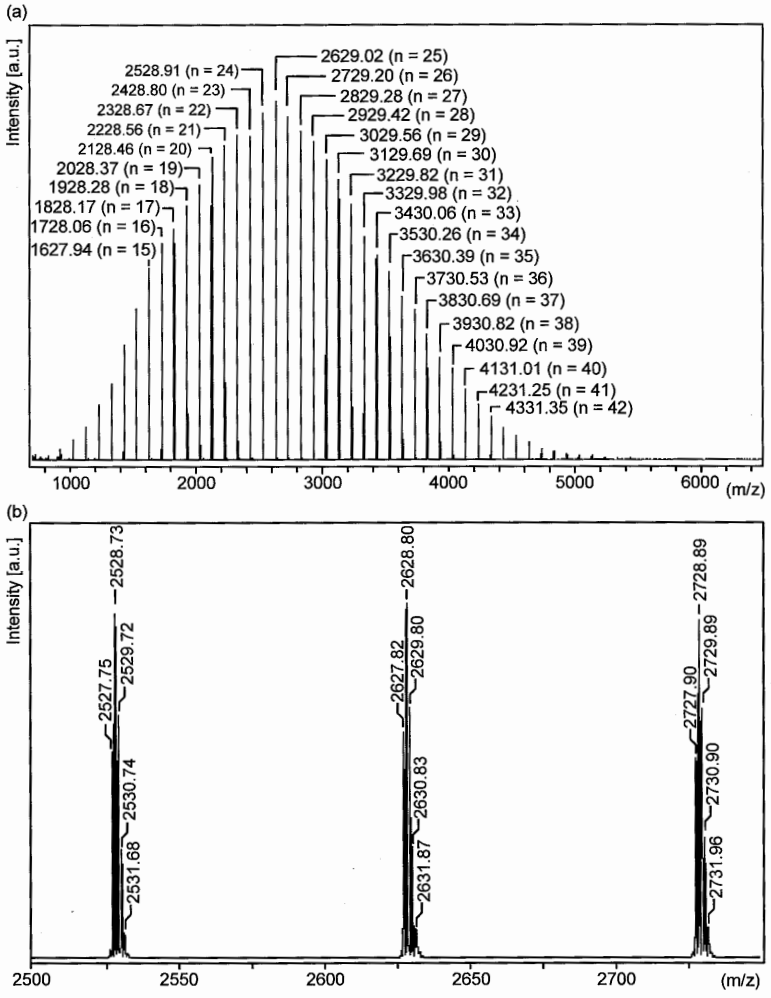

Figure 1. Full (a) and enlarged (b) TOF-MS spectra of ω-end deuterated PMMA **9F** (Table 3, entry 1).

equiv) in D_2O to give the ω-end deuterated PMMA **9F** with M_n = 3000 and M_w/M_n = 1.21 (Table 3, entry 1). The similarity of M_n and M_w/M_n before and after the exchange reaction indicated that decomposition did not occur during the exchange reaction. Matrix-assisted laser-desorption ionization time-of-flight mass (MALDI-TOF MS) spectroscopy showed only a series of peaks possessing the molecular ion masses of **9F** (Figure 1). In the ^2H NMR spectrum for **9F**, a broad singlet was observed at 2.46 ppm which corresponds to the α-ester deuterium. Treatment of PMMA **8b** having a dimethylbismuthanyl group (M_n = 3300, M_w/M_n = 1.13) with BuLi under identical conditions as those used for **8a** quantitatively transformed to **9F** (entry 2). The results clearly demonstrate that the exchange reaction involving organostibine and -bismuthine polymer end groups and BuLi is highly chemoselective despite the excess number of ester groups in PMMA **8**. The incate and magnesium enolates generated from **8b** with Me_4ZnLi_2, *t*-Bu_4ZnLi_2, and *i*-PrMgCl·LiCl also afforded **9F** quantitatively in all cases after treatment with DCl/D_2O (entries

3–5). The results clearly indicated the high reactivity of these heteroatom groups towards the exchange reaction.

The exchange reaction was successfully applied to the synthesis of ω-end functionalized PMMA by the reaction of the anionic species with various electrophiles. For example, the exchange reaction of PMMA **8a** with BuLi followed by the addition of CO_2 produced ω-carboxylic acid PMMA **9D**, which was converted to the corresponding methyl ester **9G** (M_n = 3100 M_w/M_n = 1.19) by treatment with trimethylsilyl diazomethane (entry 6). The ^{1}H NMR and MALDI-TOF MS

Table 3. Synthesis of ω-End Functionalized PMMA.

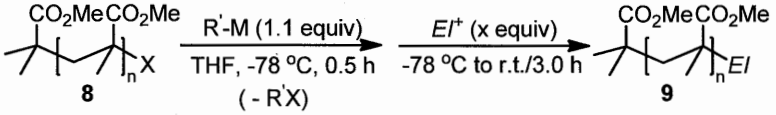

a: X = $SbMe_2$, **b**: X = $BiMe_2$.

C: *El* = COPh, **D**: *El* = CO_2H, **E**: *El* = $CH_2CH{=}CH_2$, **F**: *El* = D, **G**: *El* = CO_2Me, **F**: *El* = H

Entry	Substrate	R'-M	Electrophile (equiv)	Product	M_n/PDI	Incorp. (%)[a]
1	**8a**	BuLi	DCl/D_2O (2.0)	**9F**	3,000/1.21	>99
2	**8b**	BuLi	DCl/D_2O (2.0)	**9F**	3,400/1.13	>99
3	**8b**	Me_4ZnLi_2	DCl/D_2O (2.0)	**9F**	3,300/1.12	>99
4	**8b**	*t*-Bu_4ZnLi_2	DCl/D_2O (2.0)	**9F**	3,200/1.11	>99
5	**8b**	*i*-PrMgCl·LiCl	DCl/D_2O (2.0)	**9F**	3,300/1.11	>99
6	**8a**	BuLi	CO_2 (excess)[b]	**9D**	3,100/1.19	>99 (97)
7	**8b**	BuLi	CO_2 (excess)[b]	**9D**	3,500/1.13	>99 (97)
8	**8a**	BuLi	PhCOCl (5.0)	**9C**	3,100/1.20	99 (96)
9	**8b**	BuLi	PhCOCl (5.0)	**9C**	3,500/1.11	99 (98)
10	**8a**	BuLi	Allyl Iodide (5.0)	**9E**	3,100/1.20	98 (98)
11	**8b**	BuLi	Allyl Iodide (5.0)	**9E**	3,500/1.12	97 (95)
12	**8a**	BuLi	PhCHO (5.0)	**10**	3,100/1.20	90[c]
13	**8b**	BuLi	PhCHO (5.0)	**10**	3,400/1.13	89[c]

[a]Rate of end group incorporation determined by MALDI-TOF MS. The number in parentheses is the data derived from ^{1}H NMR analysis. [b]Carboxylic acid on ω-end was converted to methyl ester before GPC analysis with trimethylsilyldiazomethane (2.0 equiv). [c]The minor alcohol product **12** was quantitatively transformed into **10** by treatment with trifluoroacetic acid (2 equiv) in CH_2Cl_2 at room temperature.

analyses indicated a nearly quantitative conversion for **8a** to **9G**. The lithium species was also trapped with benzoyl chloride (5 equiv) and allyl iodide (5 equiv) to give the corresponding ω-end functionalized PMMA **9C** (M_n = 3100, M_w/M_n = 1.20) and **9E** (M_n = 3100, M_w/M_n = 1.20), respectively (entries 8 and 10). The desired products formed almost quantitatively on the bases of ^{1}H NMR spectroscopy and MALDI-TOF MS. When benzaldehyde (5 equiv) was used as an electrophile, PMMA **10** having a δ-lactone, formed as the major product (entry 12) via intramolecular cyclization of the initially formed lithium alkoxide **11** with the adjacent ester group (Scheme 3). MALDI-TOF MS analysis indicated the formation of two minor products, which were assigned to β-hydroxyl ester **9A** and end-protonated PMMA **9F** in a ratio of **10/9A/9F** = 90:9:1. Alcohol **9A** was cleanly converted to **10** by treatment with trifluoroacetic acid in CH_2Cl_2.

The reaction using dimethylbismuthanyl-group substituted PMMA **8b** gave virtually identical results under the same conditions as those for **8a**, and the desired ω-functionalized PMMAs with nearly quantitative end group transformation were obtained in all cases (entries 7, 9, 11, and 13). These results clearly demonstrated the successful synthesis of highly controlled PMMAs in terms of molecular weights, molecular weight distributions, and the end groups by successive living radical polymerization and end group transformation.

Scheme 3. Formation of **10** and **9A** and transformation from **9A** to **10**. *a*) 1. BuLi (1.1 equiv), THF, –78 °C, 0.5 h, 2. PhCHO (5 equiv), –78 °C to rt, 3 h. *b*) trifluoroacetic acid (2.0 equiv), CH_2Cl_2, reflux, 3h.

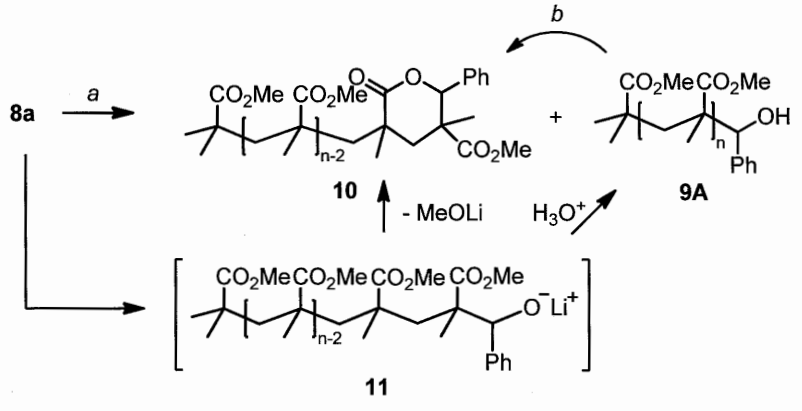

The scope of the exchange reaction was further investigated by employing various functionalized polymers with an acidic hydrogen in the main chain. For example, the reaction of poly(butyl acrylate) (PBA) **12** having a ω-dimethylstibanyl group (M_n = 4000, M_w/M_n = 1.08) with BuLi followed by the addition of benzoyl chloride (5 equiv) gave the desired ω-benzoylated PBA

13 together with cyclic β-ketoester **14** and ω-end protonated product in a ratio of 57:36:7 on the basis of MALDI-TOF MS (Scheme 4). The formation of **14** must be due to intramolecular condensation of the initially formed lithium species with the nearby ester group.[63-65] In contrast, the exchange reaction of **12** (M_n = 4100, M_w/M_n = 1.09) with *t*-Bu_4ZnLi_2 instead of BuLi selectively gave **13** (M_n = 4000, M_w/M_n = 1.10) with nearly quantitative incorporation of the benzoyl group (97%).

Introduction of an electrophile to the mid chain of the polymer to give **15** might occur via anion migration followed by trapping with benzoyl chloride. However, this possibility was ruled out on the basis of labeling experiments using ^{13}C-labeled benzoyl chloride, Ph^{13}COCl. In the ^{13}C NMR spectra of ^{13}C-labeled PBA **13-^{13}C**, the signals corresponding to the carbonyl carbon of the benzoyl group in the range of 193–194 ppm was greatly enhanced than those of **13**, and the chemical shifts were similar to that for the benzoyl group in methyl 2-benzoylpropionate (196 ppm).[66] The peak for the ketone carbon of **15**, which has a quaternary carbon adjacent to the benzoyl group, should appear lower field by ~10 ppm from that of **13**. However, they were not observed at all. The results unambiguously prove the structure of the product and thus the stability of the polymer-end anionic species.

Scheme 4. Functionalization of poly(butyl acrylate). Reaction conditions; *a*) 1. *t*-Bu_4ZnLi_2 (1.1 equiv), THF, –78 °C, 0.5 h, 2. PhCOCl (5 equiv), –78 °C to rt, 3 h. *b*) 1. *t*-Bu_4ZnLi_2 (1.1 equiv), THF, –78 °C, 0.5 h, 2. Ph^{13}COCl (5 equiv), –78 °C to rt, 3 h.

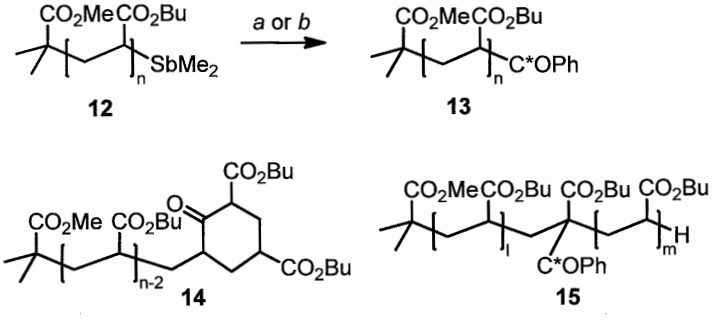

The exchange reactions with zincate were compatible with free hydroxyl groups and amide protons (Scheme 5). The exchange reaction of poly(*N*-isopropyl acrylamide) (PNIPAM) **16** having dimethylstibanyl ω-end group (M_n = 3400, M_w/M_n = 1.09) with *t*-$BuZnLi_2$ (1.1 equiv) selectively took place in DMF at –60 °C without protection of the amide protons. Subsequent addition of benzoyl chloride (5.0 equiv) gave the desired product **17** (M_n = 3500, M_w/M_n = 1.10) with

quantitative incorporation (> 99%) of the benzoyl group (Scheme 5a). The exchange reaction in DMSO at room temperature also gave **17** quantitatively after addition of benzoyl chloride. Although the exchange reaction in THF, MeOH, and H_2O proceeded efficiently, subsequent reactions with electrophiles gave ω-protonated PNIPAM as the major product. A polymer-end anion could be generated from poly(2-hydroxyethyl methacrylate) **18** (M_n = 3800, M_w/M_n = 1.28) by treatment with *t*-$BuZnLi_2$ in DMSO, and subsequent reaction with allyl iodide (5 equiv) gave desired allylated product **19** (M_n = 4000, M_w/M_n = 1.28) quantitatively (Scheme 5b).

Scheme 5. Functionalization of PNIPAM and poly(hydroxyethyl methacrylate).

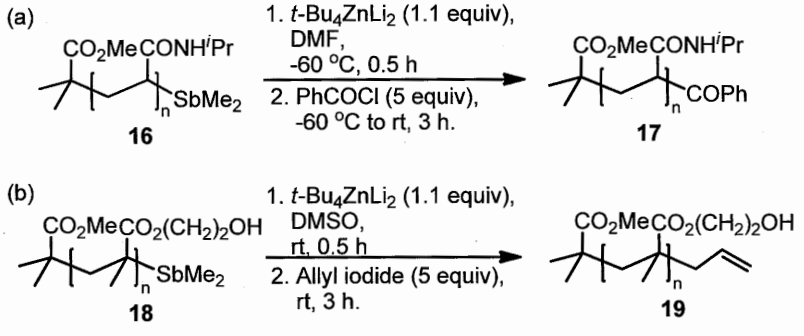

On the basis of the high chemoselectivity, the current method was applied to the synthesis of an ω-biotinylated polymer (Scheme 6). Treatment of PNIPAM **16** with *t*-$BuZnLi_2$ in DMF followed by the addition of biotinyl chloride (5 equiv) exclusively afforded ω–biotinylated PNIPAM **20** (M_n = 3900, M_w/M_n = 1.11). The structure of **20** was unambiguously confirmed by using ^1H NMR and MALDI-TOF MS analyses (Figure 2). PNIPAM is a thermoresponsive polymer and possesses lower critical solution temperature in water. On the other hand, biotin is a good ligand for proteins, such as avidin and streptavidin. Therefore, this polymer and its analogs would make it possible to thermally modulate the properties of biomaterials for biological applications.[67]

Scheme 6. Synthesis of ω–biotinylated PNIPAM **20**.

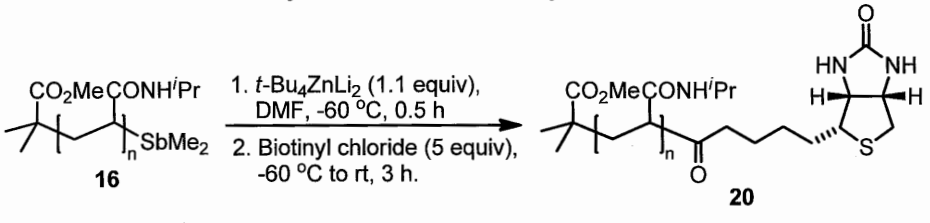

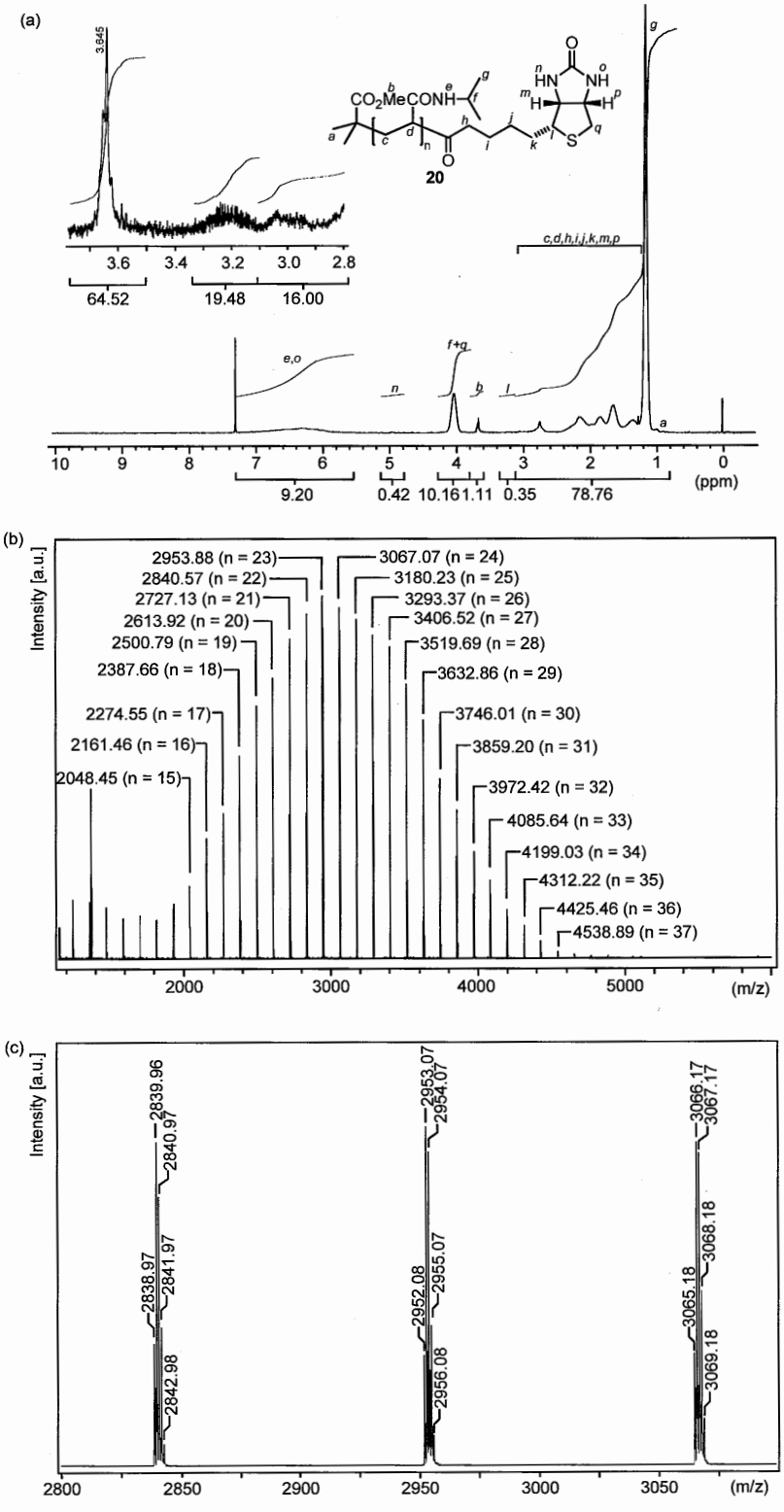

Figure 2. (a) ^{1}H NMR and (b) full and (c) expanded TOF-MS spectra of ω–biotinylated PNIPAM **20**. In TOF MS spectra, the molecular ions were observed as sodium ion adducts [$m/z = (M + Na)^{+}$].

Relative reactivities of heteroatom compounds towards exchange reactions. In order to clarify the reactivity of organostibines and -bismuthines towards the exchange reactions, we carried out competition experiments using organoiodides as references. In addition, we examined the reactivity of organotellurium compounds in conjunction with living polymerization methods that we developed. We first compared the reactivity of α-heteroatom-substituted esters **3** and **2f** (Table 4). BuLi (1.0 equiv) was added to a mixture of organobismuthine **3b** (5.0 equiv), ethyl 2-iodo-2-methylpropionate (**2f**, 5.0 equiv), and benzaldehyde (15 equiv) in THF at –78 °C. After stirring for 15 min at this temperature, the reaction was quenched by adding AcOH/MeOH. After work-up, the yields of alcohols **3A**, **2A**, and 1-phenyl-1-pentanol (**21**) were determined by GC analysis with tetradecane as an internal standard. The same reaction was repeated six times, and the yields of four experiments excluding the highest and lowest yields were averaged (see Table 4, entry 1). The same experiments were carried out with a combination of organostibine **3a** and **2f** and organotellurium **3g** and **2f** (entries 2 and 3). In addition, the effects of the ester moiety on the exchange reaction were examined by using **2f** and 2-iodo-2-methylpropionate (**3f**) (entry 4), and the reactivity of each heteroatom compound was corrected in relation to this data. These results clearly show that the organobismuthine has the highest reactivity followed by the organostibine, and Then the organotelluride, and the organoiodide is the least reactive. In other words, the relative reactivity increased in the order of iodine, telluride, stibine, and bismuthine in a ratio of 1.0:1.8:2.7:4.7 in THF at –78 °C.

Table 4. Competition Experiments of Alkylheteroatom Compounds.

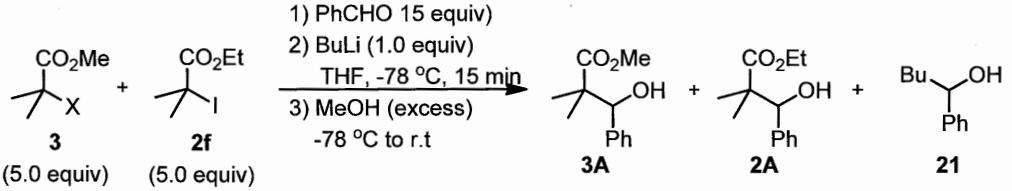

Entry	X	Yield (%)[a]			3A/2A	Reactivity
		3A	**2A**	**21**		(X/I)[b]
1	$BiMe_2$ (**3b**)	54.5	9.0	35.0	6.1	4.7
2	$SbMe_2$ (**3a**)	43.0	12.5	32.5	3.5	2.7
3	TeMe (**3g**)	25.5	11.0	26.5	2.3	1.8
4	I (**3f**)	14.5	11.0	31.0	1.3	-

[a]Determined by gas chromatography with hexadecane as an internal standard.
[b]Reactivity of heteroatom group after compensation of the effect of the ester group.

It is worth noting that the exchange reaction of **3b** and **3a** giving **3A** took place much faster than the direct addition of BuLi to benzaldehyde giving **21**. This result is consistent with the selective exchange reaction observed for the PMMA polymer-end organobismuthine and organostibine species as mentioned above. Moreover, when a three-fold excess of benzaldehyde over heteroatom species was employed in the experiments, the exchange reaction between **3g** and **2f** took place considerably faster than the addition of BuLi to benzaldehyde. The result suggests that a similar polymer-end group transformation using (meth)acrylate derivatives is possible for organotellurium and organoiodine polymer ends.[61]

We next carried out the competition experiments using aryl-substituted heteroatom compounds with phenyliodide as a reference (Table 5). The competition between tri(*p*-tolyl)bismuthine (**6e**) and phenyliodide in the presence of benzaldehyde gave **6A**, diphenylmethanol (**22**), and 1-phenylbutanol (**23**) in 0.1%, 7.5%, and 23% yields, respectively (entry 1). The competitions between tri(*p*-tolyl)stibine (**6d**) and phenyliodide and between di(*p*-tolyl)telluride (**6h**) and phenyliodide were also examined, and the yields of the products are listed in Table 5, entries 2 and 3. Despite the low yields of **6A** and low mass balances in all cases, the relative reactivity index for each heteroatom compound was determined after compensating for the reactivity difference between phenyliodide and *p*-iodotoluene (entry 4). The results suggest that,

Table 5. Competition Experiments of Arylheteroatom Compounds.

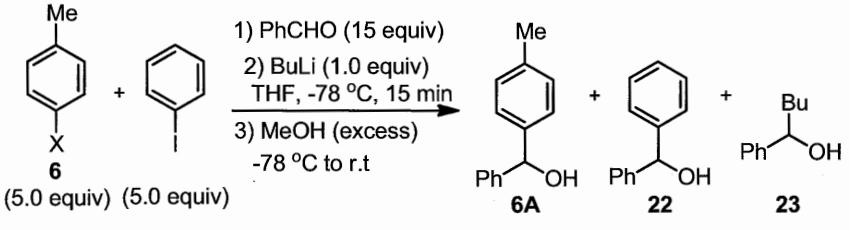

Entry	X	Yield (%)[a]			6A/22	Reactivity
		6A	**22**	**23**		(X/I)[b]
1	Bi(*p*-Tol)$_2$ (**6e**)	0.1	7.5	23.0	0.013	0.025
2	Sb(*p*-Tol)$_2$ (**6d**)	0.8	12.5	42.0	0.064	0.12
3	Te(*p*-Tol) (**6h**)	1.9	8.0	50.5	0.24	0.47
4	I	4.6	9.0	54.5	0.52	-

[a]Determined by gas chromatography using tetradecane as an internal standard.
[b]Reactivity of heteroatom group after compensation of the effect of the aryl group.

in contradiction to the results using **2** and **3**, the reactivity of aryl-substituted heteroatom compounds increases in reverse order: aryliodides > diaryltellurides > triarylstibines > triarylbismuthines in a ratio of 1:0.47:0.12:0.025 in THF. However, since the mass balance of the reaction was low, especially when **6e** and **6d** were employed, we concluded that this ratio did not reflect the kinetic reactivity of the heteroatom species for the following reason.

The exchange reaction takes place via ate complex **1** (Scheme 1), which is inert to carbonyl compounds.[68] Therefore, the formation of alcohols **2A**, **3A**, **6A**, and **22** are affected by boththe kinetic reactivity in forming the ate complex and the ease of generating a free anion from the ate complex. The pK_a of the conjugate acid of lithium enolate, mehyl isobutyrate, and BuLi, butane, are ca. 25 and 50, respectively, suggesting that the formation of lithium enolate is highly exothermic. Therefore, the liberation of the enolate from the ate complex should take place spontaneously, and the reactivity ratio using **3** and **2f** strongly reflects the kinetic reactivities of the heteroatom compounds in forming the ate complex. On the other hand, the stability of aryl lithiums (the pK_a of benzene is 43) is close to butyl lithium, and the ate complexes become more stable when aryl groups are present.[20,22] Therefore, the liberation of a reactive, free anion from the ate complex becomes slow in the case of aryl-substituted heteroatom compounds. Consequently, the results in Table 5 can be explained by the rapid formation of the ate complex, from which the liberation of the free anion is very slow. In other words, the low yields of **6A** reflect the rapid formation of stable ate complexes and indicate the high reactivity of these heteroatom compounds.

Our reactivity index between organotellurium and organoiodide is opposite to the one reported by Sonoda and coworkers.[69] We believe that the results must be due to the substituent on the tellurium atom. Sonoda and coworkers used butylphenyltelluride, and we used **3g** and **6h**. In the case of **3g**, the formation of stable enolate species decreases the activation energy for the formation of the ate complex. In the case of **6h**, the presence of two aryl groups in the molecule stabilizes the ate complex and, thus, decreases the activation energy for forming the ate complex. Furthermore, the results suggest that the substituent on the heteroatom influences the reactivity of the exchange reaction.

Conclusions

Generation of carbanions from organostibine and organobismuthine compounds through stibine-metal and bismuth-metal exchange reactions was investigated. The exchange reactions

proceeded quantitatively generating the corresponding carbanions with several organometallic reagents. The exchange reactions occurred with high chemoselectivity, and a variety of polar functional groups could be tolerated. The resulting highly functionalized carbanions were utilized for carbon-carbon bond formation with various electrophiles. The advantage of this method was exemplified in the selective functionalization of polymer ends, prepared by organostibine- and organobismuthine-mediated living radical polymerization giving a variety of structurally well-defined ω-functionalized polymers. In addition to the synthetic utility, this work provides insight into the relative reactivities of heavier organoheteroatom compounds in heteroatom-metal exchange reactions. We believe that this work opens new possibilities for synthetic application of organostibines and organobismuthines in carbanion chemistry.

Experimental Section

General. All reaction conditions dealing with air- and moisture sensitive compounds were carried out in a dry reaction vessel under nitrogen atmosphere. ^{1}H and ^{13}C NMR (400 and 100 MHz, respectively) spectra were measured for a $CDCl_3$, CD_2Cl_2, or CD_3OD solution of a sample and are reported in parts per million (δ) from internal tetramethylsilane or residual solvent peak. IR spectra (absorption) are reported in cm^{-1}. High resolution mass spectra (HRMS) were obtained under electron impact ionization conditions. Matrix-assisted laser-desorption ionization time-of-flight mass (MALDI-TOF MS) spectrum was obtained on a spectrometer in the positive reflection mode and at 20 kV acceleration voltage. Samples were prepared from a tetrahydrofuran (THF) solution by mixing sample (5 mg/mL), dithranol (10 mg/mL), and sodium trifluoroacetate (5 mg/mL) in a ratio of 1:2:1. The gel permeation chromatography (GPC) was performed with two linearly connected polystyrene mixed gel columns, which were calibrated with poly(methyl methacrylate) (PMMA) standards. Analyses were made using chloroform as an eluant for PMMA and poly(butyl acrylate) (PBA) samples with a flow rate of 0.3 mL/min and 0.01 mol/L lithium chloride solution of *N*,*N*-dimethylformamide (DMF) as an eluant for poly(*N*-isopropyl acrylamide) (PNIPAM) and poly(2-hydroxyethyl methacrylate) samples with a flow rate of 1.0 mL/min with a refractive-index (RI) detector at 40 °C. Gas chromatography (GC) analysis was performed on Shimadzu GC-14B instrument equipped with a capillary column, CBP1-M25-025 (Shimadzu, 25 m × 0.25 mm).

Materials. Unless otherwise noted, commercially available materials were used without purification. Tetrahydrofuran (THF) was distilled from sodium benzophenone ketyl and stored

under nitrogen atmosphere. DMF and dimethylsulfoxide (DMSO) were distilled over P_2O_5 and calcium hydride under reduced pressure, respectively, and were stored over molecular seives. Water content in solvents were determined by Karl-Fisher water titrater. Methyl methacrylate (MMA) and butyl acrylate (BA) were washed with 5% aqueous sodium hydroxide solution and were distilled over calcium hydride under reduced pressure and stored under nitrogen atmosphere. 2-Hydroxyethyl methacrylate was purified as reported.[70] *N*-Isopropylacrylamide (NIPAM) and dimethyl 2,2'-azobis(2-methylpropionate) (V-601) were recrystallized from hexane and cold methanol, respectively. Ethyl 2-dimethylstibanyl-2-methylpropionate (**2a**),[28] methyl 2-dimethylbismuthanyl-2-methylpropionate (**3b**),[31] ethyl 2-methyltellanyl-2-methylpropionate (**3g**),[52] 2-diphenylbismuthanyl-2-methylpropionitrile (**4c**),[3] 1-dimethylstibanyl-1-phenylethane (**5a**),[2] were prepared as reported. Tri-(*p*-tolyl) stibine (**6d**)[71] and tri-(*p*-tolyl) bismuthine (**6e**)[72] were prepared by the reaction of trichlorostibine and bismuthine with *p*-tolyl magnesium bromide, which were prepared from *p*-tolylbromide and magnesium. ^{13}C-Benzoyl chloride[73] and biotinyl chloride[74] were prepared by the reaction of ^{13}C-labeled benzoic acid and biotin with thionyl chloride, respectively. Ethyl α-iodoisobutyrate (**2f**),[75] methyl α-iodoisobutyrate (**3f**),[75] di-(*p*-tolyl) telluride (**6i**)[76] were prepared as reported. MeLi in Et_2O, *n*-BuLi in hexane, and *t*-BuLi in pentane were titrated before use.[77,78] Me_4ZnLi_2[53], *t*-Bu_4ZnLi_2[56], and *i*-PrMgCl·LiCl[59] were prepared as reported and used immediately.

Preparation of methyl 2-dimethylstibanyl-2-methylpropionate (2b). Methyl isobutyrate (6.4 mL, 56 mmol) was added to a THF solution of lithium diisopropylamide, which was prepared by adding *n*-butyllithium (37.6 mL, 1.57 M in hexane, 59 mmol) to a solution of diisopropylamine (8.3 mL, 59 mmol) in THF (100 mL) at -78 °C, and the resulting solution was stirred at this temperature for 0.5 h. Dimethylstibanyl bromide[79] (13.0 g, 56 mmol) was added to this solution, and the resulting mixture was stirred for 2 h at this temperature. Water, which was deoxygenated by passing through a nitrogen gas for 0.5 h before use, was added to this solution, and the aqueous layer was separated under nitrogen atmosphere. The remaining organic phase was washed successively with deoxygenated saturated aqueous NH_4Cl solution and saturated aqueous NaCl solution, dried over Na_2SO_4, and filtered under nitrogen atmosphere. Solvent was removed under reduced pressure followed by distillation under reduced pressure (b.p. 43-45 °C/1.1-1.3 mmHg) to give a colorless oil (49% yield, 6.94 g). ^{1}H NMR ($CDCl_3$, 400 MHz) 0.74 (s, 6H, Sb*Me*$_2$), 1.43 (s, 6H, -C*H*$_3$), 3.67 (s, 3H, CO_2*Me*); ^{13}C NMR ($CDCl_3$, 100 MHz) -1.7, 23.5, 31.7, 50.9, 177.2; HRMS

(EI) *m/z*: Calcd for $C_{16}H_{16}NSb$ $(M)^+$, 252.0110; Found 252.0118; IR (neat) 815, 1135, 1185, 1270, 1460, 1695, 2940.

General procedure of the exchange reaction with BuLi (Table 1, entry 1). A solution of **2a** (20.6 μL, 0.10 mmol) in THF (0.5 mL) was treated with BuLi (71.4 μL, 1.54 M solution in hexane, 0.11 mmol) at -78°C. After stirring for 0.5 h at this temperature, benzaldehyde (10.6 μL, 0.11 mmol) was added, the resulting mixture was slowly warmed to room temperature over 0.5 h. The reaction mixture was quenched with saturated aqueous NH_4Cl solution (0.5 mL), and was extracted with ethyl acetate (0.5 mL x 3). The organic layer was washed with saturated aqueous NaCl solution, dried over $MgSO_4$, filtered and concentrated under reduced pressure to give a crude mixture. The yield (97%) of **2A** was determined by ^1H NMR using pyrazine as an internal standard. Purification by silica gel chromatography (ethyl acetate/ hexane = 25 : 75, R_f = 0.32) afforded **2A** in 92 % yield (20.4 mg) as a colorless solid. mp: 39.8-41.6 °C. ^1H NMR ($CDCl_3$) 1.10 (s, 3H, -C*H*$_3$), 1.13 (s, 3H, -C*H*$_3$), 1.27 (t, *J* = 7.2 Hz, 3H, -$CO_2CH_2CH_3$), 3.57 (s, 1H, -O*H*), 4.18 (q, *J* = 7.2 Hz, 2H, -$CO_2CH_2CH_3$), 4.91 (s, 1H, -C*H*OH), 7.25-7.36 (m, 5H, -*Ph*); ^{13}C NMR ($CDCl_3$) 14.3, 19.1, 23.3, 47.7, 61.1, 78.9, 127.8, 127.9, 140.1, 178.1; HRMS (EI) *m/z*: Calcd for $C_{13}H_{18}O_3$ $(M)^+$, 222.1256; Found 222.1254; IR (KBr) 710, 1049, 1153, 1267, 1705, 2980, 3499.

General procedure for the exchange reaction with Me_4ZnLi_2 (Table 1, entry 2). A solution of **2a** (20.6 μL, 0.10 mmol) in THF (0.5 mL) was treated with Me_4ZnLi_2 (1.0 mL, 0.11 M solution in THF, 0.11 mmol) at -78°C. After stirring for 0.5 h at this temperature, benzaldehyde (10.6 μL, 0.11 mmol) was added by a syringe, and the resulting mixture was slowly warmed to room temperature over 0.5 h. The reaction mixture was quenched with saturated aqueous NH_4Cl solution (0.5 mL), and was extracted with ethyl acetate (0.5 mL x 3). The organic layer was washed with saturated aqueous NaCl solution, dried over $MgSO_4$, filtered and concentrated under reduced pressure to give a crude mixture. The yield (99%) of **2A** was determined by ^1H NMR using pyrazine as an internal standard.

General procedure for the exchange reaction with *t*-Bu_4ZnLi_2 (Table 1, entry 3). A solution of **2a** (20.6 μL, 0.10 mmol) in THF (0.5 mL) was treated with *t*-Bu_4ZnLi_2 (0.79 mL, 0.14 M solution in THF, 0.11 mmol) at -78°C. After stirring for 0.5 h at this temperature, benzaldehyde (10.6 μL, 0.11 mmol) was added by a syringe, and the resulting mixture was slowly warmed to room temperature over 0.5 h. The reaction mixture was quenched with saturated aqueous NH_4Cl solution (0.5 mL), and was extracted with ethyl acetate (0.5 mL x 3). The organic layer was washed with saturated aqueous NaCl solution, dried over $MgSO_4$, filtered and concentrated under reduced

pressure to give a crude mixture. The yield (95%) of **2A** was determined by ^{1}H NMR using pyrazine as an internal standard.

General procedure for the exchange reaction with *i*-PrMgCl·LiCl (Table 1, entry 4). A solution of **2a** (20.6 μL, 0.10 mmol) in THF (0.5 mL) was treated with *i*-PrMgCl·LiCl (0.12 mL, 0.897 M solution in THF, 0.11 mmol) at 0°C. After stirring for 1 h at this temperature, benzaldehyde (10.6 μL, 0.11 mmol) was added by a syringe, and the resulting mixture was slowly warmed to room temperature over 0.5 h. The reaction mixture was quenched with saturated aqueous NH_4Cl solution (0.5 mL), and was extracted with ethyl acetate (0.5 mL x 3). The organic layer was washed with saturated aqueous NaCl solution, dried over $MgSO_4$, filtered and concentrated under reduced pressure to give a crude mixture. The yield (93%) of **2A** was determined by ^{1}H NMR using pyrazine as an internal standard.

The exchange reaction of **3b**, **4c**, **5a**, **6d**, and **6e** with BuLi, Me_4ZnLi_2, *t*-Bu_4ZnLi_2, or *i*-PrMgCl·LiCl was carried also carried out according to the above general procedure to give **3A**, **4A**, **5B**, and **6A**, respectively. Spectroscopic data for each product are given as follows.

Methyl 3-hydroxy-2,2-dimethyl-3-phenylpropionate (3A):[80] ^{1}H NMR ($CDCl_3$) 1.10 (s, 3H, -C*H*$_3$), 1.15 (s, 3H, -C*H*$_3$), 3.13 (s, 1H, -O*H*), 3.72 (s, 3H, -CO_2C*H*$_3$), 4.89 (s, 1H, -C*H*OH), 7.25-7.36 (m, 5H, -*Ph*); ^{13}C NMR ($CDCl_3$) 19.2, 23.3, 47.8, 52.3, 78.9, 127.8, 128.0, 140.0, 178.4.

3-Hydroxy-2,2-dimethyl-3-phenylproprionitrile (4A):[81] ^{1}H NMR ($CDCl_3$) 1.23 (s, 3H, -C*H*$_3$), 1.44 (s, 3H, -C*H*$_3$), 2.38 (s, 1H, -O*H*), 4.56 (s, 1H, -C*H*OH), 7.25-7.45 (m, 5H, -*Ph*); ^{13}C NMR ($CDCl_3$) 23.0, 23.9, 39.0, 78.4, 123.8, 127.4, 128.3, 128.7, 139.1.

1,1,2-triphenyl-1-propanol (5B): mp: 71.4-73.8 °C. ^{1}H NMR ($CDCl_3$) 1.33 (d, *J* = 6.8 Hz, 3H, -CHC*H*$_3$), 3.99 (q, *J* = 6.8 Hz, 1H, -C*H*CH$_3$), 7.03-7.13 (m, 8H, -*Ph*) 7.22-7.35 (m, 5H, -*Ph*), 7.61-7.63 (m, 2H, -*Ph*); ^{13}C NMR ($CDCl_3$) 16.7, 47.7, 80.6, 125.8, 126.4, 126.5, 126.6, 127.8, 127.9, 128.3, 129.6, 139.1, 142.0, 145.8, 146.6; HRMS (EI) *m/z*: Calcd for $C_{21}H_{20}O$ $(M)^+$, 288.1514; Found 288.1516; IR (KBr) 694, 749, 1350, 1450, 1506, 2976, 3545.

4-Methylphenyl(phenyl)methanol (6A):[82] ^{1}H NMR (400 MHz, $CDCl_3$) 2.20 (brs, 3H, -O*H*), 2.32 (s, 3H, -C*H*$_3$), 5.71 (s, 1H, -C*H*OH), 7.08-7.33 (m, 9H, -*Ar*); ^{13}C NMR (100 MHz, $CDCl_3$) 21.0, 76.3, 126.6, 126.7, 127.7, 128.7, 129.4, 137.5, 141.0, 144.1.

General procedure for the reaction of "zincate enolate" with elctrophiles.

Synthesis of 3,3-Dimethyl-4,4-diphenyl-2-oxetanone (7):[83] A solution of **2a** (20.6 μL, 0.10 mmol) in THF (0.5 mL) was treated with Me_4ZnLi_2 (1.0 mL, 0.11 M solution in THF, 0.11 mmol) at -78°C. After stirring for 0.5 h at this temperature, a solution of benzophenone (20.0 mg, 0.11

mmol) in THF (0.5 mL) was added through a cannula, and the resulting mixture was slowly warmed to room temperature over 3.0 h. The reaction mixture was quenched with saturated aqueous NH_4Cl solution (0.5 mL), and was extracted with ethyl acetate (0.5 mL x 3). The organic layer was washed with saturated aqueous NaCl solution, dried over $MgSO_4$, filtered and concentrated under reduced pressure to give a crude mixture. The yield (61%) of **7** was determined by ^1H NMR using pyrazine as an internal standard. Purification by silica gel chromatography (ethyl acetate/hexane = 20:80, R_f = 0.31) afforded **7** in 58 % yield (14.6 mg) as a colorless solid. ^1H NMR (400 MHz, $CDCl_3$) 1.22 (s, 6H, -C*H*$_3$), 7.27 (t, *J* = 7.2 Hz, 2H, -*Ph*), 7.38 (t, *J* = 7.2 Hz, 4H, -*Ph*), 7.50 (d, *J* = 7.2 Hz, 4H, -*Ph*); ^{13}C NMR (100 MHz, $CDCl_3$) 21.0, 59.3, 88.9, 124.4, 128.1, 128.6, 139.6, 175.6.

Synthesis of Ethyl 2,2-dimethyl-3-oxo-3-phenylpropanoate (2C):[84] A solution of **2a** (20.6 μL, 0.10 mmol) in THF (0.5 mL) was treated with Me_4ZnLi_2 (1.0 mL, 0.11 M solution in THF, 0.11 mmol) at -78°C. After stirring for 0.5 h at this temperature, benzoyl chloride (12.8 μL, 0.11 mmol) was added by a syringe, and the resulting mixture was slowly warmed to room temperature over 1.0 h. The reaction mixture was quenched with saturated aqueous $NaHCO_3$ solution (0.5 mL), and was extracted with ethyl acetate (0.5 mL x 3). The organic layer was washed with saturated aqueous NaCl solution, dried over $MgSO_4$, filtered and concentrated under reduced pressure to give a crude mixture. The yield (97%) of **2C** was determined by ^1H NMR using 1,2-dibromoethane as an internal standard. Purification by silica gel chromatography (ethyl acetate/hexane = 15/85, R_f = 0.30) afforded **2C** in 97 % yield (21.3 mg) as a colorless oil. ^1H NMR ($CDCl_3$) 1.05 (t, *J* = 7.2 Hz, 3H, -$CO_2CH_2CH_3$), 1.55, (s, 6H, -C*H*$_3$), 4.12 (q, *J* = 7.2 Hz, 2H, -$CO_2CH_2CH_3$), 7.40-7.44 (m, 2H, -*Ph*), 7.51-7.53 (m, 1H, -*Ph*), 7.82 -7.85 (m, 2H, -*Ph*); ^{13}C NMR ($CDCl_3$) 13.9, 24.1, 53.4, 61.5, 128.6, 128.8, 132.9, 135.3, 175.2, 198.0.

Synthesis of Methyl 2,2-dimethyl-3-oxo-3-phenylpropanoate (3C):[85] The synthesis was carried out by using the similar procedure to the synthesis of **2C**. ^1H NMR ($CDCl_3$) 1.55 (s, 6H, -C*H*$_3$), 3.65 (s, 3H, -CO_2CH_3), 7.42-7.45 (m, 2H, -*Ph*), 7.52-7.53 (m, 1H, -*Ph*), 7.81-7.84 (m, 2H, -*Ph*); ^{13}C NMR (100 MHz, $CDCl_3$) 24.1, 52.7, 53.3, 128.7, 128.7, 132.9, 135.2, 175.8, 197.7.

Synthesis of 2,2-dimethylmalonic acid monoethyl ester (2D): A solution of **2a** (20.6 μL, 0.10 mmol) in THF (0.5 mL) was treated with Me_4ZnLi_2 (1.0 mL, 0.11 M solution in THF, 0.11 mmol) at -78°C. After stirring for 0.5 h at this temperature, to this solution was bubbled into carbon dioxide for 5 min. the resulting mixture was slowly warmed to room temperature over 1.0 h. The reaction mixture was quenched with 1 mol/L aqueous HCl solution (0.5 mL), and was extracted with ethyl acetate (0.5 mL x 5). The organic layer was washed with saturated aqueous NaCl solution,

dried over $MgSO_4$, filtered and concentrated under reduced pressure to give pure **2D** (91%, 14.6 mg). The yield (92%) of **2D** was also determined by ^{1}H NMR using 1,2-dibromoethane as an internal standard.^{1}H NMR ($CDCl_3$) 1.27 (t, J = 7.2 Hz, 3H, -$CO_2CH_2CH_3$), 1.47, (s, 6H, -CH_3), 4.21 (q, J = 7.2 Hz, 2H, -$CO_2CH_2CH_3$), 9.00 (brs, 1H, -COO*H*); ^{13}C NMR ($CDCl_3$) 14.1, 22.9, 50.0, 61.8, 172.9, 178.7; HRMS (EI) *m/z*: Calcd for $C_7H_{13}O_4$ $(M + H)^+$, 161.0814; Found 161.0812; IR (neat) 1144, 1283, 1470, 1718, 2633, 2990, 3520.

Synthesis of 2,2-dimethylmalonic acid monomethyl ester (3D): The synthesis was carried out by using the similar procedure to the synthesis of **2D**. ^{1}H NMR ($CDCl_3$) 1.40 (s, 6H, -CH_3), 3.68, (s, 3H, -CO_2CH_3), 3.68, (s, 3H, -CO_2CH_3), 10.00 (brs, 1H, -COO*H*); ^{13}C NMR ($CDCl_3$) 22.9, 50.0, 52.9, 173.2, 179.1; HRMS (EI) *m/z*: Calcd for $C_6H_{11}O_4$ $(M + H)^+$, 147.0657; Found 147.0661; IR (neat) 1146, 1230, 1431, 1716, 2641, 2980, 3522.

Synthesis of Ethyl 2,2-dimethyl-4-pentenoate (2E): A solution of **2a** (20.6 μL, 0.10 mmol) in THF (0.5 mL) was treated with Me_4ZnLi_2 (1.0 mL, 0.11 M solution in THF, 0.11 mmol) at -78°C. After stirring for 0.5 h at this temperature, allyl iodide (10.0 μL, 0.11 mmol) was added by a syringe, and the resulting mixture was slowly warmed to room temperature over 5.0 h. The reaction mixture was quenched with saturated aqueous NH_4Cl and $Na_2S_2O_3$ solution (0.5 mL), and was extracted with ethyl acetate (0.5 mL x 3). The organic layer was washed with saturated aqueous NaCl solution, dried over $MgSO_4$, filtered and concentrated under reduced pressure to give a crude mixture. The yield (85%) of **2E** was determined by ^{1}H NMR using pyrazine as an internal standard. Purification by silica gel chromatography (ethyl acetate/ hexane = 4 : 96, R_f = 0.30) afforded **2E** in 82 % yield (12.9 mg) as a colorless oil.^{1}H NMR ($CDCl_3$) 1.17 (s, 6H, -CH_3), 1.25 (t, J = 7.2 Hz, 3H, -$CO_2CH_2CH_3$), 2.28 (d, J = 8.0 Hz, 2H, -$CH_2CH{=}CH_2$), 4.12 (q, J = 7.2 Hz, 2H, -$CO_2CH_2CH_3$), 5.03-5.06 (m, 2H, -$CH_2CH{=}CH_2$), 5.69-5.76 (m, 1H, -$CH_2CH{=}CH_2$); ^{13}C NMR ($CDCl_3$) 14.4, 25.0, 42.3, 44.9, 60.5, 118.0, 134.5, 177.7; HRMS (EI) *m/z*: Calcd for $C_9H_{16}O_2$ $(M)^+$, 156.1150; Found 156.1154; IR (neat) 918, 1028, 1154, 1472, 1640, 1734, 2980.

Synthesis of Methyl 2,2-dimethyl-4-pentenoate (3E):[86] The synthesis was carried out by using the similar procedure to the synthesis of **2E**. ^{1}H NMR ($CDCl_3$) 1.17 (s, 6H, -CH_3), 2.28, (d, J = 7.2 Hz, 2H, -$CH_2CH{=}CH_2$), 3.66 (s, 2H, -CO_2CH_3), 5.02-5.06 (m, 2H, -$CH_2CH{=}CH_2$), 5.69-5.76 (m, 1H, -$CH_2CH{=}CH_2$); ^{13}C NMR ($CDCl_3$) 25.0, 42.5, 44.9, 51.9, 118.1, 134.4, 178.2.

Synthesis of Ethyl 2-methyl-2-phenylpropionate (2F):[87] A solution of **2a** (41.1 μL, 0.20 mmol) in THF (0.5 mL) was treated with Me_4ZnLi_2 (2.0 mL, 0.11 M solution in THF, 0.22 mmol) at -78°C. After stirring for 0.5 h at this temperature, a solution of $Pd(PPh_3)_4$ (5.78 mg, 5.0 x 10^{-3}

mmol) in THF (0.5 ml) and iodobenzene (44.8 μL, 0.40 mmol) were added through a cannula, and the resulting mixture was stirred for 24 h at room temperature. The reaction mixture was quenched with saturated aqueous NH_4Cl solution (1.5 mL), and was extracted with ethyl acetate (0.5 mL x 3). The organic layer was washed with saturated aqueous NaCl solution, dried over $MgSO_4$, filtered and concentrated under reduced pressure to give a crude mixture. The crude yield (59%) of **2F** was determined by ^{1}H NMR using pyrazine as an internal standard. Purification by silica gel chromatography (ethyl acetate/hexane = 10/90, R_f = 0.38) afforded **2F** in 58 % yield (22.3 mg) as a colorless oil. ^{1}H NMR ($CDCl_3$) 1.15 (t, J = 4.8 Hz, 3H, -$CO_2CH_2CH_3$), 1.37, (s, 6H, -CH_3), 4.10 (q, J = 4.8 Hz, 2H, -$CO_2CH_2CH_3$), 7.45 (m, 5H, *-Ph*); ^{13}C NMR ($CDCl_3$) 14.2, 26.7, 46.6, 61.0, 125.8, 126.8, 128.5, 145.0, 177.0.

Synthesis of Methyl 2-methyl-2-phenylpropionate (3F):[62] The synthesis was carried out by using the similar procedure to the synthesis of **2F**. ^{1}H NMR ($CDCl_3$) 1.67 (s, 6H, -CH_3), 3.68 (s, 3H, -CO_2CH_3), 7.45 (m, 5H, *-Ph*); ^{13}C NMR ($CDCl_3$) 26.7, 46.7, 52.4, 125.8, 126.9, 128.6, 144.8, 177.5.

The reactions of lithium enolates generated from **2a** and **3b** with electrophiles were also examined as references, and the results were summarized in Table 6.

Table 6. Reaction of lithium enolates generated from **2a** or **3b** with elctrophiles [a]

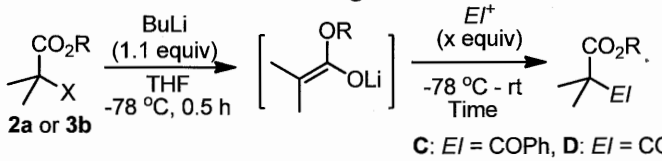

C: *El* = COPh, **D**: *El* = CO_2H,
E: *El* = $CH_2CH{=}CH_2$, **F**: *El* = Ph

Entry	Substrate	El^+ (equiv)	Time (h)	Product	Yield (%)[a]
1	**2a**	PhCOPh (1.1)	1.1	--	0
2	**3b**	PhCOPh (1.1)	1.1	--	0
3	**2a**	PhCOCl (1.1)	1.0	**2C**	100
4	**3b**	PhCOCl (1.1)	1.0	**3C**	92
5	**2a**	CO_2 (excess)	2.0	**2D**	95
6	**3b**	CO_2 (excess)	2.0	**3D**	99
7	**2a**	Allyl Iodide (5.0)	3.0	**2E**	92
8	**3b**	Allyl Iodide (5.0)	3.0	**3E**	91
9	**2a**	PhBr[b] (2.0)	24	**3F**	82
10	**3b**	PhBr[b] (2.0)	24	**3F**	79

[a]Determined by ^{1}H NMR using pyrazine as an internal standard. [b]2.5 mol% $Pd(dba)_2$ and Cy_2NH (1equiv to Pd catalyst) was added.

Preparation of PMMA 8a. A solution of MMA (3.2 mL, 30 mmol), **3a** (179.0 μL, 1.0 mmol), and V-601 (23.0 mg, 0.10 mmol) was heated at 60 °C for 3 h. A small portion of the reaction mixture was taken and dissolved in $CDCl_3$. The conversion of monomer (97%) was determined by ^1H NMR. The rest of reaction mixture was dissolved in $CHCl_3$ (15 mL), which was deoxygenated by bubbling nitrogen gas for 0.5 h before use, and was poured into vigorously stirred 500 mL of hexane, which was deoxygenated by bubbling nitrogen gas for 0.5 h before use, under nitrogen atmosphere in a glove box. The precipitated polymer was collected by filtration and was dried under reduced pressure to give 2.73 g of **8a** (91 % yield). GPC analysis indicated the polymer formed with $M_n = 3000$ and $M_w/M_n = 1.21$.

Preparation of PMMA 8b. A solution of MMA (3.2 mL, 30 mmol) and **3b** (183.0 μL, 1.0 mmol) was heated at 100 °C for 1 h. A small portion of the reaction mixture was taken and dissolved in $CDCl_3$. The conversion of monomer (99%) was determined by ^1H NMR. The rest of reaction mixture was dissolved in $CHCl_3$ (15 mL), which was deoxygenated by bubbling nitrogen gas for 0.5 h before use, and was poured into vigorously stirred 500 mL of hexane, which was deoxygenated by bubbling nitrogen gas for 0.5 h before use, under nitrogen atmosphere in a glove box. The precipitated polymer was collected by filtration and was dried under reduced pressure to give 2.82 g of **8b** (94 % yield). GPC analysis indicated the polymer formed with $M_n = 3300$ and $M_w/M_n = 1.13$.

Preparation of PNIPAM 16. A solution of NIPAM (3.39 g, 30 mmol), **3b** (179.0 μL, 1.0 mmol), and V-601 (23.0 mg, 0.10 mmol) in DMF (3 mL) was heated at 60 °C for 3 h. A small portion of the reaction mixture was taken and dissolved in $CDCl_3$. The conversion of monomer (96%) was determined by ^1H NMR. The rest of reaction mixture was dissolved in $CHCl_3$ (10 mL), which was deoxygenated by bubbling nitrogen gas for 0.5 h before use, and was poured into vigorously stirred 200 mL of hexane, which was deoxygenated by bubbling nitrogen gas for 0.5 h before use, under nitrogen atmosphere in a glove box. The precipitated polymer was collected by filtration and was dried under reduced pressure to give 3.11 g of **16** (92 % yield). GPC analysis indicated the polymer formed with $M_n = 3400$ and $M_w/M_n = 1.09$.

Preparation of PHEMA 18. A solution of HEMA (1.09 mL, 9.0 mmol), **3b** (54.0 μL, 0.30 mmol), and V-601 (6.90 mg, 0.03 mmol) was heated at 60 °C for 2 h. A small portion of the reaction mixture was taken and dissolved in CD_3OD. The conversion of monomer (90%) was determined by ^1H NMR. The rest of reaction mixture was dissolved in acetone (10 mL), which was deoxygenated by bubbling nitrogen gas for 0.5 h before use, and was poured into vigorously stirred

200 mL of hexane, which was deoxygenated by bubbling nitrogen gas for 0.5 h before use, under nitrogen atmosphere in a glove box. The precipitated polymer was collected by filtration and was dried under reduced pressure to give 1.04 g of **18** (89 % yield). GPC analysis indicated the polymer formed with M_n = 3900 and M_w/M_n = 1.28.

General procedure for synthesis ofω–deuterated PMMA 9F. A solution of **8a** (M_n = 3000, M_w/M_n = 1.21, 186.3 mg, 0.062 mmol) in THF (1.2 mL) was treated with *n*-BuLi (45.0 μL , 1.51 M solution in hexane, 0.068 mmol) at -78°C. After stirring for 0.5 h at this temperature, DCl (18.5 μL, 6.49 M in D_2O, 0.12 mmol) was added. The resulting mixture was stirred for 1 h at this temperature, and was slowly warmed to room temperature over 2 h. The reaction mixture was quenched with saturated aqueous $NaHCO_3$ solution (0.5 mL), and was extracted with $CHCl_3$ (0.5 mL x 3). The organic layer was washed with saturated aqueous NaCl solution, dried over $MgSO_4$, filtered and concentrated under reduced pressure. The residue was dissolved in CHCl3 (1 mL) and poured into vigorously stirred hexane (50 mL). The precipitated polymer was collected by suction and was dried under vacuum at 40 °C to give PMMA in 99% (185.8 mg) with M_n = 3000 and M_w/M_n = 1.21. Incorporation of ω-deuterium was confirmed by ^2H NMR (Figure 3). MALDI-TOF MS analysis also indicated the formation of the desired ω-end deuterated PMMA with M_n = 2700 and M_w/M_n = 1.04 (Figure 1).

The synthesis of **9F** was also carried out according to general procedure by using **8b** and *n*-BuLi, Me_4ZnLi_2, *t*-Bu_4ZnLi_2, or *i*-PrMgCl·LiCl. MALDI-TOF MS spectra were shown in Figure 4-7.

General Procedure for the synthesis of ω-carboxylic acid PMMA 9D (Table 3, entry 6)**.** A solution of **8a** (M_n = 3000, M_w/M_n = 1.21, 195.2 mg, 0.065 mmol) in THF (3 mL) was treated with *n*-BuLi (47.0 μL, 1.54 M solution in hexane, 0.072 mmol) at -78°C. After stirring for 0.5 h at this temperature, to this solution was bubbled into carbon dioxide for 5 min. The resulting mixture was stirred for 1 h at this temperature, and was slowly warmed to room temperature over 2 h. The reaction mixture was quenched with 1N aqueous HCl solution (0.5 mL), and was extracted with $CHCl_3$ (0.5 mL x 3). The organic layer was washed with saturated aqueous NaCl solution, dried over $MgSO_4$, filtered and concentrated under reduced pressure. The residue was dissolved in CHCl3 (1 mL) and poured into vigorously stirred hexane (50 mL). The precipitated polymer was collected by suction and was dried under vacuum at 40 °C to give ω-carboxylic acid PMMA **9D** in 97% (189.2 mg).

A colorless solution of the obtained polymer (60.2 mg, 0.020 mmol) in MeOH (0.2 mL) and toluene (0.8 mL) was treated with $TMSCHN_2$ solution (20.0 μL, 2.0 M solution in Et_2O, 0.040 mmol) at room temperature. The resulting yellow solution was stirred for 2 h at this temperature. Acetic acid was added until the solution decolorized and the excess amount of $TMSCHN_2$ was decomposed. The solvent was concentrated under reduced pressure, and the residue was dissolved in $CHCl_3$ (1 mL) and poured into vigorously stirred hexane (30 mL). The precipitated polymer was collected by suction and was dried under vacuum at 40 °C to give PMMA in 95% (57.2 mg) with M_n = 3100 and M_w/M_n = 1.19. The ^1H NMR analysis revealed the existence of characteristic signal at 3.61~3.73 ppm (Figure 8). A comparison of the integrals of these two methyl ester moiety (6H) at the ω-polymer end with those of methyl ester moiety (δ = 3.50~3.60, 3H + 84 H) at the α-polymer end and in a polymer chain revealed 97% efficiency of the ω-end group transformation. MALDI-TOF MS analysis also indicated the formation of the desired ω-methyl ester PMMA **9G** with M_n = 2700 and M_w/M_n = 1.05 as a major product (>99% pure) (Figure 9).

The same experiment using **8b** (M_n = 3300, M_w/M_n = 1.13, 214.2 mg, 0.065 mmol) gave **9F** in 99% (212.3 mg), which was converted to **9G** (M_n = 3500 M_w/M_n = 1.13) upon treatment with $TMSCHN_2$. The ^1H NMR analysis revealed 97% efficiency of the ω-end group transformation as judged by a comparison of the integrals of two methyl ester moiety (δ = 3.67~3.74, 6H) at the ω-polymer end with those of methyl ester moiety (δ = 3.53~3.66, 3H + 87 H) at the α-polymer end and in a polymer chain (Figure 10). MALDI-TOF MS analysis also indicated the formation of the desired ω-methyl ester PMMA **9G** with M_n = 3400 and M_w/M_n = 1.03 as a major product (>99% pure, Figure 11).

General Procedure for the synthesis of ω-benzoyl PMMA 9C (Table 3, entry 8). A solution of **8a** (M_n = 3000, M_w/M_n = 1.21, 184.6 mg, 0.062 mmol) in THF (1.2 mL) was treated with *n*-BuLi (44.0 μL , 1.54 M solution in hexane, 0.068 mmol) at -78°C. After stirring for 0.5 h at this temperature, benzoyl chloride (36.0 μL, 0.31 mmol) was added by a syringe. The resulting mixture was stirred for 1 h at this temperature, and was slowly warmed to room temperature over 2 h. The reaction mixture was quenched with saturated aqueous $NaHCO_3$ solution (0.5 mL), and was extracted with $CHCl_3$ (0.5 mL x 3). The organic layer was washed with saturated aqueous NaCl solution, dried over $MgSO_4$, filtered and concentrated under reduced pressure. The residue was dissolved in CHCl3 (1 mL) and poured into vigorously stirred hexane (50 mL). The precipitated polymer was collected by suction and was dried under vacuum at 40 °C to give PMMA in 96% (177.3 mg) with M_n = 3100 and M_w/M_n = 1.20. The ^1H NMR analysis revealed the existence of

characteristic signal at 7.36~7.60 and 7.66~7.83 ppm (Figure S12). A comparison of the integrals of these phenyl protons (5H) at the ω-polymer end with those of methyl ester moiety (δ = 3.50~3.71, 3H + 87 H) at the α-polymer end and in a polymer chain revealed 96% efficiency of the ω-end group transformation. MALDI-TOF MS analysis also indicated the formation of the desired ω-benzoyl PMMA **9C** with M_n = 2,700 and M_w/M_n = 1.04 as a major product (99% purity) (Figure 13). The MS also indicated the 1 % formation of ω-end protonated PMMA.

The same experiment using **8b** (M_n = 3300, M_w/M_n = 1.13, 191.7 mg, 0.058 mmol) gave **9C** in 96% (184.0 mg) with M_n = 3500 and M_w/M_n = 1.11 (Table 3, entry 9). The ^{1}H NMR analysis revealed 96% efficiency of the ω-end group transformation as judged by a comparison of the integrals of phenyl protons (δ = 7.33~7.60 and 7.64~7.83, 5H) at the ω-polymer end with those of methyl ester moiety (δ =3.38~3.77, 3H + 90 H) at the α-polymer end and in a polymer chain (Figure 14). MALDI-TOF MS analysis also indicated the formation of the desired ω-benzoyl PMMA **9C** with M_n = 3500 and M_w/M_n = 1.04 as a major product (99.3% purity) (Figure 15). The MS also indicated the 0.7% formation of ω-end protonated PMMA.

General Procedure for the synthesis of ω-allyl PMMA 9E (Table 3, entry 10). A solution of **8a** (M_n = 3000, M_w/M_n = 1.21, 183.4 mg, 0.061 mmol) in THF (1.2 mL) was treated with *n*-BuLi (43.5 μL , 1.54 M solution in hexane, 0.067 mmol) at -78°C. After stirring for 0.5 h at this temperature, allyl iodine (28.0 μL, 0.31 mmol) was added by a syringe. The resulting mixture was stirred for 1 h at this temperature, and was slowly warmed to room temperature over 2 h. The reaction mixture was quenched with saturated aqueous NH_4Cl and $Na_2S_2O_3$ solution (0.5 mL), and was extracted with CHCl3 (0.5 mL x 3). The organic layer was washed with saturated aqueous NaCl solution, dried over $MgSO_4$, filtered and concentrated under reduced pressure. The residue was dissolved in CHCl3 (1 mL) and poured into vigorously stirred hexane (50 mL). The precipitated polymer was collected by suction and was dried under vacuum at 40 °C to give PMMA in 97% (177.9 mg) with M_n = 3,100 and M_w/M_n = 1.20. The ^{1}H NMR analysis revealed the existence of characteristic signal at 4.96~5.10 and 5.50~5.78 ppm (Figure 16). A comparison of the integrals of these olefinic protons (3H) at the ω-polymer end with those of methyl ester moiety (δ = 3.37~3.79, 3H + 87 H) at the α-polymer end and in a polymer chain revealed 98% efficiency of the ω-end group transformation. MALDI-TOF MS analysis also indicated the formation of **9E** with M_n = 2800 and M_w/M_n = 1.05 as a major product (98% purity) (Figure 17). The MS also indicated the 2 % formation of ω-end protonated PMMA.

(Table 3, entry 11) The same experiment using **8b** (M_n = 3,300, M_w/M_n = 1.13, 204.6 mg, 0.062 mmol) as substrate was also carried out according to the above general procedure to give **9E** in 95% (198.3 mg) with M_n = 3,500 and M_w/M_n = 1.12. The ^{1}H NMR analysis revealed 95% efficiency of the ω-end group transformation as judged by a comparison of the integrals of olefinic protons (δ = 4.84~5.25 and 5.46~5.80, 3H) at the ω-polymer end with those of methyl ester moiety (δ = 3.38~3.79, 3H + 90 H) at the α-polymer end and in a polymer chain (Figure 18). MALDI-TOF MS analysis also indicated the formation of the desired ω-allyl PMMA **9E** with M_n = 3,500 and M_w/M_n = 1.04 as a major product (97% purity) (Figure 19). The MS also indicated the 3 % formation of ω-end protonated PMMA.

General Procedure for the synthesis of ω-(δ-lactonyl) PMMA 10 (Table 3, entry 12). A solution of **8a** (M_n = 3,000, M_w/M_n = 1.21, 183.2 mg, 0.061 mmol) in THF (1.2 mL) was treated with *n*-BuLi (44.0 μL, 1.53 M solution in hexane, 0.067 mmol) at -78°C. After stirring for 0.5 h at this temperature, benzaldehyde (31 μL, 0.31 mmol) was added by a syringe. The resulting mixture was stirred for 1 h at this temperature, and was slowly warmed to room temperature over 2 h. The reaction mixture was quenched with saturated aqueous NH_4Cl solution (0.5 mL), and was extracted with $CHCl_3$ (0.5 mL x 3). The organic layer was washed with saturated aqueous NaCl solution, dried over $MgSO_4$, filtered and concentrated under reduced pressure. The residue was dissolved in CHCl3 (1 mL) and poured into vigorously stirred hexane (50 mL). The precipitated polymer was collected by suction and was dried under vacuum at 40 °C to give PMMA in 98% (179.8 mg) with M_n = 3,100 and M_w/M_n = 1.20. MALDI-TOF MS analysis also indicated the formation of the desired ω-(δ-lacton)-substituted PMMA **10** with M_n = 2900 and M_w/M_n = 1.05 as a major product (90% purity) (Figure 20). The mass also indicated the 9 and 1% formation of β-hydroxyl ester PMMA **9A** and ω-end protonated PMMA **9F**, respectively. The incorporation yield could not be judged from ^{1}H NMR analysis since the characteristic signal for aryl protons of **10** overlap those of **9A**.

General procedure for the transformation of 9A into 10. A solution of PMMA (**10/9A/9F** = 90/9/1, 62.2 mg, 0.020 mmol), which was obtained in Table 3, entry 12, and trifluoroacetic acid (2.93 μL, 0.040 mmol) in CH_2Cl_2 (0.60 mL) was heated at reflux for 3 h. The reaction mixture was quenched with saturated aqueous $NaHCO_3$ solution (0.5 mL), and was extracted with $CHCl_3$ (0.5 mL x 3). The organic layer was washed with saturated aqueous NaCl solution, dried over $MgSO_4$, filtered and concentrated under reduced pressure. The residue was dissolved in CHCl3 (0.5 mL) and poured into vigorously stirred hexane (30 mL). The precipitated polymer was collected by suction

and was dried under vacuum at 40 °C to give PMMA in 96% (59.6 mg) with M_n = 3100 and M_w/M_n = 1.19. The ^{1}H NMR analysis in CD_2Cl_2 revealed the existence of characteristic signal at 7.16~7.48 ppm (Figure 21). A comparison of the integrals of these aryl protons (5H) at the ω-polymer end with those of methyl ester moiety (δ = 3.38~3.79, 3H + 84 H) at the α-polymer end and in a polymer chain revealed 98% efficiency of the ω-end group transformation. MALDI-TOF MS analysis also indicated the quantitative transformation of **9A** into **10** with M_n = 2800 and M_w/M_n = 1.04 (99% purity) (Figure22). The MS also indicated the quantitative transformation of **9A** into **10** and 1% formation of ω-end protonated PMMA.

The same experiment using **8b** (M_n = 3300, M_w/M_n = 1.13, 203.8 mg, 0.062 mmol) gave PMMA in 95% (193.4 mg) with M_n = 3400 and M_w/M_n = 1.13 (Table 3, entry 13). MALDI-TOF MS analysis also indicated the formation of the desired ω–(δ-lacton)-substituted PMMA **10** with M_n = 3300 and M_w/M_n = 1.04 as a major product (89% purity) (Figure 23). The mass also indicated the 10 and 1% formation of **9A** and **9F**, respectively. In order to transform **9** into **10**, the obtained PMMA (**10/9A/9F** = 89/10/1, 50.1 mg, 0.015 mmol) was treated with trifluoroacetic acid as described above to give PMMA in 98% (48.9 mg) with M_n = 3100 and M_w/M_n = 1.13. The ^{1}H NMR analysis revealed 97% efficiency of the ω-end group transformation as judged by a comparison of the integrals of aryl protons (δ = 7.18~7.46, 5H) at the ω-polymer end with those of methyl ester moiety (δ = 3.40~3.79, 3H + 87H) at the α-polymer end and in a polymer chain (Figure 24). MALDI-TOF MS analysis also indicated the quantitative transformation of **9A** into **10** with M_n = 3400 and M_w/M_n = 1.03 (99% purity, Figure 25). The MS also indicated the quantitative transformation of **9A** into **10** and 1% formation of ω-end protonated PMMA.

Syntheisis of ω-benzoyl PBA 13. A solution of BA (0.22 mL, 1.5 mmol), **3a** (9.0 μL, 5.0 x 10^{-2} mmol), and V-601 (1.15 mg, 5.0 x 10^{-3} mmol) were heated at 60 °C for 1.5 h under a nitrogen atmosphere in a glovebox. A small portion of the reaction mixture was withdrawn and was dissolved in $CDCl_3$. The conversion of monomer (95%) was determined by ^{1}H NMR. THF (1 mL) was added, and the remaining monomer was azeotropically removed under reduced pressure. GPC analysis indicated ω-dimethylstibanyl PBA **12** formed with M_n = 4100 and M_w/M_n = 1.09. A solution of **12** in THF (1.2 mL) was treated with *t*-Bu_4ZnLi_2 (0.31 mL, 0.17 M solution in hexane, 0.052 mmol) at -78°C. After stirring for 0.5 h at this temperature, benzoyl chloride (28 μL, 0.24 mmol) was added. The resulting mixture was stirred for 1 h at this temperature, and was slowly warmed to room temperature over 2 h. The reaction mixture was quenched with saturated aqueous $NaHCO_3$ solution (0.5 mL), and was extracted with $CHCl_3$ (0.5 mL x 3). The organic layer was

washed with saturated aqueous NaCl solution, dried over $MgSO_4$, filtered and concentrated under reduced pressure. The residue was purified by preparative GPC to give PBA in 98% (175.4 mg) with M_n = 4000 and M_w/M_n = 1.10. The ^1H NMR analysis in $CDCl_3$ revealed the existence of characteristic signal at 7.36~7.64 and 7.72~8.06 ppm (Figure 26). A comparison of the integrals of these aryl protons (5H) at the ω-polymer end with those of methyl ester moiety (δ = 3.63, 3H) at the α-polymer end and ester methylene protons of butyl group (δ = 3.81~4.22, 57H) in a polymer chain revealed 97% efficiency of the ω-end group transformation. The ^{13}C NMR analysis revealed the signal for the carbonyl carbon of benzoyl group resonated at 193.4~196.5 ppm (Figure 27). MALDI-TOF MS analysis also indicated the formation of the desired ω-benzoyl PBA **13** with M_n = 3500 and M_w/M_n = 1.01 as a major product (98% purity) (Figure 28). The MS also indicated the 1 % formation of ω-end protonated PBA.

Syntheisis of ω-^{13}C-benzoyl PBA 13-^{13}C. A solution of BA (0.22 mL, 1.5 mmol), **3a** (9.0 μL, 5.0 x 10^{-2} mmol), and V-601 (1.15 mg, 5.0 x 10^{-3} mmol) were heated at 60 °C for 1.5 h under a nitrogen atmosphere in a glovebox. A small portion of the reaction mixture was withdrawn and was dissolved in $CDCl_3$. The conversion of monomer (99%) was determined by ^1H NMR. THF (1 mL) was added, and the remaining monomer was azeotropically removed under reduced pressure. GPC analysis indicated ω-dimethylstibanyl PBA **12** formed with M_n = 3500 and M_w/M_n = 1.09. A solution of **12** in THF (1.2 mL) was treated with *t*-Bu_4ZnLi_2 (0.39 mL, 0.14 M solution in hexane, 0.054 mmol) at -78°C. After stirring for 0.5 h at this temperature, benzoyl chloride (29 μL, 0.25 mmol) was added. The resulting mixture was stirred for 1 h at this temperature, and was slowly warmed to room temperature over 2 h. The reaction mixture was quenched with saturated aqueous $NaHCO_3$ solution (0.5 mL), and was extracted with $CHCl_3$ (0.5 mL x 3). The organic layer was washed with saturated aqueous NaCl solution, dried over $MgSO_4$, filtered and concentrated under reduced pressure. The residue was purified by preparative GPC to give PBA in 96% (184.51 mg) with M_n = 3,800 and M_w/M_n = 1.09. The ^1H NMR analysis revealed 95% efficiency of the ω-end group transformation as judged by a comparison of the integrals of aryl protons (δ = 7.35~7.68 and 7.85~8.10, 5H) at the ω-polymer end with those of methyl ester moiety (δ = 3.63, 3H) at the α-polymer end and ester methylene protons of butyl group (δ = 3.91~4.18, 60H) in a polymer chain (Figure 29). The comparison of the ^{13}C NMR spectra of **13** and **13-^{13}C** revealed that the intensity of the signals at 193.4~195.4 ppm was greatly enhanced (Figure 30). MALDI-TOF MS analysis also indicated the formation of the desired ω-^{13}C-benzoyl PBA **13-^{13}C** with M_n = 3600 and M_w/M_n =

1.01 as a major product (99% purity) (Figure 31). The MS also indicated the 1 % formation of ω-protonated PBA.

Syntheisis of ω-benzoyl PNIPAM 17. A solution of PNIPAM **16** (M_n = 3400, M_w/M_n = 1.09, 158.2 mg, 0.047 mmol) in DMF (1 mL) was treated with *t*-Bu_4ZnLi_2 (0.30 mL , 0.16 M solution in THF, 0.052 mmol) at -60°C. After stirring for 0.5 h at this temperature, benzoylchloride (21.5 μL, 0.24 mmol) was add. The resulting mixture was stirred for 1 h at this temperature, and was slowly warmed to room temperature over 2 h. The reaction mixture was quenched with saturated aqueous $NaHCO_3$ solution (0.5 mL), and was extracted with $CHCl_3$ (0.5 mL x 3). The organic layer was washed with saturated aqueous NaCl solution, dried over $MgSO_4$, filtered and concentrated under reduced pressure. The residue was dissolved in $CHCl_3$ (1 mL) and poured into vigorously stirred hexane (50 mL). The precipitated polymer was collected by suction and was dried under vacuum at 40 °C to give PNIPAM in 99% (155.9 mg) with M_n = 3500 and M_w/M_n = 1.10. The ^1H NMR analysis in $CDCl_3$ revealed the existence of characteristic signal at 7.38~7.90 ppm (Figure 32). A comparison of the integrals of these aryl protons (5H) at the ω-polymer end with that of methyl ester moiety at the α-polymer end (δ = 3.62, 3H) and amide methylene protons of *i*-propyl group in a polymer chain (δ = 3.77~4.40, 29H) revealed 97% efficiency of the ω-end group transformation. MALDI-TOF MS analysis also indicated the formation of the desired ω-benzoyl PNIPAM **17** with M_n = 2900 and M_w/M_n = 1.05 as a major product (>99% purity) (Figure 33).

The exchange reactions of **16** and the subsequent reaction with electrophiles in various solvent were examined according to the above general procedure (Table 7).

Table 7. Solvent effect on the exchange reaction of **16**.

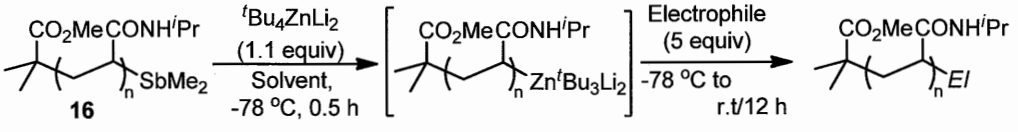

Entry	Solvent	Electrophile	Products (%)	
			El (%)[a]	*El* = H (%)
1	THF	PhCHO	CH(OH)Ph (30%)	69
2	THF	PhCOCl	COPh (10%)	88
3	MeOH	PhCHO	CH(OH)Ph (0%)	>99
4	H_2O	PhCHO	CH(OH)Ph (0%)	>99
5	DMSO	PhCOCl	COPh (93%)	0

[a]Determined by MALDI-TOF MS analysis.

Syntheisis of ω-allyl PHEMA 19. A solution of PHEMA **18** (M_n = 3900, M_w/M_n = 1.28, 175.5 mg, 0.045 mmol) in DMSO (1.2 mL) was treated with *t*-Bu_4ZnLi_2 (0.31 mL , 0.16 M solution in THF, 0.050 mmol) at room temperature. After stirring for 0.5 h at this temperature, allyl iodine (20.5 μL, 0.23 mmol) was added. The resulting mixture was stirred for 3 h at this temperature. To the reaction mixture was added MeOH and the reaction was quenched by adding DOWEX 50WX4. After solution was separated, the resulting solution was concentrated under reduced pressure. The residue was dissolved in acetone (~ 1 mL) and poured into vigorously stirred hexane (50 mL). The precipitated polymer was collected by suction and was dried under vacuum at 60 °C to give PHEMA in 95% (166.6 mg) with M_n = 4000 and M_w/M_n = 1.28. The ^{1}H NMR analysis in CD_3OD revealed the existence of characteristic signal at 5.18~5.43 and 5.68~5.80 ppm (Figure 34). A comparison of the integrals of the olefinic protons (3H) at the ω-polymer end with protons of methyl ester at the α-polymer end and two sets of methylene protons of hydoroxy ethyl group (δ = 3.53~4.18, 3H + 54H + 54H) in a polymer main chain revealed >99% efficiency of the ω-end group transformation.

Syntheisis of ω-biotinylated PNIPAM 19. A solution of PNIPAM **16** (M_n = 3400, M_w/M_n = 1.09, 102.0 mg, 0.030 mmol) in DMF (0.7 mL) was treated with *t*-Bu_4ZnLi_2 (0.24 mL , 0.14M solution in THF, 0.033 mmol) at -60°C. After stirring for 0.5 h at this temperature, a solution of biotinyl chloride (39.4 mg, 0.15 mmol) in DMF (1.0 mL) was added through a cannula. The resulting mixture was stirred for 1 h at this temperature, and was slowly warmed to room temperature over 2 h. The reaction mixture was quenched with saturated aqueous $NaHCO_3$ solution (0.50 mL), and was extracted with $CHCl_3$ (1.0 mL x 3). The organic layer was washed with saturated aqueous NaCl solution, dried over $MgSO_4$, filtered and concentrated under reduced pressure. The residue was dissolved in $CHCl_3$ (~ 1 mL) and poured into vigorously stirred hexane (50 mL). The precipitated polymer was collected by suction and was dried under vacuum at 40 °C. The polymer was further purified by preparative GPC to give PNIPAM in 95% (96.5 mg) with M_n = 3900 and M_w/M_n = 1.11. The ^{1}H NMR analysis in $CDCl_3$ revealed the existence of characteristic signal for biotin moiety (Figure 2a). The ^{1}H NMR analysis revealed 95% efficiency of the ω-end group transformation as judged by a comparison of the integrals of protons *l* (δ = 3.10~3.32, 1H) at the ω-polymer end with those of methyl ester moiety (δ = 3.65, protons *b*, 3H) at the α-polymer end. MALDI-TOF MS analysis also indicated the formation of the desired ω-benzoyl PNIPAM **17** with M_n = 2900 and M_w/M_n = 1.05 as a major product (>99% purity).

General procedure for competition experiments between 3 and 2f. A solution of **3b** (22.4 μL, 0.2 mmol), **2f** (22.4 μL, 0.2 mmol) and benzaldehyde (61.0 μL, 0.60 mmol) in THF (1.0 mL) was cooled to -78 °C, and *n*-BuLi (26.3 μL, 0.04 mmol) was added to this mixture. After 15 min stirring at this temperature, the reaction was quenched by the addition of AcOH/MeOH. After extractive work-up, the yields of alcohols **3A**, **2A**, and **21** were determined by GC analysis with tetradecane as an internal standard. The same reaction was repeated for six times (Table 8), and the yields of four experiments excluding the highest and lowest yields were averaged (Table 4).

Table 8. Competition between **3** and **2f** by employing BuLi.

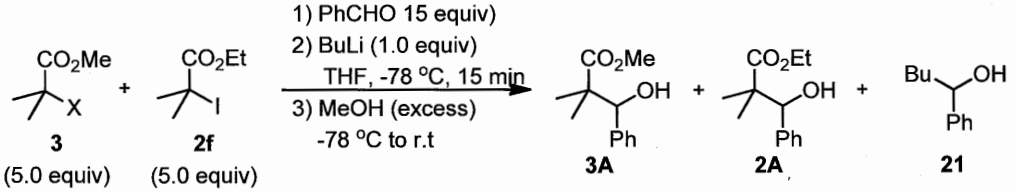

Entry	X	GC Yield (%)			3A/2A
		3A	**2A**	**21**	
1	$BiMe_2$ (**3b**)	45.1	8.7	16.6	5.20
2	$BiMe_2$ (**3b**)	59.9	4.5	68.5	13.45
3	$BiMe_2$ (**3b**)	65.7	9.0	28.5	7.30
4	$BiMe_2$ (**3b**)	38.5	10.3	32.4	3.73
5	$BiMe_2$ (**3b**)	48.1	8.0	31.5	6.05
6	$BiMe_2$ (**3b**)	44.1	8.7	43.0	5.10
7	$SbMe_2$ (**3a**)	53.4	14.1	32.1	3.80
8	$SbMe_2$ (**3a**)	47.9	17.5	40.4	2.73
9	$SbMe_2$ (**3a**)	5.61	8.6	35.0	3.28
10	$SbMe_2$ (**3a**)	63.7	24.1	28.4	2.65
11	$SbMe_2$ (**3a**)	39.4	8.8	34.6	4.47
12	$SbMe_2$ (**3a**)	30.7	8.2	23.5	3.77
13	TeMe (**3g**)	28.6	9.2	21.4	3.33
14	TeMe (**3g**)	28.5	15.2	19.7	1.88
15	TeMe (**3g**)	17.8	2.4	7.55	7.62
16	TeMe (**3g**)	47.3	16.4	33.8	2.88
17	TeMe (**3g**)	26.2	11.5	30.8	2.27
18	TeMe (**3g**)	37.9	15.0	39.0	2.53
19	I (**3f**)	17.0	19.9	24.4	0.85
20	I (**3f**)	11.1	10.2	32.2	1.09
21	I (**3f**)	10.7	8.3	27.7	1.29
22	I (**3f**)	14.7	10.5	31.6	1.40
23	I (**3f**)	18.9	12.0	60.7	1.74
24	I (**3f**)	14.5	12.2	32.6	1.19

General procedure on competition experiments between 6 and 19. A solution of **6e** (79.0 mg, 0.20 mmol), iodobenzene **19** (22.4 μL, 0.2 mmol) and benzaldehyde (61.0 μL, 0.60 mmol) in THF (1.0 mL) was treated at -78°C with a 1.52 M solution of *n*-butyllithium (26.3 μL, 0.04 mmol), in hexane. After stirring for 15 min, methanol (80.9 μL, 2.0 mmol) was added by a syringe, and the reaction mixture then warmed to room temperature. The crude yields were determined by GC analysis (tetradecane as an internal standard). The same reaction was repeated for six times (Table 9), and the yields of four experiments excluding the highest and lowest yields were averaged (Table 5).

Table 9. Competition between **6** and iodobenzene by employing BuLi.

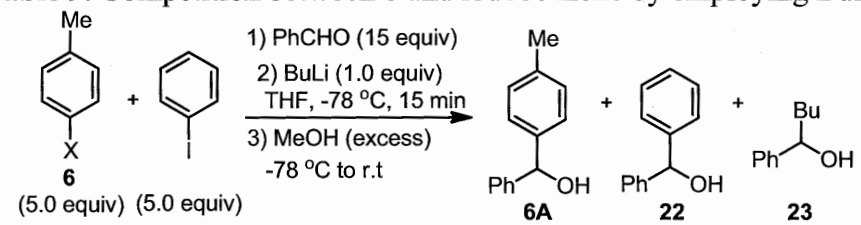

Entry	X	GC Yield (%)			6A/22
		6A	**22**	**23**	
1	Bi(*p*-Tol)$_2$ (**6e**)	0.62	10.0	22.7	0.062
2	Bi(*p*-Tol)$_2$ (**6e**)	ND	ND	9.9	-
3	Bi(*p*-Tol)$_2$ (**6e**)	ND	9.6	21.9	0
4	Bi(*p*-Tol)$_2$ (**6e**)	0.40	13.6	41.8	0.029
5	Bi(*p*-Tol)$_2$ (**6e**)	ND	5.3	14.8	0
6	Bi(*p*-Tol)$_2$ (**6e**)	ND	5.7	32.2	0
7	Sb(*p*-Tol)$_2$ (**6d**)	0.35	10.5	43.9	0.024
8	Sb(*p*-Tol)$_2$ (**6d**)	ND	11.4	35.7	0
9	Sb(*p*-Tol)$_2$ (**6d**)	0.75	15.9	43.4	0.047
10	Sb(*p*-Tol)$_2$ (**6d**)	1.05	12.5	52.1	0.084
11	Sb(*p*-Tol)$_2$ (**6d**)	1.35	11.5	41.3	0.118
12	Sb(*p*-Tol)$_2$ (**6d**)	1.05	10.3	39.1	0.102
13	Te(*p*-Tol) (**6i**)	2.65	5.4	56.7	0.495
14	Te(*p*-Tol) (**6i**)	0.65	7.1	56.7	0.092
15	Te(*p*-Tol) (**6i**)	1.50	5.3	44.4	0.286
16	Te(*p*-Tol) (**6i**)	2.60	10.2	19.5	0.255
17	Te(*p*-Tol) (**6i**)	0.90	8.5	44.4	0.106
18	Te(*p*-Tol) (**6i**)	3.75	13.2	67.9	0.284
19	I	4.90	9.5	56.7	0.519
20	I	5.25	9.8	55.9	0.538
21	I	3.55	7.3	51.3	0.486

Unless otherwise noted, ^{1}H and ^{13}C NMR spectra were measured in $CDCl_3$. Additionally, a major series of peaks as indicated by average mass number in TOF MS spectrum were observed as sodium ion adduct $(M + Na)^{+}$.

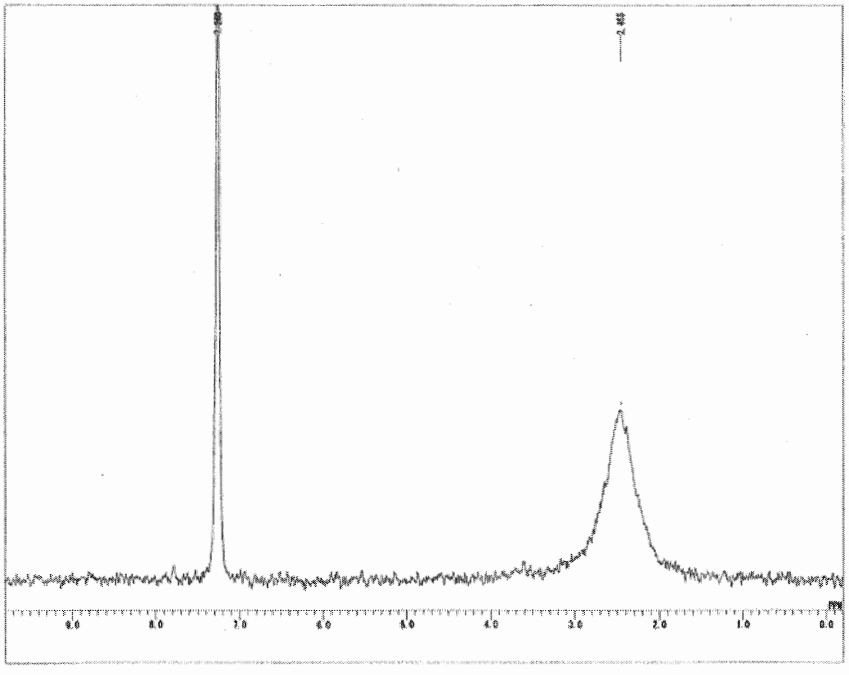

Figure 3. ^{2}H NMR specrta of the **9F** in $CHCl_3$ (Table 3, entry 2).

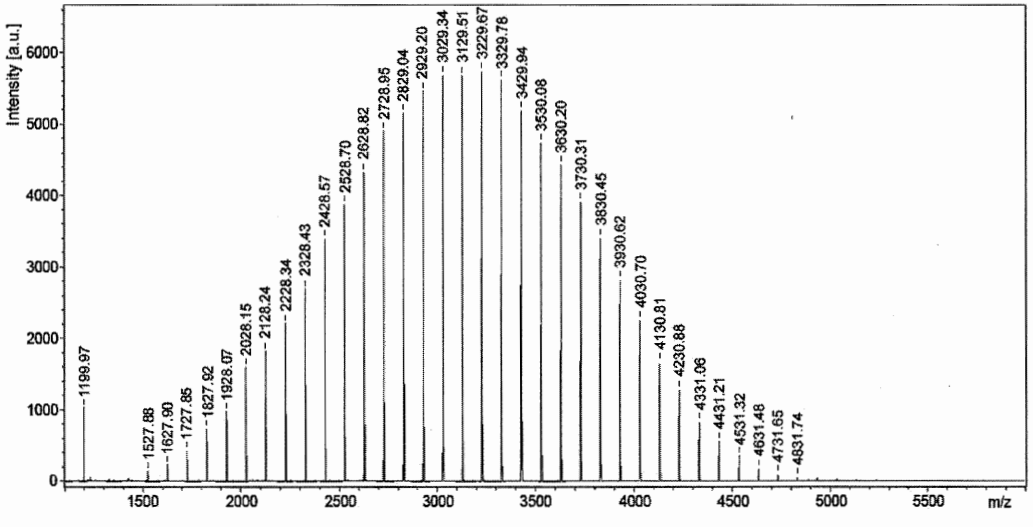

Figure 4. MALDI-TOF MS spectra of **9F** (Table 3, entry 2).

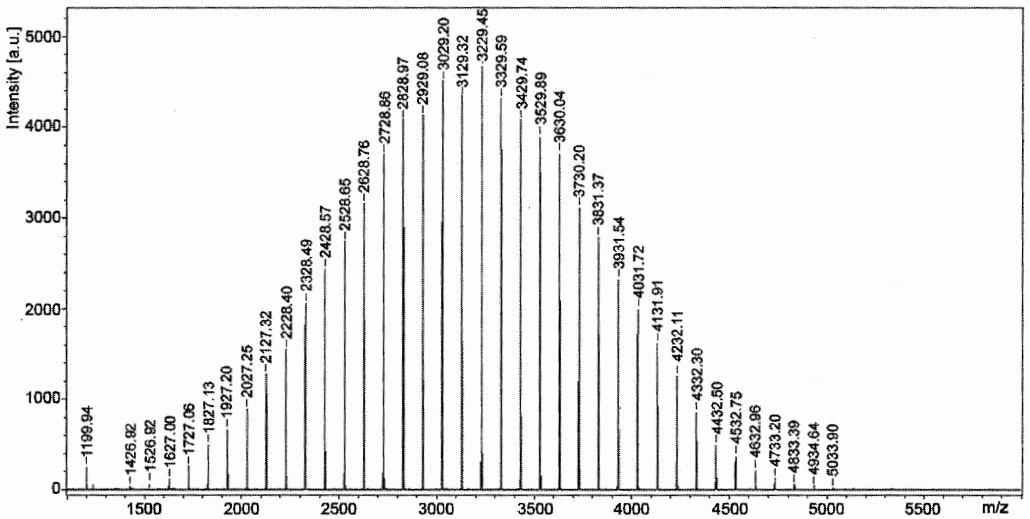

Figure 5. MALDI-TOF MS spectra of **9F** (Table 3, entry 3).

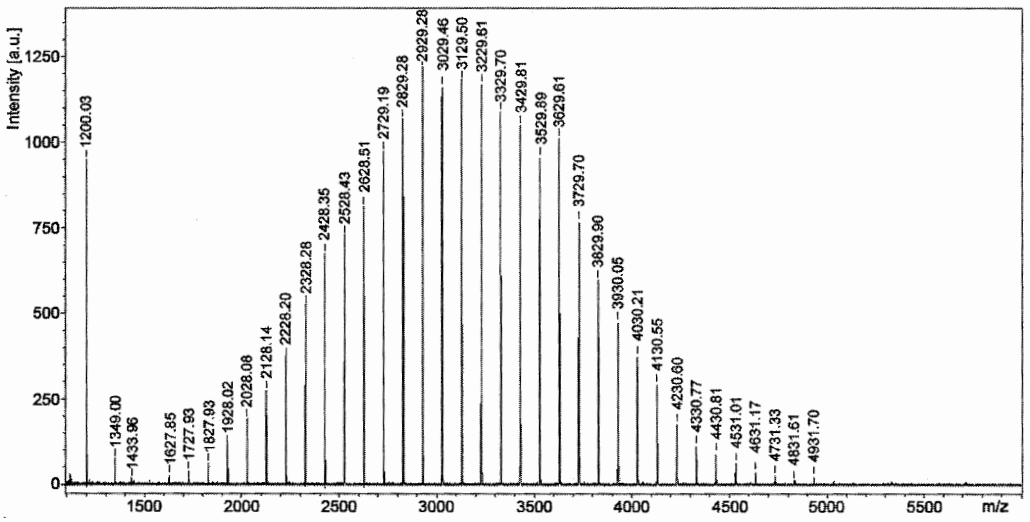

Figure 6 MALDI-TOF MS spectra of **9F** (Table 3, entry 4).

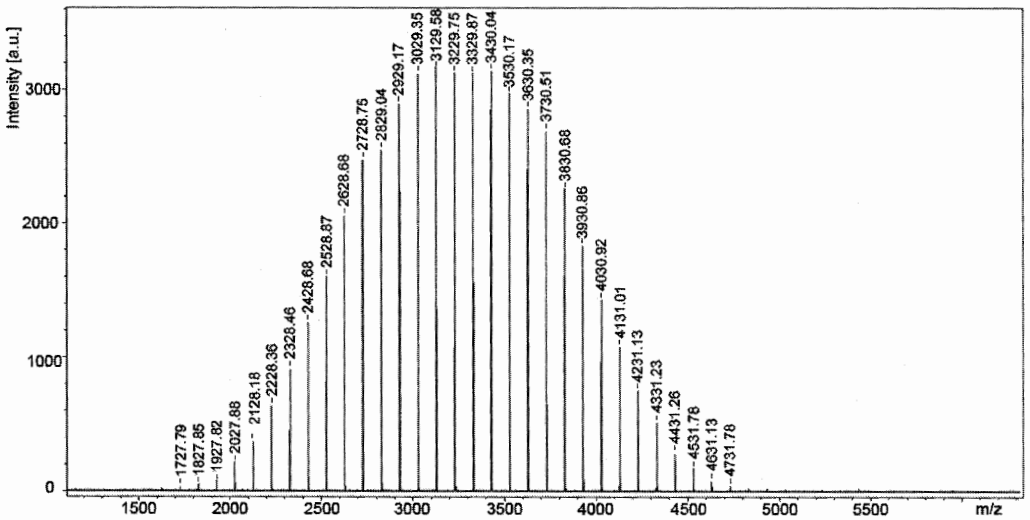

Figure 7. MALDI-TOF MS spectra of **9F** (Table 3, entry 5).

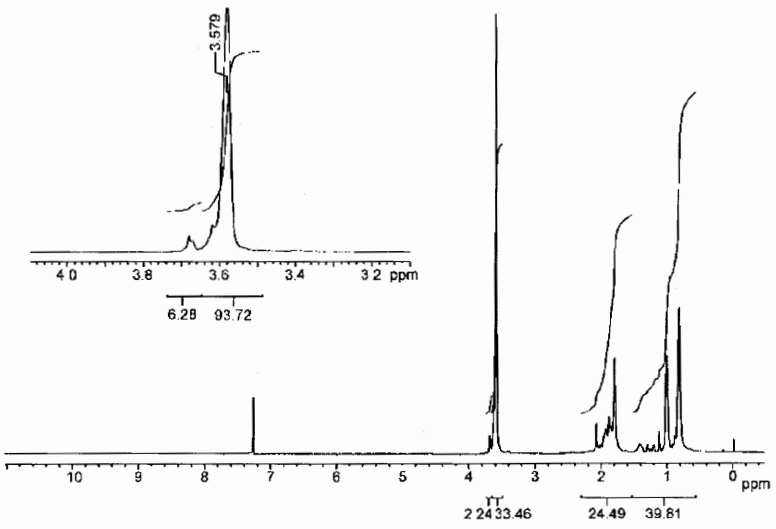

Figure 8. ^{1}H NMR specrta of **9G** (Table 3, entry 6).

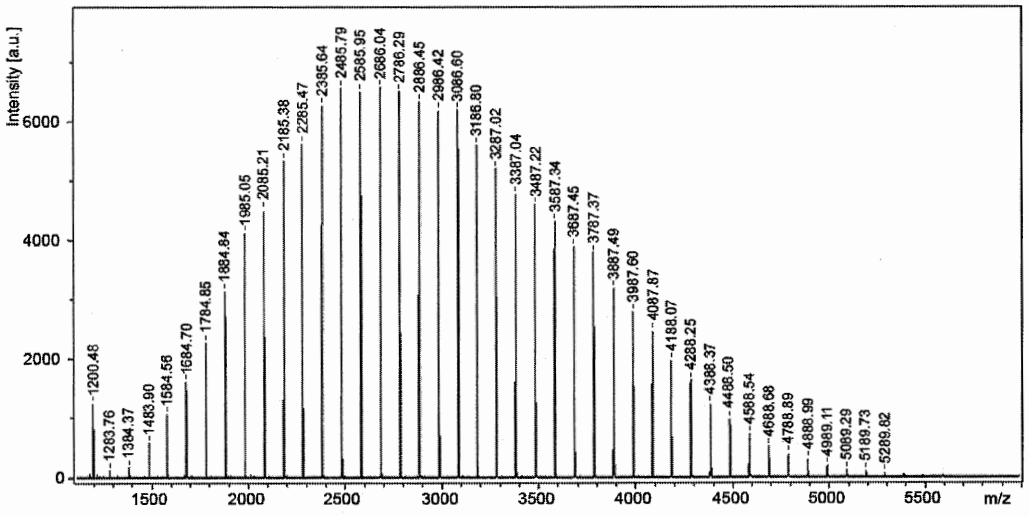

Figure 9. MALDI-TOF MS spectra of **9G** (Table 3, entry 6).

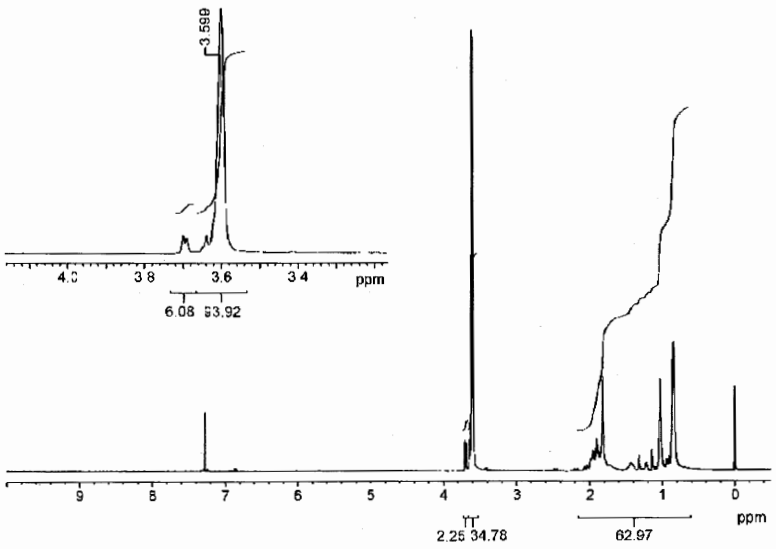

Figure 10. ^{1}H NMR specrta of **9G** (Table 3, entry 7).

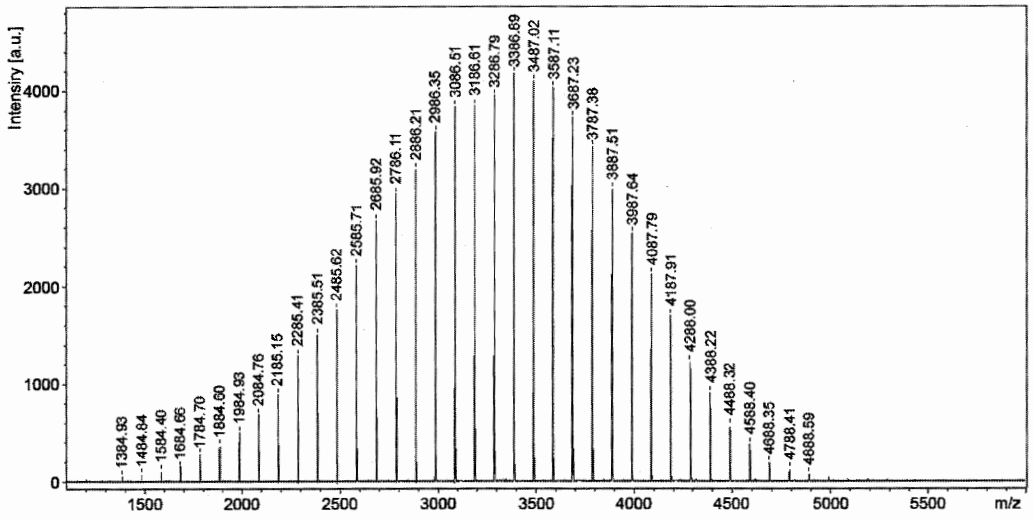

Figure 11. MALDI-TOF MS spectra of **9G** (Table 3, entry 7).

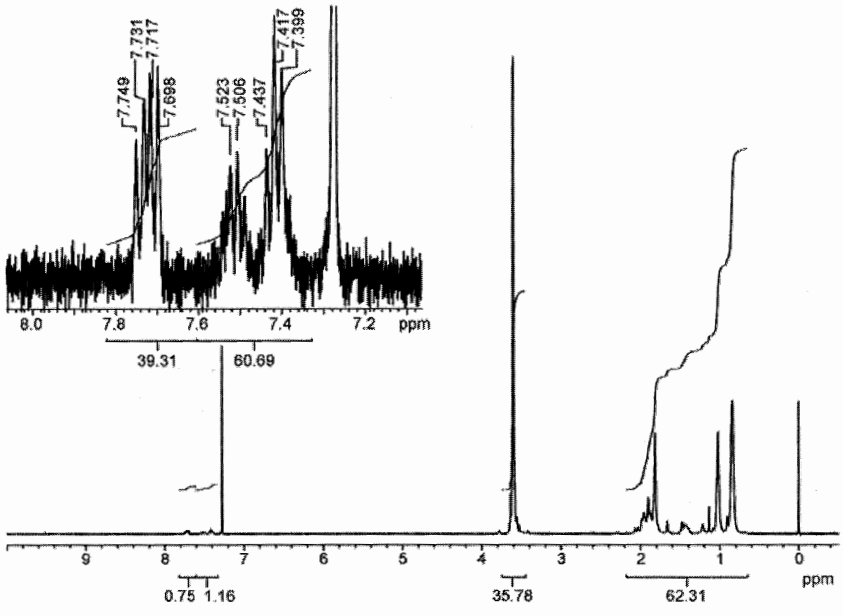

Figure 12. ^{1}H NMR specrta of **9C** (Table 3, entry 8).

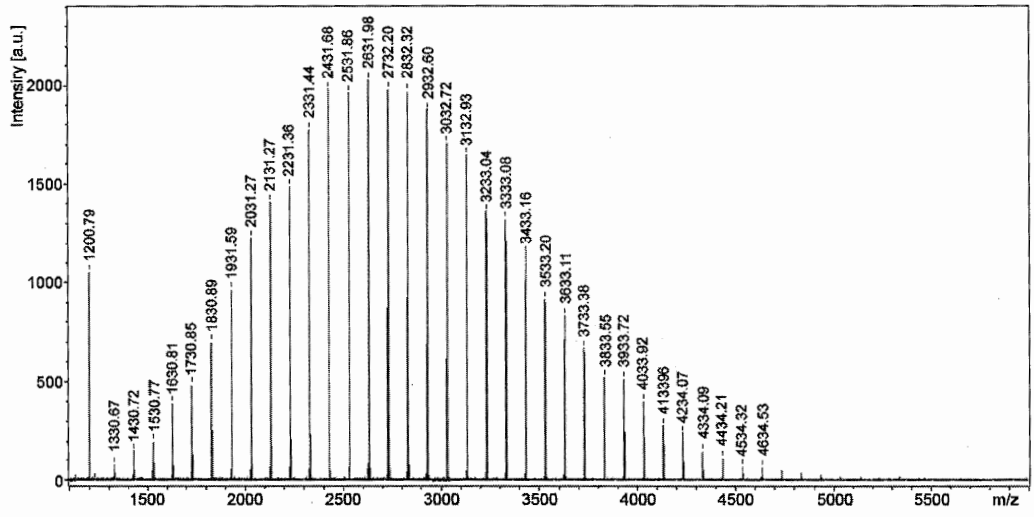

Figure 13. MALDI-TOF MS spectra of **9C** (Table 3, entry 8).

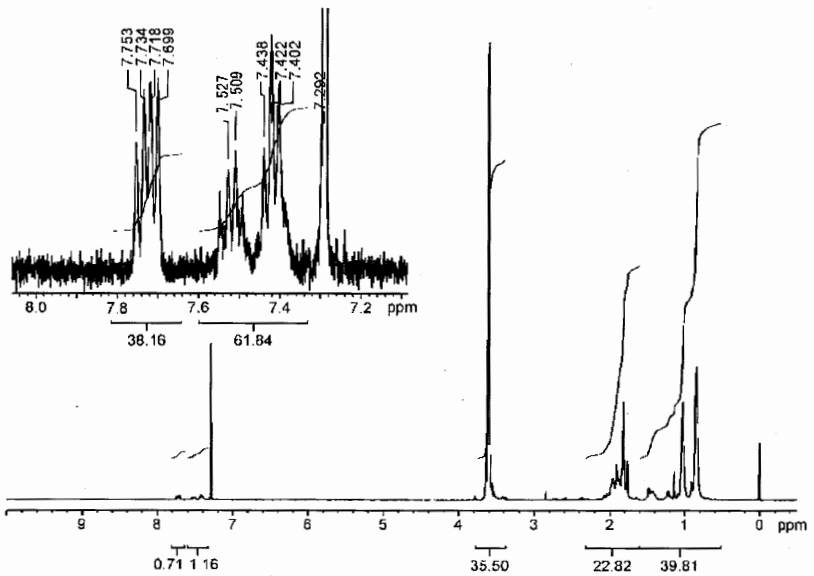

Figure 14. ^{1}H NMR specrta of **9C** (Table 3, entry 9).

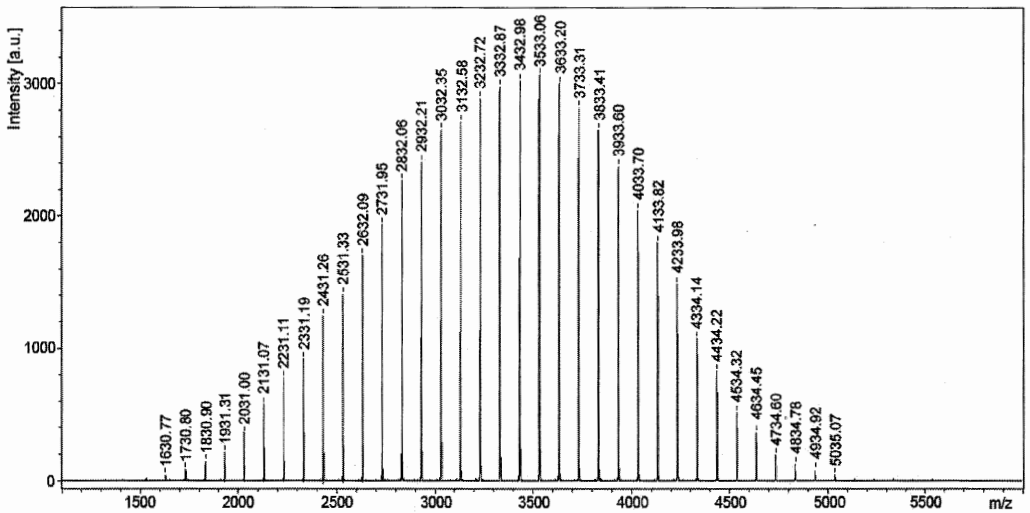

Figure 15. MALDI-TOF MS spectra of **9C** (Table 3, entry 9).

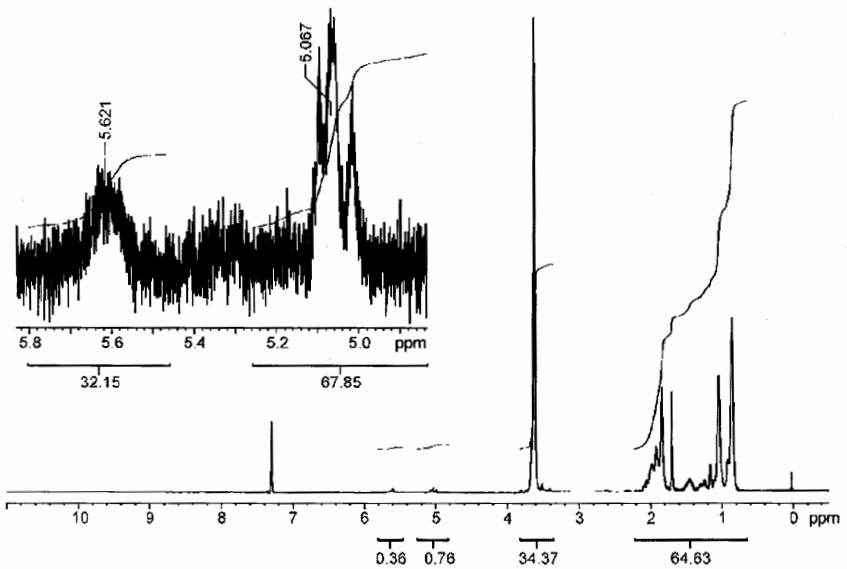

Figure 16. ^{1}H NMR specrta of **9E** (Table 3, entry10)

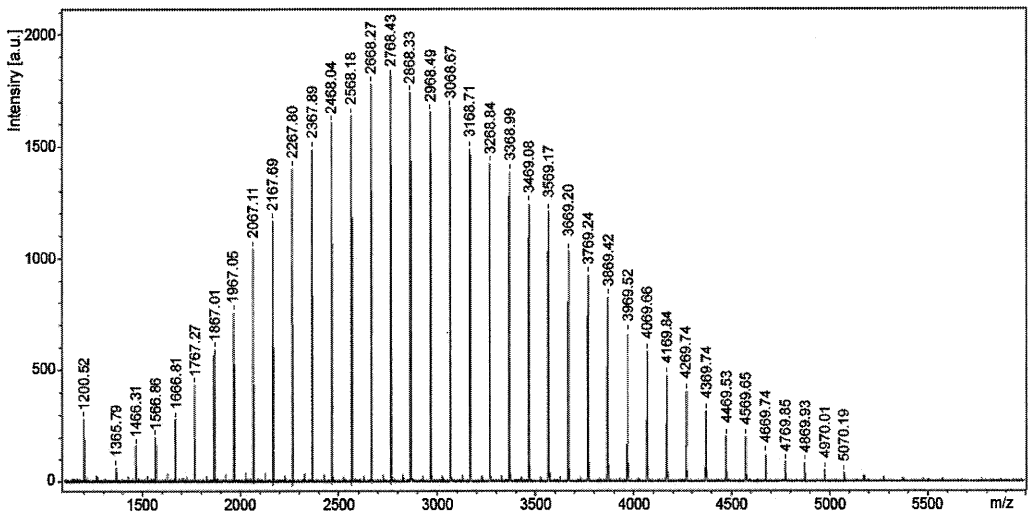

Figure 17. MALDI-TOF MS spectra of **9E** (Table 3, entry 10)

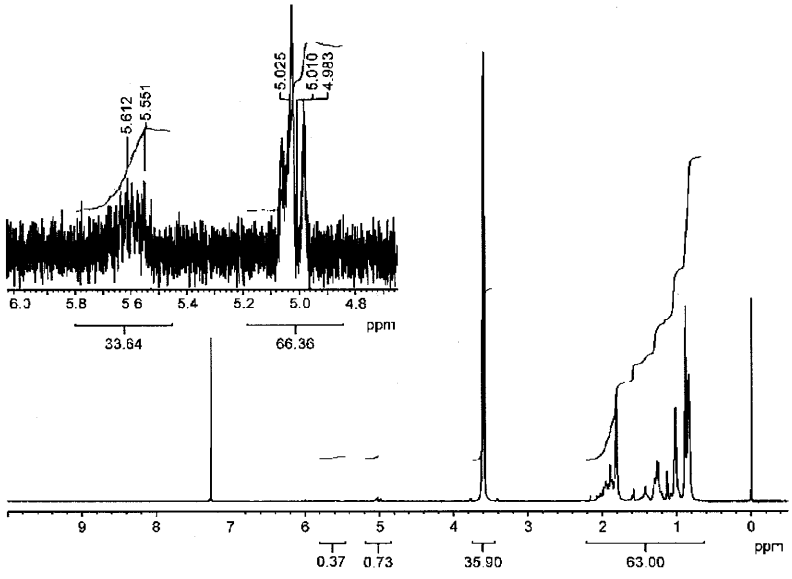

Figure 18. ^{1}H NMR specrta of **9E** (Table 3, entry 11)

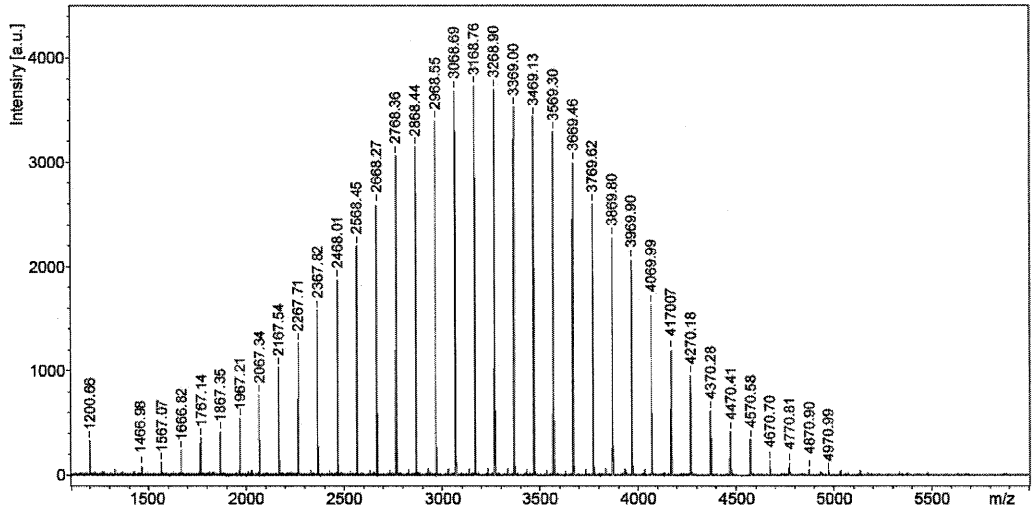

Figure 19. MALDI-TOF MS spectra of **9E** (Table 3, entry 11).

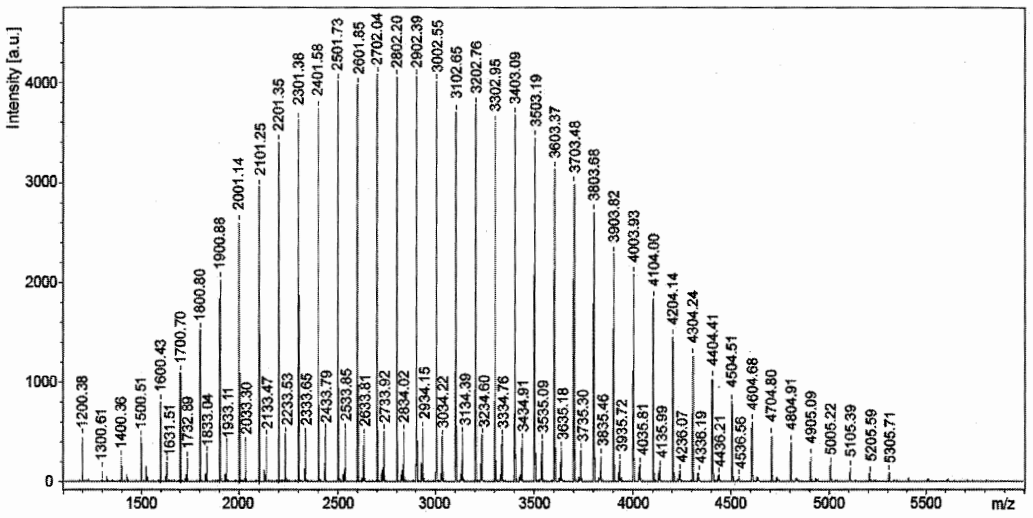

Figure 20. MALDI-TOF MS spectra of **10** (Table 3, entry 12)

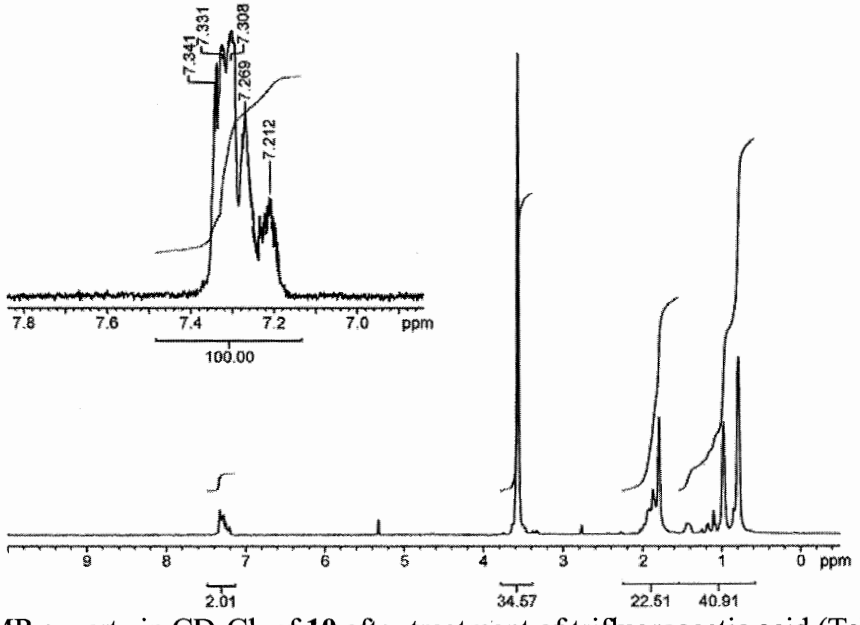

Figure 21. ^{1}H NMR specrta in CD_2Cl_2 of **10** after treatment of trifluoroacetic acid (Table 3, entry 12).

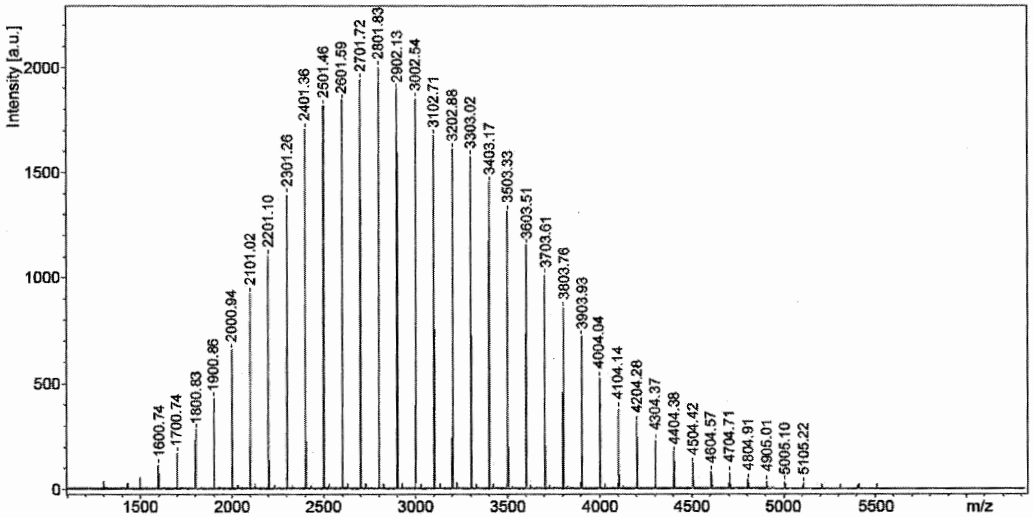

Figure 22. MALDI-TOF MS spectra of **10** after treatment of trifluoroacetic acid (Table 3, entry 12).

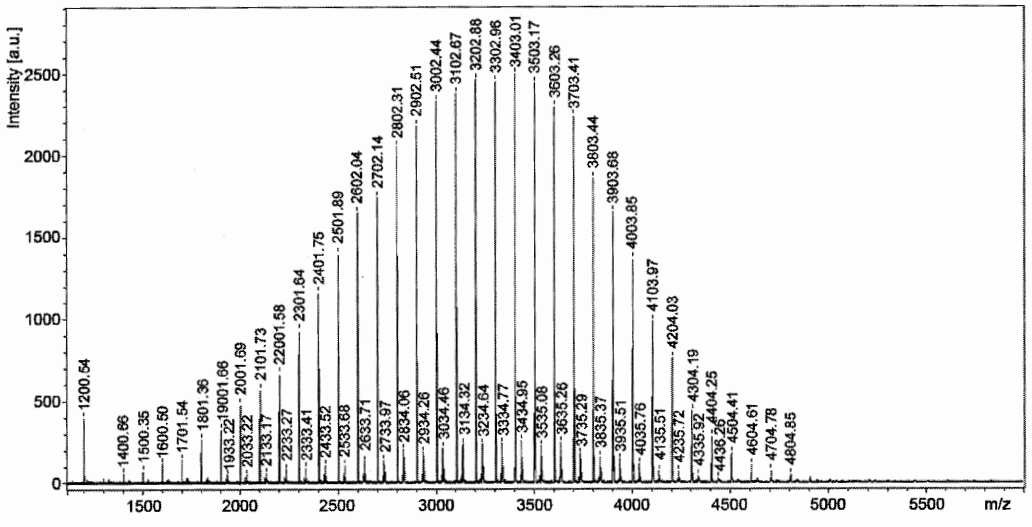

Figure 23. MALDI-TOF MS spectra of **10** (Table 3, entry 13).

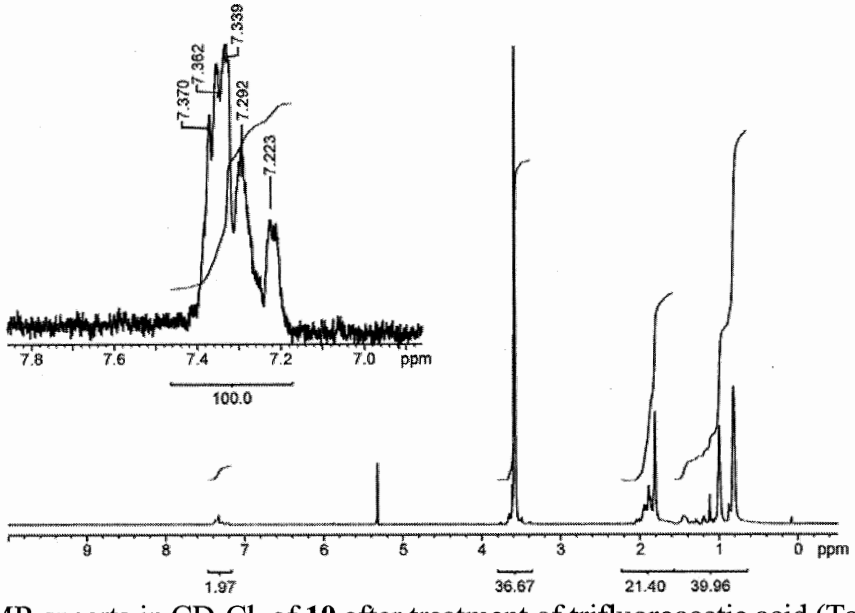

Figure 24. ^{1}H NMR specrta in CD_2Cl_2 of **10** after treatment of trifluoroacetic acid (Table 3, entry 13).

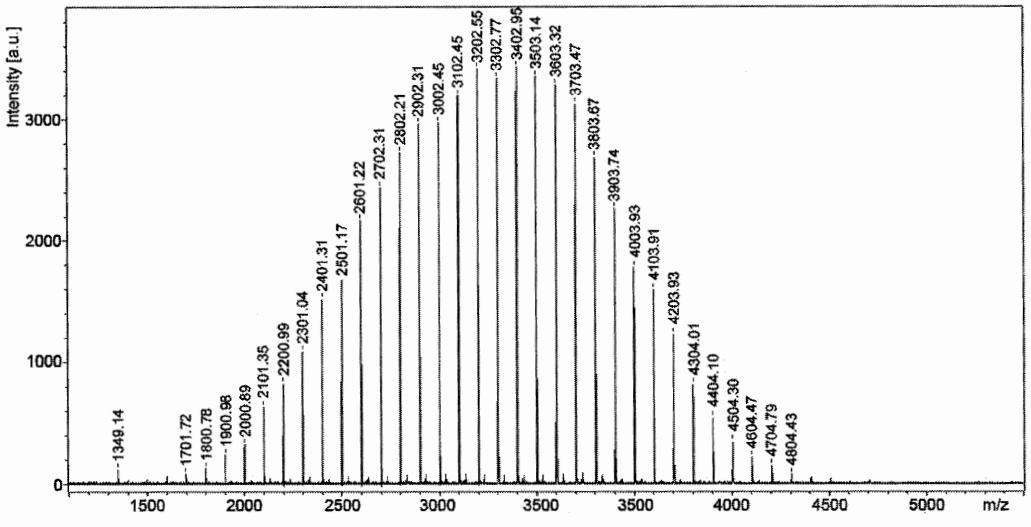

Figure 25. MALDI-TOF MS spectra of **10** after treatment of trifluoroacetic acid (Table 3, entry 13).

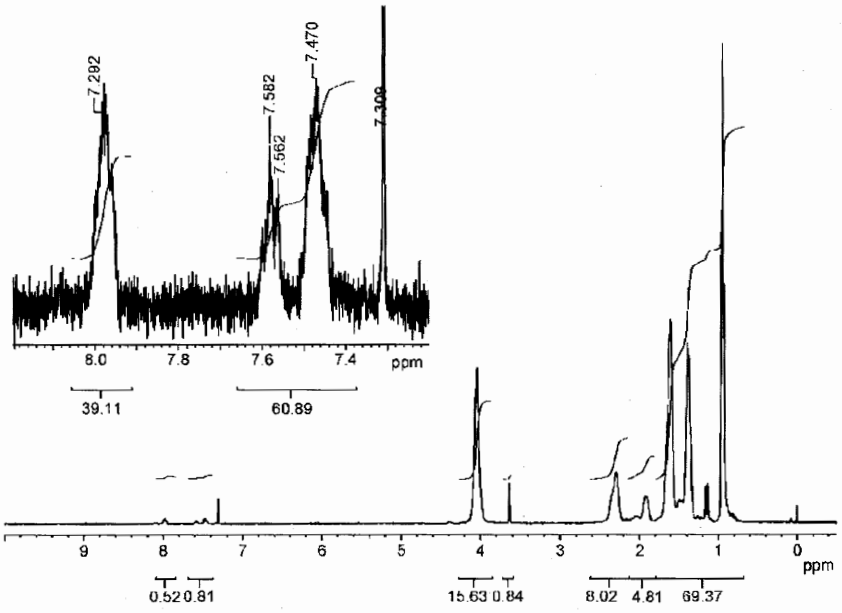

Figure 26. ^{1}H NMR specrta of **13**.

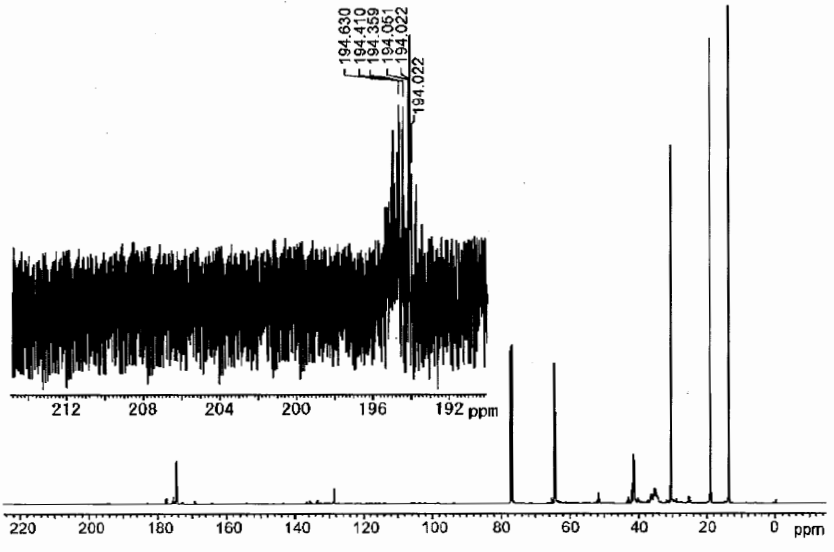

Figure 27. ^{13}C NMR specrta of **13**.

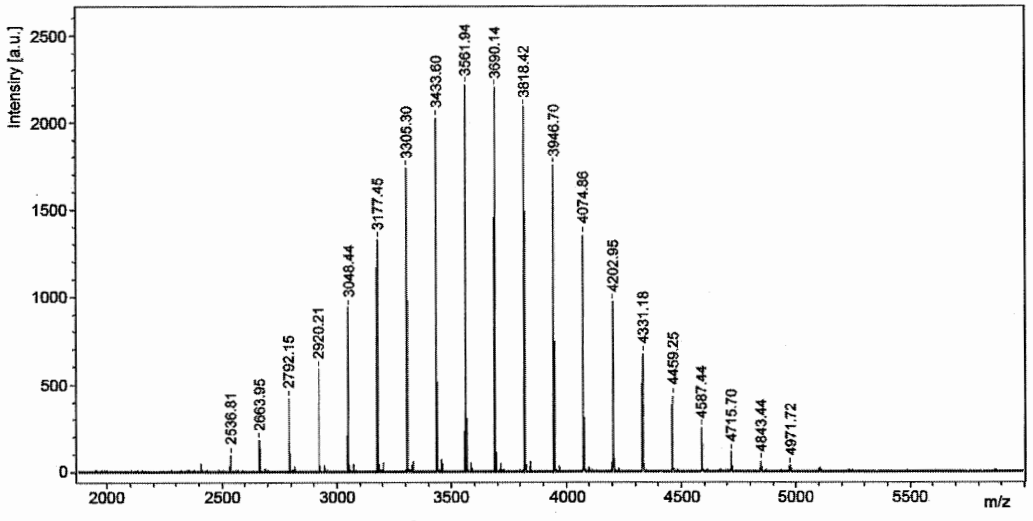

Figure 28. MALDI-TOF MS spectra of **13**.

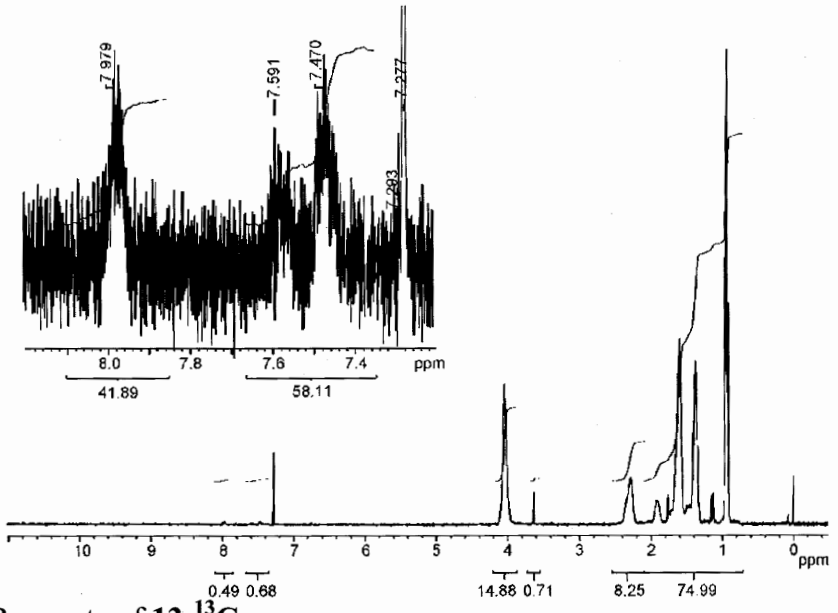

Figure 29. ^{1}H NMR specrta of **13-^{13}C**.

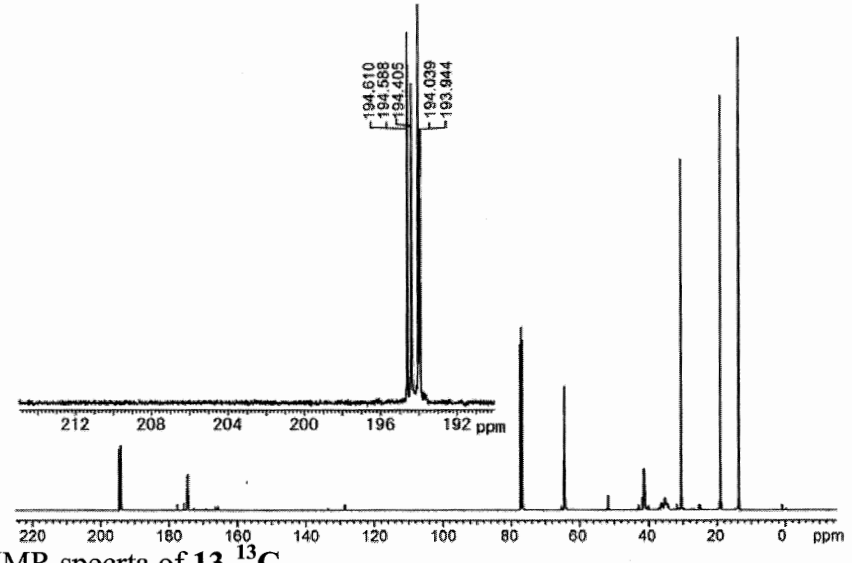

Figure 30. ^{13}C NMR specrta of **13-^{13}C**.

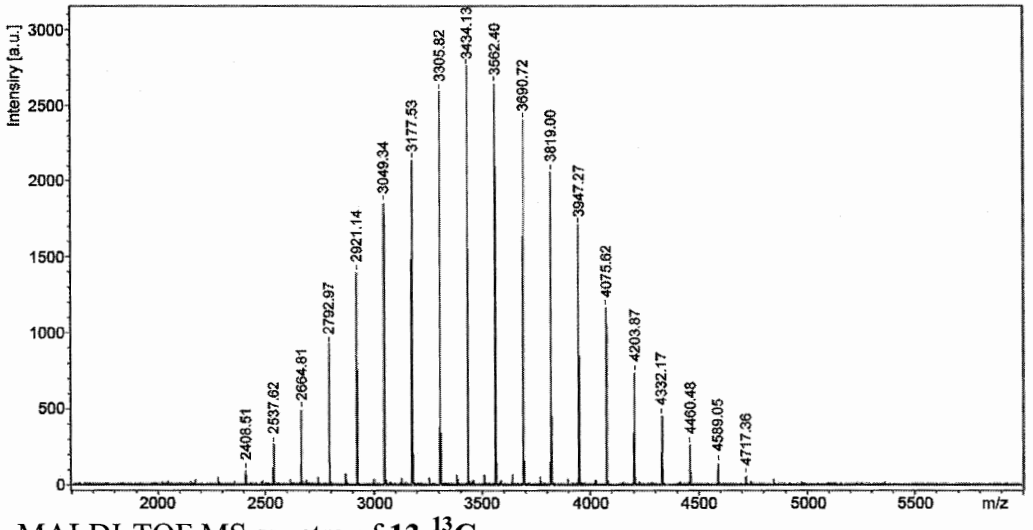

Figure 31. MALDI-TOF MS spectra of **13-^{13}C**.

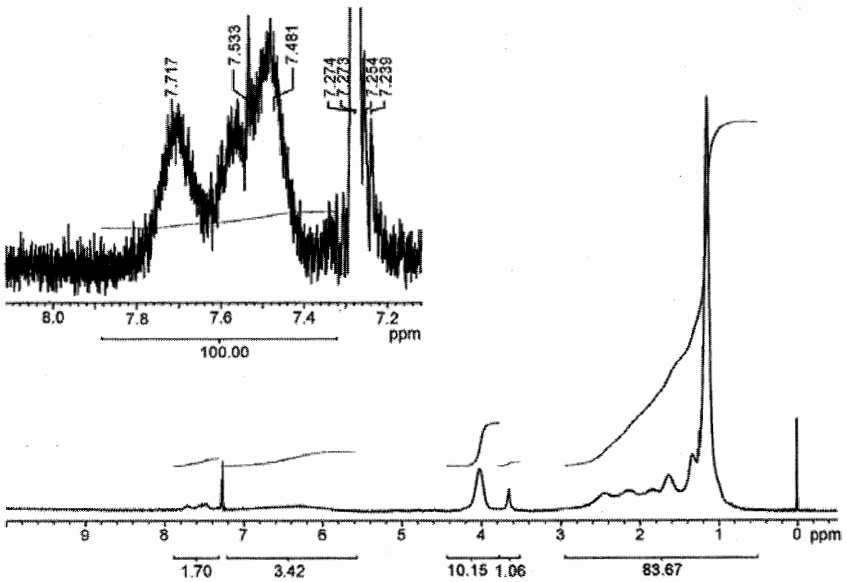

Figure 32. ^{1}H NMR specrta of **17**.

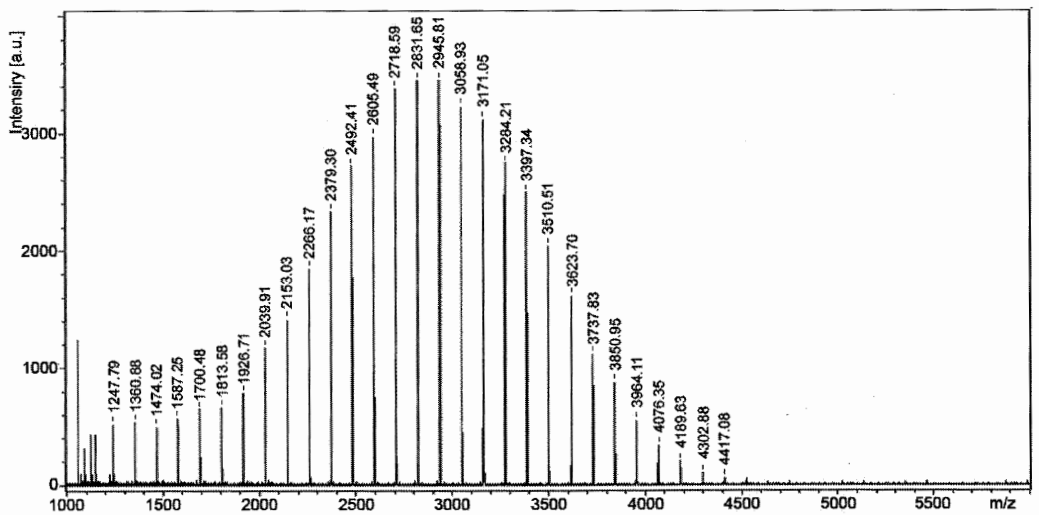

Figure 33. MALDI-TOF MS spectra of **17**.

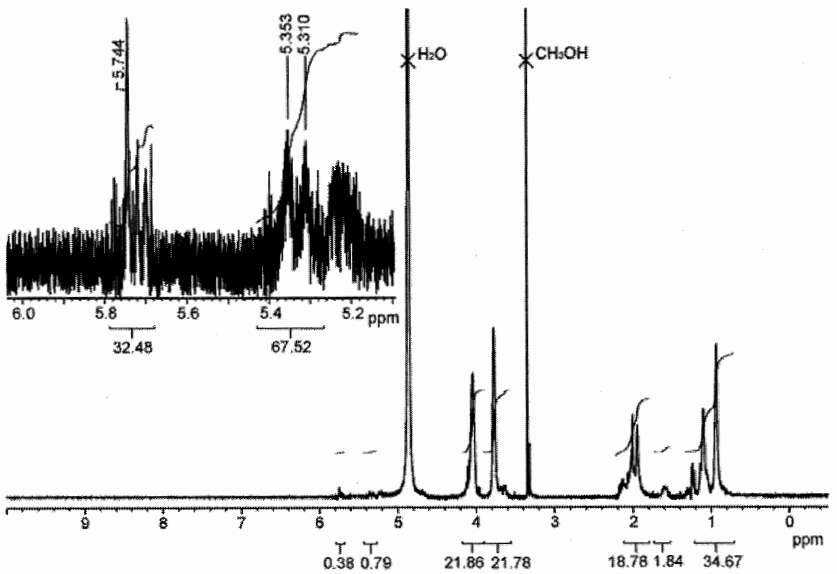

Figure 34. ^{1}H NMR specrta of **19** in CD_3OD.

References

(1) Negishi, E. *Organometallics in Organic Synthesis*; John Willy and Sons: New York, 1980.

(2) *Main Group Metals in Organic Synthesis*; Yamamoto, H.; Oshima, K., Eds.; Wiley-VCH: Weinheim, 2005.

(3) Kauffmann, T. *Top. Curr. Chem.* **1980**, *92*, 109-147.

(4) Kauffmann, T. *Angew. Chem. Int. Ed. Engl.* **1982**, *21*, 410-429.

(5) Parham, W. E.; Bradsher, C. K. *Acc. Chem. Res.* **1982**, *15*, 300-305.

(6) Sotomayor, N.; Lete, E. *Curr. Org. Chem.* **2003**, *7*, 275-300.

(7) Najera, C.; Yus, M. *Current Organic Chemistry* **2003**, *7*, 867-926.

(8) Knochel, P.; Dohle, W.; Gommermann, N.; Kneisel, F. F.; Kopp, F.; Korn, T.; Sapountzis, I.; Vu, V. A. *Angew. Chem. Int. Ed.* **2003**, *42*, 4302-4320.

(9) Chinchilla, R.; Najera, C.; Yus, M. *Chem. Rev.* **2004**, *104*, 2667-2722.

(10) Schlosser, M. *Angew. Chem. Int. Ed.* **2005**, *44*, 376-393.

(11) Seyferth, D. *Organometallics* **2006**, *25*, 2-24.

(12) Seyferth, D. *Organometallics* **2009**, *28*, 2-33.

(13) Gilman, H.; Yablunky, H. L.; Svigoon, A. C. *J. Am. Chem. Soc.* **1939**, *61*, 1170-1172.

(14) Gilman, H.; Yale, H. L. *J. Am. Chem. Soc.* **1950**, *72*, 8-10.

(15) Talalaeva, T. V.; Kocheshkov, K. A. *Bull. Acad. Sci. U.S.S.R., Div. Chem. Sci. (Engl. Transl.)* **1953**, 263-266.

(16) Wittig, G.; Maercker, A. *J. Organomet. Chem.* **1967**, *8*, 491-494.

(17) Steinseifer, F.; Kauffmann, T. *Angew. Chem. Int. Ed. Engl.* **1980**, *19*, 723-724.

(18) Suzuki, H.; Murafuji, T. *J. Chem. Soc., Chem. Commun.* **1992**, 1143-1144.

(19) Reich, H. J.; Green, D. P.; Phillips, N. H. *J. Am. Chem. Soc.* **1991**, *113*, 1414-1416.

(20) Reich, H. J.; Green, D. P.; Phillips, N. H.; Borst, J. P.; Reich, I. L. *Phosphorus, Sulfur, and Silicon* **1992**, *67*, 83 - 97.

(21) Kanda, T.; Kato, S.; Kambe, N.; Kohara, Y.; Sonoda, N. *J. Phys. Org. Chem.* **1996**, *9*, 29-34.

(22) Reich, H. J.; Phillips, N. H.; Reich, I. L. *J. Am. Chem. Soc.* **1985**, *107*, 4101-4103.

(23) Reich, H. J.; Phillips, N. H. *J. Am. Chem. Soc.* **1986**, *108*, 2102-2103.

(24) Reich, H. J.; Green, D. P.; Phillips, N. H. *J. Am. Chem. Soc.* **1989**, *111*, 3444-3445.

(25) Ogawa, S.; Masutomi, Y.; Erata, T.; Furukawa, N. *Chem. Lett.* **1992**, *21*, 2471-2474.

(26) Zefirov, N. S.; Makhon'kov, D. I. *Chem. Rev.* **1982**, *82*, 615-624.

(27) Ogawa, S.; Sato, S.; Furukawa, N. *Tetrahedron Lett.* **1992**, *33*, 7925-7928.

(28) Yamago, S.; Ray, B.; Iida, K.; Yoshida, J.; Tada, T.; Yoshizawa, K.; Kwak, Y.; Goto, A.; Fukuda, T. *J. Am. Chem. Soc.* **2004**, *126*, 13908-13909.

(29) Ray, B.; Kotani, M.; Yamago, S. *Macromolecules* **2006**, *39*, 5259-5265.

(30) Yamago, S.; Kayahara, E.; Yamada, H. *React. Func. Polym.* **2009**, *69*, 416-423.

(31) Yamago, S.; Kayahara, E.; Kotani, M.; Ray, B.; Kwak, Y.; Goto, A.; Fukuda, T. *Angew. Chem. Int. Ed.* **2007**, *46*, 1304-1306.

(32) Kayahara, E.; Yamago, S. *J. Am. Chem. Soc.* **2009**, *131*, 2508-2513.

(33) Coessens, V.; Pintauer, T.; Matyjaszewski, K. *Prog. Polym. Sci.* **2001**, *26*, 337-377.

(34) Matyjaszewski, K.; Gnanou, Y.; Leibler, L. *Macromolecular Engineering*; Wiley-VCH: Weinheim, 2007.

(35) Boutevin, B.; David, G.; Boyer, C. *Adv. Polym. Sci.* **2007**, *206*, 31-135.

(36) Matyjaszewski, K.; Tsarevsky, N. V. *Nature Chem.* **2009**, *1*, 276-288.

(37) Destarac, M. *Macromol. React. Eng.* **2010**, *4*, 165-179.

(38) Yamago, S.; Iida, K.; Yoshida, J. *J. Am. Chem. Soc.* **2002**, *124*, 13666-13667.

(39) Goto, A.; Kwak, Y.; Fukuda, T.; Yamago, S.; Iida, K.; Nakajima, M.; Yoshida, J. *J. Am. Chem. Soc.* **2003**, *125*, 8720-8721.

(40) Yamago, S. *Synlett* **2004**, 1875-1890.

(41) Yamago, S. *J. Polym. Sci. Part A: Polym. Chem.* **2006**, *44*, 1-12.

(42) Sugihara, Y.; Kagawa, Y.; Yamago, S.; Okubo, M. *Macromolecules* **2007**, *40*, 9208-9211.

(43) Yusa, S.; Yamago, S.; Sugahara, M.; Morikawa, S.; Yamamoto, T.; Morishima, Y. *Macromolecules* **2007**, *40*, 5907-5915.

(44) Kayahara, E.; Yamago, S.; Kwak, Y.; Gota, A.; Fukuda, T. *Macromolecules* **2008**, *41*, 527-529.

(45) Hasegawa, J.; Kanamori, K.; Nakanishi, K.; Hanada, T.; Yamago, S. *Macromolecules* **2009**, *42*, 1270-1277.

(46) Yamago, S.; Ukai, Y.; Matsumoto, A.; Nakamura, Y. *J. Am. Chem. Soc.* **2009**, *131*, 2100-2101.

(47) Hiiro, T.; Kambe, N.; Ogawa, A.; Miyoshi, N.; Murai, S.; Sonoda, N. *Angew. Chem. Int. Ed. Engl.* **1987**, *26*, 1187-1188.

(48) Hiiro, T.; Morita, Y.; Inoue, T.; Kambe, N.; Ogawa, A.; Ryu, I.; Sonoda, N. *J. Am. Chem. Soc.* **1990**, *112*, 455-457.

(49) Kanda, T.; Kato, S.; Sugino, T.; Kambe, N.; Sonoda, N. *J. Organomet. Chem.* **1994**, *473*, 71-83.

(50) Petragnani, N.; Stefani, H. A. *Tetrahedron* **2005**, *61*, 1613-1679.

(51) Comasseto, J. o. V.; Dos Santos, A. A. *Phosphorus, Sulfur, and Silicon* **2008**, *183*, 939-947.

(52) Yamago, S.; Iida, K.; Yoshida, J. *J. Am. Chem. Soc.* **2002**, *124*, 2874-2875.

(53) Uchiyama, M.; Koike, M.; Kameda, M.; Kondo, Y.; Sakamoto, T. *J. Am. Chem. Soc.* **1996**, *118*, 8733-8734.

(54) Uchiyama, M.; Kondo, Y.; Miura, T.; Sakamoto, T. *J. Am. Chem. Soc.* **1997**, *119*, 12372-12373.

(55) Uchiyama, M.; Kameda, M.; Mishima, O.; Yokoyama, N.; Koike, M.; Kondo, Y.; Sakamoto, T. *J. Am. Chem. Soc.* **1998**, *120*, 4934-4946.

(56) Uchiyama, M.; Furuyama, T.; Kobayashi, M.; Matsumoto, Y.; Tanaka, K. *J. Am. Chem. Soc.* **2006**, *128*, 8404-8405.

(57) Furuyama, T.; Yonehara, M.; Arimoto, S.; Kobayashi, M.; Matsumoto, Y.; Uchiyama, M. *Chem. Eur. J.* **2008**, *14*, 10348-10356.

(58) Nakamura, S.; Liu, C.-Y.; Muranaka, A.; Uchiyama, M. *Chem. Eur. J.* **2009**, *15*, 5686-5694.

(59) Krasovskiy, A.; Knochel, P. *Angew. Chem. Int. Ed.* **2004**, *43*, 3333-3336.

(60) Ila, H.; Baron, O.; Wagner, A. J.; Knochel, P. *Chem. Lett.* **2006**, *35*, 2-7.

(61) When benzaldehyde was added after the exchange reaction, the reaction gave a mixture of **3A** and **2A**, regeneration of the starting substrate **3** and **2f** due to the rapid equilibrium between the anionic and heteroatom compounds.

(62) Jørgensen, M.; Lee, S.; Liu, X.; Wolkowski, J. P.; Hartwig, J. F. *J. Am. Chem. Soc.* **2002**, *124*, 12557-12565.

(63) Hsieh, H. L.; Quirk, R. P. *Anionic Polymerization: Principles and practical applications*; Marcel Dekker: New York, 1996.

(64) Janata, M.; Lochmann, L.; Müller, A. H. E. *Makromol. Chem.* **1990**, *191*, 2253-2260.

(65) Janata, M.; Lochmann, L.; Vlček, P.; Dybal, J.; Müller, A. H. E. *Makromol. Chem.* **1992**, *193*, 101-112.

(66) Cho, D. W.; Lee, H.-Y.; Oh, S. W.; Choi, J. H.; Park, H. J.; Mariano, P. S.; Yoon, U. C. *J. Org. Chem.* **2008**, *73*, 4539-4547.

(67) Lutz, J.-F.; Bo¨rner, H. G. *Prog. Polym. Sci.* **2008**, *33*, 1-39.

(68) Chen, X.; Yamamoto, Y.; Akiba, K.-Y. *Heteroatom Chem.* **1995**, *6*, 293-303.

(69) Kanda, T.; Kato, S.; Kambe, N.; Kohara, Y.; Sonoda, N. *J. Phys. Org. Chem.* **1996**, *9*, 29-34.

(70) Yoshikawa, C.; Goto, A.; Tsujii, Y.; Fukuda, T.; Yamamoto, K.; Kishida, A. *Macromolecules* **2005**, *38*, 4604-4610.

(71) Ouchi, A.; Ebina, F.; Uehiro, T.; Yoshino, Y. *Bull. Chem. Soc. Jpn.* **1978**, *51*, 2427-2428.

(72) DesEnfants Ii, R. E.; Gavney Jr, J. A.; Hayashi, R. K.; Rae, A. D.; Dahl, L. F.; Bjarnason, A. *J. Organomet. Chem.* **1990**, *383*, 543-572.

(73) Cywar, D. A.; Tirrell, D. A. *J. Am. Chem. Soc.* **1989**, *111*, 7544-7553.

(74) Ting, R.; Adam, M. J.; Ruth, T. J.; Perrin, D. M. *J. Am. Chem. Soc.* **2005**, *127*, 13094-13095.

(75) Arnold, R. T.; Kulenovic, S. T. *J. Org. Chem.* **1978**, *43*, 3678-3684.

(76) Engman, L.; Stern, D. *Organometallics* **1993**, *12*, 1445-1448.

(77) Watson, S. C.; Eastham, J. F. *J. Organomet. Chem.* **1967**, *9*, 165-168.

(78) Kofron, W. G.; Baclawski, L. M. *J. Org. Chem.* **1976**, *41*, 1879-1880.

(79) Mlynek, P. D.; Dahl, L. F. *Organometallics* **1997**, *16*, 1641-1654.

(80) Chen, S.-L.; Ji, S.-J.; Loh, T.-P. *Tetrahedron Lett.* **2004**, *45*, 375-377.

(81) Spaccini, R.; Pastori, N.; Clerici, A.; Punta, C.; Porta, O. *J. Am. Chem. Soc.* **2008**, *130*, 18018-18024.

(82) Yamamoto, T.; Ohta, T.; Ito, Y. *Org. Lett.* **2005**, *7*, 4153-4155.

(83) Hatano, M.; Takagi, E.; Ishihara, K. *Org. Lett.* **2007**, *9*, 4527-4530.

(84) Ohkuma, T.; Sandoval, C. A.; Srinivasan, R.; Lin, Q.; Wei, Y.; Muñiz, K.; Noyori, R. *J. Am. Chem. Soc.* **2005**, *127*, 8288-8289.

(85) Iida, A.; Nakazawa, S.; Okabayashi, T.; Horii, A.; Misaki, T.; Tanabe, Y. *Org. Lett.* **2006**, *8*, 5215-5218.

(86) Wender, P. A.; Koehler, M. F. T.; Sendzik, M. *Org. Lett.* **2003**, *5*, 4549-4552.

(87) Salome′, C.; Kohn, H. *Tetrahedron* **2009**, *65*, 456-460.

Chapter 7

Theoretical Studies on Homolytic Substitution Reaction of Dicalcogenides with Carbon-centered Radical

Abstract

Homolytic substitution (S_H2) reaction on dimethyl dichalcogenides (XCH_3) (X = S, Se, and Te) with 2-cyano-2-propyl radical has been theoretically investigated using the density functional theory (DFT) calculation at M06-2X, B3LYP, or BHandHLYP level of theory. The calculations suggested that the S_H2 reactions proceed colinear transition state (TS) with respect to the incoming radical and leaving methylchalcogenyl radical. The activation energies of the radical addition step become lower in the order of dimethyl disulfide > dimethyl diselenide > dimethyl ditelluride. The deformation/interaction analysis suggested that the high kinetic reactivity of ditelluride is mainly due to the low deformation energy associated with the smaller bending of carbon-centered radical and elongation of Te-Te bond of ditelluride. Similarly, the activation energies of the radical dissociation step are also the lowest for X = Te followed by X = Se and X = S. The difference is largely controlled by interaction energy rather than deformation energy. As the results, the organotellurium compounds formed by the substitution reaction is thermodynamically least stable and the corresponding reaction is most endothermic among the reactions. The Kohn-Sham molecular orbital analysis revealed that both reaction steps take place through the SOMO-HOMO three-electron interaction, which derived from the interaction between the p orbital of carbon (or heteroatom)-centered radical (SOMO) and n orbital of the dicalcogenide (or calcogenide) (HOMO).

Introduction

Diheteroatom compounds which contain a heteroatom-heteroatom σ bond of group 15, 16, and 16 elements in the periodic table, e.g., diphosphine,[1-3] distibine,[4] disulfide,[5,6] diselenide,[7-11] ditelluride,[12-14] iodine[15,16] react with carbon-centered radicals to give corresponding organoheteroatom compounds (Scheme 1). Since the reaction takes place under neutral conditions, it is useful for the synthesis of functionalized heteroatom compounds with significant importance as metal ligands, pharmaceuticals, electroconducting materials, and building blocks in organic synthesis. Diheteroatom compounds possessing σ bond between the different heteroatoms, thiostibine[17-19] and thiobismuthine,[19] have also been reported as excellent precursor for organostibine and organobismuthine compounds, respectively. Additionally, stannylphosphine, silylphosphine,[20] and thiophosphine[21] have been recently applied for the synthesis of organophosphine compounds.

Scheme 1. S_H2 reaction of diheteroatom compounds and carbon-centered radicals. R = alkyl, aryl, or vinyl; X = heteroatom; L = alkyl or aryl.

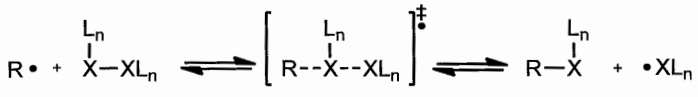

The reactivity of dichalcogenides, namely diphenyl disulfide, diphenyl diselenide, and diphenyl ditelluride toward 5-hexenyl radical has been already examined thorough kinetic studies by Russel and coworkers; the reactivity becomes higher when the element become heavier; the rate constant of S_H2 reactions increases 150 and 4 times in going from the diphenyl disulfide to diphenyl diselenide and further to diphenyl ditelluride.[22,23] However, the origin of the differences in the reactivity among these dichalcogenides remains elusive.

During our research on the development for organotellurium-, stibine-, and bismuthine-mediated living radical polymerization, which are abbreviated as TERP,[24-31], SBRP,[32,33] and BIRP,[34] respectively, we have shown that the addition of ditellurides,[35] distibines,[36] and thiobismuthine[37] in TERP, SBRP, and BIRP, respectively are effective to increase the control on molecular weight distributions of the resulting polymers. Kinetic studies revealed that ditelluride reacts with polymer-end radical (P•) through S_H2 reaction forming organotellurium compound P-TeR (Scheme 2).[38] The rate of the S_H2 reaction is 100 times faster than S_H2 reaction of the P

radical with P-TeL, and the high reactivity of the ditelluride is responsible for the increased control of molecular weight distribution. The liberated tellanyl radical (LTe•) selectively reacts with P-TeL to regenerate P radical and ditelluride. The effect of tetrametyl- and tetraphenyl distibine on SBRP and iodide on iron catalyzed polymerization and reversible chain-transfer catalyzed polymerization using organoiodides, respectively, to increase the control of molecular weight distribution have been also reported by us,[36] Sawamoto,[39] and Goto.[40]

Scheme 2. Mechanisms on the reaction of Polymer-end radical (P•) with ditelluride $(TeL)_2$ or distibine $(SbL_2)_2$.

We have also reported a new synthetic route to organotellurium compounds, which are used for controlling agents in TERP, by the reaction of 2,2-azobisisobutyronitrile (AIBN) and dimethyl- and diphenylditelluride. However, the corresponding tellurium compounds were obtained only in low yields (8-18%). The results were surprising for us, because ditellurides are one of the most reactive radical traps so far reported. On the other hand, the reaction of AIBN with diphenyldiselenide took place in 56% yield to give 2-phenylselenyl-2-methylpropionitrile.[41] Since about 40% of the radicals generated from the azo initiators dimerize within a solvent cage, the result indicated that almost all radicals diffused from the cage was captured by the diselenide. Similar high coupling efficiency is also reported in the reaction of AIBN with tetramehyldisbitine,[36] tetraphenyldiphosphine,[1] and iodine.[15] These results seem to apparently contradict to the kinetic reactivities of these dichalcogenides reported by Russel.

To clarify this point, we carried out the theoretical studies on S_H2 reaction of dichalcogenides, namely dimethyl sulfide, dimethyl diselenide, and dimethyhl ditelluride, with carbon-centered radical. The reaction pathways were studied by the density functional theoretical (DFT) method using several different functional.

Mechanism for S_H2 reaction of dialkyl- and diaryl disulfide with an alkyl radical was already examined thorough experimentally[42-45] and theoretically[46] by Pryor and coworkers. The results revealed that the S_H2 reaction predominantly proceed through the backside attack mechanism involving the collinear transition state (**TS**) with respect to the attacking radical, heteroatom, and

leaving heteroatom-centered radical. Contribution of the frontside attack mechanism, in which the attacking radical approach from the same side with the leaving radical, is negligible. Therefore, only the backside attack pathway is investigated in this study. We especially focused on to clarify the origin of reactivity difference among the heteroatom species of dichalcogenides, and the doformation/interaction and molecular orbital analyses were carried out for this purpose. Detailed results are presented in this manuscript.

Results and Discussion

Chemical Models and Computational Methods. We selected the S_H2 reaction of 2-cyano-2-propyl radical **1**, which forms by decomposition of AIBN, with dimethyl dichalcogenide $(XMe)_2$ (X = S, Se, Te) **2** as a model reaction (Scheme 2).

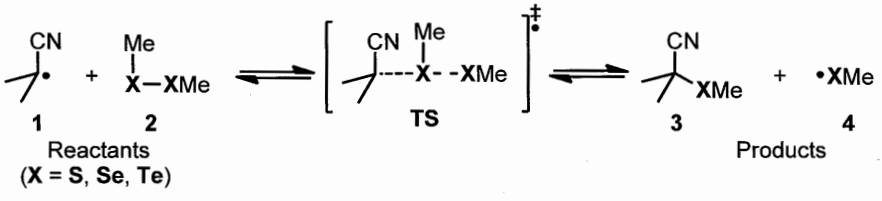

Scheme 2. Chemical model for S_H2 reaction of dichalcogens.

Extensive search of the potential energy surface was carried out for the backside attack in this study based on the Pryor's result.[42] All geometrical optimizations were performed by the density functional theoretical (DFT) method with the M06-2X,[47,48] the B3LYP, and the BHandHLYP functionals in Gaussian 03[49] or Gaussian 09[50] program package. The Hey-Wadt effective core potential (ECP) and the outermost valence electron basis set was applied for chalcogen atom X[51] and the 6-311G(d,p) basis set for C, H, and N (denoted as M06-2X/6311DZP, B3LYP/6311DZP, and BHandHLYP/6311DZP, respectively). While B3LYP is the most widely used functional, previous studies pointed out that transition states calculated at the B3LYP level might, in some cases, be too early with underestimated associated energy barriers.[52] Thus, we also performed calculations using the BHandHLYP or M06-2X functional, which has been shown to be well suited for calculating barrier heights in radical processes. This latter functional was developed particularly to address the failings of B3LYP and has been successfully used for organic reactions involving radicals.[53-55] The intrinsic reaction coordinate (IRC) method was used to track minimum energy

paths from transition structures to the corresponding local minima. Single-point energy calculations were performed at CCSD(T)/6311DZP level of theory by using the optimized geometry at M06-2X/6311DZP, B3LYP/6311DZP, and BHandHLYP/6311DZP (denoted as CCSD(T)/6311DZP//M06-2X/6311DZP,CCSD(T)/6311DZP//B3LYP/6311DZP, and CCSD(T)/6311DZP//BHanHLYP/6311DZP, repectively).

Energy surface of S_H2 reaction of 1 with 2. The potential surface energy diagrams obtained at M06-2X/6311DZP and CCSD(T)/6311DZP//M06-2X/6311DZP level of theories are summarized in Figure 1, in which the sulfur, selenium, and tellurium series are denoted with letters after hyphen, namely S, Se, and Te, respectively. The relative energies of each species were shown in Table 1. The corresponding structures to **TS**s were successfully located in all cases. The IRC calculations showed the obtained **TS**s could be connected to both reactant and product complexes (**RC**s and **PC**s, respectively), which are found by the subsequent geometry optimizations at M06-2X/6311DZP level of theory. Thus, the reaction of **1** and **2** initially forms an energetically stable **RC** by about 25 (10) kJ/mol (the values in the parenthesis were obtained by CCSD(T)/6311DZP//M06-2X/6311DZP), in all cases, which leads to the corresponding **TS**. The relative activation energies ($\Delta E_1^{\ddagger}$s) from the **RC**s to **TS**s for X = S, Se, and Te are 47.4 (58.2), 28.1 (37.6), and 16.1 (21.4) kJ/mol, respectively. The results are consistent with the Russel's experimental results.[22] The **TS**s lead to the formation of **PC**s then to the products; heteroatom compound **3** and methylchalcogenyl radical **4**. The energy changes ($-\Delta E_2^{\ddagger}$s) in formation of **PC**s from **TS**s for X = S, Se, and Te are 39.9 (77.0), 28.2 (47.8), and 15.7 (14.9) kJ/mol, respectively. The results suggested that the kinetic reactivity for the reverse reaction, namely the S_H2 reaction of **3** and **4**, is also most favorable for X = Te, followed by X = Se and S. Overall energy balance is endothermic in all cases at M06-2X/6311DZP with 4.8, 8.2, and 15.8 kJ/mol for X = S, Se, and Te, respectively, while that at CCSD(T)/6311DZP//M06-2X/6311DZP level is exothermic with 6.6, 18.1, and 25.5 kJ/mol for X = S, Se, and Te, respectively. Despite of the differences in absolute thermodynamics, both methods reveal that the reaction with **2-Te** is least thermocynamically unfavorable followed by that with **2-Se** and **2-S.** These results indicated that the low yield of the corresponding tellurium compound in the reaction of ditelluride with AIBN is due to the low thermodyanamic stability. Interestingly, the obtained reaction pathway showed the opposite order on the kinetics and thermodynamics on the calculated S_H2 reaction.

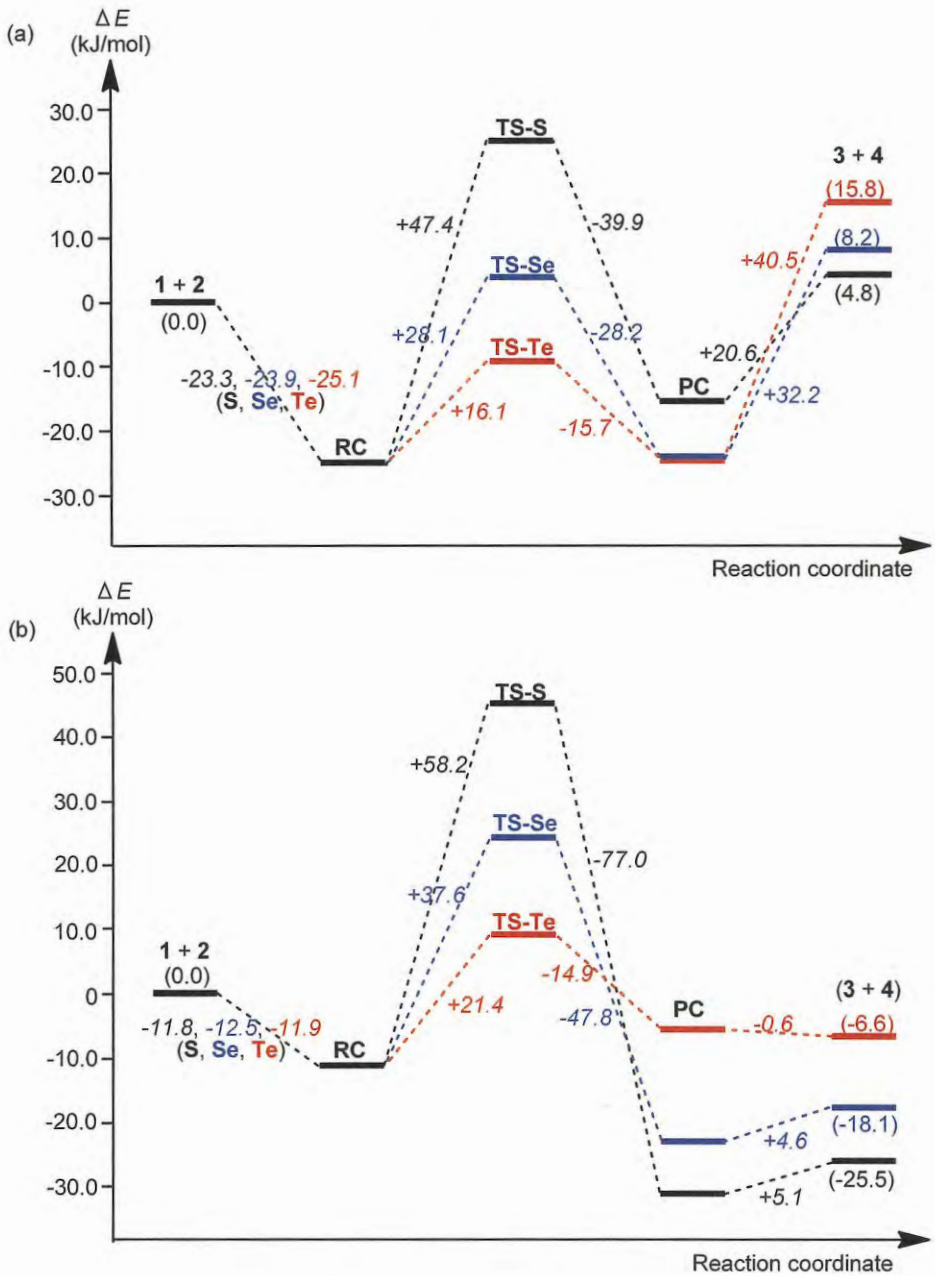

Figure 1. Potential energy surface of the reaction of dimethyl dicalcogenides **2** [$(XMe)_2$ (X = S, Se or Te)] with 2-cyano-2-propyl radical **1** obtained by a) M06-2X/6311DZP level of theory and b) CCSD(T)/6311DZP//M06-2X/6311DZP level of theory. Values in parentheses are energies relative to the reactants (**1** + **2**) in kJ/mol. Energy changes are shown in italics in kJ/mol.

Additionally, the optimization with different functional, B3LYP and BHandHLYP level of theory was also performed. Their calculations afforded qualitatively the same structures of each species as those obtained at the M06-2X method (see Experimental Section), while some relative energies were changed. IRC calculations also showed the obtained **TS**s could be connected with the similar

structure to **RCs** and **PCs** in both level of theories. However, the corresponding **RCs** and **PCs** could not be located as a minimum by using B3LYP and BHandHLYP level of theory except for **PC-Se** and **PC-Te**. According to single-point calculations at high-level CCSD(T) using the structures optimized at each level of theory, the relative energies were corrected and showed in reasonable agreement with each other. Following these results, we will discuss about the results of M06-2X from here on since the differences of functional did not alter the interpretation of the calculation obtained below.

Table 1. Calculated relative energies (kJ/mol) with different functional for RCs, TSs, PCs, and products related to reactants, namely 2-cyano-2-propyl radical **1** and dimethyl dicalcogenides **2** [$(XMe)_2$ (X = S, Se or Te)].[a,b]

	X = S				X = Se				X = Te			
Calculation Method	RC	TS	PC	Product	RC	TS	PC	Product	RC	TS	PC	Product
M06-2X	-23.3	24.1	-15.8	4.8	-23.9	4.2	-24.0	8.2	-25.1	-9.0	-24.7	15.8
M06-2X[c]	(-19.9)	(29.5)	(-6.9)	(8.5)	(-21.0)	(10.6)	(-13.3)	(17.1)	(-20.1)	(-3.8)	(-15.1)	(22.6)
B3LYP	—	51.6	—	20.4	—	33.4	—	27.4	—	21.4	17.2	38.0
B3LYP[c]	—	(57.7)	—	(23.4)	—	(39.7)	—	(31.8)	—	(27.0)	(25.9)	(43.8)
BHandHLYP	—	67.5	—	6.8	—	47.5	10.6	15.9	—	34.0	21.5	30.1
BHandHLYP[c]	—	(73.9)	—	(10.8)	—	(54.0)	(19.8)	(20.8)	—	(40.3)	(30.8)	(35.4)
CCSD(T)//M06-2X	-11.8	46.4	-30.6	-25.5	-12.5	25.1	-22.7	-18.1	-11.9	9.5	-5.4	-6.6
CCSD(T)//B3LYP	—	48.6	—	-24.8	—	26.2	-25.2	-18.3	—	11.6	-6.0	-6.6
CCSD(T)//BHandHLYP	—	49.0	—	-22.6	—	27.9	-22.8	-15.1	—	8.2	-11.0	-3.8

[a]The calculation was performed by using 6311DZP basis set in all cases. [b]Energies are given in units of kJ/mol.[c]Energy with zero-point energy (ZPE) correction are shown in parentheses.

The geometries of **RCs**, **TSs**, and **PCs** optimized by M06-2X level of theory are shown in Figure 2. All reactions take place via colinear **TSs** with respect to **1**, the heteroatom, and **4**, and the $Me_2(CN)C\bullet$-X-X angles of TSs are about 150° in all cases. Out-of-plane bending angles (θ_b) of **1** (θ_b = 2~3° in **RC**) increases to 25.7°, 23.2°, and 19.8° in **TS-S**, **TS-Se**, and **TS-Te**, respectively. As judged by the forming C-X bond length in **TSs** (2.20 Å, 2.41 Å, and 2.74 Å for X = S, Se, and Te, respectively), the higher planar character of **1** in **TS-Te** also attributes to the smaller steric hindrance between **1** and Me group on heteroatom of **2**. In other word, **1** can interact with diteluride with more far away than diselenide and disulfide. The **X-X** bond of **2** elongates by 7.7%, 4.3%, and 1.8% for **2-S**, **2-Se**, and **2-Te**, respectively, in **TSs**. The spin density at **TSs** is still retained mainly on the carbon derived from **1**, especially in **TS-Te**. These observations are consistent with the earlier TS nature in **TS-Te** than **TS-Se** and **TS-S**.

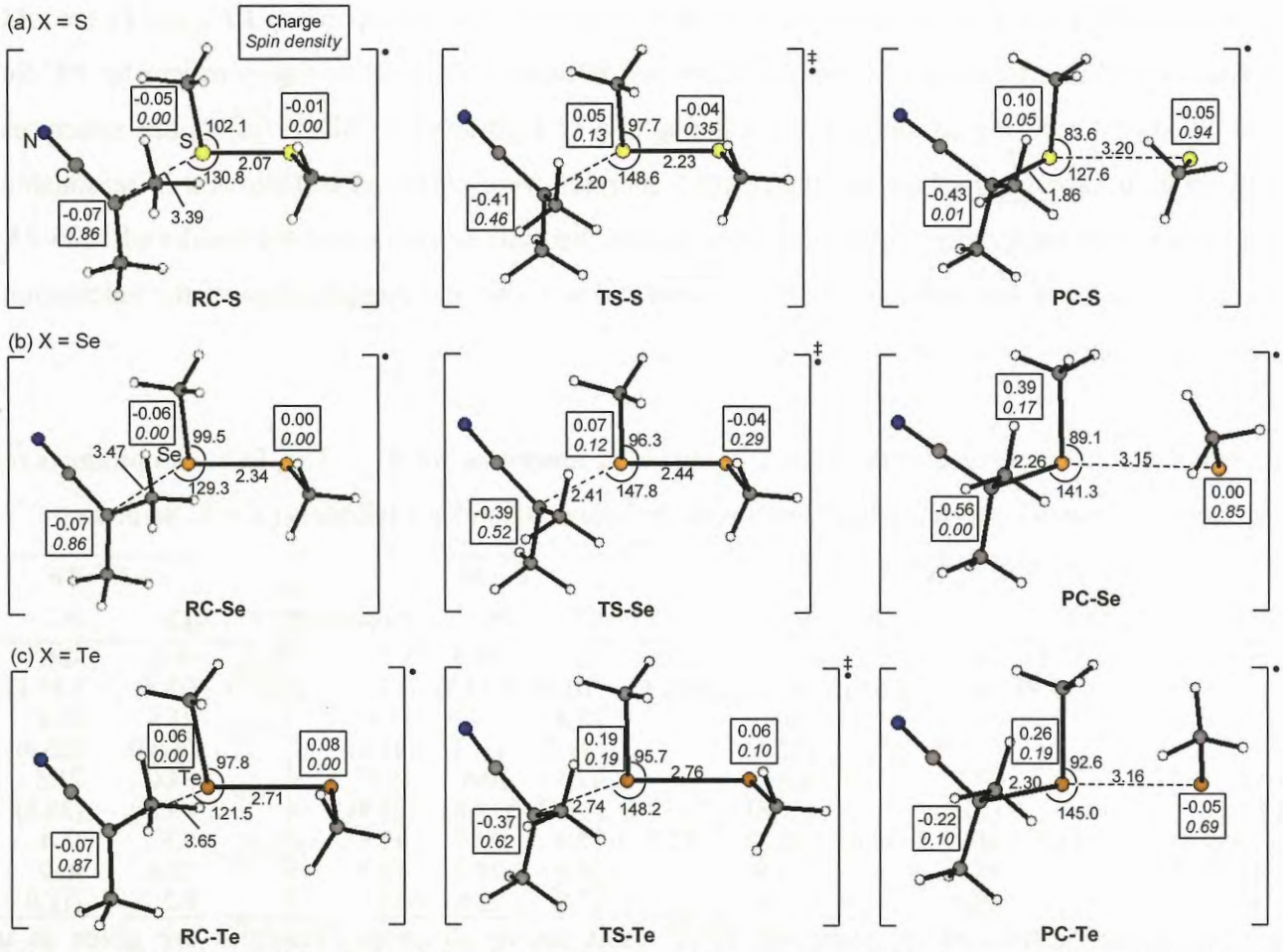

Figure 2. Geometry (Å, deg) of the RCs, TSs, PCs for reaction of the 2-cyano-2-propyl radical **1** and dimethyl dicalcogenides **2** $(XMe)_2$ (a) dimethyl disulfide (X = S), (b) dimethyl diselenide (X = Se), and (c) dimethyl ditelluride (X = Te) obtained at CCSD(T)/6311DZP//M06-2X/6311DZP level of theory. Mulliken charges and spin densities of the heavy atoms are in boxes.

Deformation/interaction analysis on radical addition reaction. The deformation/ interaction analysis[56] was performed to understand the origin of the energy difference among the heteroatom species. Thus, the activation energy $\Delta E_1^{\ddagger}$ from the **RC** to **TS** was decomposed into the deformation energy DEF_{TS1}, which is the sum of $DEF_{TS1\,(1)}$ and $DEF_{TS1\,(2)}$ required for the structural changes of **1** and **2** in **RC** to interact readily in **TS**, and the interaction energy INT_{total1}. We will discuss the energies obtained by CCSD(T)/6311DZP here. The INT_{total1} is the energy obtained by interaction between **1** and **2** as **RC** is converted to **TS**.

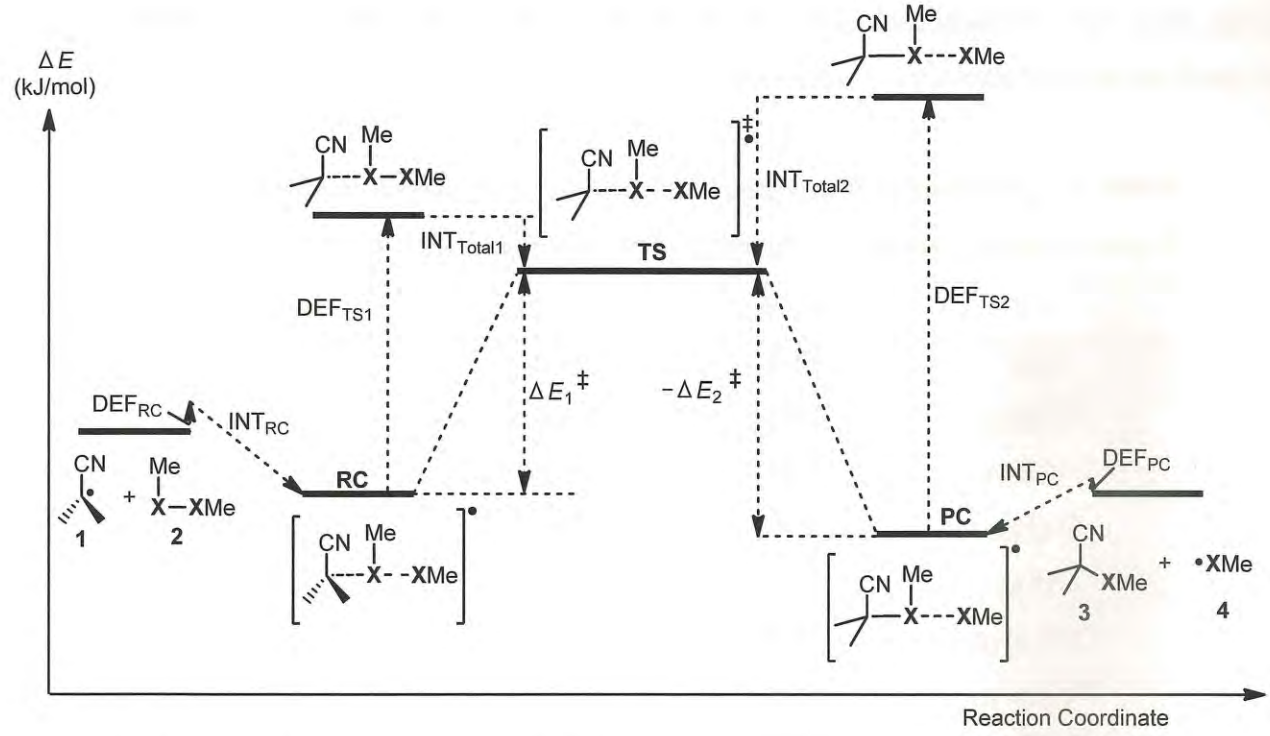

Figure 3. Deformation/interaction analysis of the radical addition and dissociation reaction.

The obtained DEF and INT were shown in Table 2. The structures derived from **1** and **2** does not change by the formation of **RC** from the reactants, and the deformation energies from reactants to **RC** are negligible in all cases (DEF_{RC} ~ 0 kJ/mol). Therefore, the stabilizing energy for the formation of RC can be exclusively attributed to the interaction energy between **1** and **2**. INT_{RC} were about 25 (12) kJ/mol in all cases. The $DEF_{TS1\ (1)}$ from **RC** to **TS** were endothermic and were calculated to be 18.0, 13.1, and 7.8 kJ/mol in the reactions with the disulfide, diselenide, and ditelluride, respectively. The energy losses are primarily due to the pyramidalization of the planer **1** with π-radical character, which are characterized by the changes in θ_b as discussed in previous section. $DEF_{TS1\ (2)}$ was the smallest in X = Te (1.0 kJ/mol), followed by X =Se (5.8 kJ/mol) and X = S (15.6 kJ/mol), which is in good agreement with smaller elongation of the Te-Te bond length in **TS-Te**. The order also correlates well with the order of the relative bond dissociation energies (BDEs) of X-X bond in **2**; the BDEs following the trend Te-Te (169.9 kJ/mol) < Se-Se (193.7 kJ/mol) < S-S (219.5 kJ/mol). Thus, the differences in $\Delta E_1^{\ddagger}$ mainly depends on both deformation energies. This is consistent with the fact that the earlier nature of the TSs is generally reflected by the smaller deformation energy. Furthermore, while the INT_{TS1}s are repulsive in all cases, INT_{TS1} become more attractive on going from X = S (+12.4 kJ/mol) to Se (+5.9 kJ/mol), and Te (+0.4 kJ/mol). Thus, the INT_{TS1} would also contribute to the determination for the height of activation

barrier, while the contribution of INT_{TS1} to $\Delta E_1^{\ddagger}$ is smaller than that of DEFs in all series because of the small absolute value.

Table 2. Deformation/interaction analysis for the radical addition step of 2-cyano-2-propyl radical **1** to dimethyl dicalcogenide $(XMe)_2$ **2**. [a]

	X = S	X = Se	X = Te
$\Delta E_1^{\ddagger}$	58.2	37.6	21.4
$DEF_{RC\ (1)}$	0.2	0.2	0.2
$DEF_{RC\ (2)}$	0.2	0.1	0.1
DEF_{RC}	0.4	0.3	0.3
INT_{RC}	-12.2	-12.8	-12.2
$DEF_{TS1\ (1)}$	18.0	13.1	7.8
$DEF_{TS1\ (2)}$	15.6	5.8	1.0
DEF_{TS1}	33.6	18.9	8.8
INT_{TS1}	12.4	5.9	0.4
INT_{Totall}	24.6	18.7	12.6
BDE[b]	219.5	193.7	169.9

[a]Energies are given in units of kJ/mol. The energies of each fragment were obtained using spin-unrestricted CCSD(T)/6311DZP level of theory. $\Delta E_1^{\ddagger} = DEF_{TS1} + INT_{Totall}$. $INT_{Totall} = INT_{TS1} - INT_{RC}$. [b]BDE: Bond dissociation energy for X-X bond of **2**.

Similarly, the analysis of the activation energy $\Delta E_2^{\ddagger}$ from **TS**s to the products was also carried out (Table 3). $DEF_{TS2\ (3)}$ is very large for all cases, and gradually became larger on going from X = (65.3kJ/mol) to Se (71.1 kJ/mol), and Te (84.0 kJ/mol). It is worth noting that these energy losses are in the opposite order as $\Delta E_2^{\ddagger}$. The C-X bonds in **TS**s are elongated by 18%, 21%, and 21% for X = S, Se, and Te, respectively, as compared with those in **PC**s. On the other hand, θ_b in **PC** are about 33-34° in all cases. Since **TS-Te** has the smallest θ_b among them as previously discussed, the larger bending is needed to transform **TS-Te** to **PC-Te**. Thus, the largest $DEF_{TS2\ (3)}$ for X = Te are due to the largest change of out-of-plane. Most importantly, the $\Delta E_2^{\ddagger}$ have the extremely large differences in interaction energy. In $\Delta E_2^{\ddagger}$, INT_{TS2}s for X = Se (-30.0 kJ/mol) and for X = Te (-72.2 kJ/mol) are rather attractive, while it is slightly repulsive for X = S (+6.4 kJ/mol). Thus, the origin of the differences in $\Delta E_2^{\ddagger}$ are strongly linked to the different INT_{TS2}.

Table 3. Deformation/interaction analysis for the radical dissociation step from transition state to heteroatom compound **3** and heteroatom-centered radical **4**.[a]

	X = S	X = Se	X = Te
$\Delta E_2^{\ddagger}$	76.9	47.8	14.9
$DEF_{TS2\,(3)}$	65.3	71.1	84.0
$DEF_{TS2\,(4)}$	0.0	0.0	0.0
DEF_{TS2}	65.3	71.1	84.0
INT_{TS2}	+6.4	-30.0	-69.1
INT_{Total2}	+11.5	-24.3	-71.1
$DEF_{PC\,(3)}$	0.1	1.1	3.2
$DEF_{PC\,(4)}$	0.0	0.0	0.0
DEF_{PC}	0.1	1.1	3.2
INT_{PC}	-5.1	-5.7	-2.0
BDE[b]	245.0	211.8	176.5

[a]Energies are given in units of kJ/mol. The energies of each fragment were obtained using spin-unrestricted CCSD(T)/6311DZP level of theory. $\Delta E_2^{\ddagger} = DEF_{TS2} + INT_{Total2}$. $INT_{Total2} = INT_{TS2} - INT_{PC}$. [b]BDE: Bond dissociation energy for C-X bond of **3**.

Molecular orbital analysis. To clarify the differences of INT_{TS} on the activation barrier, we carried out the analysis of the energy level for molecular orbitals in the reactants (Figure 4). In all cases, the highest occupied molecular orbitals (HOMOs) and lowest occupied molecular orbitals (LUMOs) in dicalcogenide are n-orbital, namely, lone pair (LP) of chalcogene and antibonding σ* orbital of X-X bonds, respectively. The energy level of the singly occupied molecular orbital (SOMO) of **1** is closer to that of HOMO than LUMO of **2** in all cases. The results suggest that the SOMO-HOMO three electron interaction between **1** and **2** is the dominant interaction in this substitution reaction.

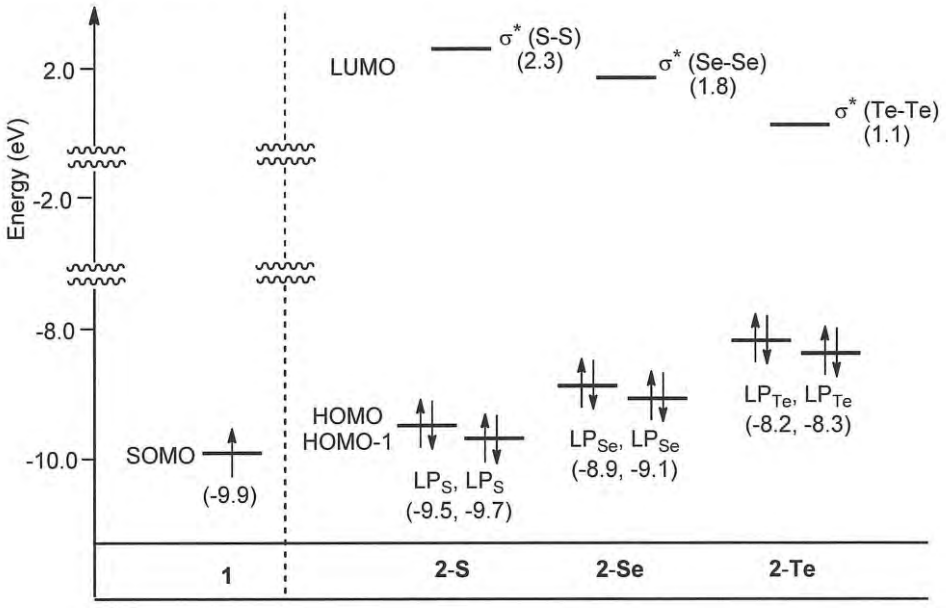

Figure 4. Energy level for Frontier MO of reactants obtained at CCSD(T)/6311DZP// M06-2X/6311DZP level of theory.

Based on the frontier orbital theory, the interaction should be more pronounced as the SOMO-HOMO gap becomes smaller. The SOMO-HOMO energy gap between **1** and **2-S**, **2-Se**, and **2-Te** are estimated to be 0.4, 1.0, and 1.7 eV, respectively. The results suggested that the interaction between **1** and the **2-Te** is the weakest followed by **2-Se** and **2-S**. However, the trend was the opposite order as INT_{TS1} obtained by deformation/interaction analysis. Generally, it have been known that DFT method often give rise to some trouble in the estimation of orbital energy level,[57] while the MO analysis give a good estimation of energy level in some cases. Then, the energy level change by used functions and basis set. ECP was also used toward the heteroatom in the current calculations. At this point, its analysis should therefore be useful only as a qualitative tool for understanding the mode of interaction in the current reaction rather than for quantitative predictions. Selected Kohn-Sham orbitals of each **TS** were shown in Figure 5. The orbital distributions are similar to each other. Kohn-Sham orbitals confirm the existence of three-electron interactions between SOMO and HOMO. The SOMOs contain a nod at the forming C-X bond, which originates from the SOMO of **1** and a LP of **2**. The LUMO, HOMO, and HOMO-1 can be assigned to σ* orbitals character of the breaking X-X bonds, LPs located on heteroatom of **4**, and σ orbitals character of the forming C-X bonds, respectively.

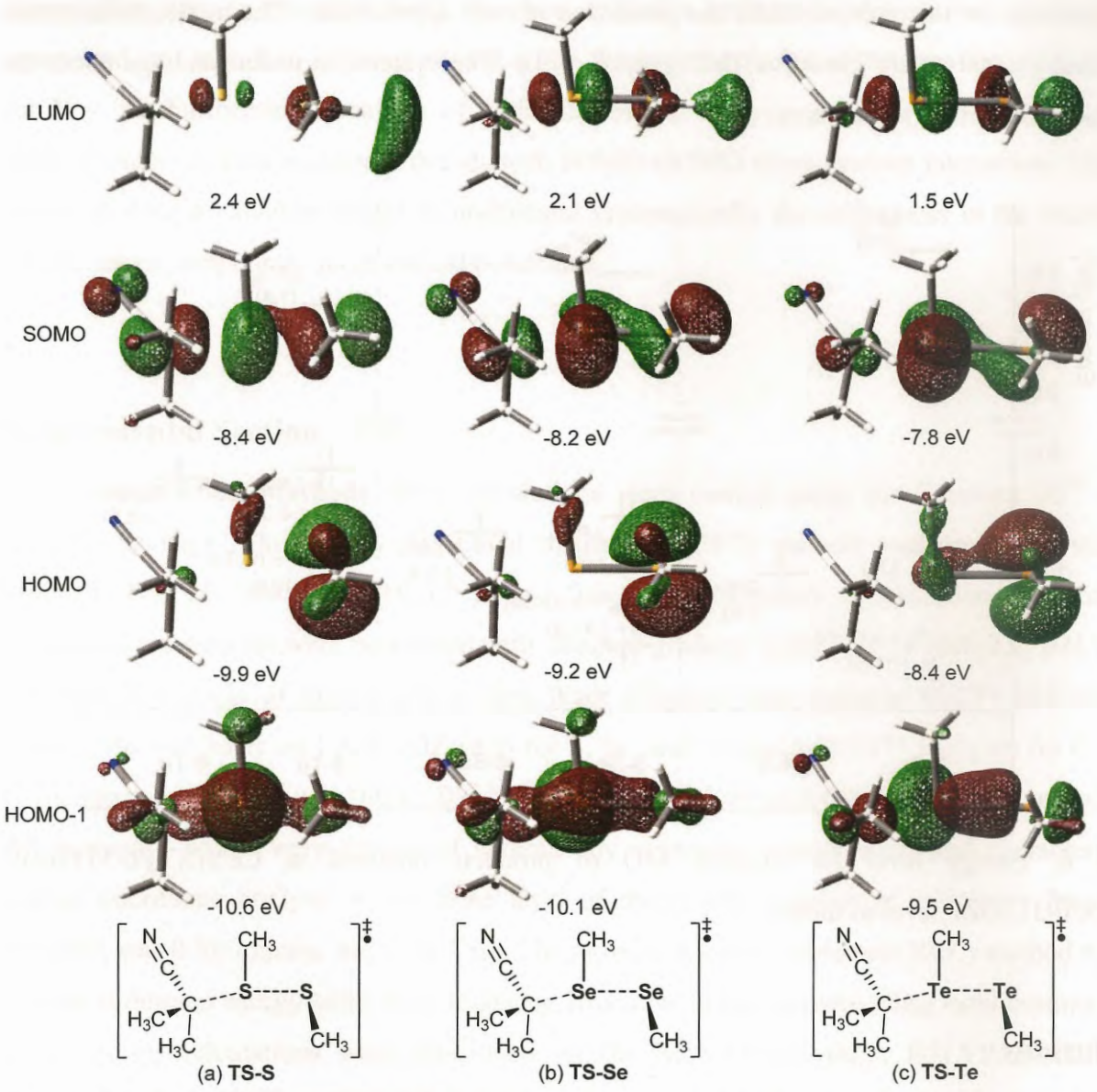

Figure 5. Selected Kohn-Sham orbitals of TSs of the addition reaction of the 2-cyano-2-propyl radical **1** to methyl substituted dicalcogenides **2** [$(XMe)_2$, (a) X = S, (b) X = Se, and (c) X = Te] obtained at CCSD(T)/6311DZP//M06-2X/6311DZP level of theory. Surfaces are drawn at an isodensity value of 0.05. The values indicate the energy level (eV).

Similarly, the energy levels of products were compared (Figure 6). In all cases, the comparisons suggested that the reverse reaction step of **3** with **4** would also take place with three-electron interaction between SOMO and HOMO for **3** and **4**, respectively. Most importantly, the energy level of SOMO for **4** is the highest for X =Te (-8.5 eV), followed by for X = Se (-9.4 eV) and X = S (-9.4 eV). It is worth noting that the higher SOMO energy of **4-Te** would suggest a higher

nucleophilicity for this radical, while the prediction in only approcimate. The nucleophilic nature may affect the extremely attractive $\mathbf{INT}_{TS2}$ for X = Te. The systematic understandings about the interaction are currently underway.

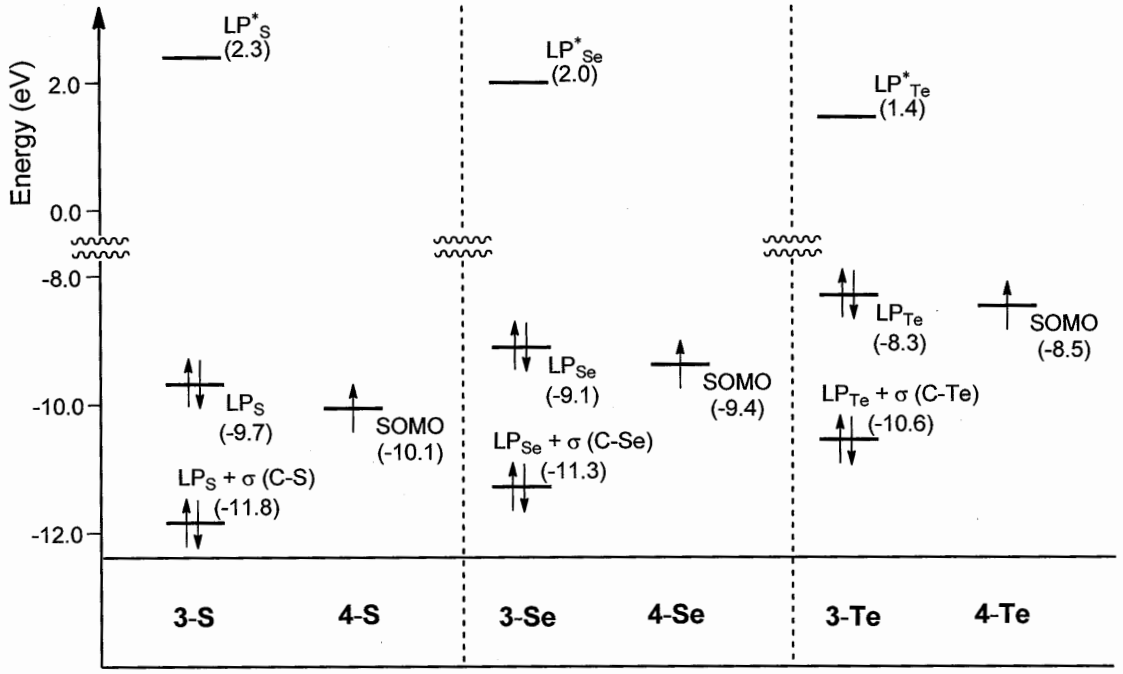

Figure 6. Energy level for Frontier MO of products obtained at CCSD(T)/6-311DZP// M06-2X/6-311DZP level of theory.

Conclusions

In summary, we have examined the reactivities of dimethyl dicalcogenides $(XCH_3)_2$ (X = S, Se, Te) under radical conditions through theoretical study to understand the origin of the similarities and differences in its reactivities. The calculation revealed that the reactivity depend on two factors, kinetic reactivity and thermodyaminc stability. Among them, ditelluride react more readily with carbon-centered radicals than diselenide and disulfide, and the reaction with ditelluride proceeds through very early transition state. Furthermore, the activation energy for the radical dissociation step also became lower in going from X =S to X = Se to X = Te. As the results, the overall cycle is thermodynamically most unfavor for X = Te, followed by X = Se, and S. Deformation/interacrtion analysis revealed that high kinetic reactivity of ditelluride in radical addition step is mainly determined by the low deformation energy, which derived from the lower elongation of Te-Te σ bond in ditelluride and the smaller bending of the attacking carbon-centered radical. In the radical

dissociation step, on the other hand, the more attractive interaction between the organotellurium compound and tellurium-centered radical is the determining factor of the low dissociation energy for X = Te. Furthermore, analysis of molecular orbital analysis gave the important information about interaction; their reaction proceeds with SOMO-HOMO three-electron interaction. This study would provide a valuable insight to understand systematically the differences in the reactivity of diheteroatom compounds under radical conditions.

Experimental Section

Computation Methods. DFT calculations were carried using the Gaussian 03[49] or 09[50] program package. The density functional theoretical (DFT) method was employed using the M06-2X, B3LYP, and BHandHLYP hybrid functional. Geometry optimizations and harmonic vibrational frequencies were performed with standard gradient techniques at M06-2X, B3LYP, and BHandHLYP levels of theory with a Hey-Wadt effective core potential (ECP) and outermost valence electron basis set LANL2DZ-(d,p) for S, Se, and Te and 6-311G** basis set for C, N, and H (denoted as M06-2X/6311DZP, B3LYP/6311DZP, and BHandHLYP/6311DZP, respectively). All stationary points were optimized without any symmetry assumptions, and characterized by normal coordinate analysis at the same level of theory (the number of imaginary frequencies, NIMAG, was 0 for minima and 1 for TSs). The intrinsic reaction coordinate (IRC) method was used to track minimum energy paths from transition structures to the corresponding local minima. Single point energy calculations were performed on the M06-2X/6311DZP, B3LYP/6311DZP, and BHandHLYP/6311DZP minimized geometries by using CCSD(T) method with same basis set (denoted as CCSD(T)/6311DZP//M06-2X/6311DZP, CCSD(T)/6311DZP//B3LYP/6311DZP, and CCSD(T)/6311DZP//BHanHLYP/6311DZP, repectively). Calculated total energies (E, hartrees), zero-point energies (ZPE, hartrees), ezero-point corrected energies (E + ZPE, hartrees), enthalpy at 298.15 K (H, hartrees), entropy at 298.15 K under 1 atomosphere of pressure (S, cal/mol·K), Gibbs free energy at 298.15 K (G, hartrees), imaginary frequencies at the TS (iω, cm^{-1}) and spin-squared expectation values ($<S^2>$) are shown in Table 4 and 5.

Table 4 Calculated total energies (E, hartrees), zero-point energies (ZPE, hartrees), zero-point corrected energies (E + ZPE, hartrees), enthalpy at 298.15 K (H, hartrees), entropy at 298.15 K under 1 atomosphere of pressure (S, cal/mol·K), Gibbs free energy at 298.15 K (G, hartrees), imaginary frequencies at the TS (iω, cm^{-1}) and spin-squared expectation values ($<S^2>$) calculated with different functional related to the S_H2 reactio of dimethyl dichalcogenides $(XMe)_2$ (X = S, Se, and Te) **2** with 2-cyano-2-propyl radical **1**.

Molecular	Calculation Method	E	ZPE	E + ZPE	H	S	G	iω	$<S^2>$
1	M06-2X/6311DZP	-210.687228	0.088895	-210.598334	-210.59099	77.967	-210.628035		0.75012
1	B3LYP/6311DZP	-210.794965	0.087854	-210.707111	-210.699696	78.826	-210.737148		0.75010
1	BHandHLYP/6311DZP	-210.657130	0.090794	-210.566337	-210.559014	78.393	-210.596261		0.75042
2-S	M06-2X/6311DZP	-99.9696531	0.078052	-99.8916011	-99.884365	77.176	-99.921034		
2-S	B3LYP/6311DZP	-100.100374	0.077013	-100.023361	-100.015909	78.434	-100.053176		
2-S	BHandHLYP/6311DZP	-99.9532140	0.079776	-99.8734381	-99.866137	77.795	-99.903100		
RC-S	M06-2X/6311DZP	-310.665738	0.168239	-310.497499	-310.48212	135.209	-310.541509		0.75012
TS-S	M06-2X/6311DZP	-310.647714	0.16902	-310.478694	-310.464705	114.447	-310.519083	342.70	0.75014
TS-S	B3LYP/6311DZP	-310.875683	0.16718	-310.708503	-310.694157	116.836	-310.749669	343.27	0.75017
TS-S	BHandHLYP/6311DZP	-310.584649	0.173017	-310.411632	-310.397581	115.423	-310.452422	459.30	0.75112
PC-S	M06-2X/6311DZP	-310.66290	0.170353	-310.49255	-310.478065	119.108	-310.534657		0.75001
3-S	M06-2X/6311DZP	-260.723469	0.131901	-260.591568	-260.581668	90.887	-260.624851		
3-S	B3LYP/6311DZP	-260.880342	0.130507	-260.749835	-260.739792	91.554	-259.897780		
3-S	BHandHLYP/6311DZP	-260.671303	0.135232	-260.536071	-260.526307	90.303	-260.569213		
4-S	M06-2X/6311DZP	-49.931604	0.036477	-49.895127	-49.891103	59.48	-49.919364		0.75000
4-S	B3LYP/6311DZP	-50.0072197	0.035478	-49.9717417	-49.967609	59.82	-49.996032		0.75000
4-S	BHandHLYP/6311DZP	-49.9364466	0.036844	-49.8996026	-49.895518	59.64	-49.923855		0.75000
2-Se	M06-2X/6311DZP	-98.2025311	0.075575	-98.1269561	-98.118888	85.354	-98.159442		
2-Se	B3LYP/6311DZP	-98.3374649	0.074843	-98.2626219	-98.254356	88.048	-98.296190		
2-Se	BHandHLYP/6311DZP	-98.1841736	0.077565	-98.1066086	-98.098568	85.339	-98.139115		
RC-Se	M06-2X/6311DZP	-308.898850	0.165573	-308.73328	-308.71699	135.209	-308.781232		0.75012

Table 4. Continued.

Molecular	Calculation Method	E	ZPE	E + ZPE	H	S	G	iω	$<S^2>$
TS-Se	M06-2X/6311DZP	-308.888152	0.166912	-308.721240	-308.706494	121.531	-308.764238	209.30	0.750217
TS-Se	B3LYP/6311DZP	-309.119726	0.165112	-308.954614	-308.939484	124.355	-308.998569	207.68	0.750188
TS-Se	BHandHLYP/6311DZP	-308.823228	0.170854	-308.652374	-308.637554	122.887	-308.695941	293.78	0.751247
PC-Se	M06-2X/6311DZP	-308.898886	0.168541	-308.730345	-308.715402	122.801	-308.773749		0.750010
PC-Se	B3LYP/6311DZP	-309.126122	0.165941	-308.960181	-308.944241	135.865	-309.008795		0.750013
PC-Se	BHandHLYP/6311DZP	-308.837280	0.17188	-308.665400	-308.649841	135.438	-308.714192		0.750020
3-Se	M06-2X/6311DZP	-259.833410	0.130842	-259.702568	-259.692318	94.673	-259.7373		
3-Se	B3LYP/6311DZP	-259.992409	0.129339	-259.863070	-259.852666	94.744	-259.821642		
3-Se	BHandHLYP/6311DZP	-259.779370	0.133951	-259.645419	-259.635285	93.757	-259.679832		
4-Se	M06-2X/6311DZP	-49.0532279	0.037015	-49.0162129	-49.012156	62.37	-49.04179		0.750006
4-Se	B3LYP/6311DZP	-49.1295679	0.035011	-49.0945569	-49.090307	62.967	-49.120224		0.750004
4-Se	BHandHLYP/6311DZP	-49.0558905	0.036293	-49.0195975	-49.015403	62.753	-49.045219		0.750007
2-Te	M06-2X/6311DZP	-95.8504523	0.073756	-95.7766963	-95.767979	92.327	-95.811846		
2-Te	B3LYP/6311DZP	-95.9838968	0.073436	-95.9104608	-95.901758	91.748	-95.94535		
2-Te	BHandHLYP/6311DZP	-95.8275580	0.075899	-95.7516589	-95.743099	91.039	-95.786354		
RC-Te	M06-2X/6311DZP	-306.547227	0.164554	-306.382673	-306.366143	137.72	-306.431579		0.750170
TS-Te	M06-2X/6311DZP	-306.541112	0.164651	-306.376461	-306.360898	129.111	-306.422242	181.84	0.750255
TS-Te	B3LYP/6311DZP	-306.770725	0.163453	-306.607272	-306.591560	131.296	-306.653943	130.75	0.750190
TS-Te	BHandHLYP/6311DZP	-306.471736	0.169091	-306.302645	-306.287268	128.986	-306.348553	196.33	0.751181
PC-Te	M06-2X/6311DZP	-306.547074	0.166281	-306.380793	-306.365990	124.33	-306.425063		0.750026
PC-Te	B3LYP/6311DZP	-306.772306	0.164611	-306.607695	-306.591585	133.195	-306.65487		0.750035
PC-Te	BHandHLYP/6311DZP	-306.476497	0.170241	-306.306256	-306.290314	136.277	-306.355064		0.750068
3-Te	M06-2X/6311DZP	-258.650084	0.129274	-258.520810	-258.510097	99.878	-258.557552		
3-Te	B3LYP/6311DZP	-258.807865	0.128302	-258.679563	-258.668850	98.076	-258.715448		
3-Te	BHandHLYP/6311DZP	-258.592125	0.132786	-258.459339	-258.448879	96.911	-258.494924		
4-Te	M06-2X/6311DZP	-47.8815950	0.035994	-47.845601	-47.841448	64.38	-47.872037		0.750004
4-Te	B3LYP/6311DZP	-47.9565184	0.035185	-47.921333	-47.917112	64.61	-47.947811		0.750004
4-Te	BHandHLYP/6311DZP	-47.8811130	0.03593	-47.845183	-47.840924	64.685	-47.871658		0.750007

Table 5. Calculated total energies (E, hartrees) by single point energy calculations on the M06-2X-, B3LYP-, and BHandHLYP-minimized geometries using CCSD(T) method.

Molecular	Calculation Method	E	Molecular	Calculation Method	E
1	CCSD(T)/6311DZP//M06-2X/6311DZP	-210.189373	**PC-Se**	CCSD(T)/6311DZP//M06-2X/6311DZP	-308.11146
1	CCSD(T)/6311DZP//B3LYP/6311DZP	-210.189552	**PC-Se**	CCSD(T)/6311DZP//B3LYP/6311DZP	-308.11222
1	CCSD(T)/6311DZP//BHandHLYP/6311	-210.189373	**PC-Se**	CCSD(T)/6311DZP//BHandHLYP/6311DZP	-308.11105
2-S	CCSD(T)/6311DZP//M06-2X/6311DZP	-99.702335	**3-Se**	CCSD(T)/6311DZP//M06-2X/6311DZP	-259.18987
2-S	CCSD(T)/6311DZP//B3LYP/6311DZP	-99.702335	**3-Se**	CCSD(T)/6311DZP//B3LYP/6311DZP	-259.18977
2-S	CCSD(T)/6311DZP//BHandHLYP/6311	-99.701833	**3-Se**	CCSD(T)/6311DZP//BHandHLYP/6311DZP	-259.18847
RC-S	CCSD(T)/6311DZP//M06-2X/6311DZ	-309.896204	**4-Se**	CCSD(T)/6311DZP//M06-2X/6311DZP	-48.919836
TS-S	CCSD(T)/6311DZP//M06-2X/6311DZP	-309.874050	**4-Se**	CCSD(T)/6311DZP//B3LYP/6311DZP	-48.919843
TS-S	CCSD(T)/6311DZP//B3LYP/6311DZP	-309.873362	**4-Se**	CCSD(T)/6311DZP//BHandHLYP/6311DZP	-48.919647
TS-S	CCSD(T)/6311DZP//BHandHLYP/6311	-309.872554	**2-Te**	CCSD(T)/6311DZP//M06-2X/6311DZP	-95.545808
PC-S	CCSD(T)/6311DZP//M06-2X/6311DZ	-309.903346	**2-Te**	CCSD(T)/6311DZP//B3LYP/6311DZP	-95.545656
3-S	CCSD(T)/6311DZP//M06-2X/6311DZP	-260.092063	**2-Te**	CCSD(T)/6311DZP//BHandHLYP/6311DZP	-95.545311
3-S	CCSD(T)/6311DZP//B3LYP/6311DZP	-260.091939	**RC-Te**	CCSD(T)/6311DZP//M06-2X/6311DZP	-305.73970
3-S	CCSD(T)/6311DZP//BHandHLYP/6311	-260.090656	**TS-Te**	CCSD(T)/6311DZP//M06-2X/6311DZP	-305.73156
4-S	CCSD(T)/6311DZP//M06-2X/6311DZP	-49.8093667	**TS-Te**	CCSD(T)/6311DZP//B3LYP/6311DZP	-305.73080
4-S	CCSD(T)/6311DZP//B3LYP/6311DZP	-49.8093927	**TS-Te**	CCSD(T)/6311DZP//BHandHLYP/6311DZP	-305.73156
4-S	CCSD(T)/6311DZP//BHandHLYP/6311	-49.8091732	**PC-Te**	CCSD(T)/6311DZP//M06-2X/6311DZP	-305.73725
2-Se	CCSD(T)/6311DZP//M06-2X/6311DZP	-97.9134604	**PC-Te**	CCSD(T)/6311DZP//B3LYP/6311DZP	-305.73750
2-Se	CCSD(T)/6311DZP//B3LYP/6311DZP	-97.9130955	**PC-Te**	CCSD(T)/6311DZP//BHandHLYP/6311DZP	-305.73886
2-Se	CCSD(T)/6311DZP//BHandHLYP/6311	-97.9129831	**3-Te**	CCSD(T)/6311DZP//M06-2X/6311DZP	-257.99714
RC-Se	CCSD(T)/6311DZP//M06-2X/6311DZ	-308.107594	**3-Te**	CCSD(T)/6311DZP//B3LYP/6311DZP	-257.99712
TS-Se	CCSD(T)/6311DZP//M06-2X/6311DZP	-308.093260	**3-Te**	CCSD(T)/6311DZP//BHandHLYP/6311DZP	-257.99575
TS-Se	CCSD(T)/6311DZP//B3LYP/6311DZP	-308.092655	**4-Te**	CCSD(T)/6311DZP//M06-2X/6311DZP	-47.740547
TS-Se	CCSD(T)/6311DZP//BHandHLYP/6311	-308.091748	**4-Te**	CCSD(T)/6311DZP//B3LYP/6311DZP	-47.740600
			4-Te	CCSD(T)/6311DZP//BHandHLYP/6311DZP	-47.740361

Cartesian Coordinates of Stationary Point.

1 (M06-2X/6311DZP)

C	0.000000	0.000000	-0.308576
C	0.000000	1.290472	-1.062711
H	-0.000227	2.152243	-0.397825
H	0.880048	1.348885	-1.712638
H	-0.879794	1.348678	-1.712994
C	0.000000	-1.290472	-1.062711
H	0.000227	-2.152243	-0.397825
H	-0.880048	-1.348885	-1.712638
H	0.879794	-1.348678	-1.712994
C	0.000000	0.000000	1.086506
N	0.000000	0.000000	2.247410

2-S (M06-2X/6311DZP)

S	-0.460309	0.927751	-0.505461
S	0.460309	-0.927751	-0.505461
C	0.460309	1.798751	0.814467
H	1.520132	1.834368	0.570553
H	0.057088	2.811873	0.851868
H	0.306679	1.315557	1.778146
C	-0.460309	-1.798751	0.814467
H	-0.306679	-1.315557	1.778146
H	-1.520132	-1.834368	0.570553
H	-0.057088	-2.811873	0.851868

RC-S (UM06-2X/6311DZP)

S	-0.805345	-0.760177	-0.643664
C	-0.469198	-1.67214	0.906662
S	-2.746631	-0.098443	-0.344382
C	-2.475984	1.44061	0.607674
H	-3.459689	1.888954	0.755698
H	-2.032825	1.224741	1.579641
H	-1.846229	2.125736	0.041735
H	0.506456	-2.143782	0.778615
H	-0.4382	-0.992656	1.758723
H	-1.232218	-2.433287	1.05588
C	2.164824	0.72042	0.02495
C	1.625948	1.297098	1.293352
H	1.81425	0.650462	2.149568
H	2.071705	2.278074	1.486139
H	0.542903	1.446323	1.194583
C	2.653737	-0.587016	0.008477
N	3.038457	-1.682894	0.00574
C	2.082571	1.515128	-1.236171
H	1.030836	1.708369	-1.478115
H	2.574093	2.484927	-1.107028
H	2.539952	0.995721	-2.076531

TS-S (UM06-2X/6311 DZP)

S	-0.338055	-0.34053	-0.507364
C	-0.288981	-1.647387	0.770289
S	-2.550747	-0.168953	-0.671958
C	-2.889621	0.74191	0.873104
H	-3.963442	0.93038	0.896088
H	-2.616228	0.15402	1.74903
H	-2.361698	1.694667	0.875883
H	0.730935	-2.026241	0.833697
H	-0.611869	-1.260315	1.736646
H	-0.95224	-2.44546	0.44651
C	1.580675	0.585139	0.042729
C	1.426467	1.081584	1.463163
H	1.304112	0.259586	2.16973
H	2.311733	1.653222	1.761159
H	0.55544	1.737754	1.526598
C	2.501786	-0.501067	-0.107532
N	3.200277	-1.415067	-0.214701
C	1.705514	1.663193	-1.010851
H	0.843463	2.332197	-0.954046
H	2.611986	2.252569	-0.842126
H	1.751659	1.234575	-2.012525

PC-S (UM06-2X/6311DZP)

S	0.102011	-0.55486	-0.783826
C	-0.087115	-1.78955	0.539413
S	-3.067448	-0.229322	-0.442687
C	-2.783473	0.911703	0.937764
H	-3.750864	1.056822	1.427486
H	-2.09095	0.494936	1.670028
H	-2.431815	1.879491	0.582937
H	0.873288	-2.256649	0.759505
H	-0.523472	-1.353906	1.438013
H	-0.776385	-2.536259	0.148444
C	1.433964	0.527064	-0.078015
C	0.969513	1.258867	1.184317
H	0.68301	0.559795	1.970951
H	1.776806	1.888157	1.566563
H	0.113538	1.887816	0.935356
C	2.585658	-0.323009	0.242189
N	3.472931	-0.999494	0.518742
C	1.809942	1.519189	-1.184879

H	0.932286	2.112489	-1.449449
H	2.594688	2.188933	-0.828791
H	2.16541	0.996159	-2.072754

3-S (RM06-2X/6311DZP)

C	2.112279	0.562479	0.302438
H	3.110795	0.477036	-0.124756
H	1.726718	1.563624	0.10647
H	2.169027	0.374002	1.373539
S	1.097086	-0.686661	-0.550219
C	-0.589966	-0.271679	0.093863
C	-1.577274	-1.143262	-0.691401
H	-1.348642	-2.195464	-0.510987
H	-2.595601	-0.941083	-0.354581
H	-1.510675	-0.942307	-1.760726
C	-0.85026	1.1462	-0.180046
N	-1.031798	2.265648	-0.367947
C	-0.705689	-0.529921	1.599644
H	-1.717349	-0.296565	1.940602
H	-0.493198	-1.581443	1.797371
H	-0.006407	0.086344	2.165208

4-S (UM06-2X/6-311DZP)

C	-1.114428	0.000051	-0.008336
S	0.69565	0.000006	-0.001866
H	-1.508619	-0.897085	-0.483072
H	-1.426495	-0.003058	1.04106
H	-1.508717	0.899737	-0.478107

2-Se (RM06-2X/6311DZP)

Se	1.134656	-0.279688	-0.318133
Se	-1.134656	0.279688	-0.318133
C	1.134656	-1.624588	1.117804
H	0.46909	-2.441652	0.852115
H	2.15906	-1.98921	1.200537
H	0.830567	-1.168452	2.057061
C	-1.134656	1.624588	1.117804
H	-0.830567	1.168452	2.057061
H	-0.46909	2.441652	0.852115
H	-2.15906	1.98921	1.200537

RC-Se (UM06-2X/6311DZP)

Se	-0.249301	-0.752163	-0.471191
Se	-2.408502	0.073413	-0.110932
C	0.134631	-1.44845	1.327876
H	-0.646576	-2.149541	1.609888
H	1.096479	-1.958003	1.261735
H	0.193633	-0.630344	2.043984
C	-1.955326	1.8197	0.673863
H	-1.438294	1.681715	1.621425
H	-1.344336	2.387879	-0.024025
H	-2.898622	2.338922	0.84664
C	2.809067	0.822433	-0.022134
C	2.760606	1.450373	-1.376022
H	3.350769	2.372769	-1.389014
H	3.135051	0.781632	-2.149237
H	1.725738	1.71864	-1.618018
C	3.233938	-0.498707	0.130469
N	3.56399	-1.604043	0.266574
C	2.307452	1.585318	1.159969
H	2.793032	2.564574	1.217683
H	1.229933	1.761763	1.046791
H	2.478352	1.051808	2.094179

TS-Se (UM06-2X/6311DZP)

Se	0.073678	-0.355945	-0.374017
Se	-2.357637	-0.115456	-0.323814
C	0.217998	-1.438236	1.255735
H	-0.476776	-2.268104	1.158265
H	1.239287	-1.812705	1.318079
H	-0.028336	-0.837878	2.129844
C	-2.443236	1.209837	1.124776
H	-2.053004	0.790029	2.04985
H	-1.886741	2.100155	0.840545
H	-3.495053	1.462169	1.257678
C	2.23446	0.660277	-0.018575
C	2.36166	1.51387	-1.25712
H	3.297834	2.082142	-1.230096
H	2.355447	0.907554	-2.163679
H	1.53311	2.224296	-1.302227
C	3.049652	-0.50825	0.009059
N	3.665222	-1.486769	0.050477
C	2.118172	1.397389	1.293727
H	3.042017	1.950051	1.499937
H	1.294707	2.112853	1.242378
H	1.943301	0.71514	2.126732

PC-Se (UM06-2X/6311DZP)

Se	-0.544093	0.633263	-0.805113
Se	2.348723	-0.44622	-0.185394

C	-0.858979	2.136564	0.400354
H	-0.546418	3.030877	-0.136505
H	-1.925241	2.198699	0.61926
H	-0.275435	2.034665	1.313637
C	2.367954	0.806553	1.326783
H	2.261543	1.829929	0.970993
H	1.586626	0.566397	2.047196
H	3.339309	0.702903	1.811392
C	-1.511814	-0.771541	0.241485
C	-1.41701	-2.061007	-0.58033
H	-1.952508	-2.860924	-0.064788
H	-1.849783	-1.933846	-1.573339
H	-0.366974	-2.346895	-0.674377
C	-2.898093	-0.316325	0.343763
N	-3.976766	0.066973	0.453784
C	-0.922429	-0.960149	1.641165
H	-1.492188	-1.728222	2.170589
H	0.115565	-1.285514	1.550826
H	-0.972319	-0.040915	2.226524

3-Se (RM06-2X/6311DZP)

Se	1.052452	-0.418741	-0.267085
C	-0.893633	-0.276164	0.157684
C	1.624894	1.282115	0.509782
H	2.675949	1.395564	0.248047
H	1.051493	2.09616	0.068061
H	1.522799	1.273655	1.592911
C	-1.590349	-1.423845	-0.581603
H	-1.191296	-2.377847	-0.229975
H	-2.662309	-1.398298	-0.374227
H	-1.438766	-1.34946	-1.658671
C	-1.359431	1.012314	-0.352904
N	-1.711387	2.042004	-0.72516
C	-1.13969	-0.354647	1.666844
H	-0.630848	0.451509	2.196099
H	-2.210493	-0.276468	1.874232
H	-0.770938	-1.310276	2.041711

4-Se (UM06-2X/6311DZP)

Se	-0.433937	0.000000	-0.000728
C	1.520403	0.000003	-0.007038
H	1.900783	0.898582	-0.486507
H	1.829863	-0.000371	1.040596
H	1.900809	-0.898229	-0.487127

2-Te (RM06-2X/6311DZP)

Te	1.324818	-0.268552	-0.241656
Te	-1.324818	0.268552	-0.241656
C	1.324818	-1.760872	1.312982
H	0.660953	-2.573803	1.031597
H	2.34647	-2.130661	1.403828
H	1.009456	-1.31508	2.252788
C	-1.324818	1.760872	1.312982
H	-1.009456	1.31508	2.252788
H	-0.660953	2.573803	1.031597
H	-2.34647	2.130661	1.403828

RC-Te (UM06-2X/6311DZP)

C	0.686794	-1.221007	1.655316
H	-0.101722	-1.787725	2.143805
H	1.617284	-1.788409	1.651954
H	0.833618	-0.264854	2.153671
C	-1.66486	2.219992	0.310856
H	-1.12992	2.315082	1.252967
H	-1.035547	2.517321	-0.524896
H	-2.560994	2.840859	0.334167
C	3.190787	1.055368	-0.026383
C	3.177621	1.612218	-1.412219
H	3.780542	2.525536	-1.459089
H	3.560355	0.900573	-2.141932
H	2.152781	1.882192	-1.691204
Te	0.140446	-0.905956	-0.40318
Te	-2.301213	0.179612	0.024894
C	3.62908	-0.249835	0.207057
N	3.967968	-1.343089	0.404793
C	2.645505	1.874149	1.097665
H	3.075692	2.880115	1.079982
H	1.559423	1.983666	0.975357
H	2.843022	1.421807	2.06879

TS-Te (UM06-2X/6311DZP)

C	0.634519	-1.190174	1.63745
H	-0.081248	-1.998508	1.763323
H	1.650712	-1.577162	1.709002
H	0.462461	-0.415113	2.381611
C	-2.328428	1.721615	1.004284
H	-1.864311	1.539314	1.97054
H	-1.790066	2.491108	0.456518
H	-3.363507	2.030681	1.149576

C	2.85634	0.740006	-0.067463
C	3.027974	1.366589	-1.42598
H	4.000856	1.869036	-1.489435
H	2.980271	0.623142	-2.22277
H	2.2507	2.115231	-1.593193
Te	0.375689	-0.382476	-0.334956
Te	-2.360265	-0.093583	-0.153937
C	3.533403	-0.482795	0.160698
N	4.034611	-1.508045	0.361347
C	2.716844	1.663567	1.113623
H	3.655126	2.208143	1.277984
H	1.928132	2.394749	0.925736
H	2.482668	1.117912	2.02848

PC-Te (UM06-2X/6311DZP)

C	-0.553437	1.625114	-1.085994
H	0.20304	1.706114	-1.863773
H	-1.537609	1.857492	-1.491688
H	-0.307598	2.288101	-0.258673
C	2.233606	1.626954	1.077638
H	2.173805	2.462072	0.383995
H	1.336254	1.578704	1.694234
H	3.101262	1.74273	1.724282
C	-2.522888	-0.110431	0.656906
C	-2.956078	-1.490432	1.153666
H	-3.902429	-1.413006	1.695953
H	-3.090516	-2.191681	0.328739
H	-2.203122	-1.890615	1.837279
Te	-0.565795	-0.404746	-0.429606
Te	2.444697	-0.231	0.006967
C	-3.445225	0.405956	-0.336622
N	-4.14907	0.840916	-1.138923
C	-2.343355	0.88444	1.803482
H	-3.291099	1.020991	2.333242
H	-1.602356	0.501161	2.508212
H	-2.014756	1.860671	1.443434

3-Te (RM06-2X/6311DZP)

C	1.259121	1.686315	0.553836
Te	0.976033	-0.309659	-0.157355
H	2.285829	1.96816	0.323263
H	0.574635	2.346643	0.022772
H	1.100959	1.741062	1.628177
C	-1.19098	-0.29104	0.172998
C	-1.77451	-1.537116	-0.504063
1	-2.856025	-1.568864	-0.349165
1	-1.577266	-1.539555	-1.576534
1	-1.339979	-2.436437	-0.060967
C	-1.696921	0.920182	-0.461462
N	-2.084184	1.897593	-0.929869
C	-1.519381	-0.263237	1.669901
H	-1.089619	0.612562	2.157844
H	-2.604094	-0.234843	1.811425
H	-1.122822	-1.160256	2.147485

4-Te (UM06-2X/6311DZP)

Te	-0.333995	0.000001	-0.000335
C	1.811011	0.000027	-0.005817
H	2.18544	-0.895994	-0.494187
H	2.130643	-0.001984	1.037424
H	2.185583	0.897743	-0.49093

1 (UB3LYP/6311DZP)

C	0.000000	0.000000	-0.306733
C	0.000000	1.294975	-1.061637
H	-0.000264	2.157944	-0.396386
H	0.879860	1.360611	-1.714032
H	-0.879567	1.360371	-1.714446
C	0.000000	-1.294975	-1.061637
H	0.000264	-2.157944	-0.396386
H	-0.879860	-1.360611	-1.714032
H	0.879567	-1.360371	-1.714446
C	0.000000	0.000000	1.080825
N	0.000000	0.000000	2.249260

2-S (RB3LYP/6311 DZP)

S	-0.464826	0.937628	-0.494846
S	0.464826	-0.937628	-0.494846
C	0.464826	1.864555	0.798546
H	1.525815	1.893732	0.55582
H	0.059381	2.878972	0.785753
H	0.309906	1.428297	1.784685
C	-0.464826	-1.864555	0.798546
H	-0.309906	-1.428297	1.784685
H	-1.525815	-1.893732	0.55582
H	-0.059381	-2.878972	0.785753

TS-S (UB3LYP/6311DZP)

S	0.325325	0.302468	-0.474448
C	0.289984	1.730435	0.684942

S	2.610752	0.076167	-0.707413
C	3.089514	-0.629146	0.919232
H	4.164215	-0.815836	0.867687
H	2.892134	0.066965	1.734604
H	2.578179	-1.57521	1.095656
H	-0.701966	2.179054	0.641573
H	0.522435	1.420969	1.70374
H	1.027229	2.449059	0.334382
C	-1.651704	-0.586486	0.068716
C	-1.546918	-1.067179	1.504963
H	-1.392994	-0.242757	2.202736
H	-2.469644	-1.582344	1.798101
H	-0.718346	-1.77131	1.602848
C	-2.542118	0.513664	-0.12268
N	-3.233405	1.434451	-0.265176
C	-1.775006	-1.682739	-0.974964
H	-0.939814	-2.381504	-0.885665
H	-2.70477	-2.242827	-0.824447
H	-1.782572	-1.274857	-1.986475

3-S (RB3LYP/6311DZP)

C	2.15477	0.56848	0.304094
H	3.154601	0.444359	-0.113463
H	1.805259	1.579121	0.091508
H	2.197889	0.394659	1.379132
S	1.111612	-0.67347	-0.549074
C	-0.603913	-0.268335	0.096929
C	-1.572528	-1.155678	-0.708204
H	-1.332955	-2.207241	-0.535911
H	-2.599454	-0.974485	-0.383131
H	-1.502249	-0.948139	-1.77649
C	-0.874579	1.145439	-0.174818
N	-1.071211	2.266661	-0.364687
C	-0.725228	-0.544766	1.605993
H	-1.739866	-0.322248	1.948594
H	-0.50798	-1.596545	1.799005
H	-0.03369	0.068582	2.184773

4-S (UB3LYP/6311DZP)

C	-1.119989	0.000042	-0.008315
S	0.69928	0.000007	-0.001867
H	-1.516941	-0.897891	-0.482638
H	-1.434463	-0.0022	1.041503
H	-1.517145	0.899719	-0.479108

2-Se (RB3LYP/6311DZP)

Se	1.117425	-0.309496	-0.382341
Se	-1.117425	-0.309496	0.382341
C	1.913779	1.08882	0.773937
H	1.775453	0.824854	1.819725
H	2.978514	1.105836	0.533091
H	1.472814	2.059246	0.557136
C	-1.913779	1.08882	-0.773937
H	-1.472813	2.059246	-0.557136
H	-1.775453	0.824854	-1.819725
H	-2.978514	1.105837	-0.533091

TS-Se (UB3LYP/6311DZP)

Se	0.115622	-0.284756	-0.371131
Se	-2.411688	-0.030689	-0.381297
C	0.235569	-1.67967	1.023404
H	-0.532861	-2.415969	0.801875
H	1.22181	-2.135717	0.95231
H	0.078624	-1.251029	2.011625
C	-2.672116	0.886392	1.351183
H	-2.357478	0.251756	2.177435
H	-2.128527	1.82901	1.359263
H	-3.741492	1.085157	1.433935
C	2.275018	0.656034	0.048009
C	2.421644	1.596434	-1.135076
H	3.37582	2.133465	-1.073159
H	2.397602	1.059929	-2.084592
H	1.618747	2.337488	-1.130604
C	3.096875	-0.506411	-0.007619
N	3.734225	-1.476406	-0.037039
C	2.208997	1.323699	1.409315
H	3.158601	1.82836	1.628031
H	1.415579	2.07339	1.421221
H	2.0243	0.605268	2.209191

PC-Se (UB3LYP/6311DZP)

Se	0.460271	-0.435447	-0.551427
Se	-2.681395	0.071125	-0.354275
C	0.496144	-1.846679	0.816108
H	-0.308997	-2.528575	0.546342
H	1.452598	-2.36564	0.779973
H	0.310001	-1.43867	1.808084
C	-2.790671	0.527315	1.562187
H	-2.331694	-0.243891	2.178537
H	-2.327771	1.494896	1.747832
H	-3.85271	0.592207	1.806487

C	2.050119	0.676969	0.080189
C	2.29632	1.718598	-1.025139
H	3.139504	2.357275	-0.749426
H	2.521664	1.242576	-1.980224
H	1.412013	2.348648	-1.144551
C	3.182342	-0.234166	0.193043
N	4.070787	-0.963162	0.307138
C	1.756447	1.344382	1.432563
H	2.616234	1.944835	1.745325
H	0.887657	1.997743	1.338188
H	1.560017	0.609151	2.213633

3-Se (RB3LYP/6311DZP)

Se	1.055811	-0.426258	-0.266451
C	-0.918375	-0.264574	0.159407
C	1.689255	1.270601	0.505796
H	2.744567	1.33906	0.241528
H	1.148774	2.104425	0.060255
H	1.587744	1.273351	1.589732
C	-1.613491	-1.411406	-0.596122
H	-1.220257	-2.371614	-0.254136
H	-2.687971	-1.389431	-0.396258
H	-1.459642	-1.330343	-1.672764
C	-1.369606	1.027687	-0.346918
N	-1.720066	2.063143	-0.71869
C	-1.166444	-0.358425	1.673994
H	-0.654111	0.437068	2.216254
H	-2.237346	-0.275153	1.884845
H	-0.806882	-1.319873	2.043752

4-Se (UB3LYP/6311DZP)

Se	-0.436312	0	-0.000715
C	1.529078	0.000002	-0.006808
H	1.909971	0.898979	-0.487822
H	1.840221	-0.000153	1.041052
H	1.909957	-0.898848	-0.488069

2-Te (RB3LYP/6311DZP)

Te	1.324966	-0.320678	-0.238193
Te	-1.324966	0.320678	-0.238193
C	1.324966	-1.859488	1.295927
H	0.614145	-2.63695	1.027545
H	2.334735	-2.272323	1.321925
H	1.077737	-1.424401	2.261001
C	-1.324966	1.859488	1.295927
H	-1.077737	1.424401	2.261001
H	-0.614145	2.63695	1.027545
H	-2.334735	2.272323	1.321925

TS-Te (UB3LYP/6311DZP)

C	0.651626	-1.406374	1.543106
H	-0.097066	-2.194735	1.551974
H	1.652174	-1.83544	1.563412
H	0.501244	-0.72962	2.381464
C	-2.512335	1.472867	1.310343
H	-2.192201	1.077766	2.271517
H	-1.894914	2.31749	1.013051
H	-3.555223	1.785092	1.368843
C	2.795438	0.726099	-0.045536
C	3.006978	1.407244	-1.386768
H	3.984092	1.906501	-1.406033
H	2.979874	0.69749	-2.215238
H	2.241237	2.168962	-1.552849
Te	0.440282	-0.339453	-0.324785
Te	-2.407576	-0.068143	-0.214693
C	3.561314	-0.456347	0.153345
N	4.150968	-1.441196	0.333057
C	2.735905	1.654796	1.154594
H	3.705206	2.151421	1.294662
H	1.981199	2.428435	0.999418
H	2.503327	1.12031	2.076721

PC-Te (UB3LYP/6311DZP)

C	-0.649637	2.029876	-0.227803
H	0.169427	2.439937	-0.814544
H	-1.604174	2.39638	-0.601357
H	-0.522731	2.280464	0.823353
C	2.576954	0.819292	1.757032
H	2.050287	1.768708	1.691894
H	2.144188	0.189007	2.530774
H	3.627643	1.000098	1.983535
C	-2.641674	-0.434203	0.5268
Te	-0.597247	-0.104914	-0.507272
Te	2.51238	-0.219486	-0.14615
C	-2.533524	-0.126846	2.025419
H	-1.78803	-0.777086	2.487464
H	-2.252606	0.911066	2.211014
H	-3.497284	-0.304162	2.515809
C	-3.548552	0.475125	-0.136892
N	-4.252942	1.227142	-0.664212
C	-3.008548	-1.899553	0.256142

H	-3.091046	-2.106692	-0.812111
H	-2.252564	-2.563131	0.683955
H	-3.969545	-2.137911	0.723467

3-Te (RB3LYP/6311DZP)

C	1.355737	1.68177	0.540075
Te	0.978101	-0.323629	-0.154257
H	2.39689	1.901342	0.303748
H	0.70654	2.370139	0.001715
H	1.201847	1.754974	1.614413
C	-1.227308	-0.272733	0.171477
C	-1.814485	-1.504076	-0.542404
H	-2.898699	-1.533358	-0.398166
H	-1.611612	-1.484912	-1.613894
H	-1.3933	-2.419889	-0.120165
C	-1.70586	0.955976	-0.442816
N	-2.084916	1.94699	-0.900464
C	-1.560866	-0.281536	1.673483
H	-2.646838	-0.248452	1.813956
H	-1.175808	-1.192872	2.133743
H	-1.129182	0.576396	2.190402

4-Te (UB3LYP/6311DZP)

Te	-0.336143	0.000001	-0.000332
C	1.824371	0.000014	-0.005442
H	2.1956	-0.897387	-0.495274
H	2.14191	-0.00101	1.038799
H	2.195686	0.898274	-0.493617

1 (UBHandHLYP/6311DZP)

C	0.000000	0.000000	-0.305671
C	0.000000	1.288917	-1.056335
H	-0.000248	2.144824	-0.393886
H	0.874925	1.352613	-1.701802
H	-0.874653	1.352388	-1.702188
C	0.000000	-1.288917	-1.056335
H	0.000248	-2.144824	-0.393886
H	-0.874925	-1.352613	-1.701802
H	0.874653	-1.352388	-1.702188
C	0.000000	0.000000	1.078777
N	0.000000	0.000000	2.233306

2-S (RBHandHLYP/6311DZP)

S	-0.460485	0.926973	-0.492531
S	0.460485	-0.926973	-0.492531
C	0.460485	1.832392	0.793874
H	1.513502	1.866107	0.550345
H	0.057376	2.839444	0.798572
H	0.312757	1.385931	1.768344
C	-0.460485	-1.832392	0.793874
H	-0.312757	-1.385931	1.768344
H	-1.513502	-1.866107	0.550345
H	-0.057376	-2.839444	0.798572

TS-S (UBHandHLYP/6311DZP)

S	-0.330698	-0.28732	-0.43197
C	-0.282504	-1.689248	0.731599
S	-2.588748	-0.137349	-0.693192
C	-3.066125	0.691377	0.853951
H	-4.137852	0.848205	0.800854
H	-2.845192	0.079034	1.718967
H	-2.577001	1.652713	0.94006
H	0.709854	-2.119698	0.707765
H	-0.531554	-1.374641	1.736806
H	-0.996581	-2.421996	0.386061
C	1.628178	0.576737	0.05563
C	1.561518	1.057768	1.484622
H	1.413313	0.2411	2.181244
H	2.489825	1.559189	1.753483
H	0.747696	1.765349	1.59658
C	2.520548	-0.519473	-0.147584
N	3.208145	-1.4234	-0.295976
C	1.746359	1.665171	-0.983479
H	0.926257	2.367659	-0.877908
H	2.679269	2.208908	-0.850491
H	1.728239	1.258689	-1.987433

3-S (RBHandHLYP/6311DZP)

C	2.130388	0.578893	0.297886
H	3.125211	0.467805	-0.11551
H	1.774146	1.580272	0.090941
H	2.174584	0.40409	1.36499
S	1.10566	-0.657323	-0.548571
C	-0.586479	-0.274036	0.094581
C	-1.550805	-1.161135	-0.695298
H	-1.30534	-2.203828	-0.524226
H	-2.568945	-0.985688	-0.364499
H	-1.489795	-0.956731	-1.757331
C	-0.878926	1.132967	-0.173789
N	-1.09549	2.236981	-0.359219
C	-0.701822	-0.543959	1.594519

H	-1.711056	-0.331484	1.935157
H	-0.475612	-1.585958	1.788753
H	-0.019454	0.073454	2.165987

4-S (UBHandHLYP/6311DZP)

C	-1.113037	0.000055	-0.00736
S	0.694297	0.000004	-0.001779
H	-1.502564	-0.889642	-0.483874
H	-1.425434	-0.003962	1.033847
H	-1.502529	0.89321	-0.477354

2-Se (RBHandHLYP/6311DZP)

Se	1.128592	-0.304204	-0.308882
Se	-1.128592	0.304204	-0.308882
C	1.128592	-1.681121	1.085576
H	0.441018	-2.471019	0.821215
H	2.13926	-2.071358	1.125385
H	0.867721	-1.251168	2.04193
C	-1.128592	1.681121	1.085576
H	-0.867721	1.251168	2.04193
H	-0.441018	2.471019	0.821215
H	-2.13926	2.071358	1.125385

TS-Se (UBHandHLYP/6311DZP)

Se	0.1145	-0.263415	-0.341715
Se	-2.396613	-0.071697	-0.374964
C	0.236449	-1.614895	1.067119
H	-0.523109	-2.354918	0.864808
H	1.216108	-2.069508	1.011067
H	0.076853	-1.169567	2.039335
C	-2.656246	0.964659	1.265139
H	-2.330783	0.404282	2.130361
H	-2.126302	1.904061	1.19755
H	-3.719563	1.157859	1.342193
C	2.247191	0.636593	0.029509
C	2.400735	1.571153	-1.145995
H	3.358671	2.085421	-1.090376
H	2.35686	1.039375	-2.088918
H	1.615878	2.320124	-1.131416
C	3.070112	-0.52528	-0.033893
N	3.703794	-1.479623	-0.067657
C	2.217166	1.301268	1.38395
H	3.174868	1.779549	1.585964
H	1.445788	2.062597	1.405284
H	2.027575	0.590883	2.179882

PC-Se (UBHandHLYP/6311DZP)

Se	0.5517	-0.467801	-0.53181
Se	-2.865867	0.004939	-0.326169
C	0.548705	-1.73865	0.944121
H	-0.241265	-2.443689	0.721082
H	1.498737	-2.253427	0.987005
H	0.334726	-1.247591	1.883502
C	-2.766389	0.754662	1.472761
H	-2.234671	0.090308	2.139223
H	-2.299057	1.728928	1.445731
H	-3.78758	0.865036	1.821152
C	2.108064	0.663217	0.010119
C	2.39811	1.591434	-1.169597
H	3.233801	2.241395	-0.929718
H	2.642945	1.030384	-2.06336
H	1.52999	2.210358	-1.371512
C	3.238029	-0.226682	0.239324
N	4.115882	-0.925466	0.445251
C	1.805536	1.457887	1.278696
H	2.663977	2.066956	1.549307
H	0.956199	2.108114	1.104246
H	1.58039	0.807585	2.115326

3-Se (RBHandHLYP/6311DZP)

Se	1.046428	-0.41628	-0.269088
C	-0.896353	-0.267717	0.15978
C	1.669913	1.261685	0.502856
H	2.717251	1.338822	0.239979
H	1.128841	2.091357	0.068336
H	1.571955	1.258277	1.579602
C	-1.592242	-1.411296	-0.578952
H	-1.197617	-2.362352	-0.236524
H	-2.657828	-1.38896	-0.372967
H	-1.446285	-1.336984	-1.649833
C	-1.366907	1.015022	-0.346042
N	-1.731074	2.031055	-0.715292
C	-1.140962	-0.352602	1.665195
H	-0.635666	0.443671	2.198211
H	-2.204636	-0.274874	1.874897
H	-0.777746	-1.303375	2.037302

4-Se (UBHandHLYP/6311DZP)

Se	-0.433036	0.000000	-0.000682
C	1.517571	0.000005	-0.006176
H	1.894524	0.891826	-0.485970

H	1.828745	-0.000540	1.033100
H	1.894546	-0.891315	-0.486875

2-Te (RBHandHLYP/6311DZP)

Te	1.318059	-0.303891	-0.236868
Te	-1.318059	0.303891	-0.236868
C	1.318059	-1.820215	1.287763
H	0.625196	-2.603198	1.017604
H	2.324784	-2.219288	1.331072
H	1.054494	-1.388491	2.241907
C	-1.318059	1.820215	1.287763
H	-1.054494	1.388491	2.241907
H	-0.625196	2.603198	1.017604
H	-2.324784	2.219288	1.331072

TS-Te (UBHandHLYP/6311DZP)

C	0.64574	-1.37948	1.525330
H	-0.104744	-2.155973	1.536062
H	1.634234	-1.817895	1.548600
H	0.503066	-0.709422	2.361191
C	-2.487569	1.485082	1.259192
H	-2.100288	1.139659	2.206607
H	-1.932212	2.342738	0.908399
H	-3.53173	1.750675	1.368923
C	2.746109	0.701979	-0.045193
C	2.979359	1.395142	-1.367617
H	3.955788	1.877933	-1.368443
H	2.949845	0.701107	-2.199577
H	2.228412	2.161991	-1.527408
Te	0.44429	-0.317793	-0.321979
Te	-2.39255	-0.083985	-0.206253
C	3.530313	-0.471639	0.145346
N	4.129121	-1.434551	0.315845
C	2.703107	1.615428	1.157454
H	3.673253	2.091846	1.298068
H	1.963267	2.394075	1.009687
H	2.464428	1.078511	2.067934

PC-Te (UBHandHLYP/6311DZP)

C	-0.731746	2.013949	-0.274074
H	0.103404	2.400147	-0.842604
H	-1.658461	2.425961	-0.648723
H	-0.602227	2.249689	0.772918
C	2.598468	0.824861	1.753951
H	2.047826	1.749226	1.65715
H	2.148553	0.186736	2.500762
H	3.62024	1.041699	2.040429
C	-2.62449	-0.450377	0.539654
Te	-0.745474	-0.097145	-0.574437
Te	2.678576	-0.210685	-0.125296
C	-2.432107	-0.200518	2.034366
H	-1.683879	-0.879055	2.427677
H	-2.117319	0.816449	2.236855
H	-3.367348	-0.372063	2.562472
C	-3.603758	0.474476	0.001094
N	-4.36435	1.221874	-0.407254
C	-3.042336	-1.894902	0.263848
H	-3.214356	-2.068429	-0.791934
H	-2.272212	-2.577933	0.608658
H	-3.95929	-2.123334	0.800209

3-Te (RBHandHLYP/6311DZP)

C	1.336986	1.667371	0.540575
Te	0.969415	-0.316834	-0.157327
H	2.373743	1.889384	0.321416
H	0.699219	2.355502	0.00288
H	1.171227	1.737205	1.606043
C	-1.20128	-0.274156	0.174412
C	-1.791513	-1.505688	-0.514649
H	-2.867091	-1.532756	-0.363324
H	-1.59725	-1.500336	-1.58059
H	-1.369301	-2.409644	-0.086824
C	-1.700711	0.939881	-0.446945
N	-2.091663	1.908335	-0.90778
C	-1.530634	-0.26445	1.667271
H	-2.608749	-0.233321	1.808679
H	-1.143921	-1.162504	2.134803
H	-1.102898	0.595772	2.168421

4-Te (UBHandHLYP/6311DZP)

Te	-0.333784	0.000001	-0.000323
C	1.81115	0.000007	-0.005124
H	2.18057	-0.890504	-0.491932
H	2.128635	-0.000298	1.03093
H	2.180656	0.890731	-0.491461

References

(1) Okazaki, R.; Hirabayashi, Y.; Tamura, K.; Inamoto, N. *J. Chem. Soc., Perkin Trans. 1* **1976**, 1034-1036.

(2) Akinori, S.; Hideki, Y.; Koichiro, O. *Angew. Chem. Int. Ed.* **2005**, *44*, 1694-1696.

(3) Cossairt, B. M.; Cummins, C. C. *New J. Chem.* **2010**, *34*, 1692-1699.

(4) Barrett, A. G. M.; Melcher, L. M. *J. Am. Chem. Soc.* **1991**, *113*, 8177-8178.

(5) Heiba, E.-A. I.; Dessau, R. M. *J. Org. Chem.* **1967**, *32*, 3837-3840.

(6) Benati, L.; Montevecchi, P. C.; Spagnolo, P. *J. Chem. Soc., Perkin Trans. 1* **1991**, 2103-2109.

(7) Perkins, M. J.; Turner, E. S. *J. Chem. Soc., Chem. Commun.* **1981**, 139-140.

(8) Back, T. G.; Krishna, M. V. *J. Org. Chem.* **1988**, *53*, 2533-2536.

(9) Ogawa, A.; Yokoyama, H.; Yokoyama, K.; Masawaki, T.; Kambe, N.; Sonoda, N. *J. Org. Chem.* **1991**, *56*, 5721-5723.

(10) Renaud, P. *Top. Curr. Chem.* **2000**, *208*, 81-112.

(11) Tsuchii, K.; Doi, M.; Hirao, T.; Ogawa, A. *Angew. Chem. Int. Ed.* **2003**, *42*, 3490-3493.

(12) Ogawa, A.; Yokoyama, K.; Yokoyama, H.; Obayashi, R.; Kambe, N.; Sonoda, N. *J. Chem. Soc., Chem. Commun.* **1991**, 1748-1750.

(13) Ogawa, A.; Yokoyama, K.; Obayashi, R.; Han, L.-B.; Kambe, N.; Sonoda, N. *Tetrahedron* **1993**, *49*, 1177-1188.

(14) Takagi, K.; Soyano, A.; Kwon, T. S.; Kunisada, H.; Yuki, Y. *Polymer Bulletin* **1999**, *43*, 143-150.

(15) Balczewski, P.; Mikolajczyk, M. *New. J. Chem.* **2001**, *25*, 659-663.

(16) David, G.; Boyer, C.; Tonnar, J.; Ameduri, B.; Lacroix-Desmazes, P.; Boutevin, B. *Chem. Rev.* **2006**, *106*, 3936-3962.

(17) Barton, D. H. R.; Bridon, D.; Zard, S. Z. *J. Chem. Soc. Chem. Commun.* **1985**, 1066-1068.

(18) Ziegler, F. E.; Wang, Y. *J. Org. Chem.* **1998**, *63*, 7920-7930.

(19) Barton, D. H. R.; Bridon, D.; Zard, S. Z. *Tetrahedron* **1989**, *45*, 2615-2626.

(20) Santiago, E. V.; Christian, M. k.-L.; Stefan, G.; Armido, S. *Angew. Chem. Int. Ed.* **2007**, *46*, 6533-6536.

(21) Wada, T.; Kondoh, A.; Yorimitsu, H.; Oshima, K. *Org. Lett.* **2008**, *10*, 1155-1157.

(22) Russell, G. A.; Tashtoush, H. *J. Am. Chem. Soc.* **1983**, *105*, 1398-1399.

(23) Newcomb, M. *Tetrahedron* **1993**, *49*, 1151-1176.

(24) Yamago, S.; Iida, K.; Yoshida, J. *J. Am. Chem. Soc.* **2002**, *124*, 2874-2875.

(25) Goto, A.; Kwak, Y.; Fukuda, T.; Yamago, S.; Iida, K.; Nakajima, M.; Yoshida, J. *J. Am. Chem. Soc.* **2003**, *125*, 8720-8721.

(26) Yusa, S.; Yamago, S.; Sugahara, M.; Morikawa, S.; Yamamoto, T.; Morishima, Y. *Macromolecules* **2007**, *40*, 5907-5915.

(27) Sugihara, Y.; Kagawa, Y.; Yamago, S.; Okubo, M. *Macromolecules* **2007**, *40*, 9208-9211.

(28) Kayahara, E.; Yamago, S.; Kwak, Y.; Gota, A.; Fukuda, T. *Macromolecules* **2008**, *41*, 527-529.

(29) Hasegawa, J.; Kanamori, K.; Nakanishi, K.; Hanada, T.; Yamago, S. *Macromolecules* **2009**, *42*, 1270-1277.

(30) Hasegawa, J.; Kanamori, K.; Nakanishi, K.; Hanada, T.; Yamago, S. *Macromol. Rapid Commun.* **2009**, *30*, 986-990.

(31) Yamago, S.; Ukai, Y.; Matsumoto, A.; Nakamura, Y. *J. Am. Chem. Soc.* **2009**, *131*, 2100-2101.

(32) Yamago, S.; Ray, B.; Iida, K.; Yoshida, J.; Tada, T.; Yoshizawa, K.; Kwak, Y.; Goto, A.; Fukuda, T. *J. Am. Chem. Soc.* **2004**, *126*, 13908-13909.

(33) Ray, B.; Kotani, M.; Yamago, S. *Macromolecules* **2006**, *39*, 5259-5265.

(34) Yamago, S.; Kayahara, E.; Kotani, M.; Ray, B.; Kwak, Y.; Goto, A.; Fukuda, T. *Angew. Chem. Int. Ed.* **2007**, *46*, 1304-1306.

(35) Yamago, S.; Iida, K.; Yoshida, J. *J. Am. Chem. Soc.* **2002**, *124*, 13666-13667.

(36) Yamago, S.; Yamada, T.; Togai, M.; Ukai, Y.; Kayahara, E.; Pan, N. *Chem. Eur. J.* **2009**, *15*, 1018-1029.

(37) Kayahara, E.; Yamago, S. *J. Am. Chem. Soc.* **2009**, *131*, 2508-2513.

(38) Kwak, Y.; Tezuka, M.; Goto, A.; Fukuda, T.; Yamago, S. *Macromolecules* **2007**, *40*, 1881-1885.

(39) Kamigaito, M.; Onishi, I.; Kimura, S.; Kotani, Y.; Sawamoto, M. *Chem. Comm.* **2002**, 2694-2695.

(40) Goto, A.; Hirai, N.; Nagasawa, K.; Tsujii, Y.; Fukuda, T.; Kaji, H. *Macromolecules* **2010**, *43*, 7971-7978.

(41) Janousek, Z.; Piettre, S.; Gorissen-Hervens, F.; Viehe, H. G. *J. Organomet. Chem.* **1983**, *250*, 197-202.

(42) Pryor, W. A.; Pickering, T. L. *J. Am. Chem. Soc.* **1962**, *84*, 2705-2711.

(43) Pryor, W. A.; Platt, P. K. *J. Am. Chem. Soc.* **1963**, *85*, 1496-1500.

(44) Pryor, W. A.; Guard, H. *J. Am. Chem. Soc.* **1964**, *86*, 1150-1152.

(45) Pryor, W. A.; Smith, K. *J. Am. Chem. Soc.* **1970**, *92*, 2731-2738.

(46) Krenske, E. H.; Pryor, W. A.; Houk, K. N. *J. Org. Chem.* **2009**, *74*, 5356-5360.

(47) Zhao, Y.; Truhlar, D. *Theor. Chem. Acc.* **2008**, *120*, 215-241.

(48) Zhao, Y.; Truhlar, D. G. *Acc. Chem. Res.* **2008**, *41*, 157-167.

(49) Frisch, M. J.; Trucks, G. W.; Schlegel, H. B.; Scuseria, G. E.; Robb, M. A.; Cheeseman, J. R.; Montgomery, J. A.; Vreven, T., Jr.; Kudin, K. N.; Burant, J. C.; Millam, J. M.; Iyengar,

S. S.; Tomasi, J.; Borone, V.; Mennucci, B.; Cossi, M.; Scalmani, G.; Rega, N.; Peterson, G. A.; Nakatsuji, H.; Hada, M.; Ehara, M.; Toyota, K.; Fukuda, R.; Hasegawa, J.; Ishida, M.; Nakajima, T.; Honda, Y.; Kitao, O.; Nakai, H.; Klene, M.; Li, X.; Knox, J. E.; Hratchian, H. P.; Cross, J. B.; Bakken, V.; Adamo, C.; Jaramillo, J.; Gomperts, R.; Stratmann, R. E.; Yazyev, O.; Austin, A. J.; Cammi, R.; Pomelli, C.; Ochterski, J.; Ayala, P. Y.; Morokuma, K.; Voth, G. A.; Salvador, P.; Dannenberg, J. J.; Zakrzewski, V. G.; Dapprich, S.; Daniels, A. D.; Strain, M. C.; Farkas, O.; Malick, D. K.; Rabuck, A. D.; Raghavachari, K.; Foresman, J. B.; Ortiz, J. V.; Cui, Q.; Baboul, A. G.; Clifford, S.; Cioslowski, J.; Stefanov, B. B.; Liu, G.; Liashenko, A.; Piskorz, P.; Komaromi, I.; Martin, R. L.; Fox, D. J.; Keith, T.; Al-Laham, M. A.; Peng, C. Y.; Nanayakkara, A.; Challacombe, M.; Gill, P. M. W.; Johnson, B. G.; Chen, W.; Wong, M. W.; Gonzalez, C. J.; Pople, A. *Gaussian 03, ReVision B. 05*; Gaussian Inc: Pittsburgh, PA, 2003.

(50) Frisch, M. J.; Trucks, G. W.; Schlegel, H. B.; Scuseria, G. E.; Robb, M. A.; Cheeseman, J. R.; Scalmani, G.; Barone, V.; Mennucci, B.; Petersson, G. A.; Nakatsuji, H.; Caricato, M.; Li, X.; Hratchian, H. P.; Izmaylov, A. F.; Bloino, J.; Zheng, G.; Sonnenberg, J. L.; Hada, M.; Ehara, M.; Toyota, K.; Fukuda, R.; Hasegawa, J.; Ishida, M.; Nakajima, T.; Honda, Y.; Kitao, O.; Nakai, H.; Vreven, T.; Montgomery, J., J. A.; Peralta, J. E.; Ogliaro, F.; Bearpark, M.; Heyd, J. J.; Brothers, E.; Kudin, K. N.; Staroverov, V. N.; Kobayashi, R.; Normand, J.; Raghavachari, K.; Rendell, A.; Burant, J. C.; Iyengar, S. S.; Tomasi, J.; Cossi, M.; Rega, N.; Millam, J. M.; Klene, M.; Knox, J. E.; Cross, J. B.; Bakken, V.; Adamo, C.; Jaramillo, J.; Gomperts, R.; Stratmann, R. E.; Yazyev, O.; Austin, A. J.; Cammi, R.; Pomelli, C.; Ochterski, J. W.; Martin, R. L.; Morokuma, K.; Zakrzewski, V. G.; Voth, G. A.; Salvador, P.; Dannenberg, J. J.; Dapprich, S.; Daniels, A. D.; Farkas, O.; Foresman, J. B.; Ortiz, J. V.; Cioslowski, J.; Fox, D. J. *Gaussian 09, Revision A.02,*; Gaussian Inc: Wallingford CT, 2009.

(51) Hay, P. J.; Wadt, W. R. *J. Chem. Phys.* **1985**, *82*, 284-298.

(52) Wang, Y.; Grimme, S.; Zipse, H. *J. Phys. Chem. A.* **2004**, *108*, 2324-2331.

(53) Zhao, Y.; Truhlar, D. G. *J. Phys. Chem. A* **2008**, *112*, 1095-1099.

(54) Hohenstein, E. G.; Chill, S. T.; Sherrill, C. D. *J. Chem. Theory Comput.* **2008**, *4*, 1996-2000.

(55) Valdes, H.; Pluhackova, K.; Pitonak, M.; Rezac, J.; Hobza, P. *Phys. Chem. Chem. Phys.* **2008**, *10*, 2747-2757.

(56) Morokuma, K. *J. Chem. Phys.* **1971**, *55*, 1236-1244.

(57) Stowasser, R.; Hoffmann, R. *J. Am. Chem. Soc.* **1999**, *121*, 3414-3420.

Concluding Remarks

This thesis entitled in "**Studies on the Precision Control of Polymer Structure Based on Heteroatom-Mediated Living Radical Polymerization Reaction**" described new and powerful methods for the precise control of macromolecular structures in terms of molecular weights, molecular weight distributions, and end groups based on organoheteroatom-mediated living radical polymerization. By elucidating basic reactivities of heavier organoheteroatom compounds, this author succeeded in synthesizing several new heteroatom compounds which are highly efficient to control the molecular weights and molecular weight distributions of the resulting polymers prepared under radical conditions. Furthermore, findings of new reactivities of heavier organoheteroatom compounds under radical and non-radical conditions enabled the precise control of polymer end structures.

In Chapters 1-4, the factors that affect the control of group transfer radical addition reaction were optimized. The ability of the hemolytic substitution (S_H2) reaction was affected by the heteroatom species as well as the substituents on the heteroatom. The substituent effects on the tellurium atom in TERP and on the antimony atom in SBRP were examined in Chapters 1 and 2. The development of organobismuthine-mediated living radical polymerization (BIRP) was discussed in Chapter 3. The studies revealed that aryl-substituted organotellurium and organobismuthine chain transfer agents are especially effective for the control of macromolecular structures giving polymers with desired molecular weights and narrow MWDs. In chapter 4, the development of bismuth-based new cocatalyst for the further control of BIRP was described. A thiobismuthine compound possessing bismuth-sulfur σ bond was newly designed and synthesized as cocatalyst of BIRP. The addition of the cocatalyst in BIRP significantly increased the MWD control and allowed the controlled synthesis of high-molecular-weight polystyrenes and ultrahigh-molecular-weight polyacrylates.

In chapter 5-6, the selective functionalizations of the living polymer-end under the radical and anionic conditions are described. Structurally well-defined ω-vinylidene polymethacrylates were successfully obtained by the reaction of polymethacrylates bearing organotellanyl, organostibanyl, and organobismuthanyl ω-polymer end groups with TEMPO free radical under thermal or photochemical conditions. The carboanions were generated from organostibines and bismuthines polymer end through heteroatom-metal exchange reaction, and subsequent reaction of the anion with electrophiles afforded ω-functionalized polymers. The exchange reaction proceeded with

highly chemoselective manner and tolerated a variety of polar functional groups.

In chapter 7, the reactivity of dichalcogenides towards the S_H2 reaction with carbon-centered radicals was theoretically investigated. The theoretical calculations revealed that their reactivity was controlled by both kinetic reactivity of the diheteroatom compounds and thermodynamic stability of the generated calcogenide compunds and calcogen-centered radical species.

These results not only considerably expand the ability of macromolecular engineering for the design and production of functional polymeric materials in materials science, but also shed new lights on the basic chemistry of radical chemistry as well as heteroatom chemistry. The basic chemistry clarified in this thesis would open new possibilities in designing new controlling agent in radical reaction and living radical polymerization reaction. Also, this author believe that, with further progress of these works, the methods developed by this author will become basic tools for creating new polymer materials in both academic and industrial fields.

List of Publications

1. "Optimaization of Organotellurium Transfer Agents for Highly Controlled Living Radical Polymerization"
   Kayahara, E.; Yamago, S.; Kwak, Y.; Goto, A.; Fukuda, T. *Macromolecules* **2008**, *41*, 527-529.
   Chapter 1

2. "Substituent Effect on the Antimony Atom in Organostibine-Mediated Living Radical Polymerization"
   Kayahara, E.; Kondo, N.; Yamago, S. *Heteroatom Chem.* **2011**, Accepted for publication.
   Chapter 2

3. "Highly Controlled Living Radical Polymerization through Dual Activation of Organobismuthines"
   Yamago, S.; Kayahara, E.; Kotani, M.; Ray, B.; Kwak, Y.; Goto, A.; Fukuda, T.
   Angew. Chem. Int. Ed. **2007**, *46*, 1304-1306.
   Chapter 3

4. "Development of an Arylthiobismuthine Cocatalyst in Organobismuthine-Mediated Living Radical Polymerization: Applications for Synthesis of Ultrahigh Molecular Weight Polystyrenes and Polyacrylates"
   Kayahara, E.; Yamago, S. *J. Am. Chem. Soc.* **2009**, *131*, 2508-2513.
   Chapter 4

5. "Synthesis of Structurally Well-Controlled ω-Vinylidene Functionalized Poly(alkyl methacrylate)s and Polymethacrylonitrile by Organotellurium, Organostibine, and Organobismuthine-Mediated Living Radical Polymerizations"
   Yamago, S.; Kayahara, E.; Yamada, H. *React. Funct. Polym.* **2009**, *69*, 416-423.
   Chapter 5

6. "Generation of Carboanions via Stibine-Metal and Bismuth-Metal Exchange Reactions and Its Applications to the Precision Synthesis of ω-End Functionalized Polymers"
   Kayahara, E.; Yamada, H.; Yamago, S. *submitted*
   Chapter 6

7. "Theoretical Studies on Homolytic Substitution Reaction of Dicalcogenides with Carbon-centered Radical. Interplay between Kinetic Reactivity and Thermodynamic Stability"
   Kayahara, E.; Yamago, S.; Chung, L. W.; Morokuma, K. *to be submitted*
   Chapter 7

Other Associated Publication

"Synthesis of Structurally Well-Defined Telechelic Polymers by Organostibine-Mediated Living Radical Polymerization. *In Situ* Generation of Functionalized Transfer Agents and Selective ω-End Group Transformations"
Yamago, S.; Yamada, T.; Togai, M.; Ukai, Y.; Kayahara, E.; Pan, N. *Chem. Eur. J.* **2009**, *15*, 1018-1029.